

A programmable syringe pump for studying cellular signaling in microfluidic dynamic environments

A Major Qualifying Project Report
Submitted to the faculty of
Worcester Polytechnic Institute

In partial fulfillment for the
Degree of Bachelor of Science by:

MQP DRA-1702

Shaimae Elhajjajy

Andrea Karduss

April 26, 2018

Approved by:

Dirk Albrecht, Ph.D., Project Advisor

Amir Mitchell, Ph.D., Project Advisor

Table of Contents

Abstract.....	vi
Authorship.....	vii
Acknowledgements.....	viii
Table of Figures.....	ix
Table of Tables.....	xii
1. Introduction.....	1
2. Literature Review.....	6
2.1 Microfluidic Cell Cultures.....	6
2.1.1 Microfluidic Materials.....	6
2.1.2 Advantages of Microfluidics.....	7
2.1.3 Limitations.....	8
2.1.4 Fluid Mechanical Properties of Microfluidics.....	9
2.1.5 Cell Cultures.....	10
2.2 Current Applications.....	11
2.2.1 Cancer Biology.....	11
2.2.2 Drug Discovery.....	12
2.2.3 Lab-on-a-chip.....	12
2.3 Dynamically Changing Environments.....	13
2.4 Media Delivery.....	17
2.4.1 Peristaltic Pumps.....	17
2.4.2 Gravity-based Pumps.....	18
2.4.3 Syringe Pumps.....	19
2.4.4 Pressure Driven.....	21
2.5 Existing Solutions.....	21
2.6 Clinical Need.....	23
3. Project Strategy.....	25
3.1 Initial Client Statement.....	25
3.2 Design Requirements: Technical.....	26
3.2.1 Objectives.....	26
3.2.2 Constraints.....	29

3.2.3 Functions.....	31
3.2.4 Specifications.....	33
3.2.5 Functional Blocks.....	34
3.2.6 Design Requirements: Standards.....	35
3.3 Revised Client Statement.....	37
3.4 Management Approach.....	38
3.4.1 Financial Statement.....	39
4. Design Process.....	40
4.1 Needs Analysis.....	40
4.1.1 Design Needs.....	41
4.1.2 Design Wants.....	42
4.1.2.1 Experiment 1: Pulse Experiment.....	43
4.1.2.2 Experiment 2: Constitutive Level.....	44
4.1.2.3 Experiment 3: Slope Experiment.....	44
4.1.3 Needs and Wants Design Matrix.....	45
4.1.4 Physical Limitations.....	46
4.2 Conceptual Designs.....	47
4.2.1 Assessment of Design Components.....	47
4.2.2 Feasibility studies.....	52
4.2.3 Experimental parameters and design calculations.....	52
4.2.4 Computational Analysis.....	55
4.3 Alternative Designs.....	56
4.4 Final Design Selection.....	57
4.4.1 Gravity-based Pump.....	58
4.4.1.1 Flow Rate Testing with Torricelli’s Law.....	58
4.4.1.2 Ohm’s Law.....	64
4.4.1.3 Flow Rate Testing with Syringes and Connected Tubes.....	65
4.4.2 Syringe Pumps.....	68
4.4.2.1 Laser Cut Syringe Pump.....	69
4.4.2.2. 3D Printed Syringe Pump.....	73
5. Verification of Final Design.....	76

5.1 Stress Testing.....	76
5.1.1 Testing 1: Forward and Rewind 10 rpm with no delay.....	78
5.1.2 Testing 2: Forward and Rewind Speed: 10 rpm 1 Step, 10 ms delay.....	79
5.1.3 Testing 3: Forward and Rewind Speed: 10 rpm 1 Step, 50 ms delay.....	80
5.1.4 Testing 4: Forward and Rewind Speed of 10 rpm 1 Step, 75 ms delay.....	81
5.1.5 Testing 5: Forward and Rewind Speed: 10 rpm 1 Step, 100 ms delay.....	82
5.2 Determination of the Relationship Between Flow Rate and Motor Delay.....	84
5.3 Switch Response Testing.....	91
5.3.1 Switch Response at 5 min Interval for the Two Pumps Alternating.....	92
5.3.2 Switching Response Lag Time in Chamber Test.....	96
5.4 Flow rate testing and pump system reaction to software commands.....	102
5.5 Experiment 2 Code.....	106
5.6 Concentration Testing.....	107
5.6.1 WebCam Concentration Testing.....	107
5.6.2 Glucose Concentration Testing.....	116
5.6.3 Microscope Concentration Testing.....	120
5.7 Inlet Plug Testing.....	121
5.7.1 Fabrication of the Plug.....	121
5.7.2 Depth of the Plug.....	122
5.7.3 Tube Orientation.....	122
5.8 Mixing.....	127
5.8.1 Improving Mixing.....	127
5.8.2 Improving Equilibrium Between Inlet and Outlet.....	131
6. Final Design Validation.....	134
6.1 Biological Experiment Results.....	134
6.1.1 Testing different flow rates for cell viability.....	134
6.1.2 Pulse Experiment 1: Half hour single drug pulse, 0.02 mL/min flow rate.....	136
6.1.3 Pulse Experiment 2: Half hour single drug pulse, 0.1 mL/min flow rate.....	139
6.1.4 Pulse Experiment 3: Half hour stabilization period, one hour single drug	

pulse, 0.02 mL/min flow rate.....	141
6.1.5 Pulse Experiment 4: Half hour stabilization period, one hour drug pulses (x2), one hour relaxation periods (x2), 0.02 mL/min flow rate.....	143
6.1.6 Pulse Experiment 5: Half hour stabilization period, one hour drug pulses (x4), ½ hour relaxation periods, 0.02 mL/min flow rate.....	145
6.1.7 Pulse Experiment 6: Half hour stabilization period, one hour drug pulses (x4), ¼ hour relaxation periods, 0.02 mL/min flow rate.....	146
6.1.8 Pulse Experiment 7: Three hours starvation media, 4 hours starvation media with vemurafenib (compared with the control)	148
6.1.9 Final Pulse Experiment: 6 multi-channel starvation experiment.....	151
6.2 Reproducibility Experiment.....	156
6.3 Economics.....	157
6.4 Environmental Impact.....	158
6.5 Societal Influence.....	158
6.6 Political Ramifications.....	159
6.7 Ethical Concerns.....	159
6.8 Health and Safety Issues.....	159
6.9 Manufacturability.....	160
6.10 Sustainability.....	160
6.11 Industry Standards.....	160
7. Discussion.....	161
7.1 Final Design Analysis.....	161
7.1.1 Accomplishing Objectives.....	161
7.1.2 Satisfying Constraints.....	162
7.1.3 Meeting Design Requirements.....	163
7.2 Comparison with Existing Devices.....	163
7.3 Limitations.....	165
7.3.1 System must be stopped manually at the end of the experiment.....	165
7.3.2 Air bubbles enter the system.....	165
7.3.3 Cells suffer during experiment setup.....	165
7.4 Impact on Biological Research.....	166

7.4.1 Cell Viability under different flow rates.....	166
7.4.2 Promising studies in cancer research.....	166
8. Conclusion and Recommendations.....	168
8.1 Conclusions.....	168
8.2 Recommendations.....	168
8.2.1 Implement a method for stopping the pumps when an experiment has finished.....	168
8.2.2 Introduce a User Interface.....	168
8.2.3 Establish a solution for preventing bubbles from entering the system.....	169
8.2.4 Prevent cell suffering during experiment setup.....	170
8.2.5 Other recommendations.....	170
8.3 Future Work.....	171
References.....	173
Appendixes.....	179
Appendix A: Arduino Code.....	179
Appendix B: Code Documentation.....	194
Appendix C: User Manual.....	205
Appendix D: Biological Experiments Protocol.....	221

Abstract

Microfluidic chambers provide a useful platform for the study of cell behavior due to their ability to precisely adjust the cellular microenvironment by controlling fluid flow at microscale volumes. Automated microfluidic systems can facilitate the study of cellular signaling networks by accurately administering dynamic drug doses to cell cultures. The design team for this MQP presents a programmable, custom engineered system composed of twelve syringe pumps that controls the delivery of two alternative media types to cells growing in standard microfluidic chambers. The system is more affordable than commercially available systems, costing only around \$150. The platform can multiplex parallel, independent, live-cell microscopy imaging experiments, and control a variety of flow rates within 0.02 mL/min, 0.05mL/min, and 0.1 mL/min were tested. The functionality of the multi-pump system was demonstrated by performing six parallel biological experiments over a twelve-hour long experiment with alternating regular media and drug concentration media at different timepoints to monitor the temporal dynamics of signaling inhibition in an important model melanoma cell line. Initial biological experiments demonstrated that the system could deliver dynamic doses of vemurafenib to melanoma cell in microfluidic chambers. Starvation experiments revealed lowered proliferation due to the absence of growth factors. A final insight was that reducing drug holidays can yield less reactivation of the ERK pathway.

Authorship Page

Section	Primary Writer	Final Editor
1. Introduction	Andrea and Shaimae	All
2. Literature Review	Andrea and Shaimae	All
3. Project Strategy	Andrea and Shaimae	All
4. Design Process	Andrea and Shaimae	All
5. Verification of Final design	Andrea and Shaimae	All
6. Final Design Validation	Andrea and Shaimae	All
7. Discussion	Andrea and Shaimae	All
8. Conclusions and Recommendation	Andrea and Shaimae	All
Appendix A: Arduino Code	Shaimae	All
Appendix B: Code Documentation	Shaimae	All
Appendix C: User Manual	Andrea and Shaimae	All
Appendix D: Biological Experiments Protocol	Andrea and Shaimae	All

Acknowledgements

The team would like to acknowledge the following people for their contribution, expertise, and assistance throughout this project.

Department of Biomedical Engineering, WPI

Dirk Albrecht, Ph.D

Kyra Burnett

Elyse Favreau

Lisa Wall

Program in Systems Biology, University of Massachusetts Medical School

Amir Mitchell, Ph.D

Payam Khoshkenar

Serkan Sayin

Brittany Rosener

Clay Mangiameli

Table of Figures

Figure 1: Different frequencies of pulsatile osmotic stresses influence rate of cell proliferation.....	14
Figure 2: The mechanism by which the drug vemurafenib inhibits the BRAF mutation in melanoma cells to stop cell proliferation.	16
Figure 3: Peristaltic Pump.....	18
Figure 4: Gravity-driven Pump.....	19
Figure 5: Syringe Pump.....	20
Figure 6: Pressure Driven Pumps mechanism.....	21
Figure 7: Concept map for visualization of objectives.....	28
Figure 8: Functional Block Diagram.....	35
Figure 9: Gantt Chart for Project Timeline.....	39
Figure 10: Graphical representation of the pulse experiment.....	44
Figure 11: Graphical representation of the constitutive level experiment.....	44
Figure 12: Graphical representation of the slope experiment.....	45
Figure 13: Preliminary Design.....	51
Figure 14: The magnitude of Reynolds number affects the type of fluid flow.....	53
Figure 15: Initial model (Model 1) of the laser cut syringe pump.	57
Figure 16: Initial model of the 3D printed syringe pump.....	57
Figure 17: Draining Tank Model for Torricelli’s Law in Hydrodynamics.....	58
Figure 18: Graphs representing the change in volume over time of water draining from a syringe.....	60
Figure 19: (A) Graph of all trials plotted with the model derived from Torricelli’s Law, (B) Graph of the average flow rate vs. time, plotted against the model derived from Torricelli’s Law, and (C) Graph of the average flow rate vs. volume, plotted against the model derived from Torricelli’s Law.....	61
Figure 20: Graphs representing the change in volume over time of water draining from a syringe.....	62
Figure 21: (A) Graph of all trials plotted with the model derived from Torricelli’s Law, (B) Graph of the average flow rate vs. time, plotted against the model derived from Torricelli’s Law, and (C) Graph of the average flow rate vs. volume, plotted against the model derived from Torricelli’s Law.	63
Figure 22: Initial design from Instructables.com.....	69
Figure 23: Model 2 of the Laser Cut Syringe Pump.....	70
Figure 24: Model 3 of the Laser Cut Syringe Pump.....	71
Figure 25: Model 4 of the Laser Cut Syringe Pump.....	72
Figure 26: Results of 3D printed syringe pump experiment; 1 step with 6 second delays.....	74
Figure 27: Final System of Syringe Pump, with 2 pumps attached to a single base.....	74
Figure 28: Length Moving part travelled for different times.....	84
Figure 29: An excerpt of the code for Experiment 1, the pulse experiment.....	85
Figure 30: Relationship Between Flow Rate and Motor Delay.....	87

Figure 31: The relationship between flow rate and motor delay.....	90
Figure 32: Pump 1 on (green dye), LED light on. Pump 2 on (red dye), LED light off.....	91
Figure 33: Regions of Interest selection at different timepoints of fluid passing through the chamber.....	93
Figure 34: 0.1 mL/min FR 5 minute interval switching of pumps.....	94
Figure 35: 0.05 mL/min Flow Rate 5 minute interval switching of pumps.....	94
Figure 36: 0.02 mL/min Flow Rate 5 minute interval switching of pumps.....	95
Figure 37: Switch Response for the Three Flow Rates Tested.....	96
Figure 38: Switch Response for Lag Time Measurements.....	97
Figure 39: Curve Fitting for Lag Time.....	99
Figure 40: Curve Fitting for Tau.....	100
Figure 41: Curve Fitting for Tau Max.....	100
Figure 42: Outlet tube with 1 cm marks and bubble travelling through system.....	102
Figure 43: Bubble traveling through outlet tube at software input of 0.1 mL/min.....	103
Figure 44: Bubbles traveling through outlet tube at software input of 0.05 mL/min.....	104
Figure 45: Bubbles traveling through outlet tube at software input of 0.02 mL/min.....	104
Figure 46: The setup of the microfluidic chamber for the WebCam Concentration Testing experiment.	108
Figure 47: Color Intensity for the Known 100% Concentration.....	109
Figure 48: Color Intensity for Known 50% Concentration.....	109
Figure 49: Color Intensity for Target 50% Concentration.....	110
Figure 50: The microfluidic chamber at the end of the experiment.....	111
Figure 51: The red channel in ImageJ.....	112
Figure 52: The green channel in ImageJ.....	112
Figure 53: The results from the second trial of the 50% WebCam Concentration Testing.....	113
Figure 54: The ROIs for the microfluidic chamber.....	114
Figure 55: The results from the 75% WebCam Concentration Testing.....	115
Figure 56: The graphical results for the 25% Glucose Concentration test.....	118
Figure 57: The graphical results for the first trial of the 50% Glucose Concentration test.....	119
Figure 58: The graphical results for the second trial of the 50% Glucose Concentration test...	119
Figure 59: The graphical results for the 75% Glucose Concentration test.....	120
Figure 60: The setup of the PDMS plug in the microfluidic inlet.....	121
Figure 61: The different depths at which the PDMS inlet plug were tested, where H1 indicates Height 1, H2 indicates Height 2, and H3 indicates Height 3.....	122
Figure 62: The three different tube orientations.....	123

Figure 63: A schematic of the funnel implemented to improve mixing.....	128
Figure 64: An image of the funnel.....	128
Figure 65: The streamlines within the micropipette tip.....	129
Figure 66: The vacuum introduced at the outlet.....	132
Figure 67: Profile of fluid flow rates administered for cell viability test.....	135
Figure 68: Percent of Cell viability when exposed to different flow rates over one hour period each.....	136
Figure 69: Drug Profile for Pulse Experiment 1.....	137
Figure 70: Results of the first pulse experiment.....	138
Figure 71: Drug Profile for Pulse Experiment 2.....	139
Figure 72: Results of the second pulse experiment.....	140
Figure 73: ERK Translocation Response Times for the 0.02 mL/min and 0.1 mL/min flow rates.....	140
Figure 74: Drug Profile for Pulse Experiment 3.....	142
Figure 75: Results of the third pulse experiment.....	142
Figure 76: Drug Profile for Pulse Experiment 4.....	143
Figure 77: Results of the fourth pulse experiment.....	144
Figure 78: ERK translocation (0.02 mL/min) demonstrated reversibility for pathway activation and inhibition.....	144
Figure 79: Drug Profile for Pulse Experiment 5.....	145
Figure 80: Results of the fifth pulse experiment.....	146
Figure 81: Drug Profile for Pulse Experiment 6.....	147
Figure 82: Results of the sixth pulse experiment.....	148
Figure 83: Drug Profile for Pulse Experiment 7.....	149
Figure 84: Results of the control for the starvation experiment.....	150
Figure 85: Results of the starvation experiment.....	150
Figure 86: Results for channel 2 of the 6 pump starvation experiment.....	153
Figure 87: Results for channel 3 of the 6 pump starvation experiment.....	153
Figure 88: Results for channel 4 of the 6 pump starvation experiment.....	154
Figure 89: Results for channel 5 of the 6 pump starvation experiment.....	154
Figure 90: Results for channel 6 of the 6 pump starvation experiment.....	155
Figure 91: Starvation channel from the reproducibility experiment.....	156
Figure 92: Control channel from the reproducibility experiment.....	157
Figure 93: ElveFlow Microfluidic Bubble Trapper.....	169

Table of Tables

Table 1: Summary of main objectives.....	26
Table 2: Pairwise Comparison Chart for Prioritization of Objectives.....	29
Table 3: Summary and description of constraints.....	30
Table 4: Functions-Means Table.....	31
Table 5: Needs and Wants of the Multi-Pump System.....	40
Table 6: Summary of the 3 different experiment types.....	43
Table 7: Design Matrix of Needs and Wants.....	46
Table 8: Physical Constraints of the Design.....	46
Table 9: Pros and Cons for Achieving Optimal Cell Culture Environment.....	48
Table 10: Pros and Cons for Type of Pump.....	49
Table 11: Pros and Cons for Stepper Motors.....	50
Table 12: Pros and Cons for Controller.....	51
Table 13: Raw data for syringe experiment, using the normal/regular nozzle.....	59
Table 14: Raw data for syringe experiment, using the small/tiny nozzle.....	61
Table 15: Summary of Syringe Experiment Flow Rates for Comparison.....	66
Table 16: Acceptance Criteria for Pump outcome exposed to stress testing.....	77
Table 17: Measurements at Original Position.....	77
Table 18: Observed Results for Forward and Rewind 10 rpm with no delay.....	78
Table 19: Speed: 10 rpm 1 Step, 10 ms delay.....	79
Table 20: Speed of 10 rpm 1 Step, 50 ms delay.....	80
Table 21: Speed of 10 rpm 1 Step, 75 ms delay.....	81
Table 22: Speed: 10 rpm 1 Step, 100 ms delay.....	82
Table 23: Time vs Length Relationship.....	83
Table 24: Summary of the observed flow rates for different delay periods.....	88
Table 25: Summary of the observed flow rate for 3 different trials of the 1 second delay for the MICROSTEP.....	89
Table 26: Lag Time between code switch command and actual time media starts flowing.....	98
Table 27: Tau - Code switch command and middle point value in slope.....	98
Table 28: Tau max- Code switch and moment media completely distributed in chamber.....	98
Table 29: Coefficient of Variation for bubbles' flow rate under different flow rate software input.....	105
Table 30: Summary of the glucose concentration testing results.....	118
Table 31: Summary of inlet plug testing results.....	124
Table 32: Summary of the mixing results using the funnel.....	130
Table 33: Summary of mixing results for the vacuum at different flow rates.....	133
Table 34: Cell viability after exposure to different flow rates and in general.....	136
Table 35: Experiment summary for the six multi-pump experiment.....	152

Chapter 1: Introduction

Cancer is one of the most devastating diseases worldwide. In particular, melanoma is a form of cancer in the skin that is believed to be caused by a combination of genetic and environmental factors [1]. Unlike other types of cancer, melanoma cases have continued to increase: the incidence rose by an astounding 270% between the years 1973 and 2002, and as of 2014, 1 in 63 Americans have the risk of suffering from melanoma [1]. Furthermore, melanoma is the fifth most common cancer type in males, and the sixth most common cancer type in females [1]. Due to its increasing prevalence, and because of melanoma's severity and fatal consequences, researchers have been compelled to develop innovative therapeutic treatments for melanoma. These therapies target key genetic mutations and signaling pathways that help hinder tumor growth [2]. Nevertheless, there still remains an abundance of research questions that need to be answered in the search for cancer treatments.

Controlling cell proliferation is particularly important in melanoma treatment. Cellular signaling pathways such as the extracellular signal-regulated kinase (ERK) pathway can regulate cell proliferation in cells. A large number of melanoma cases contain a mutated protein which leads to overactivation of the ERK pathway, resulting in increased cell proliferation. Vemurafenib is a drug that can selectively target this mutated protein and inhibit the ERK pathway to control cell proliferation. This drug is used by Dr. Amir Mitchell in the Program of Systems Biology at the University of Massachusetts Medical School in their research on cellular response to dynamically changing environments. The Mitchell Lab explores these cellular responses in the context of health and disease applications by administering dynamic dosing of drugs to cell cultures over the course of an experiment. It was previously discovered that cells behave in dramatically different ways when exposed to pulses and oscillations of osmotic stress, as opposed to static or continuous ones [3]. The aim of one of Mitchell lab's most recent projects is to determine the dynamics of the extracellular signal-regulated kinase (ERK) pathway in A375 melanoma cells in response to oscillating doses of the drug vemurafenib. This research is clinically relevant because of the occurrence of vemurafenib resistance observed in patients who have been treated with the drug. Researchers in Mitchell Lab are therefore interested in the potential for dynamic doses of vemurafenib to effectively limit melanoma cell proliferation while at the same time reducing drug exposure to prevent drug resistance.

Dynamic dosings can be achieved by the use of perfusion systems for melanoma and cancer therapeutic research using microfluidic cell cultures. One approach for melanoma and cancer therapeutics research is microfluidic cell cultures. The use of microfluidics for cell culture applications has become a wide area of study, with a large number of research laboratories implementing the technology for their experiments within the last decade [4] [5]. The advantages of such a system are many, especially in the field of systems biology. Among the advantages, microfluidics are high-throughput, allow parallel tests to be performed, control physical and chemical environments, and simulate *in vivo* environments. The advantage of being high-throughput can lead to cost reduction, saved time, and more experiments run in parallel [4]. Running parallel experiments can in turn improve reproducibility, data collection, and overall efficiency of an experiment [6]. Additionally, both chemical and physical *in vitro* environments can be more accurately controlled when compared to standard use of static cell cultures on typical tissue culture plates [4], and the microfluidic chambers can achieve laminar, continuous, constant fluid flow [6]. These two features, when combined, help to more accurately simulate the natural *in vivo* environment of cells. Furthermore, drug doses can be administered with greater precision at the nano-, pico-, or even femtoliter scale, which marks a significant improvement to normal cell culture practices that are only as small as the microliter scale [6].

Perhaps most importantly, there is great potential for automated experiments that can perform periodic media replacement through the microfluidic chambers [4]. The implementation of automation in microfluidic cell cultures can help accommodate large-scale experiments by reducing the time-consuming process of manual pipetting, as well as eliminating the need for manual intervention by researchers [6]. This could vastly improve the efficiency of cell culture experiments performed in microfluidic devices.

Currently, there is a limited number of existing devices on the market capable of delivering media with a constant continuous flow via a programmable pump to cell cultures that reside in microfluidic chambers. Automated cell cultures can be made possible with the implementation of pumps for media delivery, but the majority of pump systems that are commercially available are much too large to be compatible with microfluidic chambers and are not customizable for specific user needs [7]. Furthermore, these pump systems are extremely expensive, ranging from a couple hundred US dollars to a couple thousand.

The companies Watson-Marlow and Cole-Parmer® have developed peristaltic pumps for cell culture applications which have already been employed by various labs and researchers [8] [9]. Unfortunately, products from both of these companies possess the disadvantages previously discussed. Another available brand is ibidi®, which sells an air pump system that contains a controlled valve set and is compatible with most commonly used microfluidics. However, prices of such devices are extremely high, especially for laboratory settings in which multiple pumps are required.

There do exist several research laboratories that have designed and built pump-incorporated systems for delivering media to cell cultures *in vitro*. One of the current devices being used is a perfusion bioreactor system that maintains a physicochemical environment for cell proliferation by Zhao et. al [9]. Similarly, Sasaki et al. were able to create an infusion pump-based system specifically for the application of microfluidics [7]. Britton et al. propose in their study an assembly for a continuous flow system as an alternative to those commercially available [10].

In order to perform this project, the Mitchell Lab is in need of a modular, programmable pump system that will perform the proper drug administration. Two alternative types of media (one standard cell culture media and one infused with drugs) will be delivered to each microfluidic chamber simultaneously at various drug profiles, thereby allowing for parallel experiments to take place. This will effectively control the extracellular conditions and allow for the continued research of cell responses to dynamically changing environments. Due to the nature of the project and specificity of its requirements, there are no ideal solutions for microfluidic-specific pump systems currently available. While other research labs have attempted to create similar devices as previously discussed, none of the existing devices satisfy all the Mitchell Lab's experimental needs. Therefore, such a system would need to be custom engineered to meet the specific requirements of the Mitchell Lab's new project.

The purpose of this project is to design and build a multi-pump system which is capable of delivering two alternative types of media to cell cultures in commercially available μ -Slide VI 0.4 microfluidic chambers [11]. The pump must be motor controllable, modular, and able to accommodate 6 individual experiments running in parallel. Another objective is to make the system fully programmable by implementing an Arduino. This will allow the system to autonomously deliver varying profiles of drugs to cell cultures over the course of an experiment.

Since the system will be applied to cell cultures, the flow rate and shear stress of media delivery must be at levels which realistically mimic those found in *in vitro* testing previously published so that cells remain viable and are not damaged. Melanoma are able to withstand high shear stress on the skin; however, this type of cancer cells or any other tumor cells *in vitro* are able to withstand lower shear to the limit of 1.2 dynes/cm² [11]. The system will implement a syringe pump to achieve this media delivery. The system must maintain the proper environment for cell cultures in terms of temperature and pH, as well as the correct sterilization to avoid contamination. The end goal of the project is to satisfy the client's needs in constructing such a system, thus assisting the Mitchell Lab to continue exploring melanoma cell response to dynamic doses of drug for various systems biology and cancer research applications.

The design of a multi-pump system for cell cultures in microfluidic chambers will involve various components. The project strategy will primarily deal with constructing a working system which successfully delivers two alternative types of media, one regular and one infused with drugs, to a cell culture in one single microfluidic chamber. Once it is determined that the system is working properly in terms of mechanics and programming, and once it is confirmed that the cell cultures remain viable and healthy under this method of media delivery, the system will be multiplexed to accommodate all channels within a 6-channel microfluidic chamber. The selected pump type will be connected to a motor, which in turn will be attached to an Arduino controller. The accompanying Arduino software will be implemented to make the apparatus programmable. All of these parts will constitute the system as a whole, which is expected to successfully deliver the media types to the chambers at a flow rate that will not be detrimental to the cells in culture. Following verification that the system works successfully, experimental work with cell cultures will be completed to aid the client in the continuation of their project that focuses on exploring cellular responses to dynamic dosing regimens of drugs.

The subsequent section will be a literature review to provide more in-depth background on microfluidic cell culture and its research application which determines the need for this project. The following chapter details the project strategy and presents the approach taken for engineering a possible solution to the client's problem. Afterwards, both the design process and design verification will be elaborately described, to demonstrate the steps involved in narrowing down design ideas and the methods with which different design options were tested by confirming the main design requirements were met and selecting the final design. This paper will

also present the final design of the pump system and rationale for the design by providing verification testing involving stress testing, flow rate confirmation testing, and response time to achieve uniform media distribution after pump switching. The design will also be validated by performing biological testing and support the functioning of the design with a real-time research application. Finally, the last two chapters will consist of a discussion of the results of the project, recommendations for future work, and concluding statements on the project as a whole.

Chapter 2: Literature Review

2.1 Microfluidic Cell Cultures

Microfluidics are devices that are used for the control and manipulation of fluids at the micro-, nano-, and picoscale levels [12]. A very diverse technology, microfluidics can be employed for a wide range of scientific research applications. In fact, microfluidics are suitable for studying cell cultures due to the size compatibility, and has therefore been widely utilized in this area to achieve a so-called “lab-on-a-chip” [5]. Cell cultures, or the controlled growth and maintenance of cells in a laboratory environment, are integral to the study of biology and have been one of the hallmarks of biological research since their inception [5] [12].

2.1.1 Microfluidic Materials

The most common fabrication technique for microfluidics is soft lithography of poly(dimethylsiloxane) (PDMS), a silicon-based material. It's ideal elastomeric properties (for stamping), optical transparency (for imaging), flexibility (for molding), inertness (for biocompatibility), and inexpensiveness have established PDMS as the favored material for microfluidic devices [5] [12]. However, it is not without limitations: high gas permeability leads to unwanted evaporation of water vapor, hydrophobicity leads to undesired absorption of cell culture media components, and the risk of chemical artifacts affects the integrity of its biocompatibility [12][6].

Due to these limitations, some scientists have sought alternative options for microfluidic fabrication materials [5]. Standard plastic materials that are conventionally used in traditional cell cultures present a valid alternative for PDMS. Most cell culture equipment is fabricated from polystyrene, but other options of suitable plastics are commercially available as well. Plastic microfluidic devices are relatively inexpensive and biocompatible. They are also compatible with a wide range of commonly used reagents for biological and chemical experiments, including cell culture media [13]. Fabrication techniques for plastic microfluidic devices, like casting and injection molding, are well-established [13]. For the purpose of cell cultures, these plastic devices can be given surface treatments to enhance cell adhesion.

2.1.2 Advantages of Microfluidics

Microfluidic cell cultures have many advantages over the standard tissue culture plates at the macroscopic scale. Microfluidics are a suitable vessel for cell cultures because of their ability to handle fluids at the microscale or lower, and this is also the reason why microfluidics facilitate extremely precise control of these fluids [6]. This controllability applies to many different aspects of microfluidic cell cultures. It allows very precise volumes of fluid at the microliter, nanoliter, and picoliter ranges to be delivered to cell cultures in microfluidics; hand-held pipettes that are typically used can only deliver volumes as small as microliters [6]. Since minuscule amounts of fluid are needed, especially when compared to conventional cell cultures, consumption of reagents is greatly reduced [12]. Controllability permits the investigator to not only precisely control the experimental conditions by tailoring the geometries and architecture of the microfluidic device, but it also allows control over the seeded cell density and placement in the microchannel [6][12]. Control over the cells themselves is also possible, because delivery of media, drug doses or chemical and mechanical signals can be extremely precise [6]. In essence, microfluidics has introduced the ability to tailor and control almost any parameter of the microenvironment of cell cultures, which is an invaluable advantage [5].

Fabrication of the microfluidic devices themselves can be parallelized in order to be produced more rapidly [6]. Microfluidics can often be built as integrated and compact devices that have spatially separated, independently controlled channels, each of which contains different experiments that can be performed simultaneously [6]. Additionally, the reproducibility of biological experiments can be improved with this high parallelization [6]. In short, this enables high-throughput experimentation that maximizes experimental efficiency [12].

Microfluidics can more easily accommodate automation to a larger extent in multiple forms. In conventional cell culture, automation usually comes in the form of large and expensive robots that handle fluids, which eliminates the need for manual pipetting; conversely, automation in microfluidics can be implemented both compactly and inexpensively in a way that enables consistent manipulation, monitoring, and sampling of cells in culture [6]. Within the microfluidic platform itself, automation can be introduced in the form of microvalves, which move mechanically to perform intensive tasks [6]. In all cases, automated microfluidics allow experiments that usually require tedious and laborious tasks to be performed quickly and efficiently, all while minimizing manual intervention [6]. One common method of automation is

through the use of pumps, which are either built into the microfluidic system or connected externally via tubing to the microfluidic device [5]. These pumps often include valves or other components for additional automated control. If a pump is properly programmed, it can then deliver media continuously to cell cultures in microfluidic systems.

Conventional cell cultures can often be considered as bulk cultures, which means that any averaged results obtained from large populations could be inaccurate, misleading, or non-representative [6]. Microfluidics has the ability to achieve single cell resolution, which is of huge interest in quantitative and systems biology for dynamical analysis of cells as part of biological systems [6]. By greatly reducing the size of the cell population in the microfluidic cell culture, the resolution for individual cells is immensely enhanced both spatially and temporally for more accurate analysis [12].

Materials used for microfluidics are selected in part for their ideal and stable optical features. In particular, these materials often possess optical clarity and transparency, while they ward off autofluorescence and optical abnormalities that can sometimes be introduced by cell culture media [6]. All of these optical properties allow microfluidic systems to support excellent real-time live-cell imaging, which is a valuable asset to have in biological experiments [6].

Perhaps the most significant advantage of microfluidic cell cultures is that it enables the cellular microenvironment to be tailored to the specific needs of the experiment, which is not possible through standard cell culture Petri dishes at the macroscale [5]. More importantly, microfluidics can be used to develop an *in vitro* environment that more closely matches the cell's *in vivo* environment [5]. This is a property of huge consequence, since mimicking cells' natural microenvironment can ultimately mean accurate and representative results that are more comparable to what would actually occur within the body. This can be achieved in numerous ways, such as with perfusion systems or with spatial and temporal chemical gradients [12].

2.1.3 Limitations

One major limitation of microfluidic cell cultures is the absence of standard cell culture protocols. Traditional cell cultures in conventional Petri dishes have been the foundation of biological research procedures for many years, which has allowed ample time for standardization of protocols to have been established. However, the same is not true for microfluidics, as it is a relatively new field [12]. While this may be an issue in the present, it will not likely remain so

given time; microfluidics is an ever-expanding technique, and standards will likely be formed as the field matures [12].

One such debatable protocol is the novel cell culture surfaces used in microfluidic devices [12]. While PDMS is the material of choice for the majority of microfluidic applications to cell cultures, other concerns have arisen regarding its hydrophobicity (which causes it to absorb small molecules from solution out of media) and its potential toxicity when proper curing is absent (leading to artifacts that could deleteriously impact cells in culture) [6].

One of the advantages of microfluidics can also be interpreted as a disadvantage. An attractive feature of microfluidic cell cultures is the small scale of fluid volumes that are dealt with, which results in profitable reduction of reagents and therefore a decrease in the amount of consumables. However, microscale fluid volumes (or smaller) can be challenging to work with and can make the subsequent chemical analysis of samples more difficult [12]. Furthermore, because the amount of fluid inside the cell culture is so small, even the slightest evaporation (which is itself a respectable problem) can cause drastic shifts in the osmolarity of cell culture media [12]. This could ultimately affect the viability of the cells if the media solute becomes more concentrated as a result, which is the reason that osmolarity shifts should be avoided as much as possible [12].

2.1.4 Fluid Mechanical Properties of Microfluidics

If microfluidic cell cultures are dynamic, meaning that flow of media is constantly passing through the microfluidic chamber (as opposed to static cultures, in which the sample of media remains stationary in the chamber until it is manually exchanged), then another significant limitation is the degree of shear stress that can be exerted on the cells that are residing in the microfluidic device [6]. This is most relevant with perfusion flow because shear stress is constantly being applied to the cells as the fluid flows through the chamber [12]. Flow-induced shear stress can often lead to undesired alterations in a cell's morphology, which is reason enough to minimize shear stress by decreasing the velocity and rate of fluid flow in the system [12].

Fluid flow patterns in any vessel can be described by a unitless property called Reynolds number. This is an important fluid mechanics concept for reporting the flow regime [14]. The regime can be either laminar, in which the flow is smooth and ordered; turbulent, in which the

flow is chaotic; or transitional, in which the flow is in a state between laminar and turbulent. Reynolds number can be calculated by the following equation:

Equation 2.1

$$Re = \frac{\rho v D_h}{\mu}$$

where Re is Reynolds number, ρ is the fluid's density (kg/m³), v is the fluid's velocity (m/s), Dh is the hydraulic diameter of the vessel that is dependent on the vessel geometry (m), and μ is the fluid's viscosity (Pa*s) [14]. The hydraulic diameter can be calculated based on the geometries of the channel (i.e., if the channel is circular or rectangular), and the equation can be seen below.

$$D_h = \frac{4A_c}{p}$$

where Dh is the hydraulic diameter (m), Ac is the cross-sectional area of the vessel (either circular or rectangular) (m), and p is the wetted perimeter (m) [15].

Different flow regimes can then be characterized by the value of Reynolds number: if Re < 2300, the flow is laminar; if 2300 < Re < 4000, the flow is transitional; and if Re > 4000, the flow is turbulent [14].

Past studies have established that flow within microfluidic chambers is always laminar due to the small dimensions of these chamber [14]. However, laminar flow within small chambers leads to streamlines; if more than one stream of fluid is flowing in the interior of the chamber, these streamlines will not mix with each other but instead will be visible as distinct, separated lines [14]. The only mechanism for these streams to mix naturally is via diffusion, which is the process where molecules or particles move from an area of higher concentration to an area of lower concentration so as to spread out more evenly across the dimensions of the chamber [14]. This is usually a very slow process, but research has found that increasing the time that the streams are in contact with each other can in turn increase the degree of diffusion that is observed [14].

2.1.5 Cell Cultures

There are many additional considerations to take into account when working with microfluidic cell cultures. Traditional macroscopic cell cultures have been developed

extensively for years, which is why a standard protocol for performing these cell cultures exists. However, due to the novel nature of microfluidic cell cultures and the fact that it is considered a young technique, there has been little standardization established [12].

The method for cell seeding can depend on the specific microfluidic in question; regardless, the cell seeding procedure for microfluidics differs from that of standard tissue culture plates [5]. The most common method entails the use of syringe-based injection, typically via pipetting the media into the chamber. There are some concerns associated with this approach, namely the risk of the clogging of cells due to uneven distribution across the channel surface, the rapid depletion of nutrients and accumulation of waste in the media due to high cell densities, and the consequential effects on pH and gas concentrations in the cellular environment [5]. Essentially, the method for seeding simply must not negatively affect cell viability in any way.

It is very important that the introduction of air bubbles into the microfluidic chamber be minimized. If present in the channel, air bubbles can cause a number of problems, all of which are deleterious to the cells. They could obstruct the microchannel, hamper the flow of fluid, disrupt fluid flow patterns, dry out regions of the channel, or rupture cell membranes when burst [5]. Preventing bubbles from entering the microchannel can be achieved through careful seeding of cells and handling of the microfluidic system as a whole. Despite best efforts, however, air bubbles can sometimes be unavoidable [5].

Evaporation is another complication that can arise, which often occurs if the microfluidic cell cultures are not maintained in a properly humidified environment [5]. This can be cause for concern in PDMS devices due to the high gas permeability of PDMS, which causes drying when water vapor leaves the system, or in open systems in which microwells are exposed to air [5][12]. This can lead to a decrease in media volume, which by consequence leads to an increase in solute concentration in the media. As previously stated, however, the main preventative measure for evaporation is ensuring that the microfluidic device is placed in an environment with high humidity, such as in a properly humidified incubator [6].

2.2 Current Microfluidic Applications

2.2.1 Cancer Biology

Cancer research can also be conducted using microfluidic technology. In particular, cancer models can include angiogenesis, metastasis, and organ-on-a-chip models which closely represent the microenvironment of cancer cells *in vivo* [16]. Microfluidics can also be an invaluable tool in cancer diagnosis. Because of the convenience, low cost, and ability to deal with very small fluid volumes, microfluidic devices can enable researchers to conduct extremely sensitive assays that are capable of detecting biomarkers for diagnostics [17]. In addition, microfluidic cell cultures can provide a resource for investigating tumor cell migration, as well as many other areas of cancer research [17].

Cancer is marked by uncontrolled cell proliferation, which is what gives rise to tumors. The control of cell proliferation is critical to treat cancer and is therefore a primary focus in many areas of cancer research. In general, many cellular signaling pathways govern the control and regulation of cell growth. The ERK pathway is particularly relevant in melanoma cells, in which the presence of mutations can severely amplify cell proliferative activity [26]. Cancer research has developed therapeutic drugs that can help control this pathway in order to reduce cell proliferation, such as the drug vemurafenib, and this research is still continuing today [26]. Microfluidics are a useful platform for observing cellular signaling pathways and their effect on cancer biology.

2.2.2 Drug Discovery

Drug discovery is a huge area for the implementation of microfluidic cell cultures. Conventional cell cultures lack the ability to accurately mimic the native microenvironment and therefore cannot assuredly maintain *in vivo* cell physiology and behavior, leading to unreliable and misleading results during drug testing [18]. On the other hand, microfluidic cell cultures provide precise control of the extracellular environment such that it can be accurately modeled after the *in vivo* microenvironment, allowing for better prediction and reliability of drug testing [18]. The ability for a perfusion-based system to be implemented enables decreased risk of contamination, constant supply of nutrients, and steadier environmental conditions, all of which are crucial for drug discovery research [18].

2.2.3 Lab-on-a-chip

Lab-on-a-chip is a small-scale device that includes several components of a lab in a single system that is only a few centimeters squared in size [19]. This novel technology includes

micro- and nanoscale fabrication for 3D printing and thin films, micro- and nanofluidics for multiphase flow, and micro- and nanosystems for sensors and actuators, among others [20]. These have a variety of applications that cover biological, chemical, medical, environmental, and energy applications [20]. Some specific analysis that can be done for the aforementioned applications correspond to nucleic acid biotechnology analysis for DNA or RNA sequencing, drug development for screening and delivery, cells and tissues engineering, cell and organism motility, and single cell analysis for biochemical and biophysical purposes, among others [20].

From the previously mentioned applications, one of the main trends in biology corresponds to the use of Lab-on-a-Chip (LOC) microfluidic-based platforms for single cell biophysical analysis of cancerous tissue [21]. Due to cancer heterogeneity in both cellular level and patient population, it makes it a suitable condition to be evaluated under a LOC system [21]. Even though, in most cases LOC technology used for biochemical and biophysical analysis is starting to be implemented especially for cancer research. The biophysics of cancer involve mechanics of cancer, the tumor microenvironment, and the dielectric and optical properties of the cell [21].

The mechanical characterization of cancer cells in LOC focus on three different techniques: size-based cell isolation, constriction microfluidics, and microelectromechanical systems [21]. These are used to evaluate cell size and deformability, entry-exit time and pressure drop, and cell stiffness, diameter, and viscous losses, respectively (Shukla et al., 2018). All of these techniques have the purpose of evaluating how the tumor cells adapt to different microenvironments [21]. The electrical characterization is performed to understand the spatial separation of cells to evaluate dielectric properties based on the cytoskeleton structure and cytoplasm composition. Additionally, the impedance was measured to determine different cell metastatic potentials. These studies would also allow the electrical fluctuation of the cell membrane as the malignant phenotype in cells progresses [21]. The optical properties correspond to the refractive index that would be higher in cancerous cells compared to normal ones [21].

Even though this field has gained attention in the past decade, it still has to be developed for higher throughput and precision. It not only has the potential for studying the way cancer cells behave, but it additionally shows promise for experiments that expose those cancer cells to drugs and evaluates a specific biochemical pathway or system depending on the research team's interest.

2.3 Dynamically Changing Environments

The client of this project is Dr. Amir Mitchell of the Program in Systems Biology (PSB) at the University of Massachusetts Medical School (UMMS). Dr. Mitchell's lab works on projects such as (1) characterizing the dynamics of the MAPK signaling cascade in cancer cells, (2) uncovering methods to rewire signaling and regulatory networks in cells to overcome resistance to cancer therapy, (3) investigating asymmetric cell division in yeast cells both experimentally and theoretically, (4) designing and fabricating custom-engineered, do-it-yourself (DIY) hardware to meet the specific needs of novel experiments that study cell response to dynamically changing environments, and (5) an outreach program in which international high school students remotely design automated experiments for monitoring real-time emerging bacterial drug resistance that are performed in Mitchell lab [22] [23].

One of Mitchell lab's main investigations concerns the study of cellular response to dynamically changing environments. In their Science paper, Mitchell et al. describe a study in which they induced a dynamic environment on *S. cerevisiae* by subjecting the cells to oscillating osmotic stresses [3]. Resultant cell growth observed at single cell resolution using time-lapse microscopy showed that, when cells underwent a range of different periods of osmotic stress, the cells proliferated significantly slower at intermediate frequencies of 8 minutes.

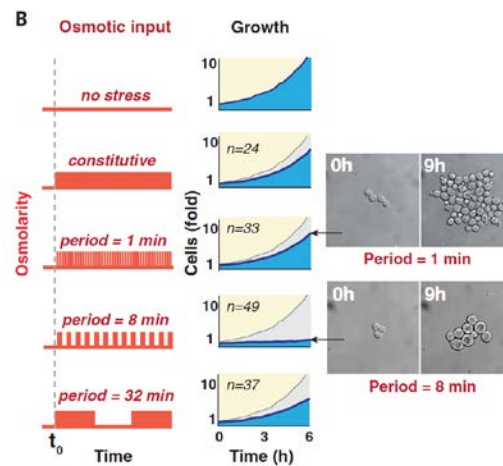


Figure 1: Different frequencies of pulsatile osmotic stresses influence rate of cell proliferation. In particular, the 8-minute frequency demonstrates considerably slower cell growth. [3]

Furthermore, they deduced that the MAPK pathway was what caused the yeast cells to mistakenly perceive the oscillating pattern of osmolarity as a continuously increasing osmolarity,

thus shedding light on methods to reveal concealed “Achilles’ Heels” in common cellular regulatory networks [3].

Mitchell Lab is pursuing similar projects related to dynamically changing environments. In their most recent studies, they are exploring the effect that oscillating drug doses have on A375 melanoma cells. In order to do this, the Mitchell Lab uses melanoma cells to run their experiments. Melanoma is a type of cancer that initiates when skin cells proliferate out of control [24]. These cells are usually called melanocytes that behave as transformed cells. This transformed cells usually enter circulation to travel through the system and reach other parts of the body, and that is how metastasis occurs [25]. However, it is still not clearly understood how the fluid microenvironment influence cancer cells’ viability and functionality [25]. Barnes et al. proposes throughout their study that cancer cells tend to be resistant to fluid shear stress by blood circulation, however Tarbell et al., demonstrates the *in vitro* resistance to fluid shear stress decreases. Therefore, melanoma cells are able to withstand high flow rates to the limit of cells exposed to 1.2 dynes/cm² [11]. This corresponds to a flow rate of 0.95 mL/min which is considered a limit flow rate for *in vitro* testing. This was calculated using the formula below, where η is the viscosity (0.0072 dynes*s/cm²), tau is the shear stress, and is the flow rate of interest in mL/min.

Equation 2.2

$$\tau = \eta * 176.1 * \phi$$

$$\phi = \frac{\tau}{\eta * 176.1}$$

$$\phi = \frac{1.2 \text{ dynes/cm}^2}{0.0072 \text{ dynes} * \frac{\text{s}}{\text{cm}^2} * 176.1}$$

$$\phi = 0.95 \text{ mL/min}$$

Pharmaceutical drugs for melanoma are being actively researched, especially those that target specific protein mutations. The BRAF protein is known to play a role in the extracellular signal-related kinase (ERK) pathway, which leads to normal cell proliferation. In the majority of metastatic melanoma cases, the BRAF protein has undergone a mutation in which the amino acid valine (V) at position 600 has been replaced by the amino acid glutamic acid (E). This

BRAF^{V600E} mutation causes the BRAF signaling to be constitutively active which, in turn, activates the downstream ERK regulatory network and causes increased cell proliferation. Vemurafenib is an FDA-approved drug that selectively targets the BRAF^{V600E} mutation [26]. By selectively inhibiting BRAF^{V600E} enzymatic activity, the downstream activation of the ERK pathway was significantly decreased, resulting in halted proliferation [26].

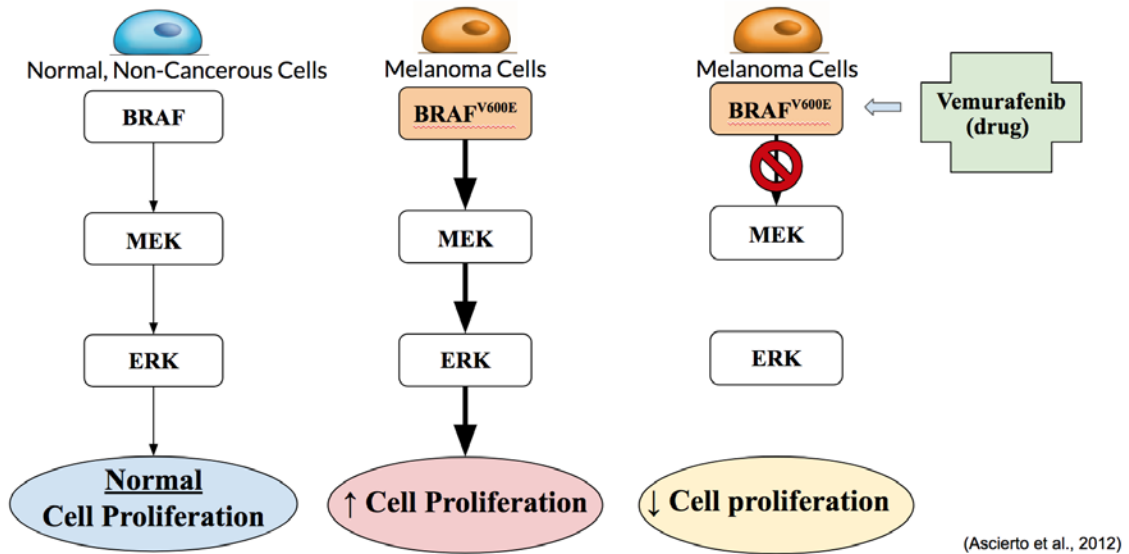


Figure 2: The mechanism by which the drug vemurafenib inhibits the BRAF mutation in melanoma cells to stop cell proliferation. Figure adapted from [27].

The ERK regulatory pathway is therefore important in cancer cell proliferation. ERK molecules initially reside in the cytoplasm of cells but will undergo nuclear translocation once activated, after which it will promote cell proliferation [28]. The dynamics of ERK activation can be visualized with kinase translocation reporters (KTRs) by their fluorescent activity. When ERK is active and inside the nucleus, KTR will reside in the cytoplasm. Conversely, when ERK is inactive and resides in the cytoplasm, KTR translocates to the nucleus [29]. ERK inactivation in melanoma cells can be studied visually by observing nuclear translocation of fluorescently-tagged KTRs that occurs in response to vemurafenib treatments.

Melanoma patients who have been treated with vemurafenib often exhibit signs of resistance. These indications usually occur between 6 to 8 months after the patient has first been treated [26]. This resistance can be attributed to either the reactivation of the ERK pathway, or the activation of other cell signaling pathways that also control cell proliferation [26]. Active

research is being conducted in the area of vemurafenib resistance, related to uncovering the exact mechanism that leads to resistance, the best therapeutic strategies to prevent this resistance, and the use of other possible drugs that can also inhibit pathways involved in proliferative activity (such as cobimetinib) [26].

2.4 Media Delivery

Cell cultures typically are done statically in Petri dishes or multiwell plates. These methods are economical and easy to use; however, they have the limitation of having to perform media changes manually, and these type interventions lead to high risk of contamination. When this process occurs, there is also a fluctuation in cell environment causing which is not ideal when trying to keep certain parameters constant and one single variable for research experimentation [30]. For these reasons, lab settings are starting to evaluate perfusion systems for cell culture. This system provides a more sterile and stable environment, since media is constantly changed adding new nutritious media and removing the waste without having manual interaction which often causes contamination. Perfusion systems additionally provide the possibility of maintaining everything in the environment constant and allow that single feature being researched as the only variable. This type of systems also allows live imaging to be taken throughout the experiment even over long-duration experiments [30].

Perfusion culture delivers fluid volumes to microfluidic devices through completed by external devices that can be connected to or built into the system [5]. The interface usually occurs through the inlet and outlet ports connecting the culture region with the external world [5]. This type of system allows constant fluid to fill the chamber with fresh media and remove it in a timely manner. The four main devices commonly used are peristaltic pumps, gravity-based pumps, syringe pumps, and pressure driven that are connected to the ports using tubing and connectors [5].

2.4.1 Peristaltic Pumps

Peristaltic pumps are positive displacement pumps that consist of a circular case or pump head with expanding and contracting cavities for suction, and discharge of the fluid contained in flexible tubing that is being pumped through the system [31]. Media being contained in the tubing enables researchers to run experiments in which sterility is required [31]. Peristaltic pumps can use a great variety of tubing sizes, which allow flow rates ranging from 0.0007

mL/min to 45 L/min [31]. Having the ability to achieve such small flow rates is one of the many advantages of cell cultures in microfluidics. Peristaltic pumps also allow bidirectional flow and recirculation, which is especially favorable for experiments that require alternating the direction of the flow [4]. However, for the purpose of this project, this particular feature is not required. This type of pump possesses self-priming properties, which is also advantageous as it allows the user to avoid manual priming and possible spills or contamination [31]. This device is also very inexpensive, which means it can be very accessible for a lab setting that requires high quantities. The downside of peristaltic pumps is that delivery of the fluid to the microfluidic chamber is administered in pulses of pressure, as demonstrated in the graph in Figure 3 [4]. These pulses of pressure for flow rates ranging between 17 ml/min to 100 ml/min correspond to 11% of variation among them [32]. However, these are not compatible with microfluidics.

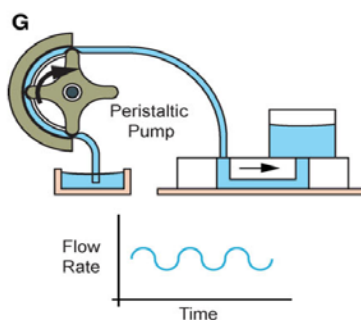


Figure 3: Peristaltic Pump [4]

2.4.2 Gravity-based Pumps

Hydrostatic or gravity-driven pumps usually consist of an open syringe held at a certain height that is connected to the microfluidic by an intervening piece of tubing. The materials used for this device are easily accessible, making this type of pump a very economic option. An advantage of this system lies in its simple mechanics and properties, which allows it to provide different flow rates depending on the diameter of the syringe, the length of the tube, and the height difference between the syringe and the chamber. Usually, the ranges of flow rate are from zero to 10 mL/min [19]. This pump can also maintain a continuous fluid flow, which is ideal when evaluating cellular response to pulses of drugs rather than to pulses of pressure.

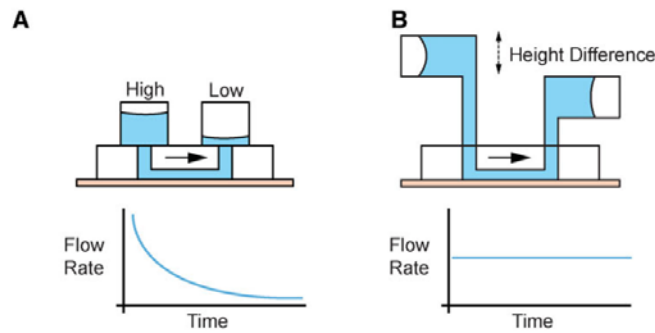


Figure 4: Gravity-driven Pump [4]

The system may include two or more gravity pumps connected to a single chamber when the experiment requires the alternation of two different types of media. In order to allow a specific media to flow, two methods are possible: 1) a valve (such as a pinch valve) can be used to open or close the tubing, thereby controlling the passage of fluid, or 2) introducing a height difference between the two pumps as shown in Figure 4 [4]. However, this system contains a significant limitation, which is that flow rate is challenging to control based on height difference; as the volume of fluid in the syringe decreases, the flow rate will also decrease [4] [33]. Thus, gravity-driven pumps are unable to provide truly constant flow rates. However, a possible option to control these flow rates would be having a closed loop system in which the reservoir of media is replenished. Applying this method to biological experiments could be a challenge since media would be in touch with cellular components and contamination could occur not making the closed, replenished loop reliable enough.

2.4.3 Syringe Pumps

A syringe pump is a small infusion device that is automated and programmed to gradually deliver a fluid into a chamber at a predesignated flow rate and speed [34]. These are used for delivering precise infusion and are able to accurately control flow rates; they are even capable of achieving very low flow rates that are ideal for cellular experiments [34]. This device is also very reliable, since it is extensively used in medical and biological research by delivering fluids to patients or by exposing cells to distinct flow rates [4]. For all the applicable flow rates, the syringe pump is able to maintain a stable, continuous flow, as demonstrated in the graph in the figure below.

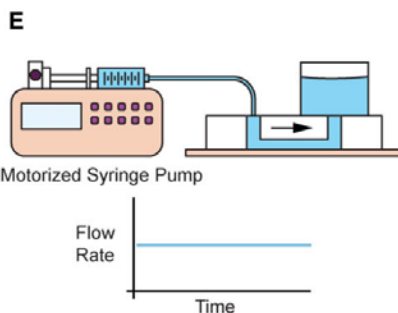


Figure 5: Syringe Pump [4]

This stable continuous flow can be achieved when media is being delivered at flow rates as low as $0.5 \mu\text{L}/\text{min}$ [30]. However, for lower flow rates around $0.1 \mu\text{L}/\text{min}$, pulses tend to appear and oscillation of the flow rate is possible due to the stepper motor used. The elasticity of the system might also be an important factor to maintain stability at such low flow rates, but this would also affect the response time of syringe pump initiation [30]. For this reason, it is important to find a balance on response time, which is determined by the resistance of the system. Stability is also a key factor to achieve continuous and smooth flow rates [30]. Finding the ideal balance would also allow the user to reduce the time the pump system takes to reach steady state, which is usually considered as a downside of this type of pump system [4].

Another downside of this type of pump is the pricing, which may range from \$300 to \$3,000. Commercially available syringe pumps are very expensive, which might be a challenge due to the project's and lab's low budget. Nonetheless, there are some ways of creating syringe pumps in lab settings, a practice which is often referred to as "DIY (do-it-yourself) syringe pumps". Britton et al. propose in their study an assembly for a continuous flow system as an alternative to those commercially available. The devices produced "in-lab" provide a flexible, versatile, and cost-effective alternative to researchers [10]. This allows the researchers to run continuous experiments and avoid high costs in research materials, as they no longer need commercially available pumps. It is also important to have a test method to assure the "in-lab" assembled device works properly and runs experiments smoothly. In this study, the team uses a sample reaction that would evaluate the functionality of the device assembly, especially to assess the construction of the device and any possible adverse events such as clogging [10].

2.4.4 Pressure driven pumps

Pressure driven pump function by having a mechanism of applying controlled pressure of air inside the reservoir of media [35]. As shown in the figure below, air is introduced through an inlet in the media container and fluid will flow through an outlet portion.

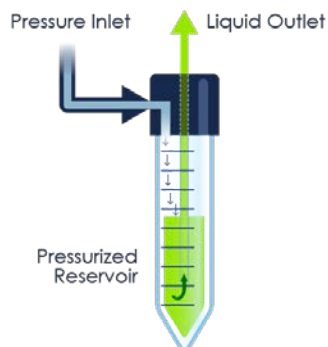


Figure 6: Pressure Driven Pumps mechanism [35].

This type of pump is considered to be stable, provides a constant flow rate, can achieve very low flow rates and provides the option for rapid switches between reservoirs. However, this it has the disadvantage of possible backflow, which is an issue during cell culture exposed to alternative types of media and only one direction of flow is required to avoid mixing of both [35]. Another downside, for lab settings with limited budget corresponds to the high prices of these systems, since researchers are just starting to use it in lab settings.

2.5 Existing Solutions

Currently there is no established gold standard for an ideal pump system utilized in microfluidic applications. However, there are several options that are commercially available and are still used for lab research settings.

Gómez-Sjöberg et al. present one of the first studies with microfluidic experimentation in which the system was built using an on-chip peristaltic pump that is located at the root of the designed microfluidic chip [36]. This pump allowed precise delivery of culture media or reagents into the channels. The three valves contained in the peristaltic pump regulated the dosage of media delivered to the channels, and at the same time controlled the flow rate based on how quickly the switch of valves was done inside the pump [36]. The amount of media delivered corresponded to 1% of the total volume capacity of the channel every 0.15 seconds. The miniature pneumatic solenoid valves were automated and controlled by an electronic that was connected to a computer by a USB. The chip was placed in an automated microscope that

maintains temperature of 37°C and 5% CO₂ [36]. The microscope imaged the chip chambers every hour to collect data on the effects of the experiment. The main limitation of this existing pump system is the type of pump being used. Peristaltic pumps usually deliver fluid in pulses of pressure which is not ideal when interested in evaluating behavior of cells to pulses of drugs, especially when keeping the fluid constant and continuous throughout the whole experiment is of vital importance.

Another device commercially available is the ibidi Pump System. This system has two components: the computer-controlled air ibidi pump, and the fluidic unit which contains the cell media reservoir, the microfluidic slide, and the electronically-controlled valve set [37]. The system provides an ideal simulation of physiological conditions in which flow acts in a unidirectional, oscillatory, and pulsatile manner. Additionally, it provides the ideal shear stress for biological tissue by mimicking shear stresses found *in vivo*, allowing the biological material to withstand long term experiments [37]. The incubator microscope performs live cell imaging and immunofluorescence to analyze shear stress response [37]. The flow rate is controlled by a software connected to the air pump, that is also able to operate over four parallel fluidic units [37]. The system can be placed in large microscope assuring ideal temperature and CO₂ concentrations. The restricted range of allowable flow rates (0.1 ml/min- 40 ml/min) as well as the high prices (\$2,500 for a single unit to \$22,500 for four units) are the limitations of this product [37].

A third type of device that can be found for purchase is an automated commercially available syringe pump; more specifically, the Microfluidic Infusion-Only Syringe Pump by Darwin Microfluidics. This pump holds only one syringe of up to 60 mL in volume [38]. It is able to deliver media at flow rates in the range of 0.000012 mL/min (by using 1 mL syringes) to 25 mL/min (by using 60 mL syringes) [38]. It is fully programmed and the user would only have to set the infusion rate for the pump to work. This system, or many similar commercial syringe pumps like it, is already being used in a great amount of lab settings, which indicates that it is very reliable. Nonetheless, the main limitations of this system is its bulkiness and its high costs that limit the amount of pumps available in a lab setting due to budget constraints. In addition, this system typically comes as a single unit and can only operate one syringe at a time, so it would not easily support experiments in which two (or more) syringes are needed for delivering alternating media; if this were the case, the lab would need multiple units.

2.6 Clinical Need

In 2016, melanoma, commonly referred to as skin cancer, caused over 75,000 cases in the United States alone, of which over 10,000 were fatal [26]. Unfortunately, the number of melanoma cases continues to rise at a faster rate than other forms of cancer, making melanoma the sixth most common form [26]. Despite making up only a small percentage of skin cancers, melanoma causes the majority of skin cancer related deaths [39]. Active cancer research has been able to develop certain therapeutic drugs that can treat specific protein mutations in the majority of melanoma cases. However, such research is still ongoing in the search for a cure.

To conduct this research, the necessary equipment that meets the needs of the biological experiments must be satisfied. In most cases, laboratories run experimental research throughout long periods of time to evaluate how cells react to a specific stimulus or how cells are engineered to grow a tissue. Manually changing cell media in experiments that last as long as 24 hours can expose cells to fluctuating environments at the moments during which media is changed, or when imaging the cells to evaluate the progress of the experiment. This exposure to temperatures different than 37°C and non-standard CO₂ concentrations can affect the overall results of the experiments. In order to obtain accurate results, the cells should be able to maintain constant all of the environmental aspects with the one single variable being studied. To accomplish this task, research labs seek the technology to run experiments through an automated and programmable system that can last long periods of time, change or alternate media automatically, and image cells throughout the whole experiment while maintaining the environmental properties needed to maintain good cell viability.

However, such a system is very specific to both the needs of the laboratory performing the experiment and the needs of the particular biological experiment that is being conducted. Existing devices have their many limitations, as previously discussed, and don't often meet the specific needs of certain types of research. Research laboratories like Mitchell Lab will often need custom-engineered systems to meet their experimental needs, as is the case for this project. Therefore, there remains a critical need for a custom engineered pump system that can support cellular signaling studies in microfluidic chambers. This Major Qualifying Project developed a multi-pump system to meet that need.

A multi-pump system will enable Mitchell Lab to conduct biological experiments in which melanoma cell response to dynamic doses of vemurafenib can be investigated. Cellular

response is measured by the study of ERK dynamics, visualized by KTRs, as a result of oscillatory drug doses. This Major Qualifying Project focuses on the design of the multi-pump system and on preliminary biological experiments that monitor the temporal dynamics of ERK signaling inhibition in an important model melanoma cell line. With this pump system, researchers in Mitchell Lab can perform experiments related to their hypothesis, in which they wish to study if dynamic dosing can inhibit the ERK pathway to stop melanoma cell proliferation just as effectively as constant dosing can. If this is the case, as they are predicting, then drug exposure to cells is limited while still providing adequate treatment. This is an important study in order to determine if dynamic treatments can help to reduce the occurrence of drug resistance.

Chapter 3: Project Strategy

3.1 Initial client statement

The challenge presented to the design team was to create a multi-pump system that would enable the research of cellular response to dynamic dosing regimens of drugs, in which these regimens are delivered as drug pulses and oscillations. The multi-pump system has been designed for use by Mitchell Lab at UMMS, which requires the device to be a fully programmable multi-pump system capable of controlling the extracellular environment of *in vitro* cell cultures. The initial client statement provided to the design team was the following:

Design and construct a perfusion system for delivering two alternative media types to a cell culture growing in a microfluidic chamber. The system should be fully programmable and modular so it can run 6 individual experiments on a multi-channel microfluidic chamber.

There is currently a limited number of automated systems that exposes microfluidic cell cultures to constant fluid flow and that enables the testing of cellular response to different drug regimens during the duration of the experiment. Such experiments can often only be performed manually and for short periods of time, which hinders the ability for accurate time-lapse microscopy to capture images for long-term experiments that can be analyzed for different cellular responses to the drug profiles. Even if those limited number of systems exist, most of them are of high cost for the lab to be able to afford and are not customizable for user needs. The device should be automated to run experiments that last between one and twenty-four hours, be compatible with a microscope for imaging during the experiments and be situated in an incubation system to provide the ideal environment for cell growth and proliferation.

The main issue also lies in the fact that no existing programmable pump system has the ability to deliver alternating flow between two different types of media to cell cultures in microfluidic chambers. Because the needs of this research are so specific, designing such a system would be beneficial for the Mitchell Lab's experiments. If the design proves to be successful, it has the potential to be used in other research labs and even in industry.

3.2 Design Requirements: Technical

3.2.1 Objectives

A set of objectives was established in the process of gaining more information for refinement of the client statement. These objectives represent various aspects of the design that were requested by the client, and are thus goals that must be achieved for the effective design of the multi-pump system. A summary of the 6 main objectives can be seen below in Table 1, followed by a brief description of each.

Table 1: Summary of main objectives

Objective	Description
Programmable	Able to perform switching of fluids with two syringe pumps while performing pulses of drugs
Automatic	Able to run without any user interaction
Maintain Cell Viability	Cells should be able to withstand and survive the shear stress generated by flow rate
Parallelization	Perform 6 experiments in parallel; Enables comparison studies
User-Friendly	Simple user interface and operation
Reproducible	Experiments produce accurate results; Other labs able to recreate the system

The details of these objectives are the following:

1. **The device must be programmable.** The pump system will consist of 6 different units, that contains 2 pumps each. The system should be able to perform switches of fluid at different time points creating profiles of pulses of drugs.
2. **The device must be automated.** The pump system should be fully programmable. An Arduino Uno board and the accompanying Arduino software can be used to write code that will operate the multi-pump system. A programmable device is advantageous in that it allows the user to specify the drug profile and length of experiment they desire (among other parameters), after which the experiment can run without user intervention.

3. **The device must maintain good cell viability.** This objective consists of three parts. The materials of the tubes, microfluidic chamber, and other pump components must be biocompatible to ensure that no chemical leaching of materials will affect the health of the cell cultures. The system must incorporate an incubation system to provide the temperature (37°C) and an addition of HEPES to the media for the pH that cell cultures need to grow. In addition, the entire system must be sterilizable, to prevent contamination of cell cultures.
4. **The device must allow parallelization.** A 6-channel microfluidic chamber (ibidi® μ -Slide VI 0.4) will be used for cell cultures. The multi-pump system should be able to deliver media to 6 microfluidic chambers at the same time, so that all 6 experiments can be run in parallel. This will have two advantages: it can make comparison studies possible if different drug profiles are administered in side-by-side experiments simultaneously, and it can improve efficiency because more experiments are being run at once.
5. **The device must be user-friendly.** The user interface should be easy to navigate when users of the system are specifying the experiment parameters that they desire. The users will achieve this by working directly with the Arduino code, which will be well documented. Furthermore, setup of the pump system, any necessary maintenance, and the overall operation of the pump system should be simple for the end user.
6. **The device must be reproducible.** There are two different aspects to this objective. First, researchers such as those working in Mitchell Lab and those who wish to perform similar experiments should be able to easily fabricate additional pump units. Therefore, the responsibility lies with the design team to thoroughly chronicle the design and construction of the system in order to provide clear instructions to these audiences. Second, the device itself must be able to produce accurate results, such that if the same experiment is performed twice at two different times, the programmable pump should produce very similar results in terms of its own functionality.

These 6 objectives can also be seen in the concept map in Figure 7 below.

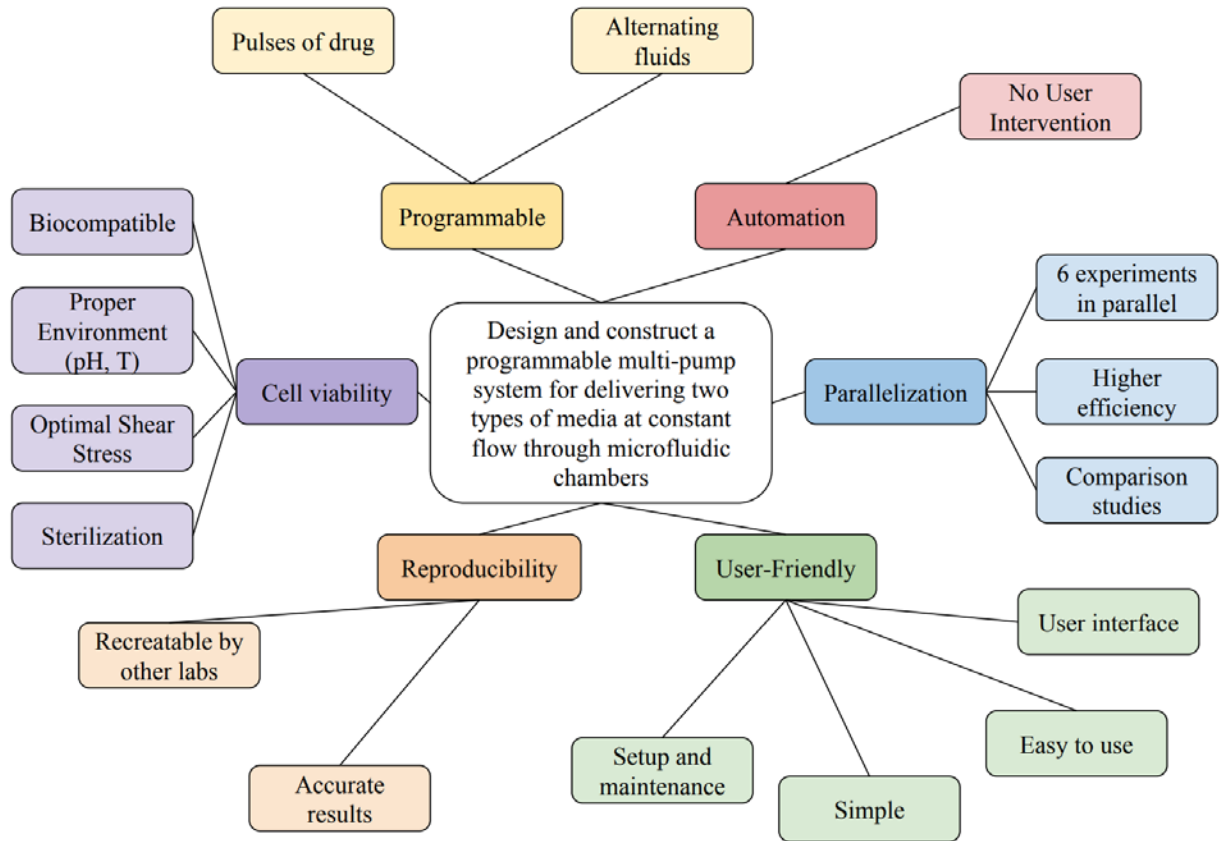


Figure 7: Concept map for visualization of objectives

To help prioritize these primary objectives, a pairwise comparison chart was also constructed. Each of the features was placed in both the leftmost column and the top row, as can be seen below in Table 2. If the objective designated in the leftmost column was deemed more important than the objective in the top row, a score of 1 was assigned; if it was determined to be less important, a score of 0 was assigned. Once the chart was completed, the scores were summed. The highest overall score indicated greatest importance, while the lowest overall score indicated least importance.

Table 2: Pairwise Comparison Chart for Prioritization of Objectives

Objective	Programmable	Automation	Parallelization	Cell Viability	Reproducibility	User-Friendly	Total Score
Programmable		0.5	1	0	1	1	3.5
Automation	0.5		1	0	1	1	3.5
Parallelization	0	0		0	1	1	2
Cell Viability	1	1	1		1	1	5
Reproducibility	0	0	0	0		0.5	0.5
User-Friendly	0	0	0	0	0.5		0.5

The results of the pairwise comparison chart helped the team realize that cell viability will be the most important feature of the design. If the cell cultures are not proliferating properly because they have inadequate growth conditions or are contaminated, then the pump itself will not have any purpose. Having a programmable and automated system are both equivalent and have the second most important attribute, as having a functional system that alternate two types of fluid and run through the long term experiments without user interactions are features of key importance to our client. Next is parallelization, which is not an indispensable feature for the pump functioning but is a requirement from the client to have 6 running experiments simultaneously in the microfluidic chamber. Lastly the two final features are reproducibility and user-friendly. The reproducibility of the device and its experiments is important because a device which produces inaccurate results each time an experiment is repeated will also be of little use because it is unreliable. The characteristic of being user-friendly will come next, since the purpose of the creation of this device is to make it simpler and easier for researchers to perform cell cultures in microfluidics within the context of their experiment constraints. This ranking demonstrates the project strategy is to first build a working system for one microfluidic chamber; upon success, the device can then be multiplexed for all microfluidic chambers with the user-friendly component.

3.2.2 Constraints

After the set of objectives was established, the design team compiled a set of constraints under two categories: technical and biological. The constraints are summarized in Table 3.

Table 3: Summary and description of constraints

Constraints		Descriptions
Biological	Cell Viability	<ul style="list-style-type: none"> • Samples need to survive the media fluid flow for the duration of the experiment. • Flow rate should be calculated depending on cells' limit to withstand shear stress
	Sterilization	<ul style="list-style-type: none"> • Samples cannot be contaminated throughout the duration of the experiment
	Biocompatible	<ul style="list-style-type: none"> • Microfluidic chamber should be biocompatible so it does not interfere with cell function
Technical	Media delivery	<ul style="list-style-type: none"> • Perfusion system should be able to deliver two types of media into each of the microfluidic chambers, at different drug profiles
	Arduino	<ul style="list-style-type: none"> • Compatible with software, stepper motor, and microfluidic chambers
	Limited Time	<ul style="list-style-type: none"> • Must be completed by end of C term (first week of March 2018)
	Cost of Materials	<ul style="list-style-type: none"> • \$250 per student + any additional cost covered by UMMS
	Size of device	<ul style="list-style-type: none"> • Device should fit on side stand of microscope incubator, with the microfluidic chamber itself placed inside the incubator.

Both biological and technical constraints are important for the outcome of the project. Regarding the biological constraints, the cells need to survive the entire experiment under a constant shear stress, while maintaining equal cell viability at the beginning and end of the experiment. In order to acquire the ideal values for shear stress, the tube dimensions and microfluidic chamber dimensions need to be considered. Sterilization also plays an important role in the biological category of the device design, since the tubing system and microfluidic chambers need to be sterile to avoid contamination once cells are cultured and media starts flowing. All the electrical components of the device cannot be sterilized but these would not be in direct contact with the cells, and thus should not affect the outcome of the experiments.

For the technical constraints, the device should be fully programmable by an Arduino and compatible with its software, in order to operate a stepper motor that controls the multi-pump

system that allows the different media types to flow into the microfluidic chambers. This device should be functioning by end of C term, which gives the design team approximately six to seven months to accomplish the project. This will also allow time for the implementation of the pump by performing biological experiments with cell cultures in D term. Additionally, the size of the device should fit the stand next to the microscope incubator, and tubes should be long enough to achieve ideal flow rate as well as reach the microfluidic chamber situated inside the microscope. The last constraint discussed is the cost of materials, for which the group has a total of \$500 and any of the available materials at the Mitchell Lab.

3.2.3 Functions

The multi-pump system designed and constructed by the team must incorporate various functions. Each of these functions will aid the team in accomplishing the objectives mentioned previously. Table 4 below contains a summary of the functions that the multi-pump system must be capable of performing, as well as possible means of achieving those functions:

Table 4: Functions-Means Table

Design Function	Possible Means of Accomplishing Function		
Delivers two alternative types of media	Two media reservoirs	Two syringe pumps in one unit	Y-connector
Control flow rate and shear stress	Low resistance of system	Dimensions of tubing (diameter and length)	Dimensions of microfluidic chamber to help minimize resistance
Maintains proper environment for cell cultures	Buffered media to maintain chemical environment (pH)	Microscope incubator to maintain temperature	Antibiotics in media to avoid contamination
Effectively remove media without damaging cells	Outlet tube long enough to reach disposal beaker	Media at the outlet collected in waste container	
Material of tubing	Polypropylene is biocompatible	Polytetrafluoroethylene (PTFE) / Teflon is chemically inert and flexible	Silicone + Platinum-cured minimizes chemical leaching
Sterility of the system	Autoclaved	Flush with ethanol	

As outlined in the initial client statement, the main goal of the multi-pump system is to deliver two types of media to cell cultures in microfluidic chambers. One type of media will be standard cell culture media, while the other type of media will be supplemented with drugs. The drug that will be used is vemurafenib. The team envisions the use of two media reservoirs, each of which is connected to the multi-pump system. The stepper motor will provide the power for fluid pumping. The two tubes for each of the media types will have a metal piece functioning as a connector and both will be inserted into an inlet plug that reaches the bottom of the inlet well of the microfluidic chamber.

It is important to consider not only the delivery of media, but also the method of media delivery. This refers to the fluid mechanics of the flowing media as it passes through both the tubes and microfluidic chamber. The multi-pump system must deliver media at a constant flow rate, in order to reduce pulses of pressure, attain constant, continuous flow throughout the experiment, and administer different doses of drugs. Furthermore, shear stress must be controlled and cannot be greater than the maximum amount the specific cell type can withstand. Another consideration which affects both flow rate and shear stress is the dimensions of tubing (namely diameter and length) and the dimensions of the microfluidic. Both of these parameters will be crucial for the fluid mechanics calculations of the project.

Since cell viability was ranked as the most important objective, the system must be capable of maintaining the proper environment for cell cultures. If the entire system was required to fit inside an incubator, as was initially thought, this would pose a size constraint on the multi-pump system. The first idea for evading this constraint was the use of buffered media, thereby sidestepping the need for the system to fit in the incubator. However, the Mitchell Lab possesses a microscope incubator inside which the microfluidic chamber will reside during experiments; the multi-pump system will remain outside the microscope incubator.

Another main function not previously described is that the system must have the ability to remove old media from the outlet of the microfluidic chamber. Since there will be continuous media flow through the chamber, there must be a way for the disposal of media once it has passed through. This could be achieved by a typical aspiration procedure which is used in standard cell culture laboratories. Another method would be to fabricate a PDMS plug at the outlet, in which a small metal connector attached to the tubing will be inserted. The fluid flow

would push the old media through the outlet tube and will be redirected to a waste disposal beaker residing inside the microscope incubator.

The materials of various components used in the device is important for biocompatibility. In particular, the choice of tubing will be essential. Common choices for microfluidic tubing are polypropylene due to its strength against chemicals across a range of pHs (The Basics of Microfluidic Tubing & Sleeves), and polytetrafluoroethylene (PTFE, or more commonly known as Teflon) for its ability to work in low-pressure situations as well as its appealing properties (non-toxic, stress resistant, chemically inert, non-porous, flexible, and transparent) (Microfluidic Tubing). Another choice for tubing would be platinum-cured silicone. This will allow for good gas permeability (CO₂ and O₂) as well as minimization of chemical leaching [40]. For the microfluidic chamber, the ibidi® μ -Slide VI 0.4 model is already prepared with surface treatments that promote cell adhesion, so it is already biocompatible. By choosing the correct materials, the multi-pump system can maintain the biocompatibility of the experiment.

Finally, proper sterilization techniques must be implemented into the system. One common method is autoclaving, which could be performed on each component of the system, especially since it will be modular. However, the design team and client agreed that the most promising approach would be to flush the system with ethanol (EtOH). The ideal way to incorporate this into the system would be to first disconnect the microfluidic chambers with cell cultures from the tubing, program and run the system to run EtOH through the tubes, then reconnect the microfluidic chambers once again.

3.2.4 Specifications

The design team needs to make sure the device maintains and simulates an accurate *in vivo* environment throughout the experiments. The design team has researched ideal shear stress that cells can withstand before reaching apoptosis. Fluid shear stress is one of the main physical forces cancer cells interact with when in contact with interstitial fluids and vascular circulation [41]. The known fluid shear stress cancer cells are exposed to interstitial fluid is within 0.1 dynes/cm². However, when exposed to blood circulation shear stress on cancer cell walls increases considerably to a range of 0.5 to 4 dynes/cm² in the venous circulation and from 4 to 30 dynes/cm² in the arterial circulation [41]. However, Tarbell et al., performed a theoretical model to estimate the shear stress over cell surface exposed to interstitial fluid, and concluded that for tumor, cancerous cells the shear stress impacting cells has the range of 0.038 dynes/cm²

to 1.2 dynes/cm² [11]. The design team decided to ideally program constant fluid flow below the limit shear stress of 1.2 dynes/cm², since Tarbell experiment results stated cancer cells exposed to a constant fluid shear stress of larger than the limit 1.2 dynes/cm² can affect the mechanobiology or the physiology of the cell [11]. For the purpose of these project, the team is only interested in performing experiments that would allow cells to survive the shear stress and stay attached to the surface of the microfluidic chamber. This shear stress is viable for the cellular experiments since it corresponds to a flow rate of 0.32 mL/min, as stated in ibidi® pump guide “Shear stress and Shear rates for ibidi μ-Slides”, which is a limit much higher than the flow rates to be tested (0.02 mL/min, 0,05 mL/min, and 0.1 mL/min) [42].

Other required specifications correspond to intervals/frequencies of drug dosage of two minutes or greater, and the number of pulses will depend on the duration of the experiment (between 1 to 24 hours). Additionally, temperature is another important specification to consider in order to maintain a high cell viability. The media being deliver to the cells should be at 37°C and properly buffered in order to maintain an ideal environment for cell proliferation.

3.2.5 Functional Blocks

Another useful way to visualize the required functions of the multi-pump system is by creating a Functional Block Diagram. The Functional Blocks for this project can be seen below in Figure 8.

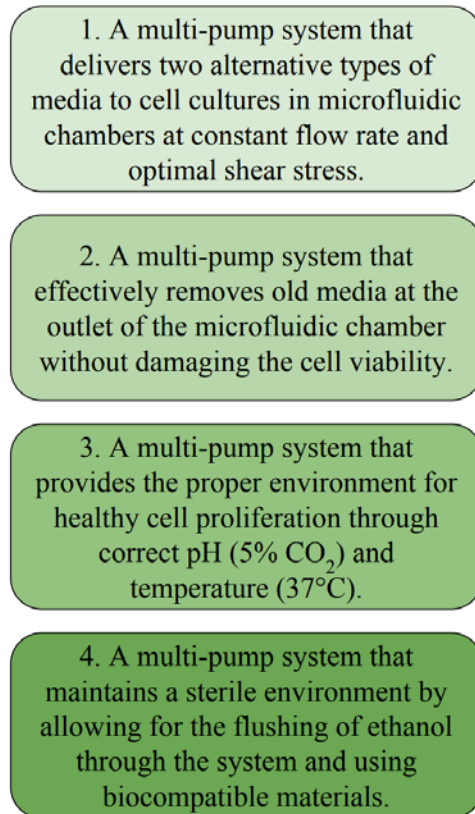


Figure 8: Functional Block Diagram

The Functional Block Diagram allows the design team to divide the functions into different categories; this helps with organizing ideas and setting incremental milestones. It could also aid the team to improve efficiency, because it may be useful to accomplish one function at a time before moving on to the next.

3.2.6 Design Requirements: Standards

3.2.6.1 Software Standards

Some standards must be incorporated into the design of the multi-pump system and mainly depend on the system's components. If the design team needs to custom engineer any part of the system, most likely by 3D printing, then it can be achieved using a computer-aided design (CAD) software like SolidWorks. In this case, the CAD files must comply with ISO standards, especially when specifying dimensions in the digital drawings. The ISO standard for CAD is number 35.240.10 [43].

The design team will be using computer and electric equipment extensively. Since an Arduino circuit board will be implemented, this is an important consideration to bear in mind. Additionally, most of the computational data analysis will be performed in MATLAB; this software was chosen because both design team members have previous experience using it, and because it is particularly suitable for calculations. In this case, the MATLAB Programming Style Guidelines must be followed when submitting the final MATLAB scripts used to generate the calculations. Arduino code will also be thoroughly documented according to common conventions, such as those in Javadoc and Doxygen, so that future users of the system will know how to program the pump according to their experiment parameters. Additionally, Arduino code documentation is provided in Appendix B. Compliance with the established standards set by each of these official, professional organizations will help the system achieve consistency, reliability, reproducibility, and safety.

3.2.6.2 Hardware Standards

In order for device to be approved, it is required to follow certain standards and regulations presented by the International Standard Organization (ISO). One of the regulations to consider is the ISO 7 (Class 10,000), which refers to the specific number of particles (or dust) found in a specific volume of air [44]. In this case ISO 7 is the most commonly used in lab ambients, especially in rooms containing Biosafety Cabinets (BSC). This standard is important for cell cultures, which will be prepared in BSCs.

The design team took in consideration the most important standards for cell culture devices, since these will be essential for the device success and cell survival. ISO 15190 refers to clinical laboratory testing and *in vitro* diagnostics test systems [45]. This is considered to be of high importance because it emphasizes the maintenance a safe working environment in a research laboratory. It consists of risk assessment for every task related to the testing performed and *in vitro* work with different types of organism or substances that might affect the performance of lab workers.

Regarding the cell culture itself, ISO 11737-2:2009 covers the sterilization of medical devices which have a large effect on cell culture performance [46]. Sterility of the designed device is essential for cell viability and survival. The device is required to be modular and detachable in order to be sterilized between experiments with 70% ethanol. Another standard of high importance to consider is ISO 10993-1, which covers the Biological Evaluation and Biocompatibility Testing of Medical Devices [47]. This standard also has a high degree of

importance due to the necessary biocompatibility required for successful cell culture experiments. The microfluidic chambers is, in this case, the key component of the system required to be biocompatible with the cell line used.

In terms of ethical considerations, there will be no human patients or testing on animals. The main consideration in this aspect will be to ensure that the multi-pump system is safe for the users throughout the experiment.

3.3 Revised client statement

Following meetings with the client and clarification of the overall project objectives, the design team was able to formulate a revised client statement. The statement was able to refine the research aims and direct the project towards the primary goal. The revised client statement is as follows:

Design and construct a programmable, modular, motor-controllable multi-pump system for delivering two types of media, one regular and the other supplemented with drugs, to cell cultures in a commercially available Ibidi® μ -Slide VI 0.4 6-channel microfluidic chamber. The system should be able to support these experiments in parallel, maintain the proper environment and sterilization for cell cultures, and supply media flow at the appropriate flow rate and shear stress for proper cell viability. The system must allow for the control of the extracellular environment by exposing the cells to different profiles of drugs over long-term experiments lasting between 1 to 24 hours, and must remove old media from the outlet of the microfluidic chamber without damaging the cells. The device will be used by the Mitchell Lab to explore cellular response to dynamic dosing regimens of drugs that are administered in pulses and oscillations.

This revised client statement highlights the key features requested by the client and the principal objectives of the project, as well as the problem, population, and outcome. The design team will aim to fulfill each of these requirements throughout the design process and for the duration of the project.

3.4 Management approach

The design team created a management plan in order to stay organized and accomplish all proposed tasks. This plan consisted of a timeline from A term to D term of the academic school year. The team decided to assign tasks on a weekly basis, intended to be accomplished by each of the weekly meetings with the project's advisors. The major milestones are divided by term. For A-term the team should complete the initial research and written drafts for Chapter 1 (September 18th), Chapter 3 (September 25th), and Chapter 4 (October 2nd). By the end of the week of October 9th, all preliminary designing should be completed. The literature review chapter is set to be started in A term but completed in B term, along with prototype building and testing. The team's goal is to complete design, construction, and testing of the multi-pump system by the end B term, on December 15th. While seemingly ambitious, the motivation behind this goal is because the team hopes to conduct experimental work with cells for the duration of C term, in order to study the effect that different profiles of drugs have on cellular response in microfluidic chambers. By C term, the team should also complete the report chapters on testing for the final design and the design verification and validation. Finally, for D term, the team will complete the concluding chapters and finish the final written report and presentation. The entire report should ideally be finished by the week of March 26th, which gives the team at least one month of time for editing. Preparing for Project Presentation Day on April 20th will ideally begin during mid-March, allowing the team ample time for practice.

In order to ensure that the project was organized, a Gantt chart was developed to create a projected timeline of the project in a more detailed manner. The Gantt chart was useful for setting incremental goals for the design team, thus helping to keep the project on track. It also helped to visualize the major milestones addressed previously. Located below (Figure 9) is the Gantt chart for terms A through D of the 2017-2018 academic year:

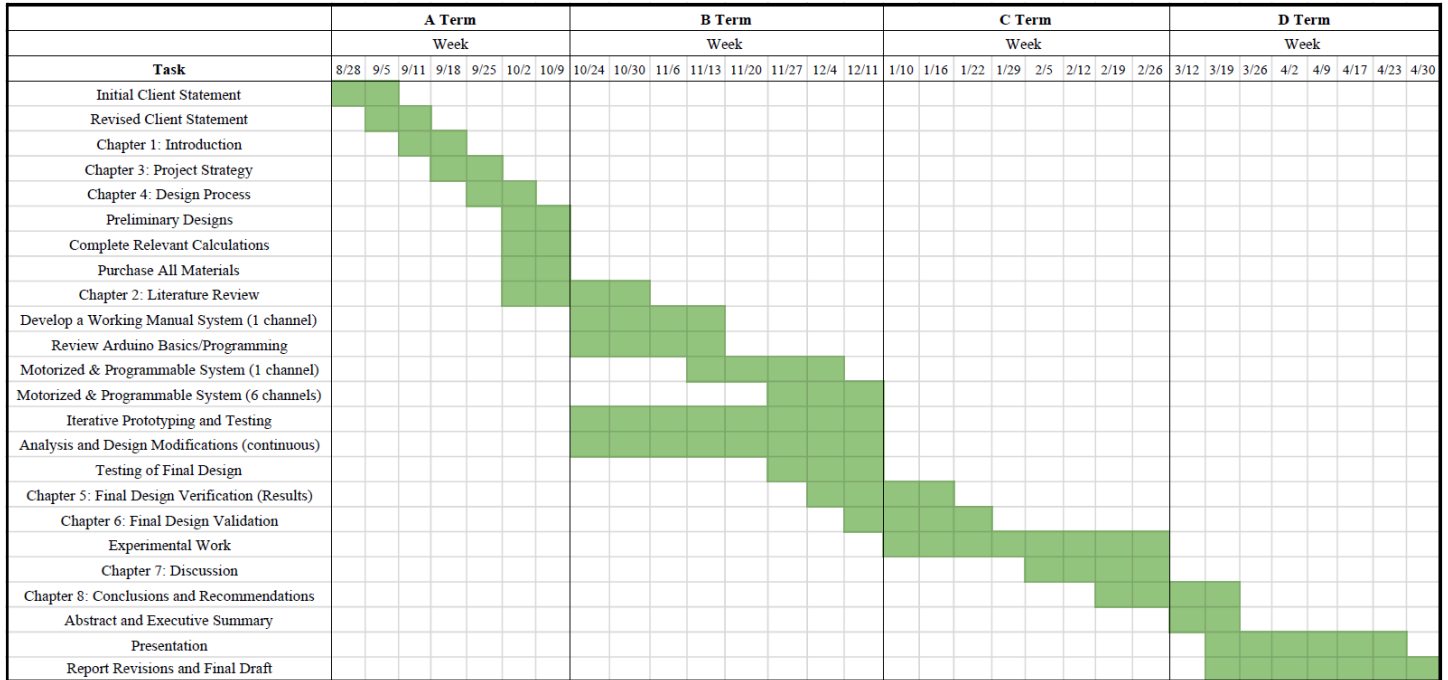


Figure 9: Gantt Chart for Project Timeline

3.4.1 Financial Statement

The team is required to work under a financial limit. The team’s budget amounts to \$500 given by the Biomedical Engineering department at WPI, with any additional expenses sponsored by Mitchell Lab. This is one of the main reasons the pump will be custom-engineered in the lab, with help from the MakerSpace in UMMS’s Program in Systems Biology. Regarding the other finances, the team must cover other parts required to construct the multi-pump system. The materials provided by UMMS are cell culture media, microfluidic chambers, and any other equipment that is available at Mitchell Lab.

Chapter 4: Design Process

In the following sections the team will discuss the needs and wants of the multi-pump system. It will also describe both the conceptual and final designs of the pump, as well as its functions and specifications.

4.1 Needs Analysis

The design team determined the needs and the wants of the multi-pump system based on the final objectives and revised client statement discussed in Chapter 3. Based on this, a list of general requirements was created and, and each of those requirements was classified as either a need or a want. The requirements that are critical to the functionality of the multi-pump system were classified as needs. On the other hand, the requirements that are desirable for the multi-pump system but are not necessary for its success were classified as wants. This means that the most important objectives were considered requirements and placed under the “Needs” category, while those with lesser importance were placed under the “Wants” category. Table 1 contains a summary of all needs and wants, with their descriptions.

Table 5: Needs and Wants of the Multi-Pump System

Needs	Description
Programmable/Automated	The system must be able to run by itself for experiments lasting between 1 and 24 hours, with minimal human intervention. Ideally, it must be compatible with an Arduino microcontroller.
Flow Rate Control	The system must be able to control the flow rate at which it delivers media to the microfluidic cell cultures, so as not to perturb the cells with shear stresses that exceed their threshold. This will prevent apoptosis due to excessive shear stresses. Less than 20% variation within the constant flow rate.
Temperature Control	The system must provide the ideal temperature of 37°C, which is required for cell function and viability.
CO ₂ Control	The system must provide the ideal pH via 5% CO ₂ , which is required for cell function and viability.
Parallelization	The system must be able to run 6 independent experiments in parallel (i.e., one experiment is running in each channel simultaneously).
Sterility	The system must be compatible with common sterilization

	techniques, primarily by disconnecting the system and spraying it with 70% ethanol (EtOH).
Size	The system must be able to fit inside the Zeiss microscope incubator in Mitchell Lab.
Two Types of Media	The system must be able to deliver two types of media: one standard media, and the other media containing drugs
Imaging	The system must be compatible with a microscope that has excellent live-cell imaging capabilities.
Wants	Description
Gravity-based pump system	The design team initially wanted the pump to be gravity-based, decided over other options primarily due to pricing, simplicity, and client request.
Open System	The design team wanted the system to be an open system, and all media used through microfluidic chamber would then be disposed of in a waste container.
Tubing size	The design team wanted the tubes to have a smaller inner diameter in order to fit 2 tubes into inlet of the microfluidic chamber and to reduce flow rate.
Multiple Types of Experiments	The system should be able to perform 3 different types of biological experiments related to the effect of dynamic dosing on cellular signaling.
LCD User Interface	The system should have a user-friendly interface for controlling the parameters of the biological experiments that are performed by the multi-pump system, possibly by implementing an LCD Display with control buttons.

4.1.1 Design Needs

The needs of the design are all features of the multi-pump system that were deemed essential for its success. In order to make sure the device was fully functional according to the client statement, it was very important to ensure that the pump could maintain high cell viability. This includes multiple components, namely the control of flow rate, temperature, CO₂, and sterilization, all of which are essential parts of standard cell culture protocol. The cells require media to survive, and the flow of media is required to be programmable and automated in order to run experiments as long as 24 hours without the need for human interaction. The control of

flow rate should be done to have less than 20% variation within that constant fluid to reduce pulses of pressure, which is an acceptable limit for DIY syringe pumps. It is also required to run 6 parallel experiments with independent conditions among each of those experiments. In addition, the size of the system must ultimately allow it to fit within the microscope incubator. All of this system requires to be compact to be standing next to the incubators and tubes connected to the system reach the microfluidic chamber that stays in the incubator during experiments.

4.1.2 Design Wants

The wants for this project were the components of the system that would improve the design outcome, but that were not required to guarantee success of the device. The design team considered using a gravity pump instead of peristaltic pump or syringe pump based on previous research done. The gravity pump resulted the most adequate for the experiment as well as the most affordable. The team also decided to have an open system in which all the media that passes through the microfluidic chambers go to waste and are not recycled. Most of the design wants have been decided through research.

The most important of these wants, however, was enabling 3 specific types of biological experiments through implementation of the final pump design. The client requested that the pump be able to support 3 different types of experiments. A summary of these experiments can be seen below in Table 6. Following the table, each of the experiments will be described in detail.

Table 6: Summary of the 3 different experiment types

Experiment	Description	Example	Parameters
Pulse Experiment	Drug will be administered in "On" and "Off" intervals for a specific duration	e.g. 2 minutes regular media, 2 minutes media with drugs	<ul style="list-style-type: none"> ● "On" Duration ● "Off" Duration ● Flow Rate ● Experiment Duration
Constitutive Level	Drug will be administered in a single-step experiment at a certain concentration, which will be maintained throughout the duration of the experiment	e.g. 30% drug concentration for an experiment duration of 24 hours	<ul style="list-style-type: none"> ● Concentration ● Flow Rate ● Experiment Duration
Slope Experiment	Drug will be administered in increasing concentrations, so as to achieve a slope profile, until it reaches a maximum concentration in a given amount of time T	e.g. reach a drug concentration of 60% in 12 hours	<ul style="list-style-type: none"> ● Max Concentration ● Time T ● Flow Rate ● Experiment Duration

4.1.2.1 Experiment 1: Pulse Experiment

For the first experiment, drugs will be administered to the cell cultures in pulses (see Figure 10). These pulses could be delivered at many different frequencies. The starting concentration of drug can be mixed to the desired concentration before the start of the experiment, since the concentration of the drug itself remains constant throughout the experiment. The user will input the duration of the "On" interval, which is the length of time for which drugs will be administered, and the duration of the "Off" interval, which is the length of time for which normal media will be administered. The two intervals can be equal in value, such as an example experiment in which regular media is applied for 2 minutes, then drug is applied for 2 minutes, in alternating cycles. Alternatively, the two intervals can have different values, such as an example experiment in which regular media is applied for 3 minutes, then drug is applied for 1 minute, in alternating cycles. The user will also need to specify a flow rate, which will dictate the speed of the pump (i.e. the length of delay between each step of the motor), as well as the experiment duration (so the experiment will end when desired). The user will input

each of these parameters directly in the Arduino code that corresponds with Experiment 1 (see Appendix A).

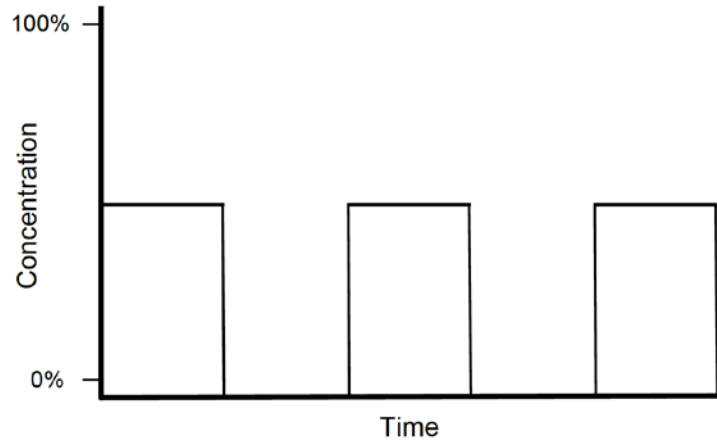


Figure 10: Graphical representation of the pulse experiment

4.1.2.2 Experiment 2: Constitutive Level

For the second experiment, the drug will be administered at a specified concentration and at a constant rate for the duration of the experiment. The user will input the desired drug concentration, the flow rate, and the duration of the experiment directly into the Arduino code. As an example, the user could achieve an experiment in which a 30% drug concentration is supplied to cell cultures at a flow rate of 0.02 mL/min for an experiment duration of 24 hours.

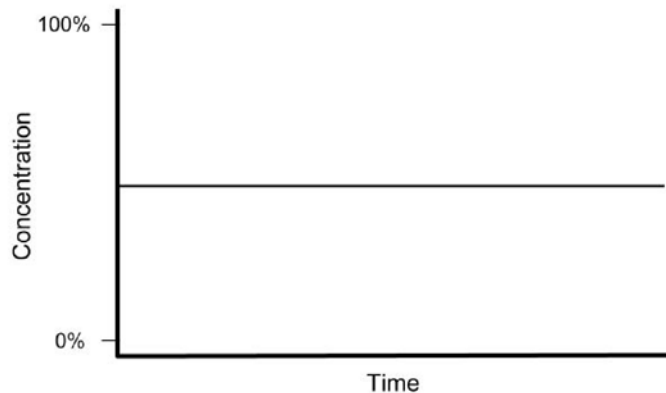


Figure 11: Graphical representation of the constitutive level experiment

4.1.2.3 Experiment 3: Slope Experiment

In the third experiment, drugs will be administered in a slope profile. The user will input the maximum concentration to be achieved throughout the experiment, and the time it takes for maximum concentration to be reached. The drug concentration will increase at a constant rate until it reaches the maximum concentration in the allotted time. The flow rate and experiment duration must also be specified. For example, the drug concentration could steadily increase during the experiment so that it reaches a final maximum concentration of 60% in a total of 12 hours.

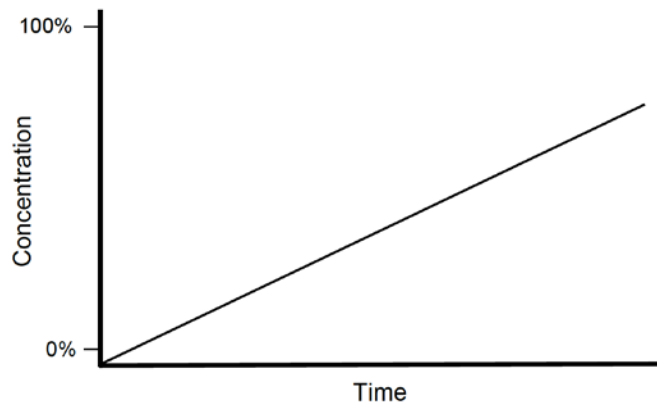


Figure 12: Graphical representation of the slope experiment

Out of these 3 experiment types, the main focus rested on the first (pulse) experiment. However, all three were ultimately investigated.

4.1.3 Needs and Wants Design Matrix

After defining the needs and wants for the design, a design matrix was created. A design matrix is used to determine which needs and wants influence each of the design considerations of the multi-pump system. Table 7 shows the complete design matrix for the needs and wants. The needs and wants are listed in the top row, while the design considerations are listed in the leftmost column. Each “X” in the table’s cells demonstrate that the particular need or want will influence the specified design consideration. The rightmost column indicates the total number of needs and wants that have an impact on the various design components. This matrix was ideal for understanding how the specifics of the design were influenced by the needs and wants of the system, and it was helpful for the design team to refine the requirements of the final design.

Table 7: Design Matrix of Needs and Wants

	Needs	Programmable Automated	Flow Rate Control	Temperature Control	CO2 Control	Parallelization	Sterility	Size	Two Types of Media	Imaging	Wants	Gravity-based Pump System	Open System	Tubing Size	Multiple Types of Experiments	LCD User Interface	Total
System Dimensions								X		X		X		X	X		5
Heating Source				X			X					X	X				4
CO2 Source					X		X					X	X				4
Media Delivery			X				X		X			X	X	X	X		7
Media Removal			X						X			X	X	X			5
Tubing			X				X		X			X	X	X			6
Plug Design							X		X				X	X			4
Arduino		X	X			X			X			X			X	X	7
Microscope Incubator				X	X		X	X		X		X					6
Multi-Channel Microfluidic Chamber						X	X		X			X			X		5

4.1.4 Physical Limitations

In order to build the device, some physical limitations had to be considered. These limitations imposed some constraints on the pump's design. Table 8 summarizes the physical constraints that the design team considered with quantitative values where applicable/available.

Table 8: Physical Constraints of the Design

Specification	Acceptable Range
Tube Diameter (D)	1/16 in < D < 1/50 in
Shear Stress	< 1.2 dynes/cm ²
Size of the pump	Must fit within the Zeiss microscope incubator chamber
Weight	Must minimize weight for easy transport and set up of experiments

The team decided to consider these limitations based on their imposed constraints on the device. The tube diameter was initially proposed to be 1/16 inches, but further research of the Hagen-Poiseuille equation indicated that a smaller tube diameter would help to achieve a slower flow rate due to the direct relationship between the two variables (see Section 4.2.3 for more details). Because the multi-pump system was required to deliver media at very low flow rates to accommodate cell cultures, the tube diameter was ultimately decreased to 1/50 inches, or 0.02 inches. These smaller dimensions also allowed two tubes to fit inside the inlet of the microfluidic chamber, which is necessary for deliver of two different media types. . The shear stress must be less than 1.2 dynes/cm², since that is the maximum level of stress cancer cells can withstand *in vitro* without losing function and exhibiting apoptosis [11]. Other physical constraints include the size and weight of the pump, both of which should be reduced as much as possible to facilitate the process of setting up an experiment and transport in case some fixing is needed.

4.2 Conceptual Designs

4.2.1 Assessment of Design Components

Evaluating design elements was an important component for deciding on the final design of the system. The necessary design elements were discussed in detail, and each have a list of possible means for achieving that particular design element. Once the advantages and disadvantages were considered for each approach, the method of choice was integrated into the final conceptual design in order to achieve the design criteria.

The system must be able to provide the proper environment for microfluidic cell cultures, whether directly or indirectly. This means that the cells must reside in a pH (around 7.2-7.4) and temperature (approximately 37°C) which closely resembles that of the cells' native *in vivo* environment. Media could contain HEPES buffer or sodium bicarbonate buffer, which maintain the pH at this ideal range. Since cells would be in contact with unsterile environment, Penicillin-Streptomycin (Pen Strep) was also added to the media in order to prevent potential contamination by microorganisms. On the other hand, while a standard incubator would provide the ideal cell culture environment, it would not accommodate the imaging needs of the biological cellular signaling experiments. Running the experiments in a microscope incubator would allow the syringe pump units to be placed on a stand adjacent to the microscope, with the microfluidic

chamber located inside and the pumps located outside. This has the added feature of allowing for live cell culture imaging because of its connection to a microscope. Although these devices are expensive, Mitchell Lab already has one in their workspace which would be at the design team's disposal.

Table 9: Pros and Cons for Achieving Optimal Cell Culture Environment

Cell Culture Environment		
Possible Means	Pros	Cons
Buffered Media	<ul style="list-style-type: none"> • DMEM contains nutrients for cellular environment • HEPES buffer maintains ideal pH (7.2-7.4). • Penicillin-Streptomycin prevents contamination 	<ul style="list-style-type: none"> • Cells will be at room temperature (25°C)
Standard Incubator	<ul style="list-style-type: none"> • Maintains both ideal pH and temperature 	<ul style="list-style-type: none"> • Imposes a size constraint on the system • Does not allow for live-cell imaging during the experiment
Microscope Incubator	<ul style="list-style-type: none"> • Maintains both ideal pH and temperature • Does not impose a size constraint on the system • Pump can be located nearby on exterior • Allows for live cell imaging 	<ul style="list-style-type: none"> • Expensive

The different types of pumps that are known to have been used in automated cell cultures each have their own advantages and disadvantages. For more in-depth analysis and visuals of these pump types, see Chapter 2: Literature Review. In short, syringe pumps allow for precise control of fluid flow but can introduce fluctuations which manifest into shear stresses applied to the cells [4] [48]. Peristaltic pumps can allow for media recirculation and bidirectional flow but only supply pulsatile flow [4]. Hydrostatic pumps can maintain a continuous fluid flow, but exhibit a gradual decrease in flow rate as the fluid volume (and therefore, hydraulic pressure) drops [4][13]. For the outlet of the microfluidic chamber, either a syringe pump or peristaltic pump could be viable options for removing media, if needed.

Table 10: Pros and Cons for Type of Pump

Pump Type		
Possible Means	Pros	Cons
Syringe Pump [4][48]	<ul style="list-style-type: none"> ● Precise control of fluid flow ● Reliable (used by many labs and in many experiments) 	<ul style="list-style-type: none"> ● Can introduce ripples, fluctuations, and shear stress ● May need to replenish media supply ● Expensive
Peristaltic Pump [4]	<ul style="list-style-type: none"> ● Bidirectional flow ● Allows for media recirculation, if desired ● Cheaper alternative 	<ul style="list-style-type: none"> ● Only provides intermittent, pulsatile fluid flow
Hydrostatic Pump [4][13]	<ul style="list-style-type: none"> ● Maintains continuous fluid flow ● Simple mechanics ● Less expensive 	<ul style="list-style-type: none"> ● Fluid flow rate can decrease as volume of media decreases (therefore, flow rate is not constant)
Pressure driven pump [19]	<ul style="list-style-type: none"> ● Stable and constant flow ● Achieves low flow rates ● Rapid switches between reservoirs 	<ul style="list-style-type: none"> ● High prices ● Delivers media in form of flow rate

Per the client's request, a stepper motor was implemented as the driving force of the pump. The stepper motor is an appealing choice because of the fact that it is compatible with a microcontroller, which will also be implemented into the system. Furthermore, since it provides a certain number of discrete steps over a period of time, it can control both position and speed. This allows more accurate control of the fluid flow rate that is delivered by the syringe pump. Since it can move very quickly, the motor will be very useful in changing the type of media that is passed through the system. Its drawbacks are that high speeds must be reached gradually because the motor may stall if accelerated too quickly; however, this does not affect this system.

Table 11: Pros and Cons for Stepper Motors

Motor		
Possible Means	Pros	Cons
Stepper Motor [49]	<ul style="list-style-type: none"> • Can be controlled directly by microcontrollers (e.g. Arduino) • Can be controlled precisely (one step for each electric pulse given) • Can move very quickly (one step every few milliseconds) or very slowly, depending on the needs of the experiment 	<ul style="list-style-type: none"> • Must accelerate gradually to reach high speeds • May stall if stepping rate is increased too quickly

The client also proposed two different options for controllers: Arduino and Raspberry Pi. Both systems are inexpensive and compatible across different platforms. The Raspberry Pi system uses a Linux OS and is essentially a mini-computer, which means it has a larger capacity to run multiple programs at the same time. Because of this fact, it is more complex to use. On the other hand, the Arduino is a simple microcontroller with open-source software that can run a limited number of programs at once. While the Raspberry Pi system does have extra capabilities, an Arduino was chosen for the microcontroller. Rationale for this decision is two-fold. First, the design team has previous experience using an Arduino but not Raspberry Pi, and second, the simple Arduino is sufficient to accomplish the tasks of this multi-pump system.

Table 12: Pros and Cons for Controller

Controller		
Possible Means	Pros	Cons
<p>Arduino [50]</p>	<ul style="list-style-type: none"> • Simple • Inexpensive • Open-source • Cross-platform • Design team members have previous experience using it 	<ul style="list-style-type: none"> • Can run limited number of programs at once
<p>Raspberry Pi [51]</p>	<ul style="list-style-type: none"> • Inexpensive • Cross-platform • Uses a Linux OS • Can run multiple programs at once 	<ul style="list-style-type: none"> • More complex to use (mini-computer) • Would require extra time to learn

The initial proposed design incorporates the design elements selected from the tables above and can be seen below in Figure 13. This was the team’s preliminary design. Most notably, this design implements a gravity-driven pump because the client had proposed the use of gravity pumps at the start of the project.

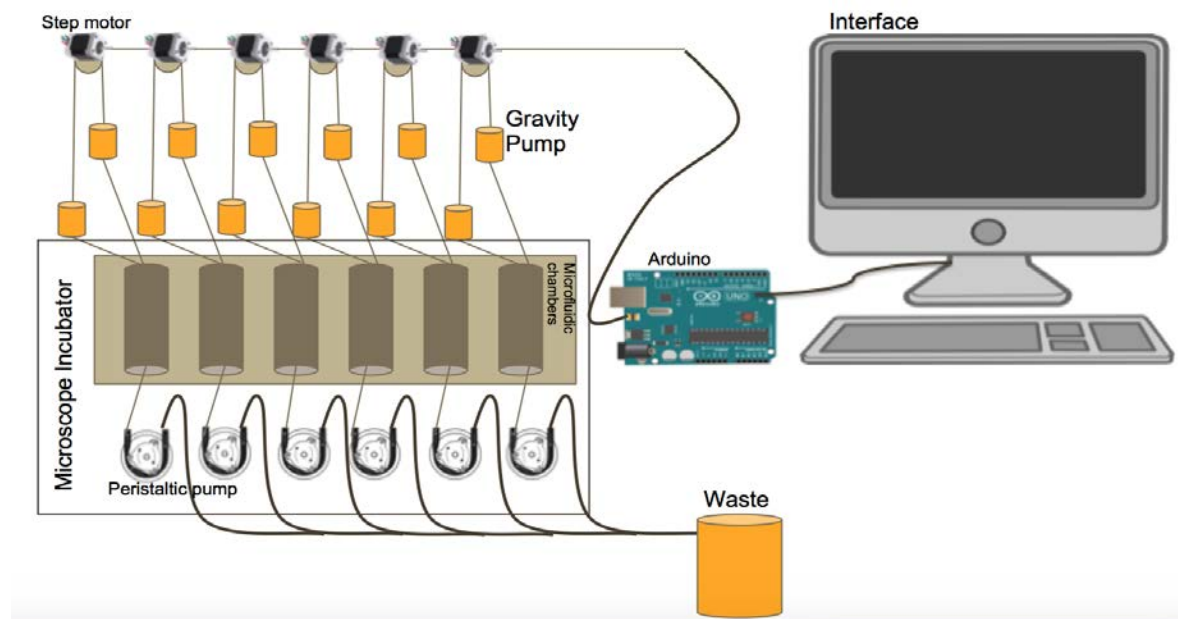


Figure 13: Preliminary Design

Two reservoirs of media are placed around a pulley as shown. The system will have an Arduino connected via USB to an interface on which the program controlling the motors will be running. The Arduino will control the motor, whose steps will turn the pulley the appropriate amount for adjusting the height of the media reservoirs. The type of media (regular vs. drug-supplemented) and the rate at which that media is delivered to the microfluidic chambers will be determined based on the height of the reservoirs as the pulley turns. The main principle behind this concept is that if one media reservoir is situated at a more elevated height than the other media reservoir, then the media in the first reservoir will flow while the media in the second reservoir will not, and vice versa. The microfluidic chambers containing the cell cultures will be located inside the microscope incubator. Lastly, the peristaltic pump will be removing media from the chamber outlets and disposing of the media in a waste container.

4.2.2 Feasibility studies

Feasibility of the multi-pump system will be mainly determined by cell viability. The accuracy with which the Arduino controls the motor will dictate how fast the motor itself will turn, and the speed of the motor will in turn affect the flow rate of the pumped fluid. If the flow rate is higher than that which the specific cell type can withstand, then it could generate a strong shear stress that will be deleterious to the cells. The design team planned to test a range of different flow rates when pumping media to the cell cultures. To determine cell viability, a simple live cell count would be performed at the beginning and end of each experiment. The difference in live cell numbers would indicate how many cells were washed away due to the shear stress or how many had undergone cell death.

4.2.3 Experimental parameters and design calculations

Many of the design calculations that necessary for this project were related to fluid mechanics. First, the Reynolds number of the fluid was an important property to consider. Reynolds number (Re) is a dimensionless parameter whose magnitude helps to determine the type of flow taking place [52]. As in Figure 5, if Re is less than 2000 ($Re < 2000$), flow is laminar; if Re is between 2000 and 4000 ($2000 < Re < 4000$), flow is transitional; and if Re is greater than 4000 ($Re > 4000$), flow is turbulent [52].

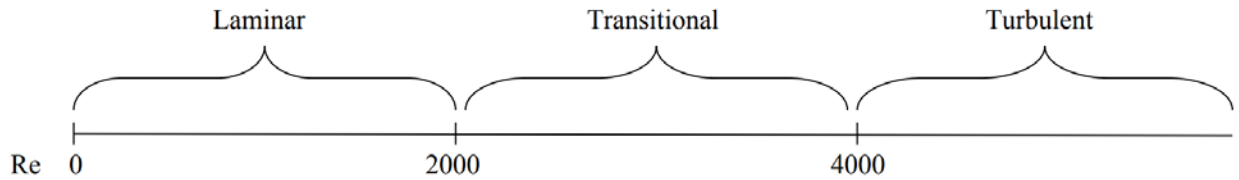


Figure 14: The magnitude of Reynolds number affects the type of fluid flow.

Since laminar flow is streamlined, organized, and doesn't involve any disturbances in fluid flow, this is the flow type the multi-pump system should achieve, both inside the tubes and the microfluidic chamber [52]. Therefore, the Reynolds number of fluids within the system must be less than 2000 at all times. The equation for Reynolds number is:

$$Re = \frac{\rho v D_h}{\mu}, \quad \text{Equation 4.1}$$

Where ρ is fluid density (kg/m^3), V is average fluid velocity (m/s), D_h is the hydraulic diameter of the chamber (m), and μ is fluid viscosity ($\text{Pa}\cdot\text{s}$) [52]. As mentioned previously, the hydraulic diameter can be calculated determined by the geometry of the vessel, which in most cases will be based on if the vessel is circular or rectangular. The density and viscosity of cell culture media can be found in the literature (but can be approximated as the density and viscosity of water), while the velocity of fluid flow and diameter of the tubes must be determined in the laboratory.

Fluid flow within small scale vessels like microfluidic chambers is almost always laminar [14]. Furthermore, if two fluids are delivered to the microfluidic cell cultures simultaneously, mixing between those fluids within the chamber will not occur except if diffusion also occurs [14]. This is particularly relevant if mixing of two different media types must be achieved by the pump system.

Hydrostatic pressure will be the main driving force for fluid flow for the gravity-based pump, which the design team was looking to implement initially. This will depend on the density of the fluid (ρ), acceleration due to gravity (g), and vertical distance between the media reservoir and the point at which it will enter the microfluidic chamber (h). The equation modeling hydrostatic pressure is the following [51]:

$$\Delta P = \rho g h \quad \text{Equation 4.2}$$

Once calculated, the hydrostatic pressure can indicate how much pressure the fluid is exerting in the tubes; the actual pressure within the microfluidic chamber may be different.

The next important consideration is the Hagen-Poiseuille equation, which is:

$$Q = \frac{\pi R^4 \Delta P}{8 \mu L},$$

Equation 4.3

Where Q is volumetric flow rate (m³/s), R is radius of the tube (m), ΔP is change in pressure (Pa), μ is fluid viscosity (Pa*s), and L is length of the tube (m) [51]. The Hagen-Poiseuille equation only holds true for laminar flow, which is yet another reason why it is important to make sure Reynolds number is less than 2000 for fluid flow pumped by the system [52]. Equation 4.3 applies for a circular cross-section, and therefore applies to the tubing of the system. Once the tube dimensions are decided upon, and once the pressure of fluid from the pump is determined by using Equation 2 above, the flow rate can be calculated. The volumetric flow rate can also be calculated using the following simple equation:

$$Q = \frac{\Delta V}{\Delta t}$$

Equation 4.4

Where the volumetric flow rate is calculated by finding the change in volume (m³) over the change in time (s).

The resistance of a system can be found by the equation:

$$R = \frac{\Delta P}{Q}$$

Equation 4.5

where R is the fluidic resistance (Pa*s/m³), ΔP is the change in pressure (Pa), and Q is the flow rate (m³/s). For a circular tubing geometry, the resistance can be calculated with the equation:

$$R = \frac{8 \eta L}{\pi r_0^4} [53]$$

Equation 4.6

where R is the fluidic resistance (Pa*s/m³), η is the fluid viscosity (Pa*s), L is the length of the tube (m), and r₀ is the radius of the tube's interior (m). For a rectangular microchannel, the resistance can be calculated with the equation:

Equation 4.7

$$R = \frac{12\eta L}{wh^3} [53]$$

where R is the fluidic resistance (Pa*s/m³), η is the fluid viscosity (Pa*s), L is the length of the channel (m), w is the width of the channel (m), and h is the height of the channel (m). Therefore by rearranging Equation 4.5 to solve for Q and plugging in Equation 4.6, the flow rate for the rectangular profile of the chamber is:

$$Q = \frac{\Delta P}{R} = \frac{\Delta P wh^3}{12\eta L}$$

Equation 4.8

With the determination of the flow rate, the shear stress can be calculated. As mentioned previously, cells are very sensitive and can die if the shear stress exerted upon them is too great. With this in mind, the shear stress for a circular vessel can be solved for as follows:

$$\tau_{wall} = \frac{8\mu Q}{2\pi R^3} = \frac{32\mu Q}{\pi D^3}$$

Equation 4.9

where τ is shear stress (Pa), μ is fluid viscosity (Pa*s), Q is volumetric flow rate (m³/s), R is radius of the tube (m), and D is the diameter of the tube (m) [51]. This is the shear stress at the wall of the tubes. For the rectangular shear stress in the microchannel, the quantity can be calculated from the following:

$$\tau_{wall} = \frac{6\mu Q}{wh^2} [54]$$

Equation 4.10

where τ is shear stress (Pa), μ is fluid viscosity (Pa*s), Q is volumetric flow rate (m³/s), w is the width of the channel (m), and h is the height of the channel (m).

Calculations for the resistance and analysis of flow rate and shear stress can be found in Sections 4.4.1.2 and 4.4.1.3. Please refer to these sections for analysis of the initially proposed gravity-driven system.

4.2.4 Computational Analysis

The main analytical software used in the design process was MATLAB from MathWorks®. This software was an extremely valuable tool in both analyzing and visualizing data. MATLAB allowed the design team to model different relationships between variables. It also assisted the design team in large amounts of computation, particularly in the modeling of

fluid flow by Torricelli's Law. MATLAB therefore provided an easy, accurate, and convenient way for multiple calculations that would otherwise be completed by hand.

MATLAB was also extremely useful in characterizing flow rate of the multi-pump system, both in performance testing and in biological testing. For much of this analysis, either ImageJ or FIJI softwares were used to determine "regions of interest" (ROIs) in particular regions of the microfluidic chamber through time-lapse microscopy. The pixel intensity was then measured for all of these ROIs across all timepoints. MATLAB was then used to plot the resultant data for visualization and characterization of the flow rate. Similar analysis using FIJI and MATLAB were applied for ERK dynamics analysis in the biological experiments.

4.3 Alternative Designs

The team proposed alternative designs for gravity-based pumps. More specifically, two different syringe pumps were constructed. Syringe pumps were the choice for alternates because of their easily controllable flow rates. Additionally, they are considered very reliable devices since most laboratory settings already run biological experiments using syringe pumps; in other words, syringe pumps are established devices in scientific research. However, commercially available syringe pumps are found within a range of expensive prices that exceed the team's budgets. Therefore, do-it-yourself (DIY) syringe pumps were selected as the most suitable alternative device, as an option described in Chapter 2: Literature Review.

The Program in Systems Biology at UMass Medical School provides a MakerSpace with all the essential equipment needed to build the basic components of the syringe pump, including both a 3D printer and a laser cutter. For this reason, the team evaluated two options: laser cut syringe pumps and 3D printed syringe pumps.

The first alternative pump constructed was the laser cut syringe pump, with the initial design coming from an open-source website. More specifically, the syringe pump replicated here can be found at Instructables.com [55]. The pieces required for this pump were laser cut from 16"-by-12" boards of acrylic using the laser cutter in the MakerSpace. All other necessary supplies were purchased from Home Depot. The very first model, built exactly as instructed from the Instructables website, can be seen in Figure 15 below.

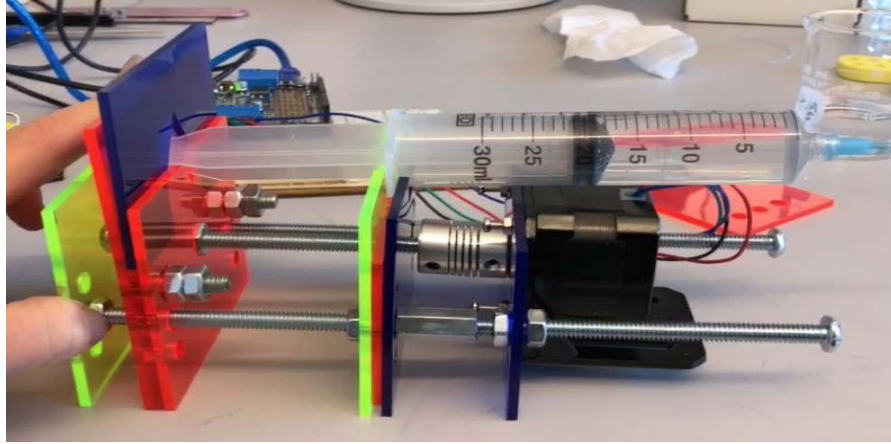


Figure 15: Initial model (Model 1) of the laser cut syringe pump.

Another alternative device was the 3D printed syringe pump, which was another open-source model built based resources by Hackaday [56]. The MakerSpace was used to 3D print the main pieces of the syringe pump. The additional pieces needed to finish building one single syringe pump were ordered online. The assembly of the pump was done as recorded in Appendix A: User Manual. The final assembly can be seen in Figure 16 below.

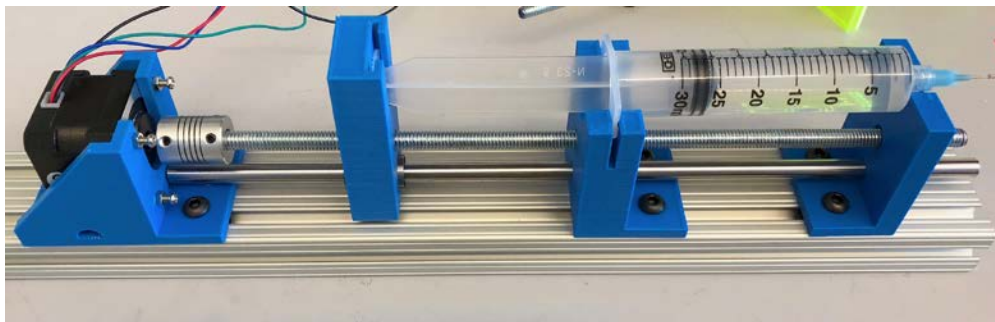


Figure 16: Initial model of the 3D printed syringe pump.

4.4 Final Design Selection

The design team evaluated each of the 3 proposed designs in turn. In order to compare the designs and select the most suitable option that meets all requirements, the main need that was tested was the flow rate. Achieving a low flow rate that allows 30 mL of media to last for a 24-hour long experiment as required by our client, and that at the same time generates a shear stress which cells are able to withstand, will define the most suitable design to be selected. The contents of this section outline the design process involved in constructing the ideal pump system for meeting the needs of the client, and the decision process when selecting the final design.

4.4.1 Gravity-based Pump

Since the client initially suggested the implementation of a gravity-based pump to deliver media to the cell cultures in microfluidic chambers, this was the first type of pump tested. There were various phases associated with this type of pump.

4.4.1.1 Flow Rate Testing with Torricelli's Law

To model the draining of media from a syringe, the draining tank model, which applies Torricelli's Law in Hydrodynamics, was used. It begins with the following proposition: suppose there is a cylindrical tank from which water drains through a hole under the influence of gravity, such as the one displayed in below.

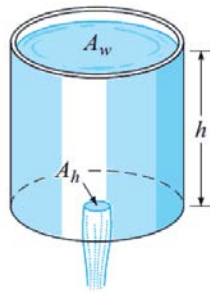


Figure 17: Draining Tank Model for Torricelli's Law in Hydrodynamics [54][55]

where A_w is the cross-sectional area of the cylinder, A_h is the cross-sectional area of the hole, and h is the height of the water. The circular cylindrical tank models the syringe, and the hole models the nozzle of the syringe. An important assumption of this law is that viscosity (or friction on the nozzle walls) is negligible.

Torricelli's Law was physically modeled by filling an open syringe with water, then recording the time it took for the syringe to empty, in 5 mL increments. The goal of this testing was to get a preliminary idea for the magnitude of the flow rate of water that is free falling from a syringe under the sole force of gravity. The test was performed for 5 trials, after which the average time was calculated followed by the volumetric flow rate. The raw data for this first syringe experiment, in which the regular nozzle of the syringe was used as the outlet, can be seen below in Table 13.

Table 13: Raw data for syringe experiment, using the normal/regular nozzle

Normal Nozzle							
	Trial 1	Trial 2	Trial 3	Trial 4	Trial 5	Average	
Volume (mL)	Time (s)	Time (s)	Time (s)	Time (s)	Time (s)	Time (s)	Flow Rate (mL/s)
30	0	0	0	0	0	0.00	3.18
25	1.42	1.67	1.52	1.56	1.69	1.57	2.88
20	3.21	3.37	3.31	3.23	3.41	3.31	2.62
15	5.12	5.33	5.18	5.15	5.3	5.22	2.26
10	7.44	7.33	7.36	7.42	7.57	7.42	1.77
5	10.31	10.14	10.18	10.22	10.41	10.25	1.12
0	14.56	14.58	14.68	14.65	15.08	14.71	0.00

Graphical results were then obtained by using the equation associated with Torricelli's Law to interpret the raw numerical collected results. The following equation will denote the change of volume of water over time:

$$\frac{dV}{dh} = -A_h \sqrt{2gh}$$

Equation 4.11

The next equation is the solution to the differential equation:

$$h = \left(-\frac{A_h}{2A_w} \sqrt{2g} * t + \frac{C}{2} \right)^2$$

Equation 4.12

Here, h is the height of the water, A_w is the cross-sectional area of the cylinder, A_h is the cross-sectional area of the hole, g is the acceleration due to gravity constant, t is time, and C is the constant of integration, which can be solved for using an initial condition.

Next, the derived equation and the results was implemented in MATLAB. The volumetric flow rate was determined from the raw results and plotted on a graph of Volume (mL) vs. Time (s). The equation from Torricelli's model was then plotted on the same graph to determine the accuracy of the model approximation. The results can be seen below in Figure 18.

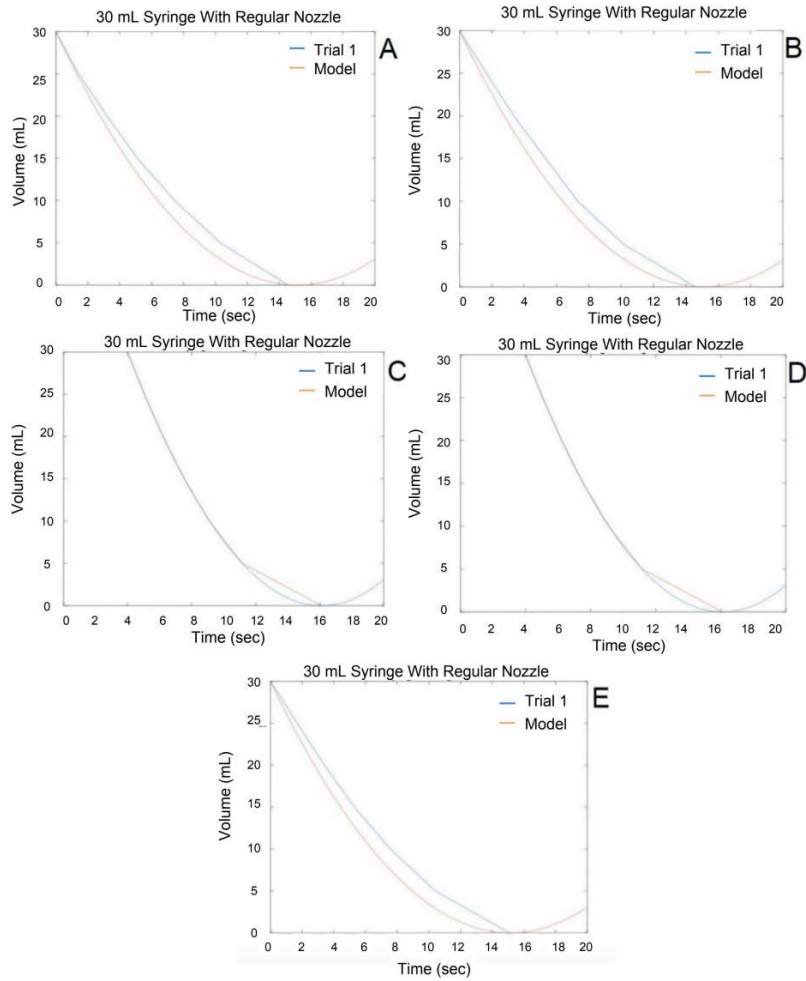


Figure 18: Graphs representing the change in volume over time of water draining from a syringe. The syringe had the regular diameter of the nozzle of the syringe. (A) Trial 1, (B) Trial 2, (C) Trial 3, (D) Trial 4, and (E) Trial 5. Each trial is plotted on the same plot as the model derived from Torricelli's Law to compare results and determine model accuracy.

Figure 19 (below) is useful for visualizing the precision of the 5 trials with respect to each other, as well as the accuracy of the trials when compared to Torricelli's model. The average flow rate across all 5 trials was calculated, then plotted against Time and Volume in two different graphs. These graphs can also be seen in Figure 19.

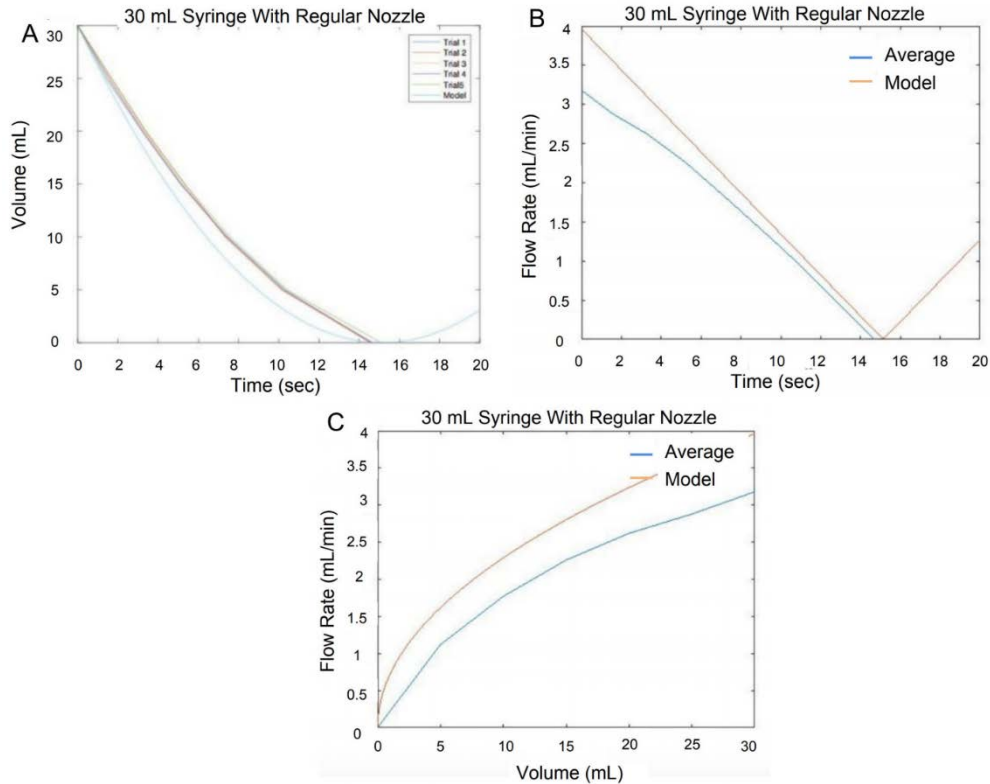


Figure 19: (A) Graph of all trials plotted with the model derived from Torricelli's Law, (B) Graph of the average flow rate vs. time, plotted against the model derived from Torricelli's Law, and (C) Graph of the average flow rate vs. volume, plotted against the model derived from Torricelli's Law.

The same procedure was then repeated, this time with the attachment of a blunt needle at the nozzle of the syringe. It was hypothesized that this needle, with a smaller inner diameter than the nozzle of the syringe, would help to slow the flow rate of the water in the open syringe. The raw results can be found in Table 14, and the graphical results in Figures 20.

Table 14: Raw data for syringe experiment, using the small/tiny nozzle

Normal Nozzle							
	Trial 1	Trial 2	Trial 3	Trial 4	Trial 5	Average	
Volume (mL)	Time (s)	Time (s)	Time (s)	Time (s)	Time (s)	Time (s)	Flow Rate (mL/s)
30	0	0	0	0	0	0.00	1.87
25	2.73	2.61	2.60	2.66	2.75	2.67	1.64
20	5.82	5.62	5.54	5.83	5.77	5.72	1.44
15	9.31	8.83	8.97	9.59	9.2	9.18	1.30
10	13.59	12.39	12.67	13.55	12.98	13.04	1.05
5	18.55	17.01	17.29	18.46	17.77	17.82	0.78
0	25.03	23.11	23.52	25.49	24.08	24.25	0.00

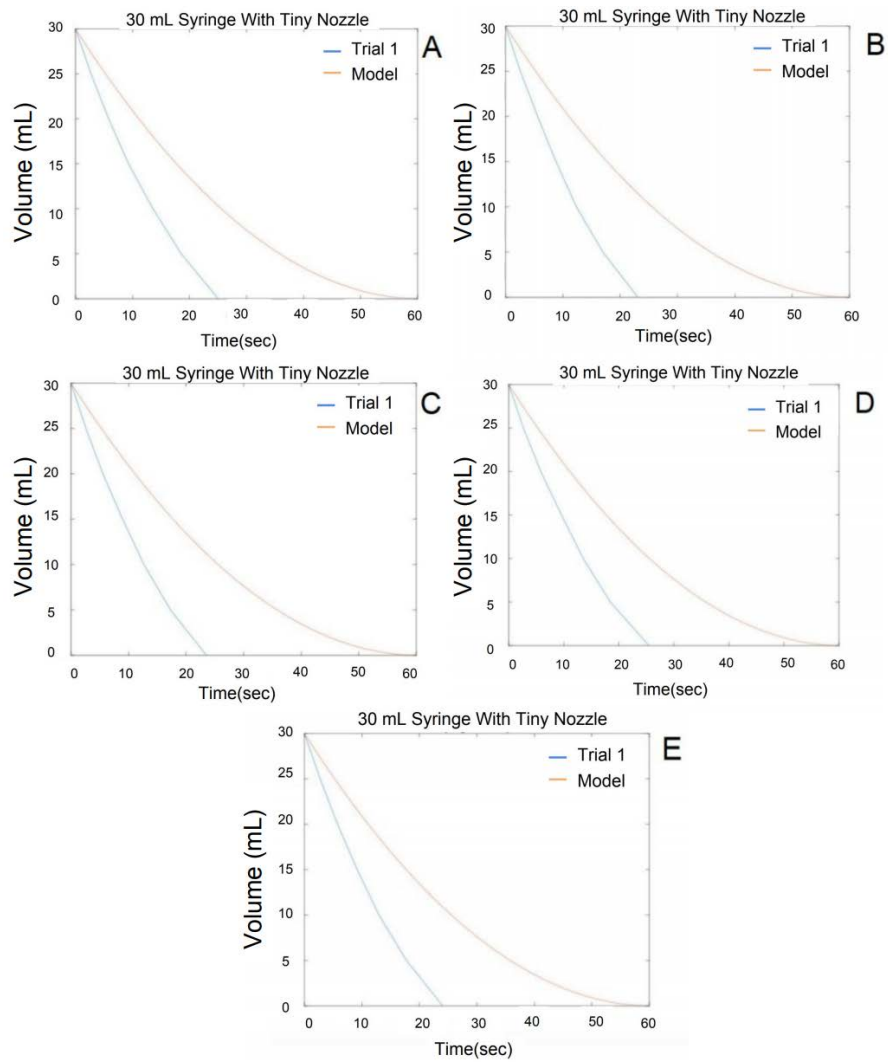


Figure 20: Graphs representing the change in volume over time of water draining from a syringe. The syringe had the smaller diameter of the attached blunt needle. (A) Trial 1, (B) Trial 2, (C) Trial 3, (D) Trial 4, and (E) Trial 5. Each trial is plotted on the same plot as the model derived from Torricelli's Law to compare results and determine model accuracy.

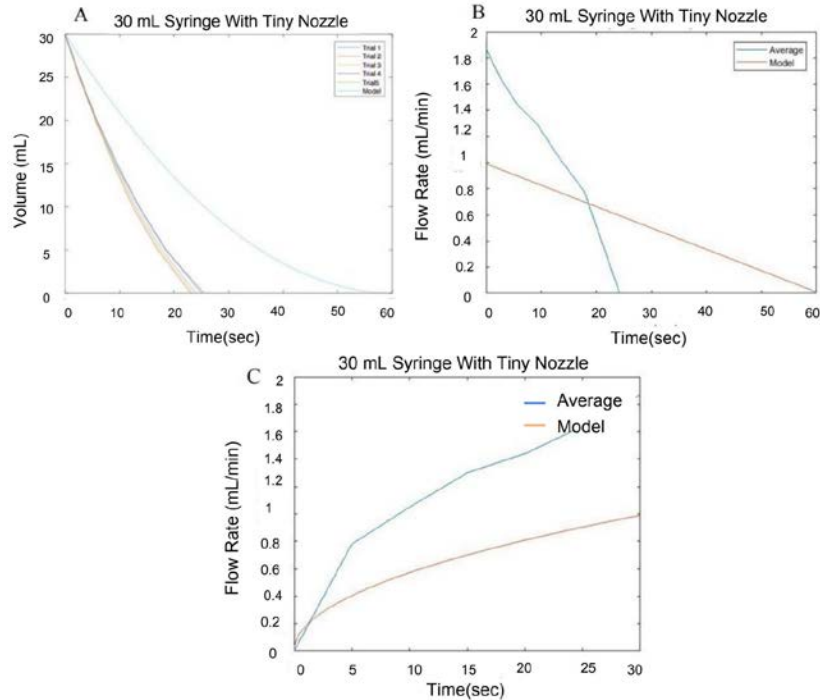


Figure 21: (A) Graph of all trials plotted with the model derived from Torricelli's Law, (B) Graph of the average flow rate vs. time, plotted against the model derived from Torricelli's Law, and (C) Graph of the average flow rate vs. volume, plotted against the model derived from Torricelli's Law.

In this case, it is clear that the normal nozzle more closely followed the predictions made with Torricelli's Law, while the blunt needle did not. This could be attributed to a variety of reasons, such as the fact that the blunt needle attachment's diameter was not constant throughout. It could also be that the reason for deviation from the model is that one of the assumptions made by Torricelli's Law is that viscosity is negligible. This assumption may not hold in real life, therefore leading to some deviation. In other words, the resistance that is present in the blunt needle caused the Torricelli Law model to not accurately model this system. It was also noticed that in all cases, whether in plots of volume vs. time where flow rate is represented by the slope of the curve or in plots involving flow rate as one of the variables, that flow rate always decreases over time. The results of these experiments demonstrate Marimuthu et al.'s description that flow rate decreases over time as a result of decreasing hydraulic pressure.

4.4.1.2 Ohm's Law

As discussed in Equation 4.5, the resistance of a system can be found by $R = \frac{\Delta P}{Q}$.

Written in its more conventional form, the equation is $Q = \frac{\Delta P}{R}$ and is known as Ohm's Law.

This equation can be used to model the resistance that is present in microfluidic gravity flow.

Equations 4.6 and 4.7 contain the information for calculating the resistance for both circular tubes and rectangular chambers, respectively, and these values can be solved here.

The known values are:

$$\eta \text{ (viscosity)} = 1 \text{ mPa}\cdot\text{s} = 0.001 \text{ Pa}\cdot\text{s}$$

$$L_t \text{ (length of tube)} = 50 \text{ cm} = 0.5 \text{ m}$$

$$r_o \text{ (radius of tube)} = 0.01 \text{ in} = 0.00025 \text{ m}$$

$$L_c \text{ (length of channel)} = 17 \text{ mm} = 0.017 \text{ m}$$

$$w \text{ (width of channel)} = 3.8 = 0.0038 \text{ m}$$

$$h_c \text{ (height of channel)} = 0.4 \text{ mm} = 0.0004 \text{ m}$$

$$h_t \text{ (height of tubes)} = 50 \text{ cm} = 0.5 \text{ m}$$

For the circular tubes:

$$R = \frac{8\eta L_t}{\pi r_o^4} = \frac{8(0.001 \text{ Pa}\cdot\text{s})(0.5 \text{ m})}{\pi(0.00025 \text{ m})^4} = 325949323452 \text{ Pa}\cdot\text{s}/\text{m}^3$$

$$R = 3.3 * 10^{11} \text{ Pa}\cdot\text{s}/\text{m}^3$$

For the rectangular chambers:

$$R = \frac{12\eta L_c}{wh^3} = \frac{12(0.001 \text{ Pa}\cdot\text{s})(0.017 \text{ m})}{(0.0038 \text{ m})(0.0004 \text{ m})^3} = 838815789.474 \text{ Pa}\cdot\text{s}/\text{m}^3$$

$$R = 8.4 * 10^8 \text{ Pa}\cdot\text{s}/\text{m}^3$$

These resistances can then be added in series together, as follows:

Equation 4.13

$$R_{series} = R_1 + R_2$$

$$R_{series} = 3.3 * 10^{11} \text{ Pa}\cdot\text{s}/\text{m}^3 + 8.4 * 10^8 \text{ Pa}\cdot\text{s}/\text{m}^3 = 330840000000 \text{ Pa}\cdot\text{s}/\text{m}^3$$

$$R_{series} = 3.3 * 10^{11} Pa * s/m^3$$

Based on these equations, the total resistance of the system, when taking both the circular tube resistance and the rectangular channel resistance into account, is $3.3 * 10^{11} Pa * s/m^3$. Here, it can be seen that the majority of resistance in the system will be contributed by the tubing. This conclusion makes sense because the dimensions of the tubing are so small, particularly the inner diameter. When the resistance for the tubing and the resistance for the rectangular chamber are added in series, the value for the tubing dominates. Furthermore, due to significant figures, R_{series} is equivalent to R_{tubing} . Therefore, the tubing contributes the most to the resistance of the system.

4.4.1.3 Flow Rate Testing with Syringes and Connected Tubes

To better model the actual situation, the next round of testing incorporated tubing, since this will be an important aspect of the final pump. Tubes with an inner diameter of 0.02 inches was selected as the optimal tube diameter for of this project. The goal of this experiment was to observe the effect that tube length had on the flow rate of fluid out of the open syringe. A length of 50 cm was chosen as the control. A length of 100 cm was chosen to observe the effect that doubling the length would have, and a length of 25 cm was chosen to observe the effect that halving the length would have. The setup involved attaching the blunt needle to the syringe, fitting one end of the plastic tube over the blunt needle, inserting a small metal tube into the other end of the plastic tube, and then placing this end into a makeshift plug that was in the inlet of the microfluidic chamber. The syringe was then extended vertically until the tube was taut, then was secured in place. Similar to the previous experiment, measurements of time were made for every 1 mL increment of water, as the water flowed out of the syringe and into the microfluidic chamber. These experiments were performed in triplicate.

MATLAB was again employed to graph the raw results for analysis. The times measured in the three different trials were averaged, then plotted against the volume. The line of best fit was displayed alongside the volume vs. time graph, which in most cases was almost nearly linear. The slope of the line of best fit was taken to be the volumetric flow rate for that particular experiment. The slopes of these graphs, and therefore the volumetric flow rate, were negative, indicating the flow rate was decreasing over time.

One experimental error occurred in which two variables were changed simultaneously, with those two variables being tube length and syringe height (since the tubes were always taut). This explains why the syringe with the 25 cm length tube actually took much longer to empty (~35 minutes) when compared to the other two tube lengths (~28 minutes), which was unexpected due to its shorter length.

Another experiment was conducted to remedy this error. The 100 cm long tube was used, except the syringe was not extended vertically until the tube was taut. Instead, the syringe was placed at half height (at approximately the height at which the syringe with 50 cm taut tube was), such that the 100 cm tube was loose and hanging limply on the lab counter. This ensured that the only one variable (tube length) was changing, while all of the others (including height) remained constant. This allowed better understanding of the exact effect that tube length has on flow rate, without any extraneous factors. The addition of an outlet tube at the other end of the microfluidic chamber through which media left the system did not cause any significant differences in flow rate. A summary of the flow rates is listed in Table 15.

Table 15: Summary of Syringe Experiment Flow Rates for Comparison

Experiment	Flow Rate (mL/min)
25 cm tube	0.8357
50 cm tube	1.0549
100 cm tube	1.1334
100 cm tube, half height	0.5969
100 cm tube, half height, with outlet tube	0.5785

The flow rate for the experiment with the 100 cm tube length at half height (0.5969 mL/min) was almost half of the flow rate for the 50 cm tube length at the same height (1.0549), thereby suggesting that flow rate is inversely proportional to the tube length. This was a positive result, since it demonstrated that the flow rate could be significantly decreased. However, flow rate always decreased over time in all gravity-based experiments.

The equations for fluid mechanics properties can be used to analyze this data. Ohm's Law allows for the calculation of flow rate from pressure and resistance, as mentioned in the previous section.

$$Q = \frac{\Delta P}{R} = \frac{\rho gh}{R}$$

The meanings of these variables have already been described in previous sections. In this version of syringe experiments, as the height of the syringe increases because the increased tube length is taut, the resistance also increases. Since both of these increase linearly, they cancel each other out because h is in the numerator while R is in the denominator. The magnitude of their respective increases will affect the subsequent value of flow rate. In the results, it was observed that the flow rates are similar for the different taut lengths of tubing for this reason.

For when the tube length remains constant but the height decreases by half, this means that in the equation height h will decrease by $\frac{1}{2}$ but the resistance R will remain the same (because tube length has not changed). Due to the direct relationship between flow rate Q and height h , the flow rate will halve. This was also observed in the results, in which the 100 cm tube length at half height produced a flow rate of 0.5969 mL/min, while the 100 cm tube length at taut height produced a flow rate of 1.1334 mL/min. The former is 52.7% of the latter, indicating that the flow rate did indeed decrease by half when the height was also halved.

Equation 4.14 can be used to calculate the experimental flow rate of the system, to demonstrate that the results gathered from this syringe experiments are accurate.

$$Q = \frac{\rho gh_t}{R_{series}} = \frac{(1000 \text{ kg/m}^3)(9.81 \text{ m/s}^2)(0.5 \text{ m})}{3.3 * 10^{11} \text{ Pa} * \text{s/m}^2} = 1.5 * 10^{-8} \text{ m}^3/\text{s} = 0.9 \text{ mL/min}$$

The expected flow rate from this experiment was 0.9 mL/min for a tube length of 50 cm. The experimental flow rate for a tube length of 50 cm was 1.05 mL/min (Table 15). The percent error here is 16.7 %, which demonstrates that the experimental flow rate can be approximated by using the governing equations.

Using these same principles, the Theoretical tube length that could provide the desired flow rate can also be calculated. The following calculation uses the same height of 50 cm to find the tube length.

$$Q = \frac{\rho gh_t}{\frac{8\eta L_t}{\pi r_0^4} + \frac{12\eta L_c}{wh^3}} \quad [50]$$

$$L_t = \left(\frac{\rho g h_t}{Q} - \frac{12\eta L_c}{wh^3} \right) * \frac{\pi r_0^4}{8\eta} \quad [50]$$

Equation 4.17

$$L_t = \left(\frac{\rho g h_t}{Q} \right) * \frac{\pi r_0^4}{8\eta}$$

$$L_t = \left(\frac{\left(1000 \frac{kg}{m^3} \right) \left(9.81 \frac{m}{s^2} \right) (0.5 m)}{3.33 * 10^{-10} \frac{m^3}{s}} \right) * \frac{\pi (0.00025m)^4}{8(0.001 Pa * s)} = 22.6 m$$

As can be seen the term for microfluidic chamber resistance was dropped in Equation 4.17, because this term is negligible since the resistance of the tubing dominates (as previously described). Therefore, at a height of 0.5 m, the tube length need to be at least 22.6 meters long in order achieve the desired flow rate of 0.02 mL/min. This tube length is not feasible, as it is extremely long and will make the setup of the pump very inconvenient for the user. This is almost 50 times the amount of tube length used previously, which makes sense because the flow rate was also decreased by a factor of ~50. An alternative would be to lowering the height by a factor of ~50, from 0.5 m to 0.01 m or 1 cm, but this may also not be feasible since the height is so low. A combination of increasing tube length and lowering the height could be implemented to achieve the desired flow rate. Decreasing the inner diameter of tubing would also be an option, maybe to as low as 0.01 in. This is ½ of the inner diameter of the tubing that was used, which would increase the resistance of the system by a factor of 4, or 16 times, and that could also help to slow the flow rate. Additionally, a valve could also be introduced in the system, which would allow for the tube length to be decreased while also controlling the passage of fluid into the microfluidic chamber.

Even though this pump has the advantage of being easy to build and accessible, the team decided to discard this design due to low accuracy of having constant flow rate throughout time and the challenge to achieve slow flow rates for the 30 mL to last 24 hours and to maintain cell viability. Furthermore, the tube length required for slow flow rates would not be feasible during the setup of this system.

4.4.2 Syringe Pumps

With the result of the gravity-based pump experiments detailed in Section 4.4.1, a conclusion was reached as a team that the gravity-based pump was not the optimal solution for

the client's problem. While it is definitely possible to achieve low flow rates using gravity-based pump systems, as demonstrated in Albrecht et al., the flow rate provided would inevitably decrease over time as a result of loss of hydraulic pressure [33], also observed in [31]. The magnitude of the decrease in flow rate can be minimized in gravity-based systems and may be negligible in certain applications, but for the purposes of this project an alternative solution was sought. The next proposal by the client was to build a do-it-yourself (DIY) syringe pump, using the materials available in the MakerSpace provided by the Program in Systems Biology at UMass Medical School.

4.4.2.1 Laser Cut Syringe Pump

Upon building the initial laser cut syringe pump in Figure 22 (below), the design team realized that the instructions provided from instructables.com were in fact incomplete. The team then made many adjustments to this design, in order to optimize it as much as possible and to customize it to our immediate needs.

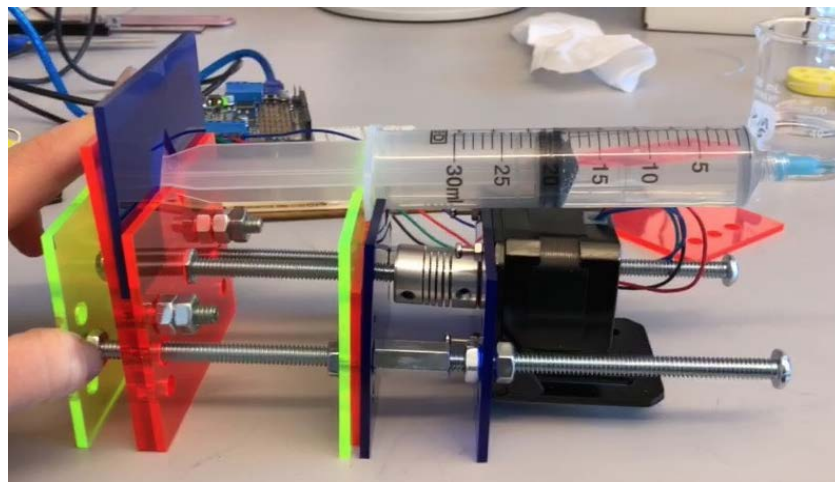


Figure 22: Initial design from Instructables.com

Unfortunately, the design provided by instructables.com kept getting stuck after a short period of time. In addition, there was not enough force applied to the back of the syringe. This is for a couple of key reasons, all of which were addressed in Model 2 (please see Model 1 in Figure 22 for comparison):

1. The single piece of acrylic behind the syringe was not strong or sturdy enough to push the syringe plunger down.

- a. Modification: Another piece of acrylic, identical to the first, was placed behind the syringe for added support and strength when pushing the syringe
2. The moving piece of the syringe pump (i.e. the piece of the pump that slid along the central rod to push the syringe plunger) was neither large nor stable enough to consistently push the syringe plunger. Because it was not aligned properly, this moving piece kept getting stuck.
 - a. Modification: All acrylic pieces were made taller in height, with two rods added to the top part. This was in an attempt to better align the pieces so the moving part would move more smoothly. A slot was custom made for the syringe to fit snugly and securely in the entire model. In addition, the rods in all four corners of the syringe pump were changed from threaded to smooth rods in order to make the movement along the rods smoother. These modifications can be seen in Figure 23.



Figure 23: Model 2 of the Laser Cut Syringe Pump

The next issue encountered was that the length of rods commercially available to the team were not long enough so that the plunger of the syringe could be fully extended. This meant that only a fraction of the full 30 mL syringe was available for holding fluid (see Figure 23). This was problematic because the entire 30 mL volume was necessary to ensure that fluid lasts for 24-hour long experiments. Another issue was that in the original design, the syringe was placed over the motor, which could lead to potential problems if leaking from the syringe was ever to occur during use of the syringe pump. These problems were addressed with a single

solution, which can be seen in Figure 24. Many of the parts were rearranged (i.e. reversed) so that the syringe was now facing away from the motor and any other electronics such as the Arduino. This reduced the risk of electronic problems associated with potential leakage and extended the range of the syringe. Now, the entire 30 mL volume of the syringe could be utilized.

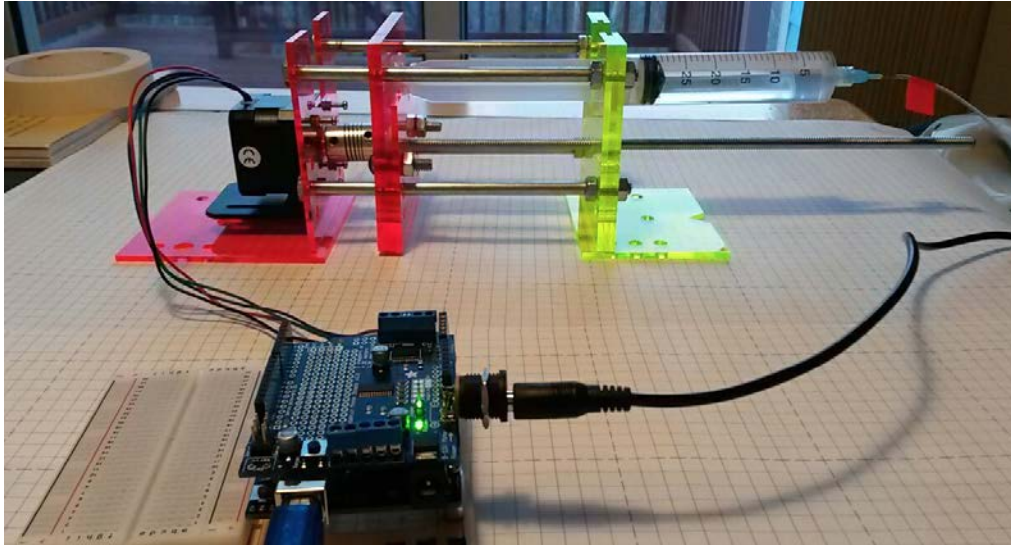


Figure 24: Model 3 of the Laser Cut Syringe Pump

However, the syringe pump was still getting stuck. While the previous modifications of the pump made the overall movement much smoother, there was still not enough force pushing on the syringe plunger, because of its positioning which was very high up in the model. To solve this issue, the custom-made slot for the syringe was lowered closer to the central rod. Since the central rod is where all of the force was coming from (via the rotation of the rod produced by the motor), the goal was to make the syringe plunger as close in proximity to the central rod as possible. This would allow the majority of the force produced by the rotating motor to then be applied to the syringe plunger, rather than being dissipated and thus weaker at a location farther away. This design can be seen below in Figure 25.

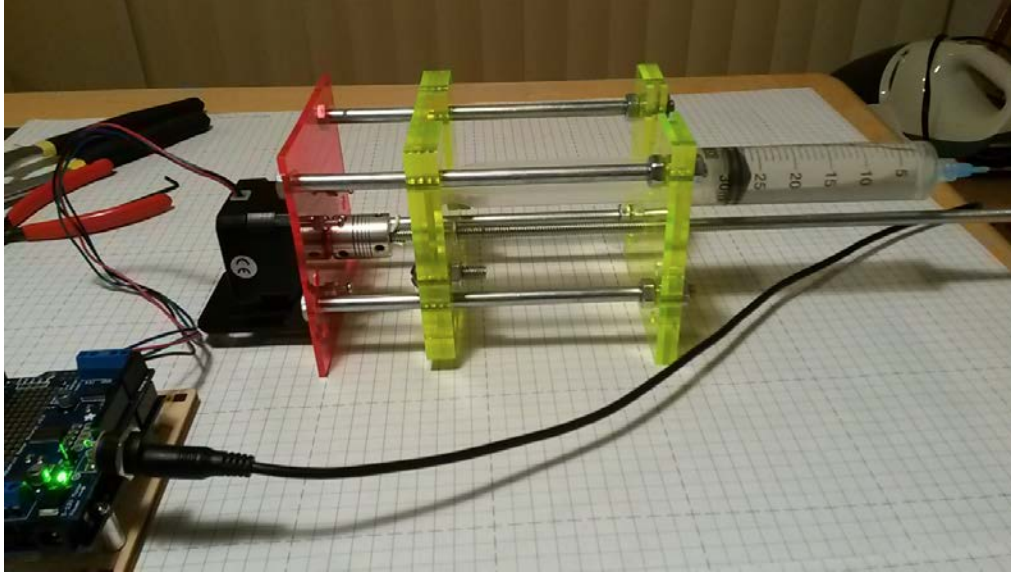


Figure 25: Model 4 of the Laser Cut Syringe Pump

With this final design, the laser cut syringe pump ran much more smoothly. A lot of valuable data was obtained from quick experiments with this model. First, the Arduino code was produced with help from the Adafruit Motor Shield library. With the use of the functions provided by this library, the motor could turn 1 step at a time. Furthermore, the insertion of delays of different time periods could slow the motor. With Model 4, the first experiment saw the motor moving 1 step, with a 1 second delay between each step. For the first milliliter increment of this experiment, it took 9.49 minutes, for a flow rate of

$$\frac{1\text{mL}}{9.49\text{ min}} = 0.101\text{ mL/min}$$

This flow rate was lower than any of the other flow rates obtained by the gravity-based syringe pump, which indicated that the syringe pump could potentially be a better option. The entire 30 mL took a total of 3 hr 55 min (235 min) to be pumped out, which gave an overall volumetric flow rate of

$$\frac{30\text{ mL}}{235\text{ min}} = 0.13\text{ mL/min}$$

The discrepancy between the flow rate of the first milliliter and the overall flow rate suggests that the flow rate produced by this pump was not constant throughout.

To reduce the flow rate even further, a 6 second delay was added between single steps of the motor. For the first milliliter, the flow rate was:

$$\frac{1 \text{ mL}}{64 \text{ min}} = 0.016 \text{ mL/min}$$

which was well below our desired flow rate of 0.02 mL/min (calculated for 30 mL fluid to last for maximum of 24 hours). The last 5 mL of the syringe produced a flow rate of

$$\frac{5 \text{ mL}}{219 \text{ min}} = 0.02 \text{ mL/min}$$

which was still close to the desired flow rate.

Ultimately, while the new and improved laser cut syringe pump provided ideal flow rates and enhanced stability, it would still get stuck occasionally. Another option for DIY syringe pumps was investigated.

4.4.2.2. 3D Printed Syringe Pump

For the 3D printed syringe pump, similar experiments to the two designs mentioned above were conducted. The syringe was filled to the 30 mL mark, and the time was measured at each 1 mL increment. The preliminary testing for this design was to determine if 1) the ideal flow rate of 0.02 mL/min could be achieved easily, and 2) the flow rate was constant regardless of the fluid volume. The volumetric flow rate was determined at each 1 mL mark and then plotted.

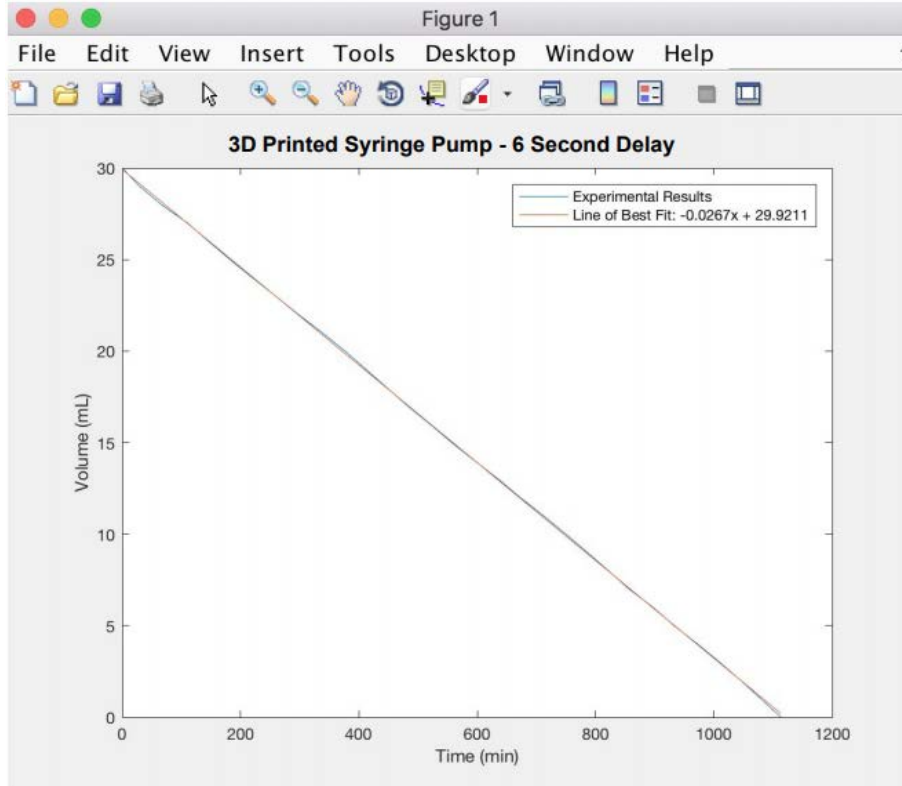


Figure 26: Results of 3D printed syringe pump experiment; 1 step with 6 second delays

The average volumetric flow rate was approximately 0.027 mL/min, as indicated by the slope of the line. Because of the lengthy nature of this experiment, only 1 trial was performed. The design team concluded that this syringe pump did not exhibit decreased flow rate as volume decreased, and that it could simply achieve the desired low flow rates by increasing the length of delay between steps.

Due to time constraints resulting from delay when ordering parts, the following modifications were made (see Figure 27).

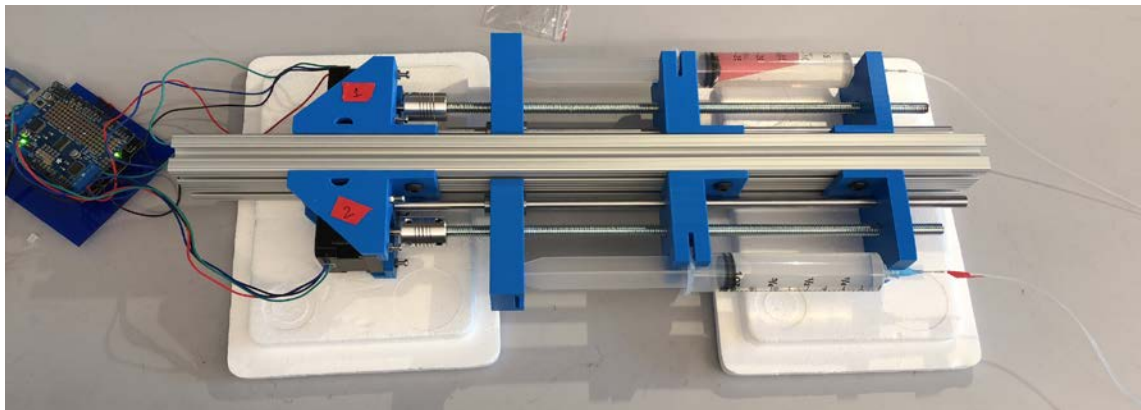


Figure 27: Final System of Syringe Pump, with 2 pumps attached to a single base.

The team decided to attach both syringes to the same base and set them sideways in order to reduce the budget and to be able to use one T-slotted extrusion base for two syringes (i.e. one base per system). The team confirmed the syringe pump worked normally when placed in this position without any challenge. It also worked well with the Arduino, since a single microcontroller can be used to operate 2 stepper motors. The team decided to name two syringe pumps attached to one single T-slotted extrusion base as a “unit”. At this point, further testing needed to be completed to ensure the device performance before performing the biological testing using melanoma cells.

From a qualitative standpoint, the 3D printed syringe pump seemed to be the most stable compared to the laser cut syringe pump that got stuck in the middle of the experiments. Additionally, it is compatible with an Arduino and the flow rate can easily be controlled and programmed through the code, which gives the advantage over the gravity-based pump system in which achieving a constant flow rate was a challenge.

The 3D printed syringe pump was ultimately selected as the final design. Out of the 3 design options, this device satisfied all of the needs discussed in Section 4.1. It is compatible with an Arduino, which allows the system to be automated and the flow rate to be precisely controlled. The setup of the system allows the microfluidic chamber alone to fit inside the microscope incubator, which fulfills the needs for temperature control, CO₂ control, size, and imaging. The setup also allows for convenient parallelization of experiments, as well as the delivery of 2 different types of media, with each syringe on one unit containing one type of media. Because the system is modular, it can be easily disassembled and sterilized using either ethanol or autoclaving. The main reason for selecting the 3D printed syringe pump as the final design was the precise control of flow rate and the attainment of the desired constant flow rate that it allowed.

Chapter 5. Final Design Verification

5.1 Stress Testing

The goal of performing stress testing corresponds to three different rationales: (1) confirm the pump hardware is sturdy and stable, (2) make sure the plastic material of the 3D printed parts do not deteriorate, and (3) evaluate that the extensive use and vibrations of the device do not affect the function of the pump.

The stress testing of the pump was performed by observation and qualitative data analysis. The pump was observed in its initial condition and was evaluated for any possible alterations of the device during and after functioning at different rates. For the mechanical and software stability of the pump, experiments were run multiple times and results were verified to be identical. In doing so, it confirmed that the multi-pump system is stable and that it can produce accurate and precise results.

The stress testing was performed under the following specifications and results will be qualitative based on observation:

1. Forward and rewind stress testing: subject pump to the max speed it can take before it starts shaking. Functioning pump experience different speeds and note observations.

Key areas of interest to look for observation:

1. The motor bed (any effects due to heat produced by the motor)
2. The small cylinder bearing inside the moving piece at the bottom (if it starts sliding out)
3. The moving piece itself (if it wobbles back and forth)
4. The joiner between the motor and the threaded rod, and the threaded rod itself (if there is any degradation of the metal due to grinding)
5. Overall vibrations of the pump

Table 16: Acceptance Criteria for Pump outcome exposed to stress testing (For details on how each part looks like, refer to Appendix C: User Manual)

Syringe pump part to evaluate	Outcome accepted	Outcome for failing
Motor bed (3D printed)	Brand new after 3D printed, intact	Melted or cracked
Syringe holder parts (3D printed)	Intact	Cracking, cut edges due to threaded rod contact
Moving part (3D printed)	Stable throughout experiment, intact	Movement from side to side or immobilized
T-slotted extrusion base	Same position before and after experiment	Moves upward or downward with an angle
Smooth rod	Stays in place	Moves forward
Threaded rod	Stays in place	Unaligned
Linear bearing	Stays in the middle of the moving 3D printed piece	Moves and becomes dislodged from the moving piece

- Motor bed had no defect, brand new after 3D printed.
- Moving part stable with linear bearing holding smooth rod exactly in the middle of the hole.
- Middle-point syringe holder part stable attached to T-slotted extrusion. Threaded rod slightly touching bottom part of middle hole. Smooth thread perfectly fits through bottom hole.
- End part syringe tip holder: tightly attached to T-slotted extrusion. Threaded rod slightly touching bottom part of middle hole. Smooth thread perfectly fits through bottom hole.

Table 17: Measurements at Original Position

Reference part	Measurement (cm)
Starting length to go forward (Measured from coupler connector to moving 3D printed part):	3
Length from coupler connector to non - moving middle point 3D part syringe holder	14
Length moving part travels	9

5.1.1 Testing 1: Forward and Rewind 10 rpm with no delay

Table 18: Observed Results for Forward and Rewind 10 rpm with no delay

Trial #	Observation	Criteria	Time (s)
Trial 1	Forward: <ul style="list-style-type: none"> ● Stable parts ● Moving part ● Threaded rod ● Smooth rod ● Linear Bearing 	Accepted Failed Accepted Fail Accepted	210
	Rewind: <ul style="list-style-type: none"> ● Stable parts ● Moving part ● Threaded rod ● Smooth rod ● linear bearing ● T-slotted extrusion base 	Accepted Fail Accepted Accepted Accepted Fail	215
	Average time Forward		219.3
	Average Time Rewind		219.3
	Average Time Total		219.3
	Speed (cm/s)		0.041

5.1.2 Testing 2: Forward and Rewind Speed: 10 rpm 1 Step, 10 ms delay

Table 19: Speed: 10 rpm 1 Step, 10 ms delay

Trial #	Observation	Criteria	Time (s)
Trial 1	Forward: <ul style="list-style-type: none"> ● Stable parts ● Moving part: ● Threaded rod: Accepted ● Smooth rod ● Linear Bearing ● T slotted extrusion base 	Accepted Failed Accepted Fail Accepted Fail	347s
	Rewind <ul style="list-style-type: none"> ● Stable parts ● Moving part ● Threaded rod Accepted ● Smooth rod ● Linear Bearing ● T slotted extrusion base 	Accepted Failed Accepted Fail Accepted Fail	353s
	Average time Forward		350.3
	Average Time Rewind		353.6
	Average Time total		350.5
	Speed		0.025 cm/s

5.1.3 Testing 3: Forward and Rewind Speed: 10 rpm 1 Step, 50 ms delay

Table 20: Speed of 10 rpm 1 Step, 50 ms delay

Trial #	Observation	Criteria	Time (s)
Trial 1	<p>Forward:</p> <ul style="list-style-type: none"> ● Stable parts ● Moving part ● Threaded rod ● Smooth rod ● Linear bearing ● T-slotted extrusion base <p>Rewind:</p> <ul style="list-style-type: none"> ● Stable parts ● Moving part ● Threaded rod ● Smooth rod ● Linear bearing ● T-slotted extrusion base 	<p>Accepted</p> <p>Fail</p> <p>Accepted</p> <p>Fail</p> <p>Accepted</p> <p>Fail</p> <p>Accepted</p> <p>Accepted</p> <p>Accepted</p> <p>Accepted</p> <p>Accepted</p> <p>Fail</p>	
	Average time Forward		1019.6
	Average Time Rewind		1028.3
	Average Time total		1024.0
	Speed		0.009 cm/s

5.1.4 Testing 4: Forward and Rewind Speed of 10 rpm 1 Step, 75 ms delay

Table 21: Speed of 10 rpm 1 Step, 75 ms delay

Trial #	Observation	Criteria	Time (min)
Trial 1	<p>Forward:</p> <ul style="list-style-type: none"> ● Stable parts ● Moving part ● Threaded rod ● Smooth rod ● T-slotted base <p>Rewind:</p> <ul style="list-style-type: none"> ● Stable parts ● Moving part ● Threaded rod ● Smooth rod ● linear bearing ● T-slotted extrusion base 	<p>Accepted</p> <p>Fail</p> <p>Accepted</p> <p>Accepted</p> <p>Accepted</p> <p>Accepted</p> <p>Fail</p> <p>Accepted</p> <p>Accepted</p> <p>Accepted v</p>	
	Average time Forward		1433.7
	Average Time Rewind		1447.0
	Average Time total		1440.4
	Speed		0.0062 cm/s

5.1.5 Testing 5: Forward and Rewind Speed: 10 rpm 1 Step, 100 ms delay

Table 22: Speed: 10 rpm 1 Step, 100 ms delay

Trial #	Observation	Criteria	Time (min)
Trial 1	Forward: <ul style="list-style-type: none"> ● Stable parts ● Moving part ● Threaded rod ● Smooth rod ● linear bearing ● T-slotted base Rewind: <ul style="list-style-type: none"> ● Stable parts ● Moving part ● Threaded rod ● Smooth rod ● linear bearing ● T-slotted extrusion base 	Accepted Fail Accepted Accepted Accepted Fail Accepted Fail Accepted Accepted Accepted Fail	
	Average time Forward		1769.6
	Average Time Rewind		1795.6
	Average Time total		1782.6
	Speed		0.005 cm/s

After performing the testing for different delays, 75 ms was found to be the most suitable speed for the user to rewind or forward the pump based on the observations for the different speeds. Based on the adequate delay, further testing was performed based on the length the moving part traveled at different time points from the beginning to the platform, instead of the syringe length as done in the testing above. The 75 ms delay was chosen to perform to get a time vs length relationship.

Table 23: Time vs Length Relationship

Time (min)	Length moving part traveled (cm)	Average Length for each timepoint
5	2.5	2.53
5	2.6	
5	2.5	
10	5.0	5.03
10	5.1	
10	5.0	
15	7.5	7.53
15	7.6	
15	7.7	
20	9.0	9.16
20	9.3	
20	9.2	

Based on the table above and graph below, the average of moving part length traveled at different times tend to be linear, having the length the moving part travelled be directly proportional to the time the code ran. However, for the final time point of 20 minutes, it falls and deviates from that proportionality, which could have been from human error measuring the distance or setting up the appropriate time.

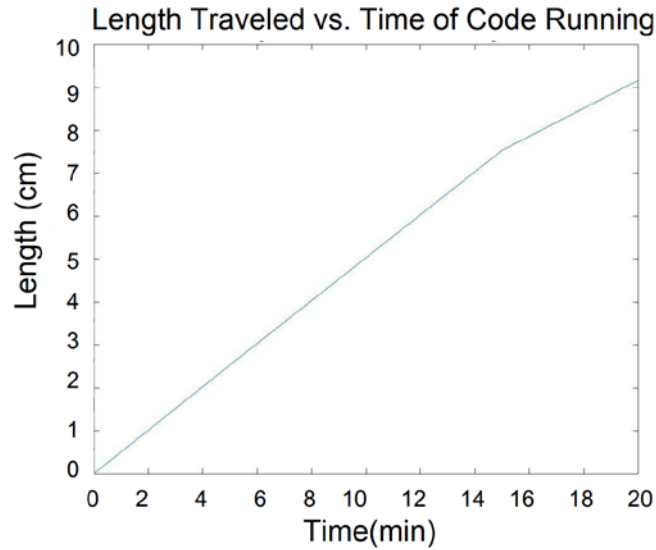


Figure 28: Length Moving part travelled for different times

5.2 Determination of the Relationship Between Flow Rate and Motor Delay

The goal of this experiment was to accurately determine the exact relationship between flow rate and motor delay. In the Arduino code for Experiment 1, the built-in function `step()` (which is a part of the Adafruit Motor Shield library; see Figure 29, line 10) is used to control the motor by moving it one step at a time. Because stepper motors move in discrete steps, it can be difficult to increase or decrease the rate at which the motors move. Another built-in function, the `delay()` function (see Figure 29, line 11, allowed the team to decrease the rate of the motor by inserting delays between each step. The duration of the delay determined the length of time between each step, and therefore would determine the flow rate of the fluid being pumped out.

```

1  switch (running_motor)
2  {
3    case MOTOR_1:
4
5      if ((end_time - start_time) <= motor1_interval)
6      {
7        digitalWrite(ledPinGreen, HIGH);
8        digitalWrite(ledPinRed, LOW);
9        Serial.print("Motor 1 On\n");
10       myMotor1 -> step(STEPS, BACKWARD, MICROSTEP);
11       delay(motor1_delay);
12     }
13
14     else
15     {
16       running_motor = MOTOR_2;
17       digitalWrite(ledPinGreen, LOW);
18       digitalWrite(ledPinRed, HIGH);
19       Serial.print("Motor 2 On\n");
20       myMotor2 -> step(STEPS, FORWARD, MICROSTEP);
21       delay(motor2_delay);
22     }
23
24     break;

```

Figure 29: An excerpt of the code for Experiment 1, the pulse experiment. This figure displays the first half of the code. The second half continues the switch statement for the case of MOTOR_2. The entire Arduino code can be found in Appendix A

The desired flow rate is a parameter of each of the 3 different cases of experiment. The multi-pump system software controls the flow rate of the fluid by computing the speed of the motor and introducing a delay. The delay length will end up determining the flow rate. Therefore, there is a relationship between flow rate and motor delay, and establishing this relationship is essential to solidifying and confirming accuracy of flow rate for the multi-pump system. The data from this experiment is crucial to confirming the accuracy of the algorithm, to make sure it ultimately delivers media at the desired flow rate. With this data, we were able to have a working pump capable of delivering pulses of drug at the correct flow rate that could be used for a real experiment.

One BD 30 mL syringe was filled with water and inserted in the syringe pump. In the Arduino code, the first parameter of the step() function was set to 1 (i.e., controlling the motor to move only 1 step at a time), and the delay() parameter was set to 1000 (i.e., inserting a 1000 ms, or 1 second, delay between each step). A timer was started when the pump began running and the time was recorded at each 1 mL mark as the volume of the fluid decreased. After all data collection, the flow rate at each measurement was calculated by dividing the volume (i.e. 1 mL)

by the time in minutes it took for that volume to be pumped out. The average flow rate was then calculated by taking the mean of these numbers.

The average length of time for each 1 mL to be pumped out was 6.464 min. The total length of the experiment was 3.232 hours. The average flow rate was once again 0.1547 mL/min.

A similar experiment was performed, but this time the delay between steps was increased to 2000 ms, or 2 seconds. The average length of time for each 1 mL to be pumped out was 12.905 min. This is almost exactly twice the amount of time it took for the 1 second motor delay experiment (6.464 min).

$$\frac{12.905 \text{ min}}{6.464 \text{ min}} = 1.9964 \approx 2$$

The total length of the experiment was 6.452 hours. Once again, this is almost exactly twice the

$$\frac{6.452 \text{ min}}{3.232 \text{ min}} = 1.9963 \approx 2$$

amount of time it took for the 1 second motor delay experiment (3.232 hours).

The average flow rate was 0.0776 mL/min. This is almost exactly half of the flow rate calculated in the 1 second motor delay experiment (0.1547 mL/min).

$$\frac{0.0776 \text{ min}}{0.1547 \text{ min}} = 0.5016 \approx 0.5$$

For the 3 second delay, the average length of time for each 1 mL to be pumped out was 19.478 min. This is almost exactly three times the amount of time it took for the 1 second motor delay experiment (6.464 min). The total length of the experiment was 9.739 hours. Once again, this is almost exactly three times the amount of time it took for the 1 second motor delay experiment (3.232 hours). The average flow rate was 0.0516 mL/min. This is almost exactly one-third of the flow rate calculated in the 1 second motor delay experiment (0.1547 mL/min).

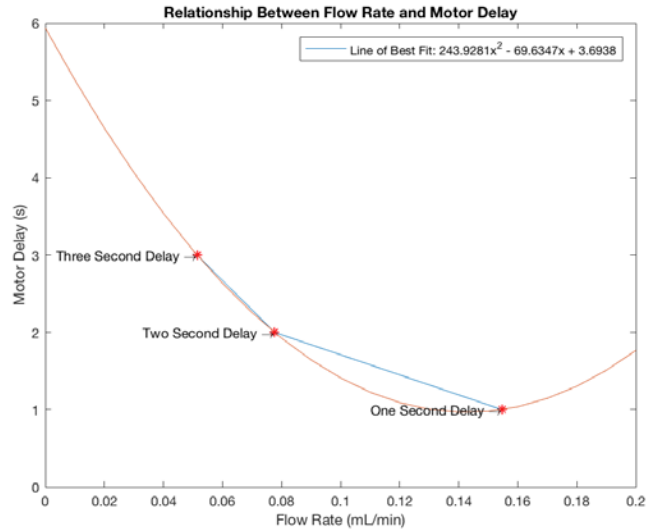


Figure 30: Relationship Between Flow Rate and Motor Delay

After completing three different experiments of this nature, there was a noticeable trend. The relationship is neither linear nor quadratic, but there was a significant pattern. The flow rate of each motor delay can be calculated as the reciprocal of the ratio of the flow rates, multiplied by the flow rate of the 1 second motor delay. Based on this, a general formula was hypothesized at this stage of experimentation:

$$\left(\frac{X \text{ second motor delay}}{1 \text{ sec motor delay}}\right)^{-1} * 0.1547 \text{ mL/min}$$

$$\left(\frac{4 \text{ sec}}{1 \text{ sec}}\right)^{-1} * 0.1547 \text{ mL/min} = 0.03868 \text{ mL/min}$$

Thus for 4 second delays, we expect the flow rate to be 0.03868 mL/min.

For 5 second delays, we expect the flow rate to be 0.03094 mL/min.

$$\left(\frac{5 \text{ sec}}{1 \text{ sec}}\right)^{-1} * 0.1547 \text{ mL/min} = 0.03094 \text{ mL/min}$$

And for 6 second delays, we expect the flow rate to be 0.02578 mL/min.

$$\left(\frac{6 \text{ sec}}{1 \text{ sec}}\right)^{-1} * 0.1547 \text{ mL/min} = 0.02578 \text{ mL/min}$$

This numbers would be confirmed or rejected in the following experiments. To save time, these experiments were conducted only on the last 5 mL of fluid in the syringe, since it was

confirmed that the flow rate appears to remain constant throughout the entire 30 mL. This will therefore give us valuable data. If correct, this pattern would allow us to easily calculate the required motor delay necessary to achieve the desired flow rate input by the user.

The same procedure was carried out for 4, 5, and 6 second delays. For these longer delays, only 5 mL were used instead of the complete 30 mL to reduce time. This is justified also by the fact that there was no observed difference in flow rates throughout the duration of the 30 mL. In other words, the flow rate remained consistent throughout the 30 mL, which demonstrates that there is no effect of fluid volume on flow rate. Thus, observing only the last 5 mL is reasonable for these purposes. The flow rates for each of these delays were calculated in the same manner as previously for the 1, 2, and 3 second delays.

Below is a summary of the flow rates associated with each of the delays mentioned above.

Table 24: Summary of the observed flow rates for different delay periods

Delay (s)	Flow Rate (mL/min)	Prediction (mL/min)	Percent Error (%)
1	0.1547	0.1547 (base)	0
2	0.0776	0.0774	0.258
3	0.0516	0.0516	0
4	0.0387	0.0387	0
5	0.0311	0.0309	0.643
6	0.0249	0.0258	3.614

The predictions for flow rate that were made based on the observed pattern were very accurate, as can be seen from the fourth column of Table 24, because of the very low percent errors. Additional testing will be used to confirm flow rate, but from this testing it is apparent that the relationship between flow rate and motor delay has been accurately determined.

It was later noted that the MICROSTEP parameter (rather than SINGLE and DOUBLE) was able to have the motor move 1 step at a time, but with much smoother movement. This is desired, since the flow of media through the microfluidic must be as continuous as possible, and must have minimal amount of pulsatile flow as possible. For testing the MICROSTEP

performance, only 5 mL was used once again to measure the flow rate. Three trials were performed for the 1 second delay. The results can be seen below in Table 10.

Table 25: Summary of the observed flow rate for 3 different trials of the 1 second delay for the MICROSTEP

Trial Number	Flow Rate (mL/min)
1	0.1395
2	0.1400
3	0.1396
Average	0.1397

Thus, the MICROSTEP parameter of the step() function which produced much smoother movement of the motors was able to produce a slower flow rate of 0.1397 mL/min, when compared with the flow rate obtained using the SINGLE parameter which was 0.1547 mL/min. This is ideal, not only for the smoother, more continuous movement but also because the flow rate of the media through the microfluidic chamber should be as low as possible so as not to perturb the cells in any way, as cells are sensitive to shear stresses.

The exact relationship between flow rate and motor delay was then determined. With the delay duration as the x-variable and the flow rate as the y-variable, a mathematical relationship between flow rate and motor delay was determined by using the data points collected from the experiment. This relationship can be seen graphically in Figure 31 below.

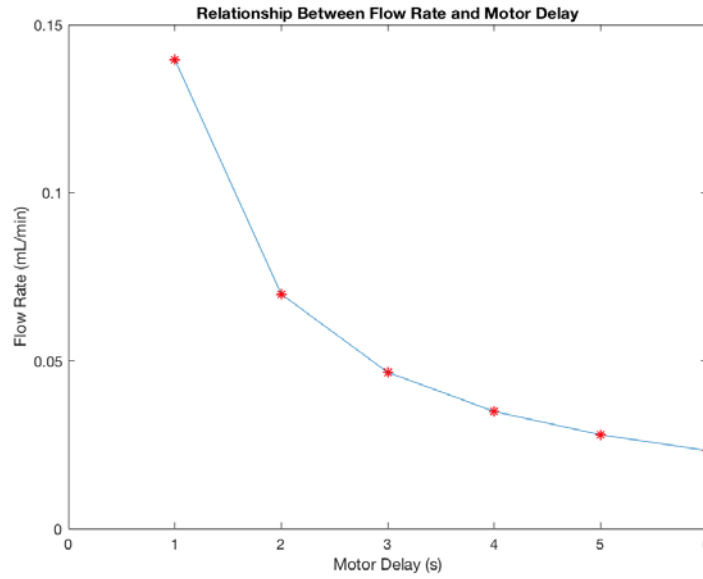


Figure 31: The relationship between flow rate and motor delay. This graph is for the MICROSTEP results

A mathematical relationship can be deduced from these results. The flow rate (mL/min) serves as the y-variable, while the motor delay (s) serves as the x-variable. Using the curve fitting tool in MATLAB (cftool), curve fitting was performed on the experimental data collected in order to find a relationship of the form $y = k/x$, since the graph demonstrates an inverse relationship between the two variables. In this tool, the X Data parameter was set as the motor delays and the Y Data parameter was set as the observed volumetric flow rates. From the drop-down menu that designates the type of relationship, “Custom Equation” was selected, and the design team specified that the desired relationship was in the form of an inverse relationship, $y = k/x$. The tool then generated the following equation to model this relationship:

Equation 5.1

$$y = f(x) = \frac{k}{x}$$

where y is the flow rate and x is the step delay. Therefore, the value of k in this relationship is 0.1396. The curve fitting tool displayed that the R-square value was 1, indicating that this equation is a very good fit.

This relationship was implemented in the code for Experiment 1. When the user enters the flow rate that he or she desires, the code will calculate the appropriate delay time to insert

between each step of the motor in order to achieve that flow rate. This inverse relationship was expected by the design team, and this flow rate testing was used to verify the hypothesis.

5.3 Switch Response Testing

The purpose of this test is to analyze the uniform media distribution at switch input of pumps determined by the user in the Arduino code. The main goal is to analyze the spread of fluid inside the microfluidic chamber as it is pumped from the system and evaluate if the desired behavior of uniform distribution of the fluid in the chamber is achieved. This test mainly tested how long it takes for the media to cover the complete surface area of the microchannel.

The experiment was performed by filling one syringe with green food coloring, representing media with no drug, and the other one with red dye, representing the media with drug. The choice of color for the dye used in both cases was based on the most contrast between the colors in the split channels (red) command in the FIJI software. This decision would facilitate data collection and observation of media switching in the chamber. Before starting the experiment, both syringes were primed by injecting fluid into the tubes making both plungers reach the 30 mL mark of the syringe. The other important factor in preparation was the Arduino Software (Experiment 1), in which both variables `motor1_interval` and `motor2_interval` were set to 360000 (so that the "On" and "Off" intervals are both 5 minutes).

The experiment was performed for two different scenarios: (1) 5 minute interval for each pump, and (2) 5 minute pump 1 running (media with no drug, green dye) and 10 minutes pump 2 running (media with drug, red dye).

In order to facilitate the user perception and observation of pumps switching and the new colored media flowing into the chamber, an LED light was placed next to the experiment.

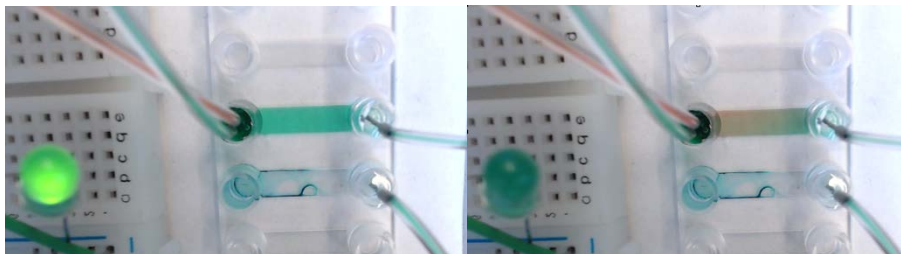


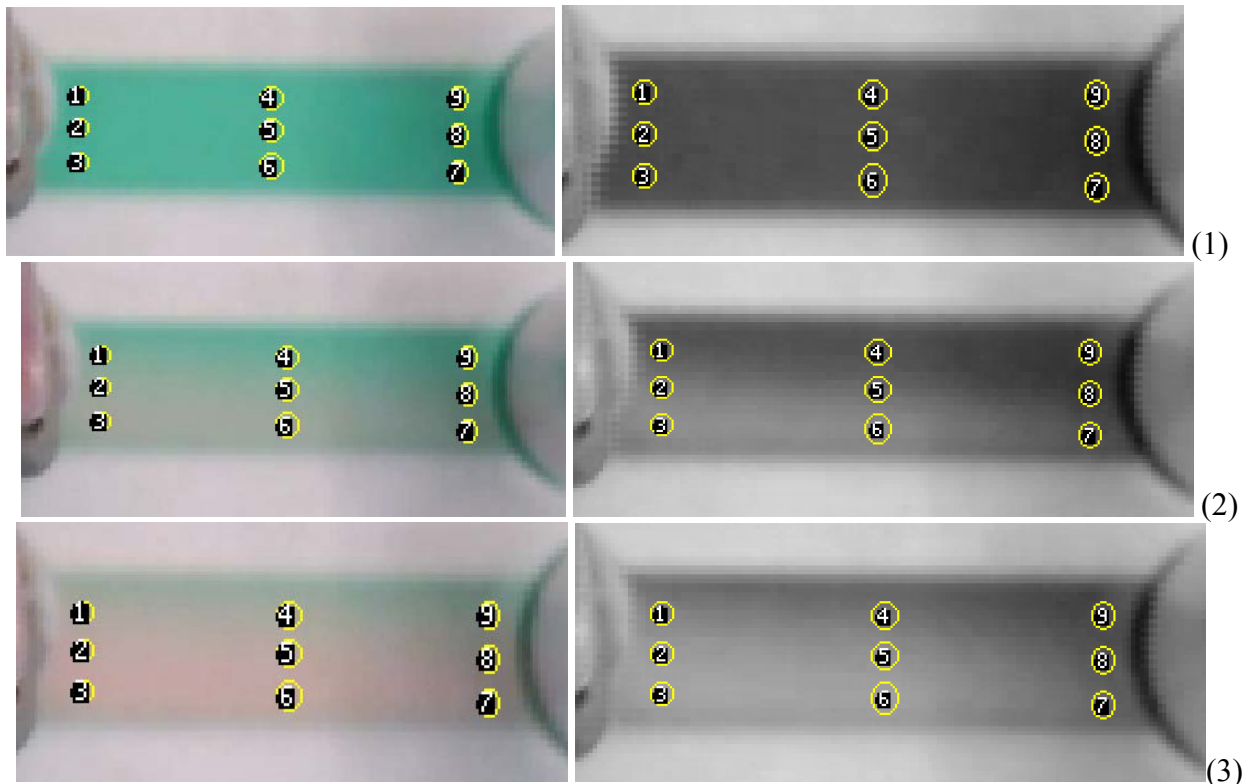
Figure 32: Pump 1 on (green dye), LED light on. Pump 2 on (red dye), LED light off

As shown in Figure 7 above, while pump 1 is running according to the code, the LED light turned on, and while pump 2 was running it would turn off. This would allow the user to observe if for example at the exact moment the LED turned off, the red dye fluid started flowing

inside the chamber. The video taken demonstrates that by observation; when the light runs off, the red dye media started flowing. More accurately, quantitative measurements and results are demonstrated in the following section 6.4.1.

5.3.1 Switch Response at 5 min Interval for the Two Pumps Alternating

This experiment was performed to analyze how accurate pump switching response occurs inside the chamber with respect to the code's input. The WebCam recorded a 30-minute video in which each pump ran three times on a 5-minute interval. The video was converted into .tif images as a readable format for FIJI, in which the Region of Interest (ROI) tool was used to analyze the intensity of color at various regions throughout the microchannel. For accurate measurements in FIJI, the video was started at the exact moment the code was uploaded to the Arduino, making both the video and code run in parallel. The regions of interest were selected as shown in the figure below.



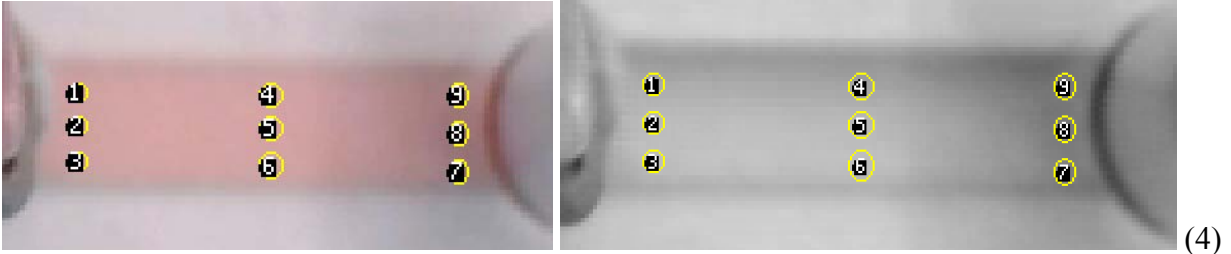


*Figure 33: **Regions of Interest selection at different timepoints of fluid passing through the chamber.** (1) Pump 1 with green dye media running. (2) Switch occurs, Pump 2 starts running at 5 min time point. (3) Delay in having uniform media distribution. (4) Complete uniform distribution of Red dye media achieved.*

In Figure 33, the four different images represent four different timepoints, regarding the switch response of fluid changing and uniform distribution in the chamber. It can be observed that the Regions of Interest 1, 4, and 9, at the top row of the chambers are the ones in which the red dye medium takes longer to reach. In result, Figure 34 demonstrates that those three regions have a lower green intensity color than the rest of the regions when the red dye medium is flowing through the chamber. In order to interpret the graph data, it is important to note that green intensity close to 0 represents higher intensity (darker), and larger numbers for green intensity represent lower intensity (lighter color, red in this case). Therefore, the intensity of green in the three regions of the top row at the microfluidic chamber contain a lower number near the 160s of green intensity, while the rest of the regions reach the 210 since the beginning of the experiment.

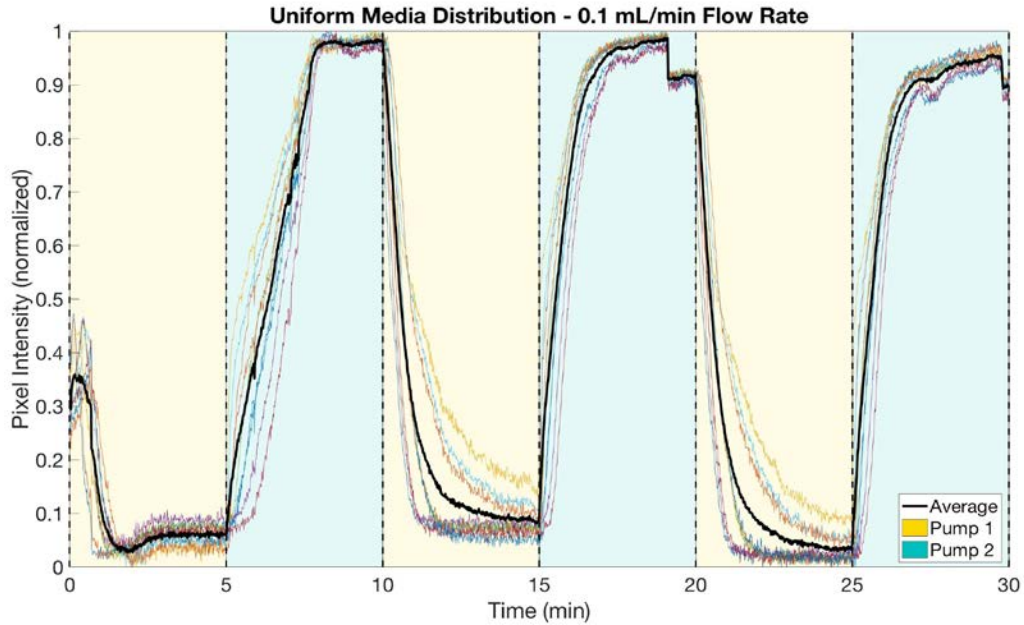


Figure 34: 0.1 mL/min FR 5-minute interval switching of pumps.

The same procedure was performed for the 0.05 mL/min and 0.02 mL/min flow rate. However, the slower the flow rate, the longer it took for uniform media distribution at the chamber to be achieved. Figure 35 demonstrates the behavior of media distribution as response of switch for the 0.05 mL/min.

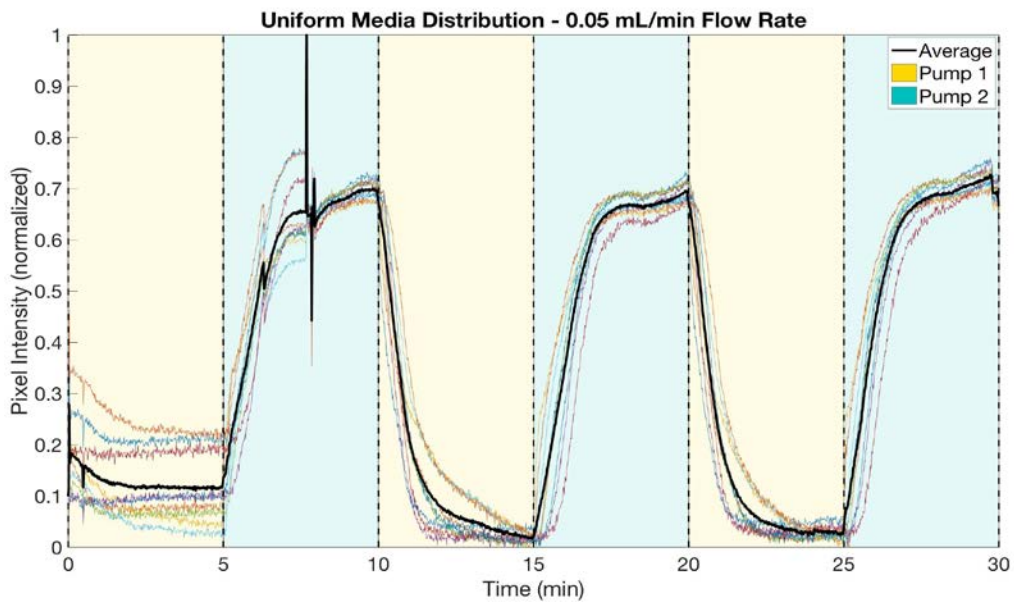


Figure 35: 0.05 mL/min Flow Rate 5-minute interval switching of pumps.

In Figure 35, the regions of interest 7, 8, and 9 correspond to the ones with lower green intensity values, which still makes sense to the images in Figure 33 (2). In this image it can be observed that the last column regions were the last to get the new media distributed. These had similar values, around the 150 s, to the lower green intensity regions for the 0.1 mL/min flow rate (1, 4, 9).

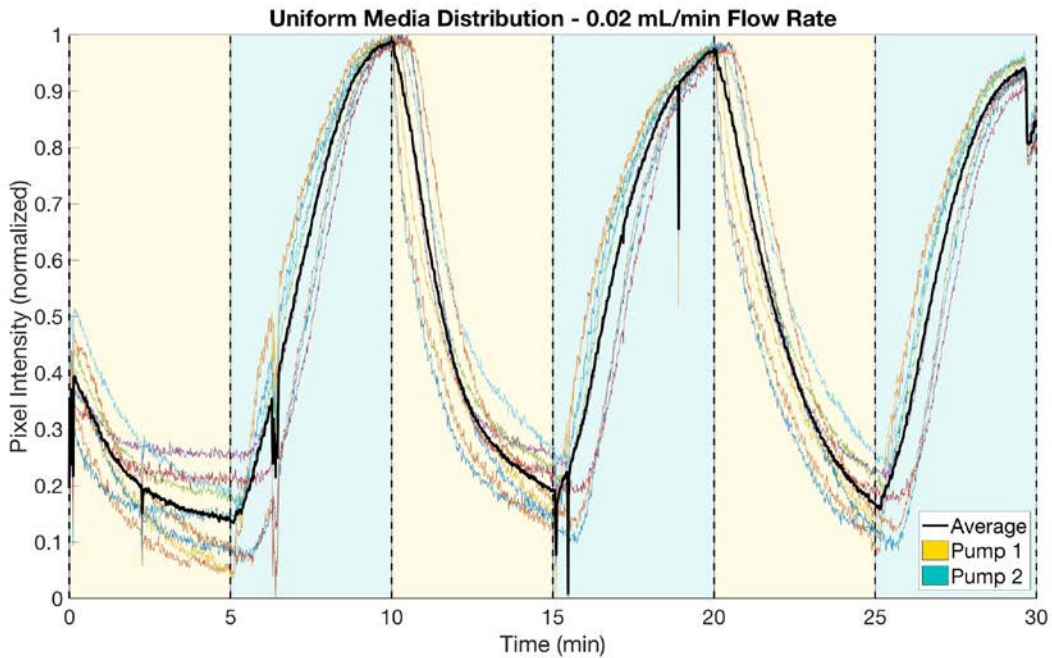


Figure 36: 0.02 mL/min Flow Rate 5-minute interval switching of pumps.

In a similar manner, regions 7, 8, 9, in Figure 36 are those with a lower intensity. In this case the 0.02 mL/min flow rate has very little period of time in which the graph behaves in a table top manner as the previous flow rate graphs.

The graph below represents all three experiments performed with different flow rates in one single graph.

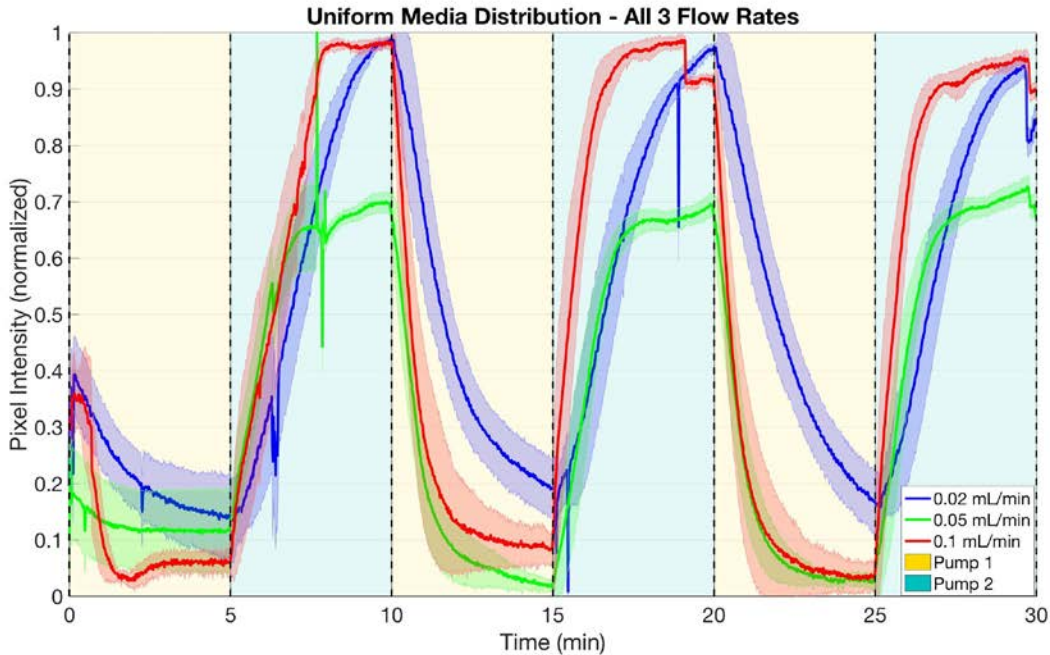


Figure 37: Switch Response for the Three Flow Rates Tested

Figure 37 demonstrates the mean of all three flow rates that have been evaluated. In this graph, it can be seen more clearly how as the flow rate decreases, the complete media distribution for the entire interval each pump is running decreases. This can be also seen by the difference between the green intensity levels of green dye is flowing (lower end of the graph) and red dye flowing (upper ends of the graph, which decreases with lower flow rates, meaning there is less of a clear differentiation between medias flowing through the chamber.

Even though this data allows the team to determine if there is an accurate switch on each pump alternating, it does not allow us to calculate the possible lag time that exists from the switch generated by the code, and the actual switch observed in the chamber.

5.3.2 Switching Response Lag Time in Chamber Test

The main purpose of this test is to calculate the lag time, τ , and τ_{max} of the pump switch response in the channel. This experiment was generated for 5 minutes of Pump 1 with green dye running and 10 minutes for Pump 1 with red dye running. The lag time corresponds to the time difference from which the code indicated the switch and the actual moment the switch occurs in the chamber. τ corresponds to the time difference from timepoint to switch by the code, and the middle value of the slope. τ_{max} corresponds to the difference in time between

the time of switch by the code and the maximum value of time when new media has completely distributed in chamber.

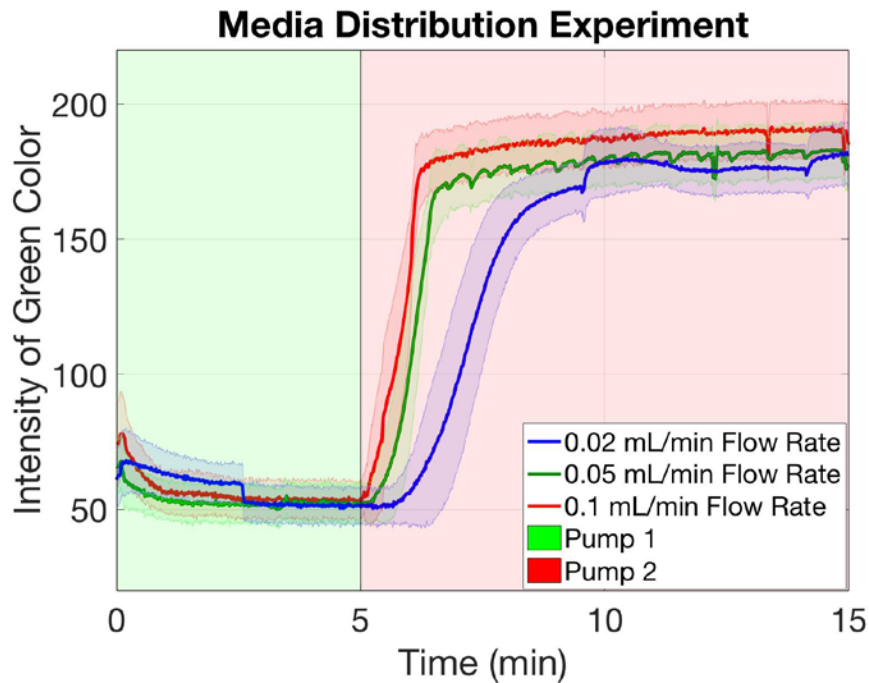


Figure 38: Switch Response for Lag Time Measurements

Figure 38 demonstrates that none of the flow rates tested have an immediate switch response in the chamber when indicated by the code. However, it is notable that as the flow rate decreases, then the lag time, τ and τ_{max} increases. These values were calculated based on the coordinates of the points of interest for this analysis. The coordinates are used for the analysis are shown in Figure 38.

The method used to calculate these values, is not the most convenient. Human error might be involved in selecting values and perception among humans might influence. Therefore, a proposed solution is given by analysis of these values by utilizing MATLAB.

The tables below summarize the behavior of the fluid at switch response for each of the flow rates tested.

Table 26: Lag Time between code switch command and actual time media starts flowing

Flow Rate (mL/min)	Time Switch in code (min)	Time Drug media starts flowing in chamber (min)	Difference between Code time and Actual time of switch (Δt) Lag Time
0.1	5.0	5.005	$5.005 - 5.000 = \mathbf{0.005}$
0.05	5.0	5.219	$5.219 - 5.000 = \mathbf{0.219}$
0.02	5.0	5.662	$5.662 - 5.000 = \mathbf{0.662}$

Table 27: Tau - Code switch command and middle point value in slope

Flow Rate (mL/min)	Time Switch in code (min)	Time Drug media starts flowing in chamber (min)	Difference between Code time and mid-point value of the slope: Tau
0.1	5.0	5.842	$5.842 - 5.000 = \mathbf{0.845}$
0.05	5.0	6.072	$6.072 - 5.000 = \mathbf{1.072}$
0.02	5.0	7.172	$7.172 - 5.000 = \mathbf{2.172}$

Table 28: Tau max- Code switch and moment media completely distributed in chamber

Flow Rate (mL/min)	Time Switch in code (min)	Time Drug media starts flowing in chamber (min)	Difference between Code time and Actual time: Tau time
0.1	5.0	6.351	$6.351 - 5.000 = \mathbf{1.351}$
0.05	5.0	6.991	$6.991 - 5.000 = \mathbf{1.991}$
0.02	5.0	9.765	$9.765 - 5.000 = \mathbf{4.765}$

The flow rate of 0.02 mL/min presented the highest lag time, tau, and tau max. It is under discretion of the client to decide if lag time is within the acceptable range or not.

In a similar approach as in Section 5.2 where the relationship between flow rate and motor delay was determined, the relationship here between flow rate and response time was also found. The curve fitting tool in MATLAB was implemented once more. The flow rate (mL/min) was the x-variable, while the response time (min) (either lag time, tau, or tau max) was the y-variable. For reference, lag time is defined here as the time between the moment when the switch between pumps is made and the moment when media starts entering the chamber. Tau is defined as the midpoint value of the increasing slope (i.e., time to 50% pixel intensity). Tau max is defined as the time between the moment when the switch between pumps is made and the moment that the new incoming media completely fills and is distributed across the entire chamber.

Curve fitting was performed according to the equation $y = k/x$. For lag time, the relationship was found for an inverse relationship:

Equation 5.2

$$y = f(x) = \frac{k}{x} = \frac{0.0125}{x}$$

with an R-square value of 0.9255, indicating a good fit by this equation to the data. The graph of this relationship can be seen below.

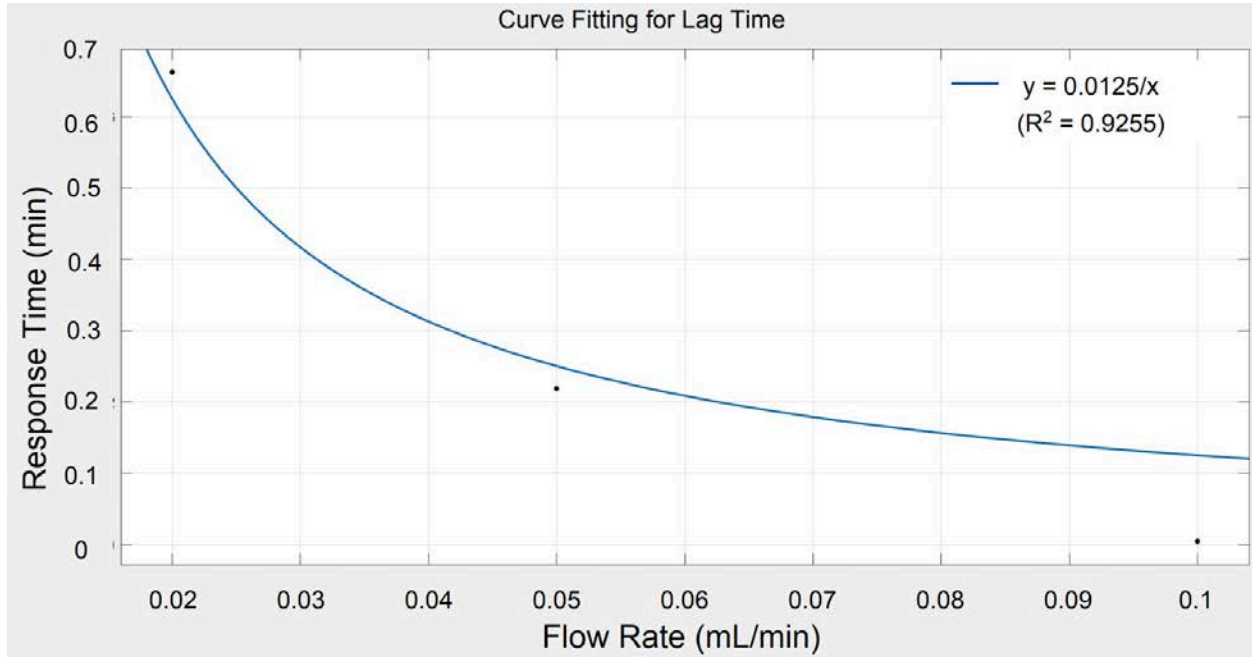


Figure 39: Curve Fitting for Lag Time

For tau, the curve fitting yielded the following result:

Equation 5.3

$$y = f(x) = \frac{k}{x} = \frac{0.0462}{x}$$

with an R-square value of 0.814, indicating a relatively good fit by this equation to the experimental data, although not as close as the previous equation. The graph of this relationship can be seen in the following plot.

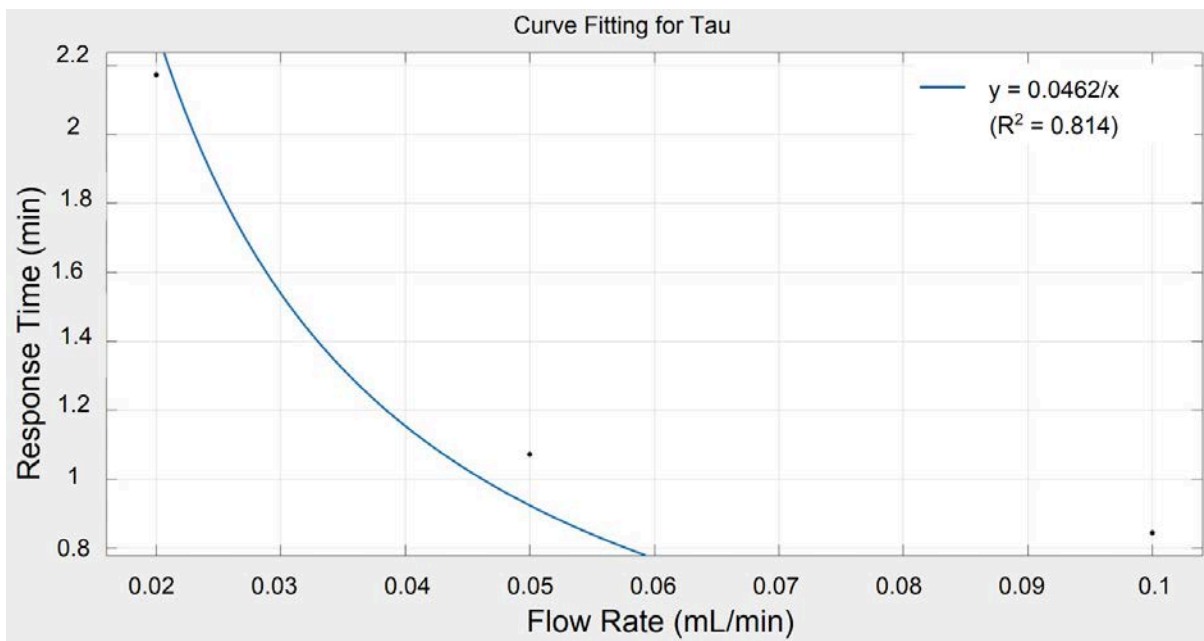


Figure 40: Curve Fitting for Tau

Finally, for tau max the curve was modeled in a similar manner to the curve for tau:

Equation 5.4

$$y = f(x) = \frac{k}{x} = \frac{0.0972}{x}$$

with an R-square value of 0.977, indicating again a very good fit by this equation to the experimental data. This relationship can be visualized in the following graph.

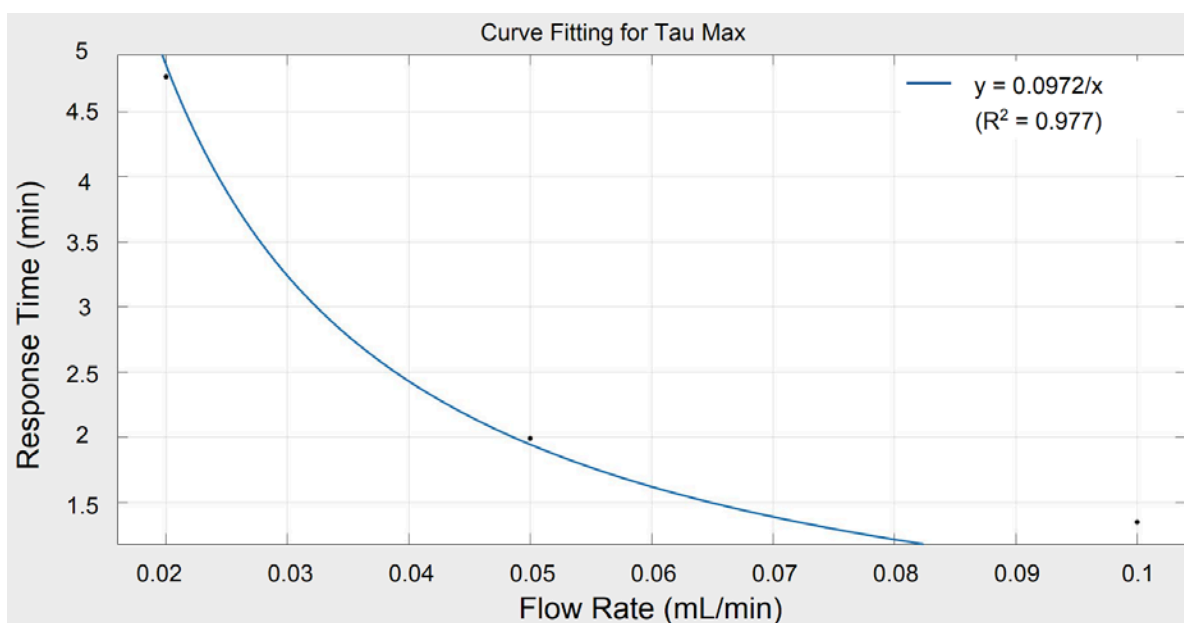


Figure 41: Curve Fitting for Tau Max

To demonstrate the usefulness of these equations, an example calculation can be performed. A hypothetical situation would be to predict the response times for a very fast flow rate of 1 mL/min. Then, the calculations would be:

$$y = \frac{0.0125}{1 \text{ mL/min}} = 0.0125 \text{ min} = 0.75 \text{ seconds}$$

$$y = \frac{0.0462}{1 \text{ mL/min}} = 0.0462 \text{ min} = 2.77 \text{ seconds}$$

$$y = \frac{0.0972}{1 \text{ mL/min}} = 0.0972 \text{ min} = 5.83 \text{ seconds}$$

For this flow rate of 1 mL/min (which would allow a 30 mL syringe to last for 30 min), the theoretical lag time is 0.75 seconds, so it will take 0.75 seconds for the media to start flowing into the chamber after the switch between pumps is made. For tau the response time would be 2.77 seconds, which means this is the time point at which the pixel intensity reaches half of the max. For tau max the response time would be 5.83 seconds, which means this is the amount of time it would take for the chamber to be completely filled with the new incoming media after the switch between pumps is made. These values show that for a very fast flow rate, response times can be predicted based on the experimental data, and that they would occur very quickly.

Another hypothetical situation would be to predict the response times for a slow flow rate of 0.01 mL/min (which would allow a 30 mL syringe to last for 3000 minutes, or 50 hours which is longer than 2 days). The calculations would be:

$$y = \frac{0.0125}{0.01 \text{ mL/min}} = 1.25 \text{ min}$$

$$y = \frac{0.0462}{0.01 \text{ mL/min}} = 4.62 \text{ min}$$

$$y = \frac{0.0972}{0.01 \text{ mL/min}} = 9.72 \text{ min}$$

In this case, the theoretical lag time is 1.25 min, the response time for tau is 4.62 min, and the response time for tau max is 9.72 min, with the same respective conclusions as mentioned previously for the 1 mL/min flow rate. These values show that for a very slow flow rate, response times can be predicted based on the experimental data, and that they would occur very

slowly. Overall, this model can help the user to select a desired flow rate based on the response time they would like for their particular experiment.

5.4 Flow rate testing and pump system reaction to software commands

The goal of this experiment was to accurately determine the exact relationship between flow rate and the motor delay for the algorithms. Achieving the desired flow rate is a parameter for all the different cases of experiments described in section 5.2. The multi-pump system software controls the flow rate of the fluid by computing the speed of the motor and introducing a delay. In order to provide data and insight on the whole system reaction to software commands on the stepper motors, the flow rate at the outlet tube was measured. The experiment was performed by gently introducing a bubble into the outlet tube, by rapidly extracting the metal connector out of the plug and connecting it again. The pump system was still running allowing the bubble to move through the outlet tube according to the flow rate that was programmed. The flow rates that were tested consist of 0.02, 0.05, and 0.1 mL/min. The outlet tube was marked at every cm and the distance the bubble travelled from the outlet to the end of the tube.

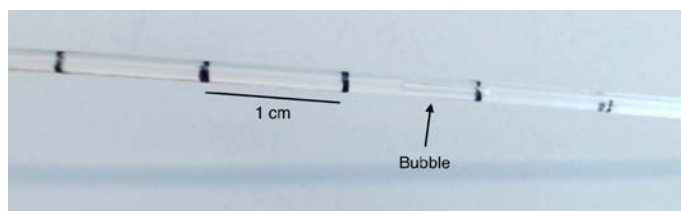


Figure 42: Outlet tube with 1 cm marks and bubble travelling through system

Bubbles were introduced consecutively every 5 second and the team timed the bubbles path during pumps alternation. For the purpose of this experiment, the software was programmed for the pumps to alternate every 30 s. The idea was to confirm bubble flow rate was maintained constant at every time point the pumps switched. The flow rate of different bubbles at different timepoints was graphed as shown below for 0.1 mL/min, 0.05 mL/min, and 0.02 mL/min respectively.

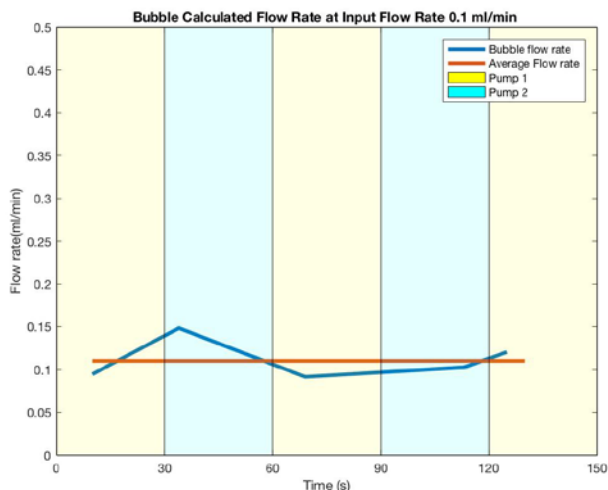


Figure 43: Bubble traveling through outlet tube at software input of 0.1 mL/min

Flow rate 0.1 mL/min was assessed by following the previously described protocol. The background of the graph indicates which pump was working while the distance the bubble traveled was timed to get the velocity of the bubble. Then the internal cross-sectional area of the outlet tubing was utilized to calculate the flow rate of the bubble. The flow rate of the bubbles of the 0.1 mL/min input flow rate in the software seems to stay within 0.09 and 0.15 giving a mean of 0.11 mL/min and a standard deviation of 0.023. The coefficient of variation was then calculated as indicated in Table 29 which summarizes the values for all the different flow rates tested. Observations of the graph indicate that possible variation in flow rate are found right after the switch of pump, as in the second time point after 30 seconds the second pump has just started to work the bubble seemed to have an increase flow rate around the 0.15 mL/min.

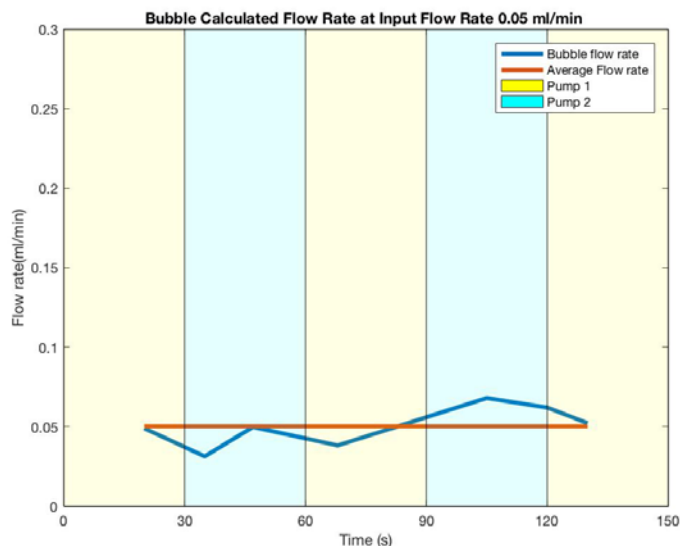


Figure 44: Bubbles traveling through outlet tube at software input of 0.05 mL/min

The procedure for calculating flow rate for the different bubbles that were introduced in the outlet tube was the same followed for flow rate 0.1 mL/min. The bubbles' flow rate seems to stay within the range of 0.03 mL/min and 0.06 mL/min giving an average flow rate of 0.0503mL/min. The coefficient of variation is given in Table 29.

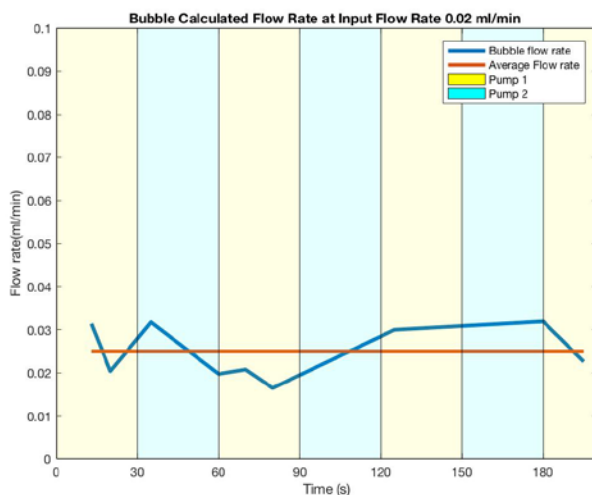


Figure 45: Bubbles traveling through outlet tube at software input of 0.02 mL/min

The bubbles traveling through the outlet tubing at 0.02mL/min flow rate seem to have a larger variation since the flow rate of each bubble under the different pumps working ranges from 0.018 mL/min to 0.03 mL/min. However, the average flow rate all bubbles under different

pumps achieved was of 0.024 mL/min as indicated by the red line in the graph. Again, this graph shows the tendency of bubbles, which flow rate was measured at timepoints right after the switch of pumps have occurred, to have either increasing or decreasing flow rates right at those points instead of maintaining constant flow rate. For example, the bubble measurement taken at 35 s, right after pump 2 had started working has an increase in flow rate to 0.03 mL/min.

The table below represents the coefficient of variation among the flow rates calculated from the bubble's distance travelled through the outlet tube at the different flow rates that had been typed into the system's software.

Table 29: Coefficient of Variation for bubbles' flow rate under different flow rate software input

Flow rate software input	0.1 mL/min	0.05 mL/min	0.02 mL/min
Mean	0.110	0.0503	0.0249
Standard Deviation	0.0234	0.0126	0.00617
Coefficient of Variation(sd/avg)	0.213	0.251	0.247
% Coefficient of Variation	21.3%	25.1%	24.7%

This table summarizes the coefficient of variation for each of the flow rates tested. This indicated that the flow rate 0.1 mL/min has the least dispersion of bubbles' measures flow rate under the different pumps working, making it have the most uniform and constant flow even during the switching of the pumps. This is followed by the 0.02 mL/min and then 0.05 mL/min, However, all of the coefficient of variations are found within the range of 20% and 26% which indicate the dispersion of flow rates calculated for each of the bubbles at the different flow rates tested are very similar. Having a range of variation from 21-25% for the flow rates tested, goes above to the variation presented for peristaltic pumps in Chapter 2, which was 11% for a higher range of flow rates. Even though it was not proven for this syringe pump to be better regarding keeping constant fluid, the reason for this could be the testing was done manually and human error can be involved, as well as this pump system is a Do-It-Yourself, which does not have the same capacities as those commercially available. Therefore, the commercially available

peristaltic pump with 11% variation in pulsation is not comparable with this Do-it-yourself syringe pump [11].

5.5 Experiment 2 Code

The Arduino code for Experiment 2 went through multiple iterations. The first version of the code calculated the ratio of steps for each motor that would be needed to deliver the desired concentration. For example, if the user desired a drug concentration of 75%, then the code would calculate that motor 1 (which controls the drug) will execute every 3 steps for every 1 step that motor 2 (which controls normal media) will execute, since a 3:1 ratio is analogous to 75%. The code would then calculate the delay based on the desired flow rate, using the aforementioned relationship between flow rate and motor delay. Each motor would deliver its corresponding number of steps all at once in succession, without any delay between each step. The delay would only be introduced after each motor delivered its calculated number of steps. For example, for a 75% concentration, motor 1 would deliver 3 steps, motor 2 would simultaneously deliver 1 step, and the delay would be inserted after both of the motors have completed these steps.

This method seemed reasonable because the pump would be delivering both types of media at the same time. Additionally, because of the way in which the media is delivered (with some force behind it), the media could have some mixing of fluids involved. The concern with this method is that it could introduce a large amount of pulsatile flow. For example, if the user required a 90% concentration, the motor 1 would deliver 9 steps all at once while motor 2 simultaneously delivered 1 step. Those 9 steps delivered by motor 1 occur very quickly, and could then introduce large pulses in the flow. This would not only affect the outcome of the biological experiments (which require flow that is as continuous as possible), but could also affect the viability of cells, which are sensitive to large amounts of shear stress.

The second version of the code was similar to the first, with one difference. Instead of inserting the delay after both motors had completed each set of steps, the delay was inserted between each step within the set. This means that the motors did not run at the same time, but rather took turns to run. For example, if the desired concentration was 75%, motor 1 would move one step, wait for the delay period, move a second step, wait for the delay period, move the third step, and wait for the delay period. After this, motor 2 would move 1 step and wait for the delay period, after which motor 1 would start running again in the same manner. This allowed the pulsatile nature of the flow observed in version 1 of the code to be significantly reduced.

However, this introduced another issue. If, for example, the desired concentration was again 90%, then motor 1 delivering 9 steps (with delays inserted in between each step) would take a larger amount of time, before motor 2 could even deliver its 1 step. This means that the cells in the microfluidic chamber would likely be exposed to pure drug concentration for the duration of motor 1 running, rather than a mixture of the two medias at the desired 90% concentration, since normal media is only added after motor 1 has completed running. Evidently, a different method was needed.

For the third and final version of the code, the AccelStepper.h library was required to allow smooth, continuous of both motors simultaneously. The library enabled this capability. Instead of calculating the correct ratio of steps based on the desired concentration, this version of the code would calculate the correct ratio of speeds based on the desired concentration (note the sum of the two rates is equal to the overall desired flow rate). For example, if the desired concentration was a 75% concentration, then motor 1 (controlling the drug) would move at a speed that is 3 times faster than the speed at which motor 2 runs, to still achieve the 3:1 ratio. With this library, the speed is dictated in steps per second (so the ratio of the steps per second for motor 1 to motor 2 would be 3:1). This code was the most successful, because it allowed for both smooth, continuous movement of both motors simultaneously, and for achieving the correct concentration by controlling the speed of the two motors. This was also the version of code used for the testing of the Experiment 2 code. All Arduino code can be found in Appendix A.

5.6 Concentration Testing

The most important part about testing Experiment 2 code was verifying that the drug concentration produced by the pump was equivalent to the desired concentration input by the user into the Arduino code. This would confirm that the code itself was working correctly, and that the pump could indeed enable biological experiments for Experiment 2: Constitutive Level. Multiple different testing methods were used to confirm drug concentration produced by the pump.

5.6.1 WebCam Concentration Testing

The first method of testing used a method similar to the Switch Response Testing. The goal of this test was to verify that the desired drug concentrations could be produced the desired in the microfluidic chamber, by using colored dyes and a WebCam. One BD 30 mL syringe was

filled with water, while the other was filled with a water solution dyed with dark blue food coloring. In the microfluidic chamber, one channel was filled with a 100% concentration (i.e., undiluted) sample of the dyed water. The channel next to the first was filled with a manually mixed sample of known 50% concentration. The channel next to the second was not filled with any liquid, but the inlet and outlet plugs were inserted; this channel would be the target 50% concentration. In other words, the first two channels served as reference channels, and the third was the channel to be observed for proper concentration. After setting up the pump and priming the tubes, the Arduino code for Experiment 2 was uploaded, and the WebCam was started. The pump ran for approximately 20-25 minutes, with the microfluidic being recorded the whole time. At the end, the .avi video file was converted to a series of .tif images using a MATLAB script.

ImageJ was used to select the ROIs in each channel and analyze the intensity of color at various regions throughout the microchannel. The goal was to compare the numerical results of the known 50% channel and the target 50% channel, to see if the pump was in fact producing the correct concentration. Below in Figure 46 is the setup of the microfluidic chamber as well as the ROIs.

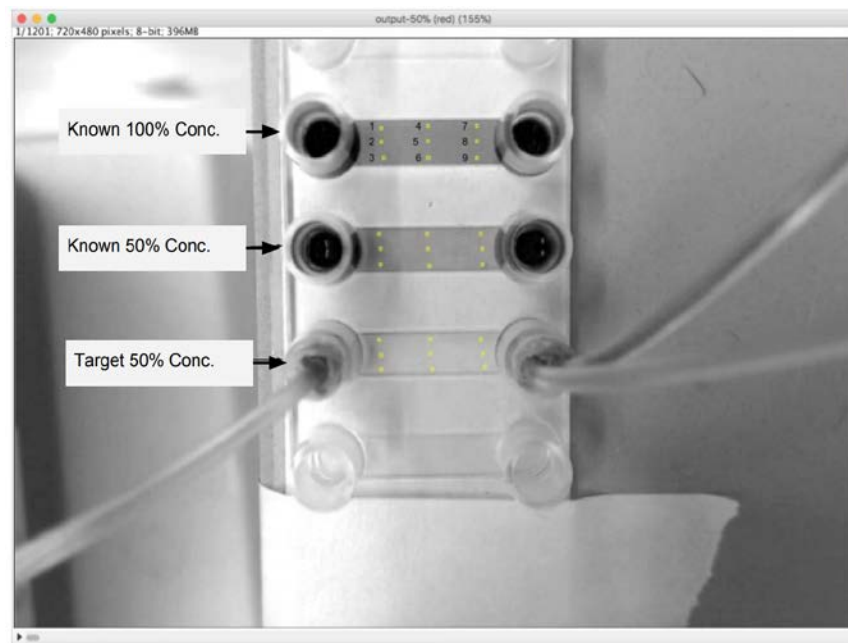


Figure 46: The setup of the microfluidic chamber for the WebCam Concentration Testing experiment. The ROIs for each are shown. Note that the ROIs for the second and third channels were selected in the same order as for the first channel.

The MultiMeasure tool was then used to measure the color intensity for the ROIs at all time points. The values for color intensity were then plotted against time.

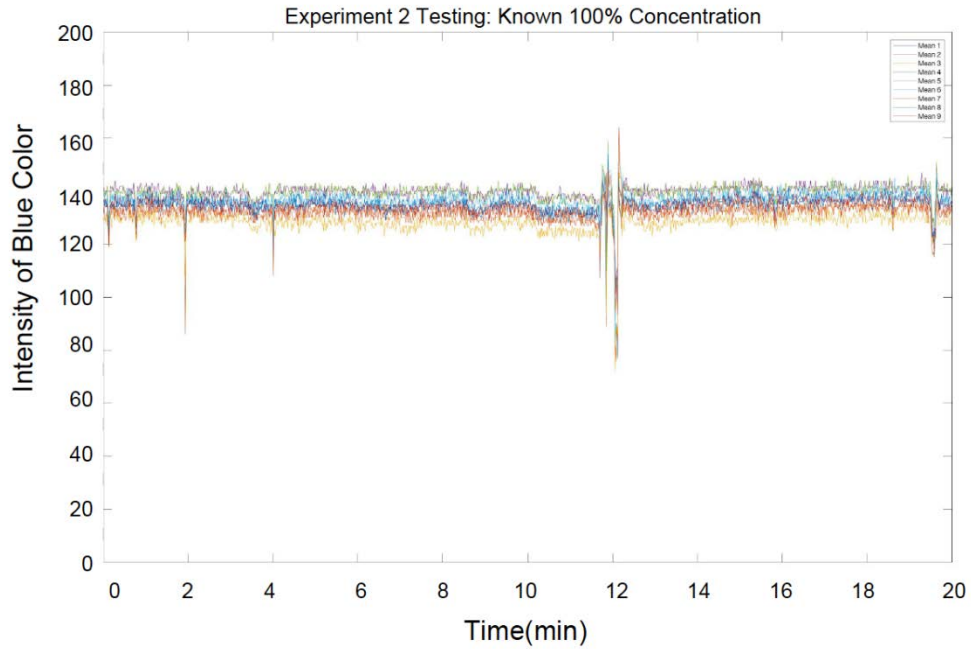


Figure 47: Color Intensity for the Known 100% Concentration

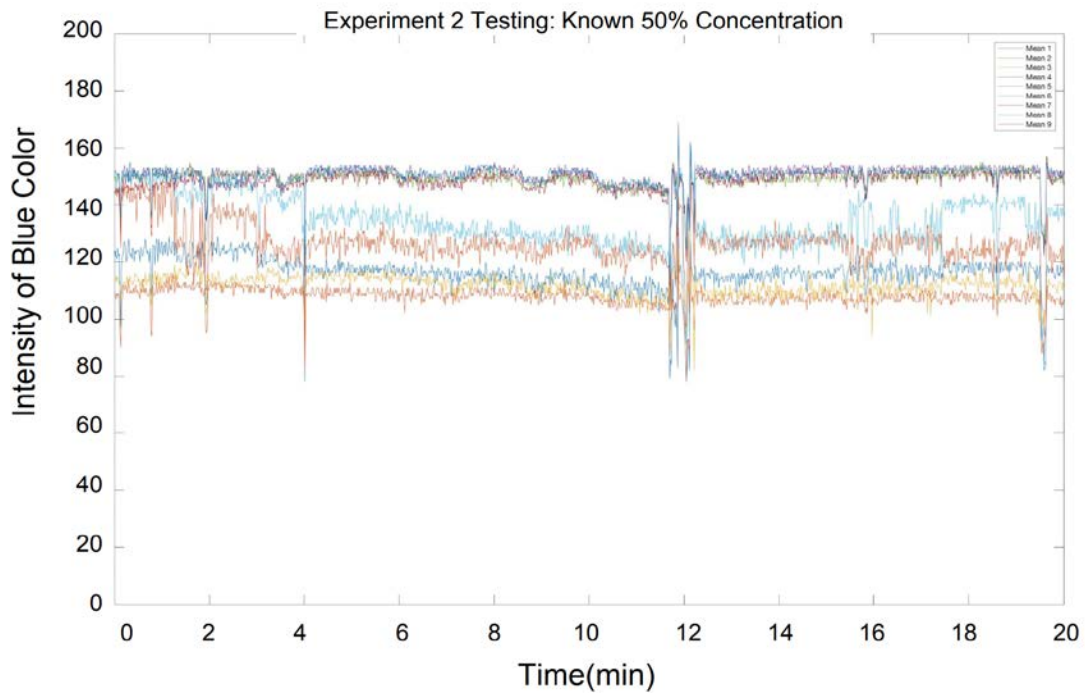


Figure 48: Color Intensity for Known 50% Concentration

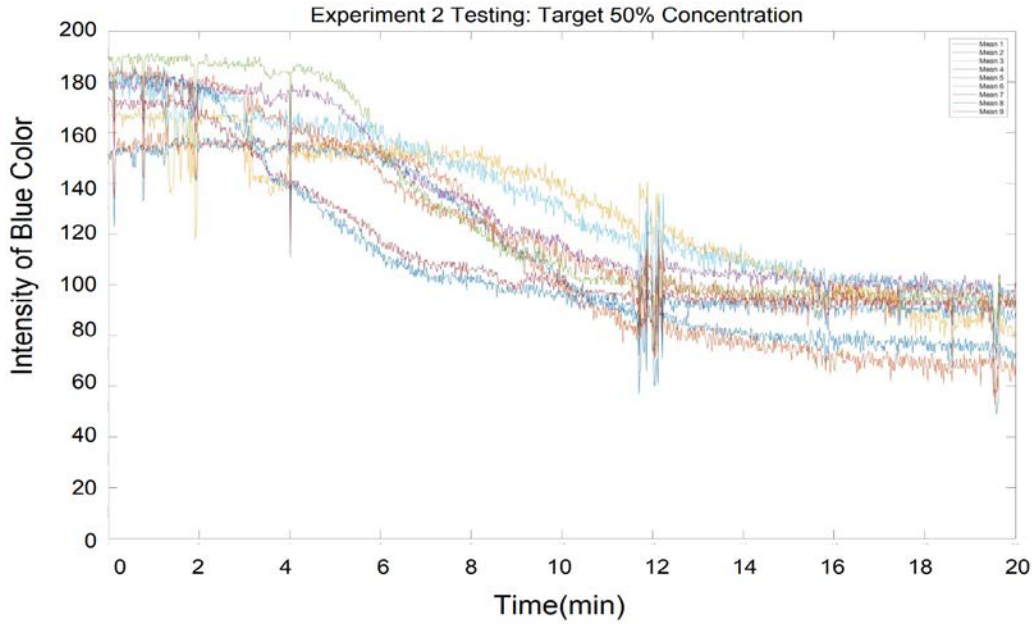


Figure 49: Color Intensity for Target 50% Concentration

The color intensity for the known 100% concentration (i.e., undiluted blue-dyed water) was around 140. The color intensity graph for the known 50% concentration had more noise, but the color intensity ranged from 110 to 150. These numbers demonstrate that there wasn't a large difference in pixel intensity when comparing the known 100% and 50% concentrations, which is a confirmation of the visual results; when visually observing the two channels, it was very difficult to note the difference between the known 100% color and the known 50% color, which can be seen below in Figure 50.

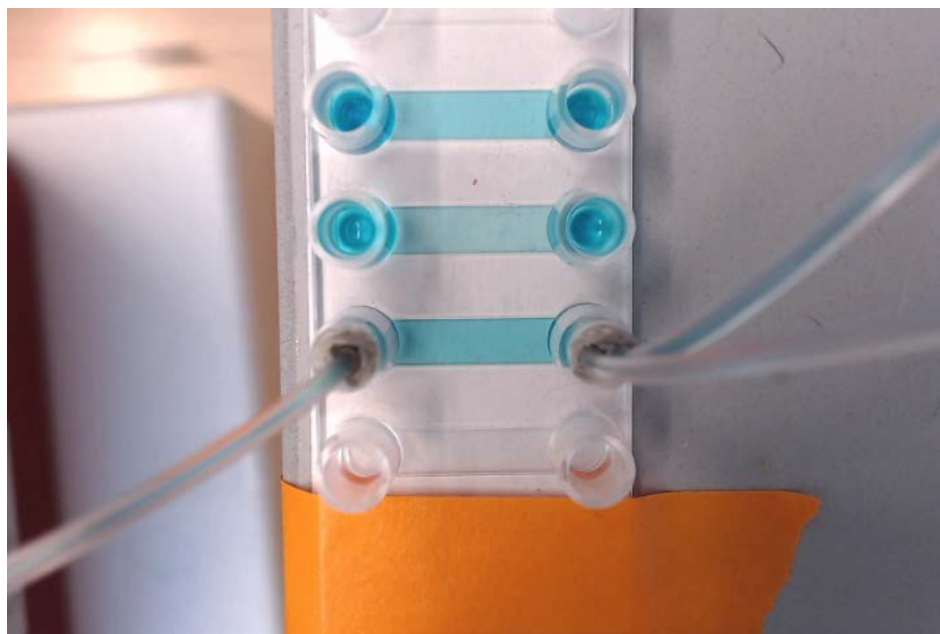


Figure 50: The microfluidic chamber at the end of the experiment. The colors in the top (known 100%) and middle (known 50%) channels are difficult to differentiate, suggesting that there is not a huge difference in color intensity; this was confirmed with the graphical results. The bottom channel (target 50%) appears darker than the other two channels.

For the target 50% channel, the color intensity started at very large values because the channel was empty and thus devoid of color. As the experiment continued, the color intensity began decreasing; this is indicative of the colored media as it begins to fill the channel over time. Finally, the color intensity near the end of the video, at which point the dyed water had completely filled the chamber was between 60 and 100. This is clearly not a match for the known 50% concentration, which had values ranging between 110 and 150. Furthermore, these values are even smaller than the known 100% concentration. This means that, overall, the color of the target 50% concentration was darker than both the known 50% and known 100% concentrations, which doesn't make sense intuitively and should not be possible. However, this can also be seen above in Figure 47, where the color of the liquid in the bottom channel seems darker than the first two channels.

Because of these unexpected results, a second trial for 50% concentration was performed, this time using a darker blue dye to try and make the color intensity easier to interpret. When the Split Channels option is opened in ImageJ, there are three different options (blue, red, and green); the analysis for this trial was performed using the green channel (previously, it had been

performed using the red channel). This is because, as a result of using darker dye, the red channel did not give much contrast between the microfluidic channels, as can be seen below in Figure 51. The green channel provided much better contrast between the microfluidic channels, so that was used for the analysis instead (see Figure 48).

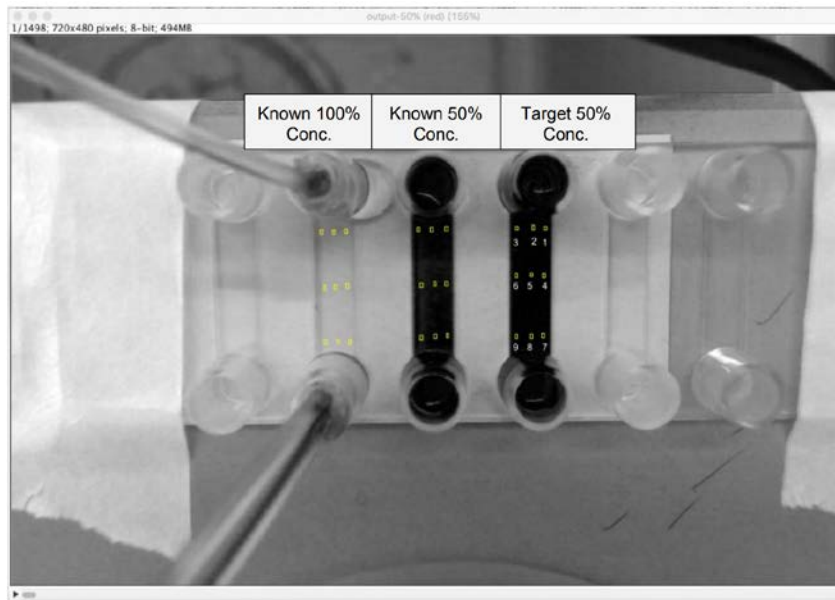


Figure 51: The red channel in ImageJ. The color intensity is so dark for it is hard to differentiate between the two reference channels on the right.

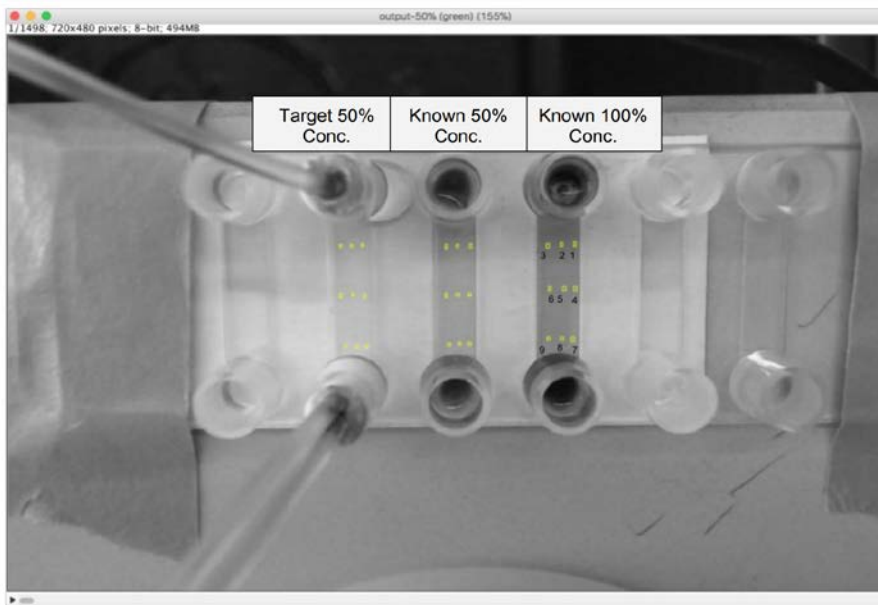


Figure 52: The green channel in ImageJ. The color intensity between the two reference channels on the right have better contrast.

The same method of analysis was used to measure the color intensity of the selected ROIs and graph the results. In this experiment, the sample from the pump was much closer to the control 50% concentration.

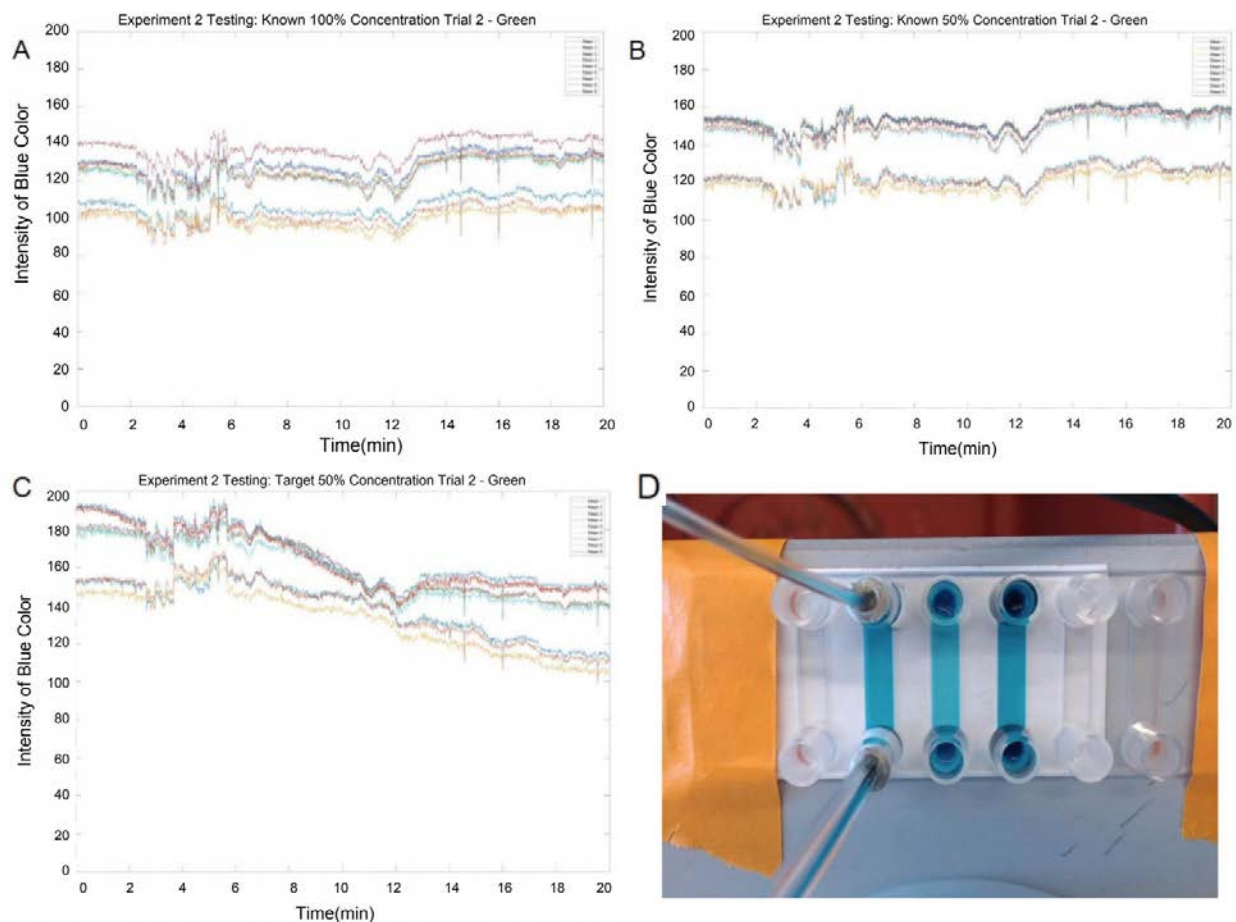


Figure 53: The results from the second trial of the 50% WebCam Concentration Testing. (A) Color intensity for the known 100% concentration, (B) Color intensity for the known 50% concentration, (C) Color intensity for the target 50% concentration, (D) Microfluidic chamber at the end of the experiment. The target 50% channel is darker than the known 50% channel but about the same color as the known 100% channel.

The results for the second trial were also inconclusive. The two reference channels for known 100% and known 50% concentrations produced very similar color intensities, as can be seen in the graphs. Additionally, while the target 50% channel at the end of the experiment was much closer to the known 50% channel in terms of color intensity, the visual difference between the two channels in the microfluidic is clear (see Figure 53).

A test was also run for a 75% concentration. In this test, the camera was accidentally moved, which shifted the ROIs at a time point about halfway through the video. To compensate for this bit of human error in the experiment, the video was split in two (at the time point where the shift occurred), and ROIs were chosen for each section separately, but at approximately the same locations.

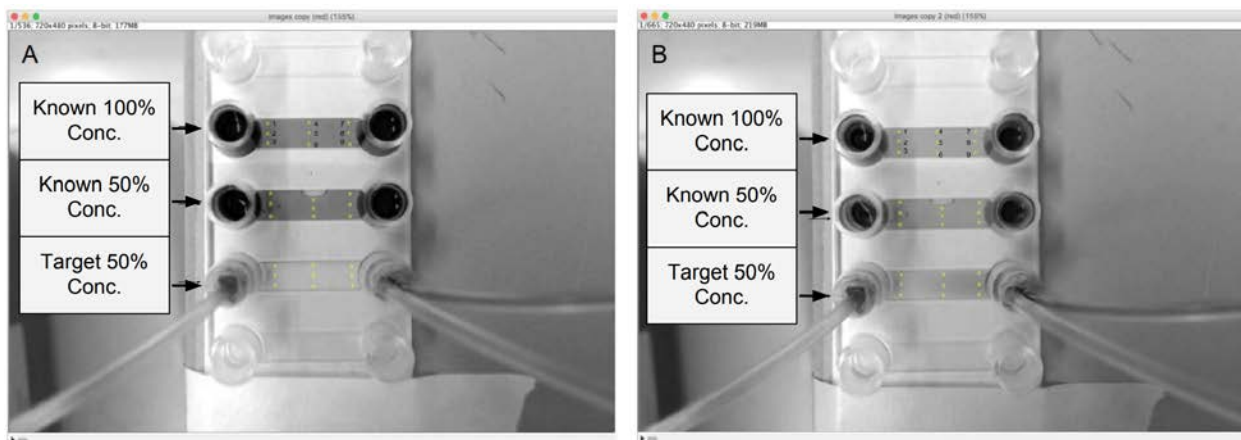


Figure 54: The ROIs for the microfluidic chamber. (A) The ROIs before the camera was moved. (B) The ROIs after the camera was moved. Notice that the movement of the camera caused colors to appear darker in (A) and lighter in (B).

The analysis was then performed similarly to before. The data for color intensity was obtained separately but was then concatenated. The graphical results can be seen in Figure 55.

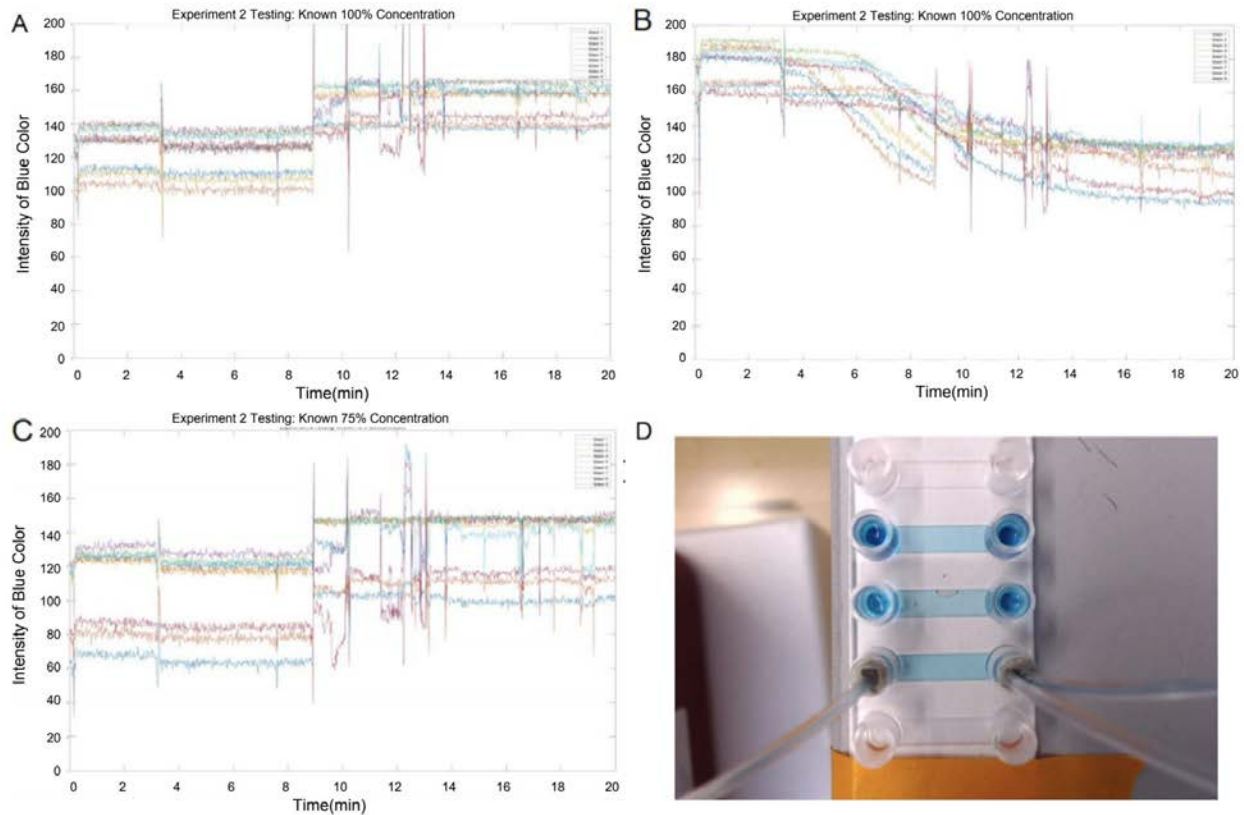


Figure 55: The results from the 75% WebCam Concentration Testing. (A) Color intensity for the known 100% concentration, (B) Color intensity for the known 75% concentration, (C) Color intensity for the target 75% concentration, (D) Microfluidic chamber at the end of the experiment. The three channels are difficult to differentiate by color.

In this experiment, the sample from the pump (target 75%) was much closer to the control 75% concentration. However, it does appear a tiny bit darker, which is represented in the data since the color intensity at the end of the experiment is lower for the target 75% concentration than for the known 75% concentration. The sudden shift in data points is due to the movement in the camera in the middle of the experiment. The shift in values corresponds to the shift because, when the camera was moved, the perceived color of the blue in the channel became lighter than before the camera was moved, as indicated by the sudden increase in values following the shift.

There were many complications encountered during this test, including:

1. Poor lighting will introduce shadows over the microfluidic chamber.
2. It was difficult to ensure a good capture of 3 channels side-by-side.

3. After consulting with advisors, it was noted that analysis based on pixels may not be accurate when using dyes, especially in cases where the analysis is based on the difference between colors. If the difference is small, it may be more difficult to confirm, especially if the camera resolution is poor.
4. The difference in color between the control 100% and the control 50% concentrations was difficult to see (due to a lighter blue dye).

Potential solutions to the aforementioned problems include:

1. Using the WormTracker Behavior Recording System from Albrecht Lab to provide a uniform, constant lighting from beneath the chamber and a steady video recorder above the chamber.
2. Using the microscope incubator in the lab to measure degree of fluorescence in the channel.
3. Using a different method of concentration confirmation, such as glucose concentration testing, conductivity of different salt concentrations using an electrode, etc.

All of these solutions were brainstormed with the help of advisor consultation. Some of these alternative methods were then explored, since concentration was still unconfirmed following this testing.

5.6.2 Glucose Concentration Testing

The main goal of this test was to verify that the code itself was working properly. This was done by testing if the desired concentrations could be produced by the pump, by using glucose solutions, a glucose meter, and test strips. This test did not include the microfluidic chamber. Although it is important to ensure that the correct drug concentration can be applied to cells within the microfluidic chamber, it was still unknown at this point whether or not the code itself was working as desired. Therefore, while this test did not necessarily measure the concentration within the channel, the purpose of this test was to verify that the code itself was working the way it was meant to be when it was written. Once this was confirmed, one variable could be eliminated and the team could then work on making sure the concentration was achieved inside the channel.

This test was performed by first making different glucose solutions. There were some problems encountered with this step.

1. The first glucose solution tested was a pre-mixed solution of glucose and distilled water from one of the research associates in Mitchell lab. This solution was autoclaved and had never been used before. However, when trying to measure the concentration, the glucose meter gave an error message, E11, which means “Abnormal Result” according to the Contour Next Blood Glucose Monitoring System manual.
2. The glucose meter functioned normally with the control solution, which is produced by the manufacturer to test that the meter functions properly.
3. New glucose solutions were made, again with glucose and distilled water. The glucose meter still gave the error message.
4. Different approaches were implemented to make the glucose meter work, including dilutions of the glucose solution so that its concentration is in the range that can be measured by the meter, and trying different solutions with different concentrations.

The problem with the glucose meter was eventually solved. After consulting with Profs. Albrecht and Page, it was confirmed that the glucose needed to be dissolved in a balanced salt solution, since the measurement taken by the glucose meter is based on an electrochemical reaction. To resolve the issue, a new glucose solution was made in DPBS with a target concentration of 500 mg/dL, which is well within the range of operation for the glucose meter (20-600 mg/dL). Upon testing this new solution, the glucose meter successfully measured the concentration at 522 mg/dL.

One syringe was filled with DPBS, while the other was filled with this glucose solution. After priming the tubes and setting up the experiment, the code for Experiment 2 was uploaded to the Arduino. For the experiment, the tubes were placed in a different well of a 96-well plate after every 1 minute, for a duration of 30 minutes. After the experiment ended, a clean micropipette was used to mix the contents of each well, after which the concentration of the solution was measured using the glucose meter.

Four different experiments were conducted, and the results can be seen in Table 30.

Table 30: Summary of the glucose concentration testing results.

Percentage	Expected Concentration (mg/dL)	Average Measured Concentration (mg/dL)	Percent Error (%)
25%	171	170.3	0.409
50% (Trial 1)	294	290.2	1.293
50% (Trial 2)	294	314.8	7.075
75%	448	469.2	4.732

The values for Expected Concentration were obtained by manually mixing 25%, 50% and 75% glucose concentrations and measuring them using the glucose meter. The measured concentrations for each of the 4 tests was found by averaging all 30 measurements to find the mean value; this is the third column in the table. The percent error in the last column demonstrates the comparison between the expected and experimental values. As the values of the percent error are very low, this demonstrates that the code was indeed producing the desired concentrations (when the solutions were mixed). In other words, the code was working as expected. The results can be seen graphically in Figures 56-59, below.

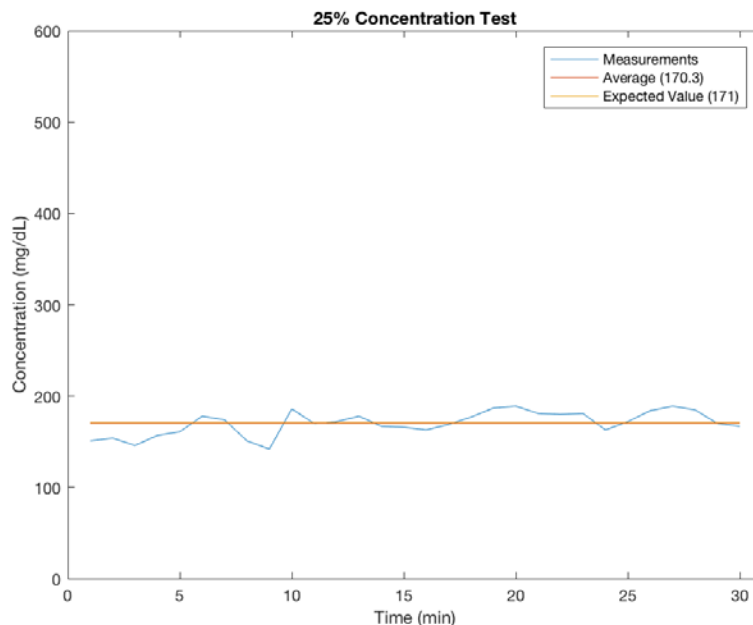


Figure 56: **The graphical results for the 25% Glucose Concentration test.** The blue line indicates measured values, the red line is the average of those values, and the yellow line is the expected value. The percent error was very low, at 0.409%.

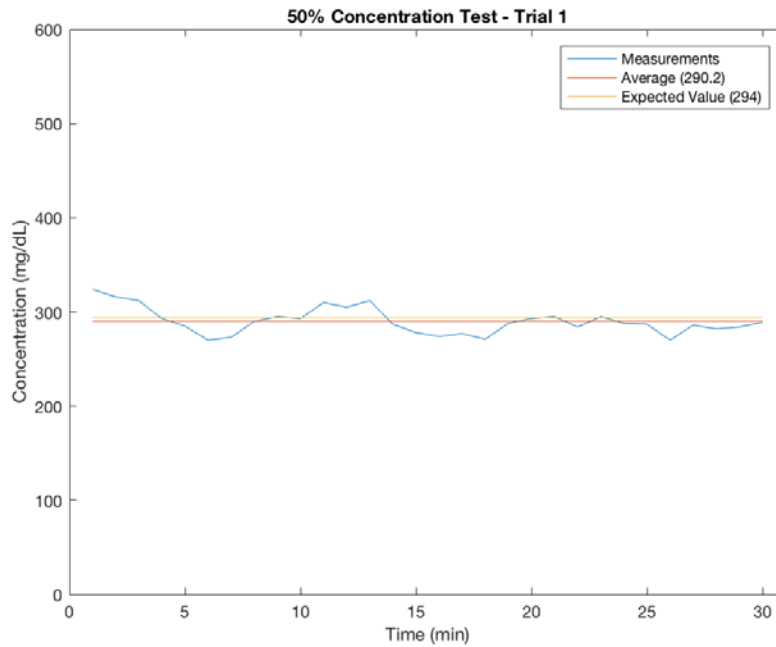


Figure 57: *The graphical results for the first trial of the 50% Glucose Concentration test. The blue line indicates measured values, the red line is the average of those values, and the yellow line is the expected value. The percent error was very low, at 1.293%.*

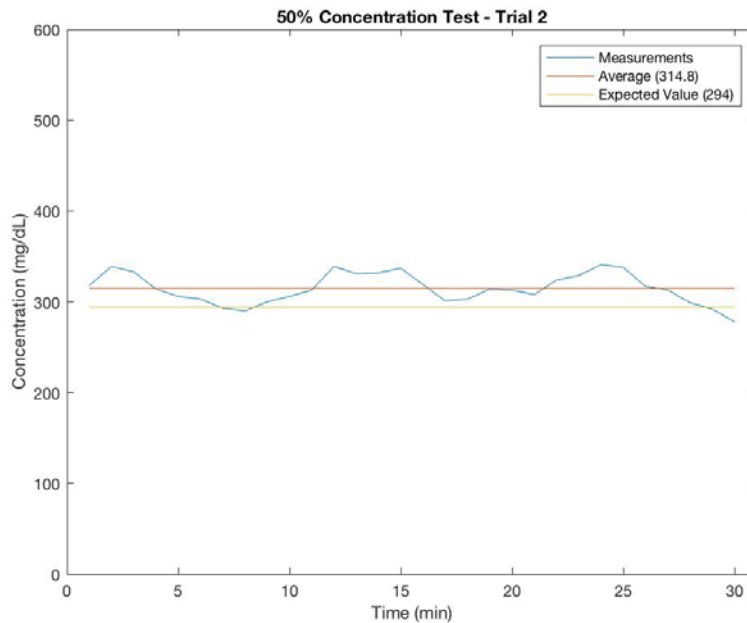


Figure 58: *The graphical results for the second trial of the 50% Glucose Concentration test. The blue line indicates measured values, the red line is the average of those values, and the yellow line is the expected value. The percent error was low, at 7.075%.*

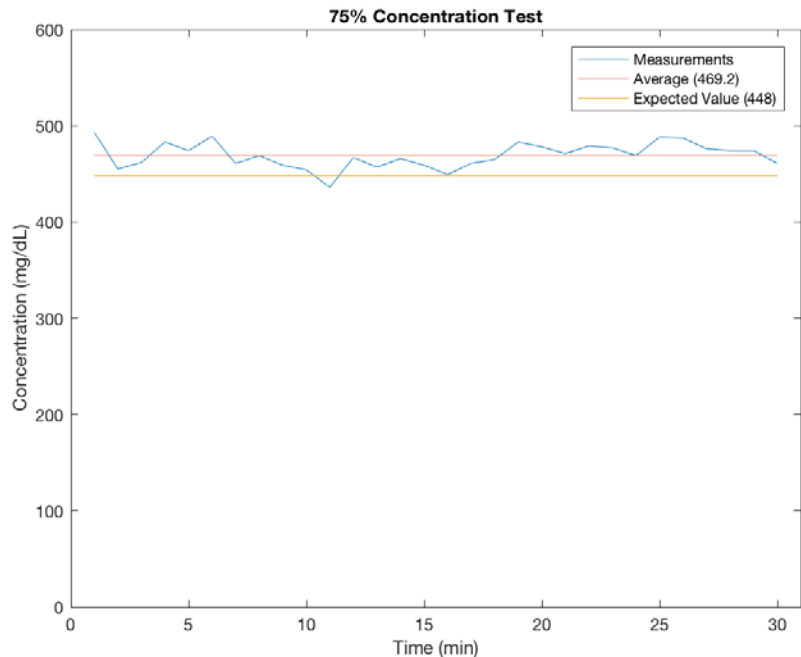


Figure 59: The graphical results for the 75% Glucose Concentration test. The blue line indicates measured values, the red line is the average of those values, and the yellow line is the expected value. The percent error was low, at 4.732%.

With these results, it was confirmed that the code produced the correct concentrations. However, a method was still needed to confirm that the concentration within the microfluidic channel was correct.

5.6.3 Microscope Concentration Testing

Because a microscope was readily available in Mitchell lab, this was planned to be the next form of testing. However, it was realized that the largest issue for achieving Experiment 2 was mixing. Because there was not a way to ensure that the two fluids in the two syringes were mixed properly before their entry into the microfluidic channel, there would be an issue with using this mode of testing to verify concentration. In fact, a time lapse video was taken for 45 minutes (with an image being taken every 30 seconds). However, due to the presence of streamlines within the channel, and due to some other issues with securing reference images for comparison, this method of concentration testing was put on hold, until mixing could be resolved.

5.7 Inlet Plug Testing

The inlet plug is an important component of the pump, as it will need to prevent leaking of media throughout the experiment while maintaining the position of the tubes for proper media delivery. This section details the fabrication and complications of the inlet plug.

5.7.1 Fabrication of the Plug

Up until this point, the inlet plug was fabricated from a hollow cylindrical connector in which the inlet tubes were placed, filled with a rope caulking material to secure the tubes in place. The client desired a plug to be made from PDMS, in which a larger surgical punch would create the plug itself while smaller surgical punches would create two smaller holes in the PDMS for placement of the inlet tubes. This would need to be completed using surgical punches of the correct diameters to ensure the right fit in the microfluidic inlet and the right fit of the tubes in the plug. Therefore, a 0.75 mm surgical punch was used to create two small holes in the plug for the inlet tubes to be placed in. This diameter was a perfect fit for the inlet tubes and did not demonstrate any leaking. Next, a 4 mm surgical punch was used to create the plug itself. While a plug of this diameter did not show any leaking at low flow rates, it did show significant leaking at higher flow rates when the pump was being primed. To overcome this limitation, a 4.5 mm surgical punch was used next to create the plug. This fit extremely snugly into the microfluidic inlet and did not allow for any leaking at either low or high flow rates. Thus, the final PDMS inlet plug was fabricated by using a 4.5 mm surgical punch to create the plug and a 0.75 mm surgical punch to create two smaller holes within the plug for tube placement. The setup of the PDMS plug in the microfluidic inlet can be seen below in Figure 60.

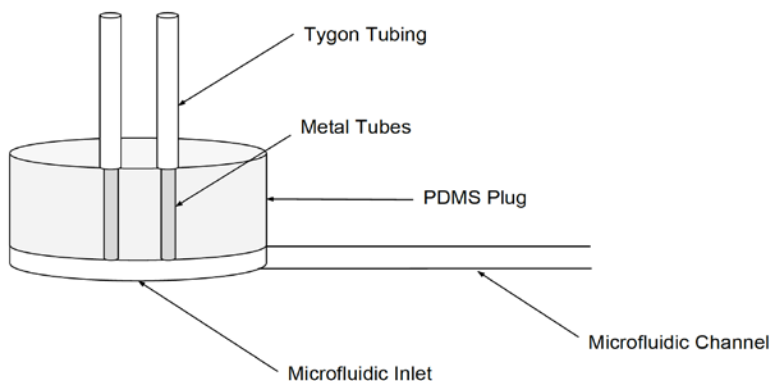


Figure 60: The setup of the PDMS plug in the microfluidic inlet.

5.7.2 Depth of the Plug

When the PDMS plug was used initially, there were significant streamlines within the microfluidic channel, which was anticipated. This means that the two fluids were not being sufficiently mixed, which poses a huge problem for Experiment 2, where mixing of fluids is essential for achieving the correct desired concentration. To try and solve this limitation, dead volume was introduced by experimenting with the depth at which the inlet plug was inserted into the microfluidic inlet. The client requested that the team find the best possible option for inlet plug placement that provides the best amount of mixing, but at the same time gives the minimum amount of dead volume. The idea behind this was that by introducing dead volume, there would be room in the microfluidic inlet for the two fluids to mix. The different heights at which the plug was inserted can be seen below in Figure 61.

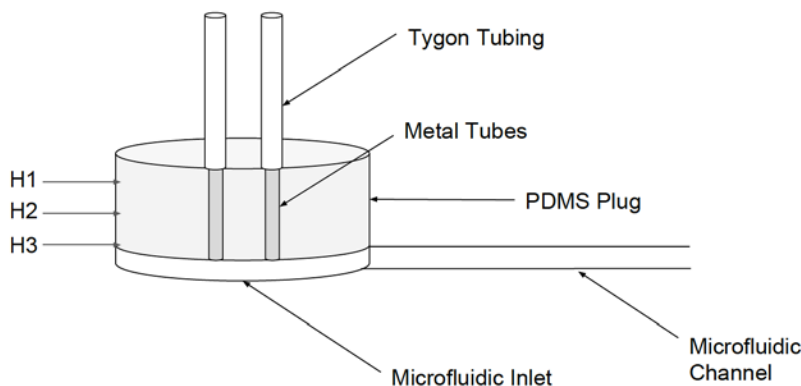


Figure 61: The different depths at which the PDMS inlet plug were tested, where H1 indicates Height 1, H2 indicates Height 2, and H3 indicates Height 3

5.7.3 Tube Orientation

The inlet plug was tested at each different height, and for each height it was tested with one of three different tube orientations. For this test, one syringe was filled with normal water (representing normal media), while the other was filled with water that was dyed with dark green food coloring (representing drug). The three different tube orientations are as follows:

1. Tubes side by side.

2. Tubes parallel to the channel, with the green water-filled tube closer to the microfluidic channel.
3. Tubes parallel to the channel, with the green water-filled tube further away from the microfluidic channel.

These three orientations can be seen in the figure below, as well as the mixing results of the different orientations.

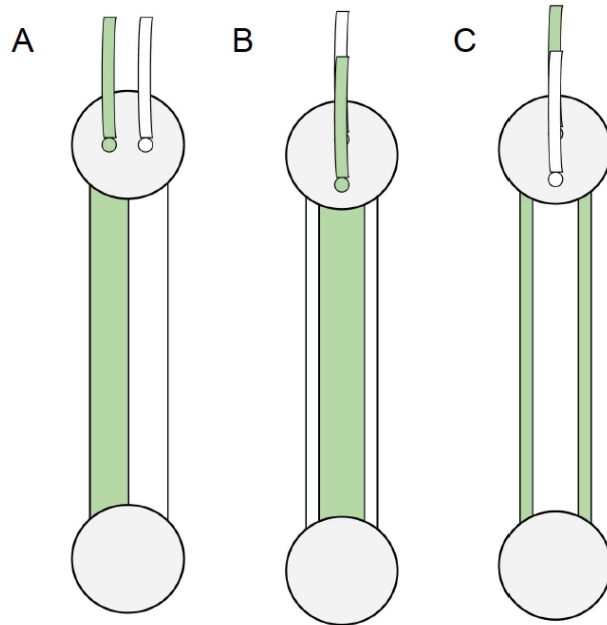


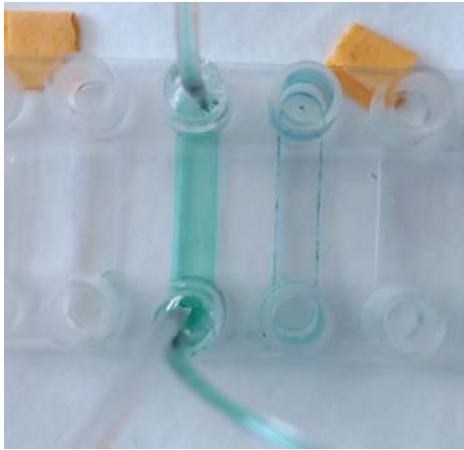




Figure 62: The three different tube orientations. The flow within the channel itself followed one of these three general patterns.




When the two tubes were placed side by side, as in Figure 62A, there were distinct streamlines that split the channel in half; one half was green, the other half was clear. When the tubes were placed one in front of the other, with the green tube in front of the clear tube as in Figure 62B, there were also distinct streamlines, with the central region of the channel green and both outer regions of the channel clear. When the tubes were placed one in front of the other, with the clear tube in front of the green tube as in Figure 62C, there were again distinct streamlines, with the central region of the channel clear and both outer regions of the channel green.


The table below displays a summary of the results of the inlet plug testing, with a combination of different plug heights and tube orientations.

Table 31: Summary of inlet plug testing results

Height	Tube Orientation	Results	Comments
H1	Side by side		<ul style="list-style-type: none"> • Noticeable streamlines • Channel split in half
H1	Green in front		<ul style="list-style-type: none"> • No apparent streamlines, but very uneven mixing (can see spots of color)
H1	Clear in front		<ul style="list-style-type: none"> • Streamlines present, but not as distinct • Uneven mixing (can see spots of color)

<p>H2</p>	<p>Side by side</p>		<ul style="list-style-type: none"> • Relatively even mixing • Some spotty colors throughout • After a while, it is clear that there are two separate colors (not as clear a line between the two but the difference is visible)
<p>H2</p>	<p>Green in front</p>		<ul style="list-style-type: none"> • Streamlines reappear • Not so much bisected in half (i.e. a greater degree of mixing than the streamlines from before) but still apparent • Amount of streamlines gradually reduced over time, but may not be enough

<p>H2</p>	<p>Clear in front</p>		<ul style="list-style-type: none"> • The larger section is clear instead of green
<p>H3</p>	<p>Side by side</p>		<ul style="list-style-type: none"> • Green starts thinly along the edges and is light in color, but gets more prominent as time passes • It then spreads through the chamber horizontally
<p>H3</p>	<p>Green in front</p>		<ul style="list-style-type: none"> • Started out streamlined • More even spread throughout the channel but still darker on one side

H3	Clear in front		<ul style="list-style-type: none"> • Green starts thinly along the edges and then spreads to midsection of chamber, but the streamlines are consistent
----	----------------	--	---

5.8 Mixing

As is evident from the results of the inlet plug testing, mixing will be an issue with Experiments 2 and 3, both of which require the mixing of two fluids to achieve the correct concentration. The attempts to improve mixing will be described in this section.

5.8.1 Improving Mixing

A funnel created to improve mixing. The rationale behind introducing this funnel was twofold: first, it would provide more time for the two fluids to mix, as this would help diffusion to occur, and second, it would allow the fluids to mix better as the diameter of the funnel decreased. The funnel was created using two PDMS plugs and a 10 μL micropipette tip, as in Figure 63 below.

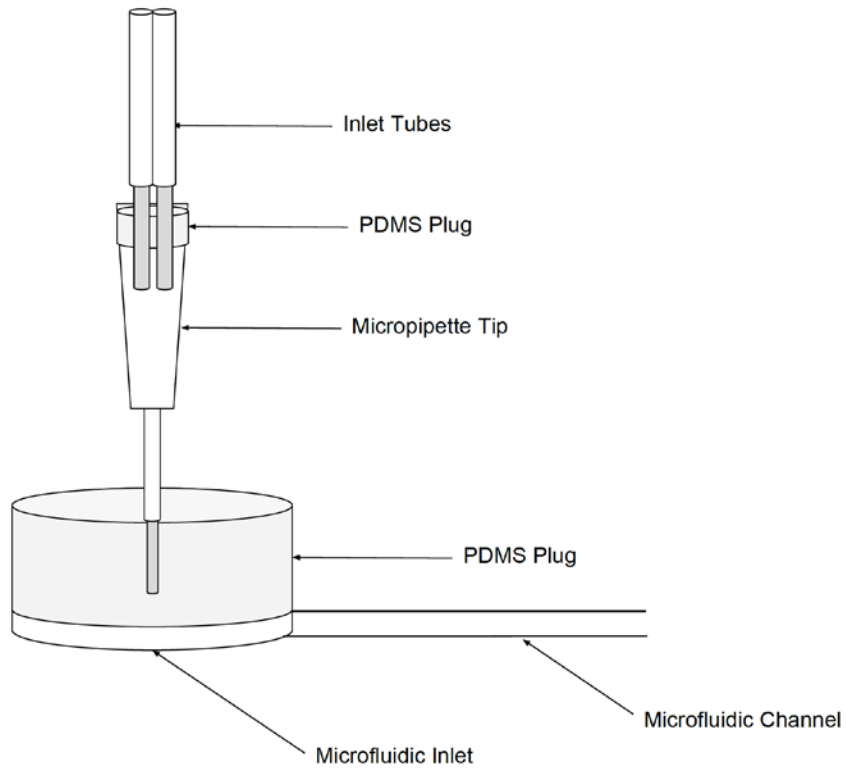


Figure 63: A schematic of the funnel implemented to improve mixing. The results demonstrated greatly improved mixing.



Figure 64: An image of the funnel.

A smaller plug was made to fit at the top of the micropipette tip, this time with a 3 mm outer diameter. Two smaller holes were made with the 0.75 mm surgical punch for the two inlet

tubes. The 4.5 mm PDMS plug was kept the same for the microfluidic inlet, but this time only one small hole (diameter = 1 mm) was made for the bottom of the micropipette tip to fit into.

The same testing as the inlet plug testing was then repeated. This time, instead of altering the tube orientation, 3 different flow rates were testing to see the effect on mixing. An interesting thing to note is that while there were no streamlines in the microfluidic channel, those streamlines were present in the micropipette tip itself.

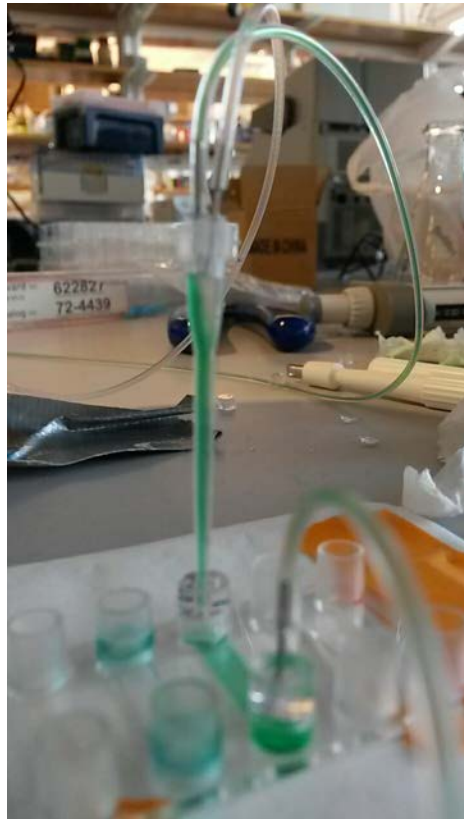
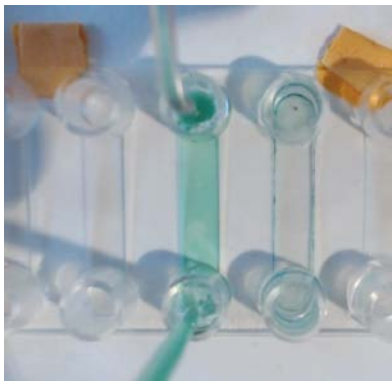
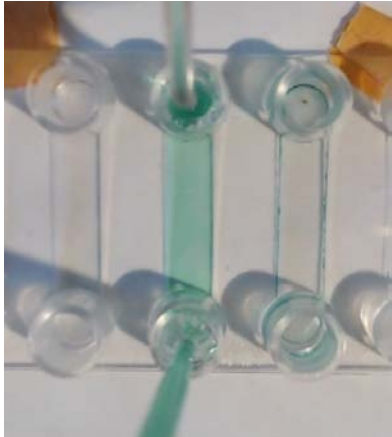



Figure 65: The streamlines within the micropipette tip. The microfluidic channel no longer had streamlines.

However, the funnel did eliminate streamlines in the channel. A summary of those results can be seen in the table below.

Table 32: Summary of the mixing results using the funnel

Flow Rate (mL/min)	Results	Comments
0.1		<ul style="list-style-type: none"> • No streamlines • Waves of different colors can be seen throughout when the droplet leaves the micropipette tip and hits the microfluidic inlet (so mixing is still not occurring ideally)
0.05		<ul style="list-style-type: none"> • Similar results as for the 0.1 mL/min flow rate, but the waves of different colors are less noticeable
0.02		<ul style="list-style-type: none"> • Waves of different colors almost unnoticeable • Best mixing so far

Overall, the funnel was able to eliminate the presence of streamlines, but the main observance was the presence of waves of different colors as the droplet left the micropipette tip and hit the bottom of the microfluidic inlet. However, the results show that as the flow rate is decreased, the degree and severity of these waves also decrease. At the 0.02 mL/min flow rate,

which is the lowest flow rate tested and also the ideal flow rate for biological testing, the waves are almost unnoticeable. This case provided the best degree of mixing so far, when compared to all other attempts to achieve mixing. In other words, the funnel at the 0.02083 mL/min provided the most uniform mixing.

The client had two concerns with this funnel:

1. The micropipette tip introduced dead volume to the system, and it would take some time before the liquid inside the tip could equilibrate.
2. The micropipette tip was large and tall, meaning it would not be able to fit within the microscope in which the biological experiments would take place.

A possible solution to these concerns would be to miniaturize the funnel. This would both reduce the dead volume and the size of the funnel for placement within the microscope.

5.8.2 Improving Equilibrium Between Inlet and Outlet

It was noticed that there was no buildup of fluid in the inlet, which was desired in the hope that it would provide some degree of mixing, but there was buildup of fluid at the outlet. Two different attempts were made to try and improve this equilibrium of fluid in the inlet and outlet.

The first involved creating a plug with a crescent shape in it at the edge. This was performed at the client's suggestion. The rationale behind this was because the plug was fitting very tightly in the inlet, and thus not allowing any passage of air for the fluids to equilibrate. However, this led to a large amount of leaking at the inlet.

The second involved introducing a vacuum at the outlet, which would continuously suction out the media as it exits the microfluidic channel.

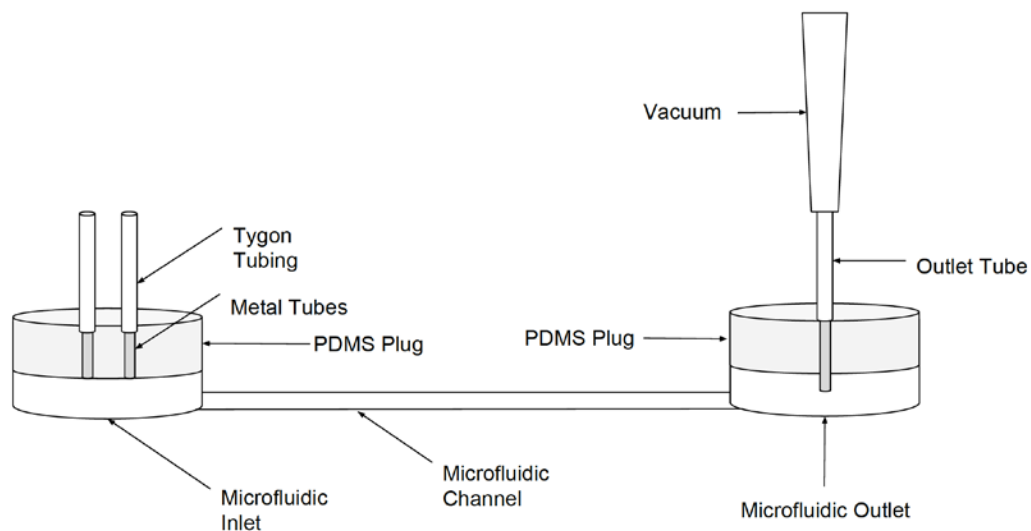
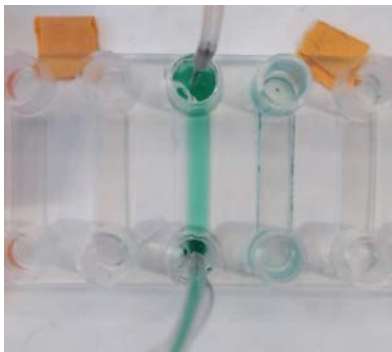
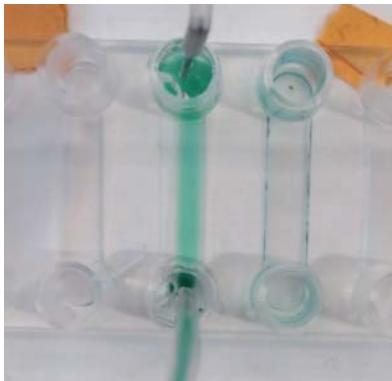
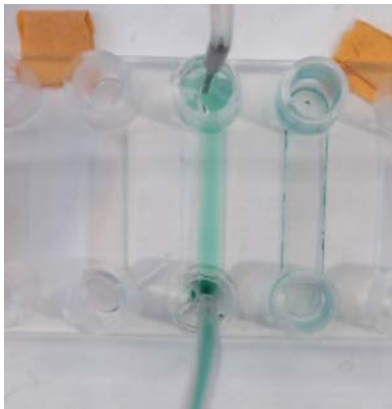


Figure 66: The vacuum introduced at the outlet

The tip of the vacuum would not touch the bottom of the microfluidic outlet but would instead be at a certain height. This would allow the media at the outlet to always maintain a certain height as well, since any media that causes the level to increase above that height would be automatically suctioned out. While this did help with establishing an equilibrium of the fluid levels at the inlet and outlet of the microfluidic, it did not however help with mixing, which was another goal of introducing the vacuum. A summary of the mixing results for the vacuum can be seen below.

Table 33: Summary of mixing results for the vacuum at different flow rates

Flow Rate (mL/min)	Results	Comments
0.1		<ul style="list-style-type: none">• Distinct streamlines present
0.05		<ul style="list-style-type: none">• Distinct streamlines present
0.02		<ul style="list-style-type: none">• Distinct streamlines present

Chapter 6: Final Design Validation

6.1 Biological Experiment Results

Upon completion of the multi-pump system design, the team performed biological experiments that further demonstrated the device's performance. This form of testing was crucial in validating that the pump functioned compatible with microfluidic cell cultures, and that the device as a whole met the needs of the client by showing its success in enabling biological experiments.

As mentioned previously, the biological experiments consisted of exposing melanoma cell cultures in microfluidic chambers to dynamic doses of the drug vemurafenib. The ERK dynamics in response to these dynamic drug treatments would then be analyzed. The following sections describe each of the biological experiments conducted by the design team with the multi-pump system. The general procedure for all biological experiments can be found in Appendix D: Biological Experiment Protocol.

6.1.1 Testing different flow rates for cell viability

Description:

The first experiment dealt with exposure of cell cultures to different flow rates. The three different flow rates used were 0.02 mL/min, 0.05 mL/min, and 0.1 mL/min. The cell cultures were exposed to the flow rates for 1 hour each in a single experiment. The purpose of this experiment was to gain insight of cell viability under shear stresses exerted by the fluid flow from the syringe pump system.

Experiment Duration: 3 hours

Imaging Frequency: Every 5 minutes

Number of Tiles for Analysis: 3

Figure:

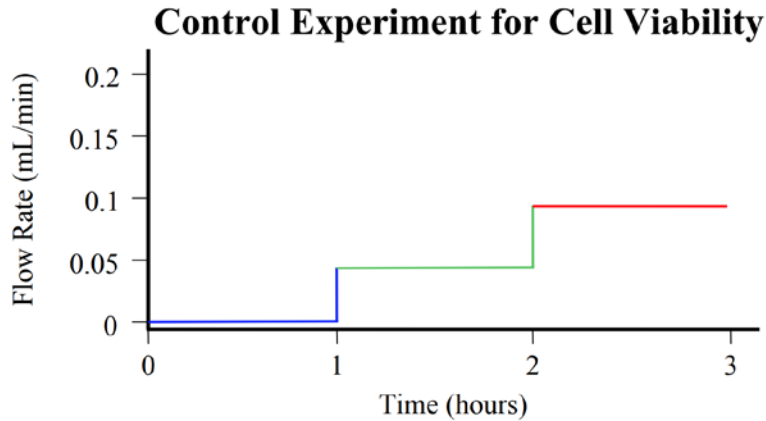


Figure 67: Profile of fluid flow rates administered for cell viability test

Results:

Cell viability was measured by cell counting. The results were obtained by using the Cell Counter plugin in FIJI. Cells were selected in each of the images of interest and the cell counter was summing up the amount of cells. Number of cells were counted at the time point 0, which was right before the experiment was started. By the end of the first hour, the image corresponding to the 60-minute mark was found and cell count was performed again to demonstrate the amount of cells that had survived the shear stress of the lowest flow rate. The last image considered for the 0.02 ml/min cell viability, was the first one used for the following flow rate in the experiment. The same procedure was done and cells were again counted at the 120-minute mark to confirm cell viability at the end of cells exposure to 0.05 ml/min flow rate. Lastly, the cell counter was used at the 180-minute mark to obtain cell viability after cells were exposed to the highest flow rate of 0.1ml/min. The measurements were considered from three different tiles that had been imaged and the average of all three was found. The table below summarizes the cell viability after cells were exposed to each flow rate and cell viability in general.

Table 34: Cell viability after exposure to different flow rates and in general

Flow Rate (ml/min)	Avg cell count at start of flow rate exposure	Avg cell count at end of flow rate exposure	% Cell Viability
0.02	132	113	85
0.05	113	123	109
0.1	123	117	95
Overall	132	117	88

Overall, cell viability results high with 88% of cell survival after exposed to all three tested flow rates. However, the cell viability in between each of the flow rates tested vary. As shown in the figure below for the 0.02 ml/min cell viability corresponds to 85%. After exposed to the 0.05 ml/min, cell survival was of 109%. Lastly, the cell viability after the final tested flow rate 0.1 ml/min.

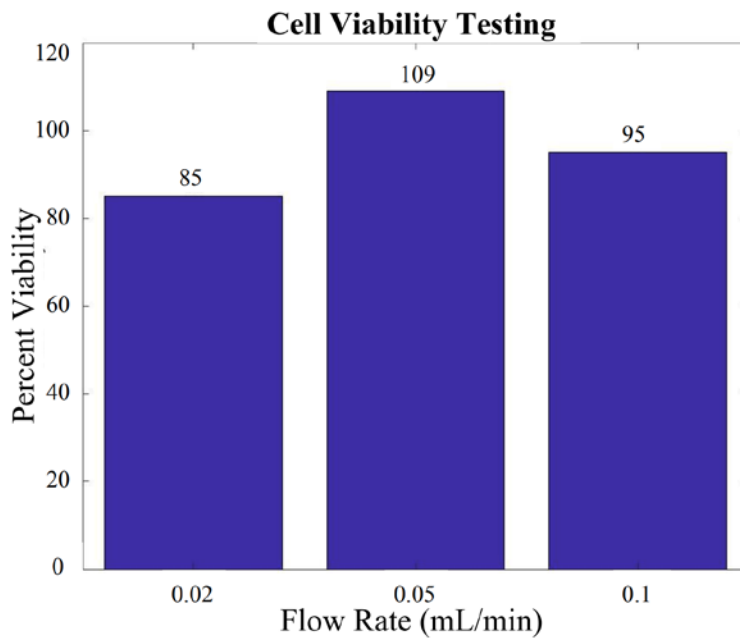


Figure 68: Percent of Cell viability when exposed to different flow rates over one hour period each.

6.1.2 Pulse Experiment 1: Half hour single drug pulse, 0.02 mL/min flow rate

Description:

The first pulse experiment took place at the lowest flow rate of 0.02 mL/min, as this would exert the least shear stress on the cells. This flow rate is indicated in Fig. 69 below, where the lines for the 0.02 mL/min flow rate are in blue. To gain a basic understanding of the ERK dynamics exhibited during a simple vemurafenib treatment, a single pulse of drug was issued to the cells. The experiment's drug profile was half an hour of media, half an hour of drug, and half an hour of media again (Fig. 69).

Experiment Duration: 1 ½ hours

Imaging Frequency: Every 5 minutes

Number of Tiles for Analysis: 4

Figure:

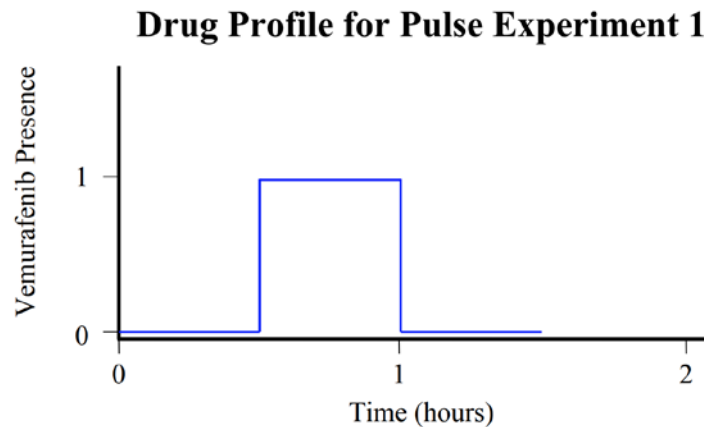


Figure 69: Drug Profile for Pulse Experiment 1

Results:

Nuclear translocation of KTR was measured to model ERK dynamics in the cell in response to the single vemurafenib pulse. The Zeiss microscope saved all images in a .czi file, which was opened in the program FIJI for analysis. Regions of Interest (ROIs) were selected within the nuclei. Since slight movement of cells was common throughout the image sequence over time, cells that were selected for analysis were those for which the ROIs remained inside the nuclei at all time points. The team tried to select as many good cell samples as possible from each of the 4 tiles. The “MultiMeasure” feature in FIJI was then employed to measure pixel

intensity of the ROIs from each of these tiles, after which pixel intensity was plotted against time.

Data was normalized using the following equation:

Equation 6.1

$$Y_i^n = \frac{(Y_i - Y_{min})}{Y_{max} - Y_{min}}$$

where Y_i is the data point at time i , Y_{min} is the minimum pixel intensity, Y_{max} is the maximum pixel intensity, and Y_i^n is the normalized data point. This ensured that values on the y-axis of the graphs remained between 0 and 1. The average was overlaid on top of the individual ROI data curves.

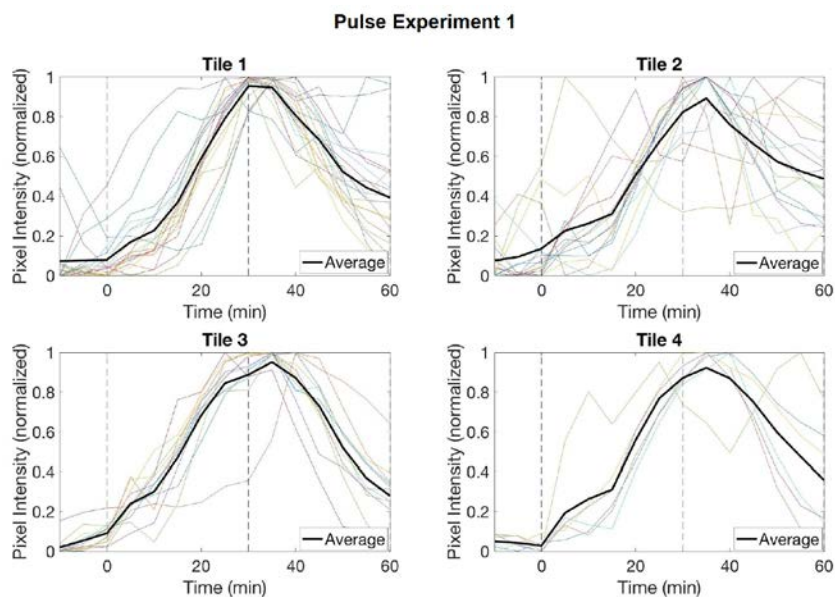


Figure 70: Results of the first pulse experiment. Each subplot contains the pixel intensity measurements for the ROIs of one tile. The different colored lines represent the data for each ROI. Data is normalized and the average is plotted.

The data across all 4 tiles was relatively consistent throughout. The switch between media and drug occurred at time $t = 0$ min, which is where ERK inhibition occurs as the curve increases due to increasing pixel intensity. At $t = 30$ min, the switch between drug and media occurred, which is why the curve decreases as pixel intensity decreases, indicating that the ERK pathway has been reactivated.

This experiment demonstrated many different things about the pump system, including that it could be used to analyze ERK dynamics of melanoma cells treated with pulses of vemurafenib, that it could be used to perform dynamic versions of the static experiments, and that its media and drug delivery could successfully induce ERK inhibition when exposing cells to the specified drug profile. Since this was the first biological experiment performed with the pump, it confirmed the functionality of the system and demonstrated that it was performing correctly and successfully as intended.

6.1.3 Pulse Experiment 2: Half hour single drug pulse, 0.1 mL/min flow rate

Description:

The second pulse experiment had exactly the same drug profile as the first pulse experiment (Fig. 69), except the flow rate was increased to the upper bound of tested flow rates, which was 0.1 mL/min. Below in the figure for pulse experiment 2's drug profile (Fig. 71), the difference in flow rate is marked by the change in line color from blue to red.

Experiment Duration: 1 ½ hours

Imaging Frequency: Every 5 minutes

Number of Tiles for Analysis: 4

Figure:

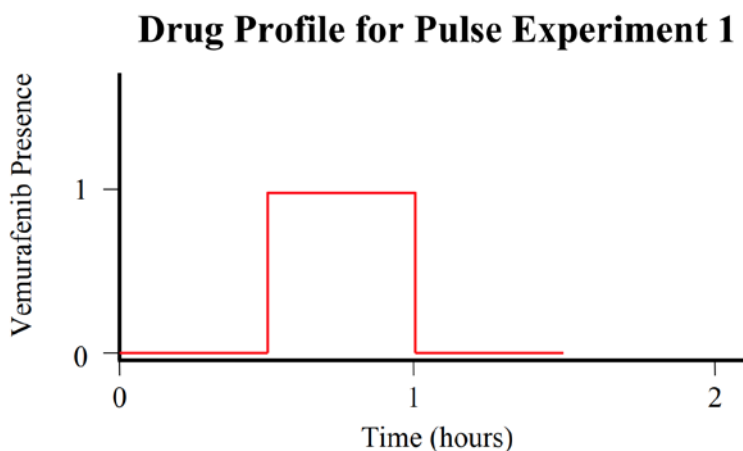


Figure 71: Drug Profile for Pulse Experiment 2

Results:

The same analysis in FIJI was performed, with the following results:

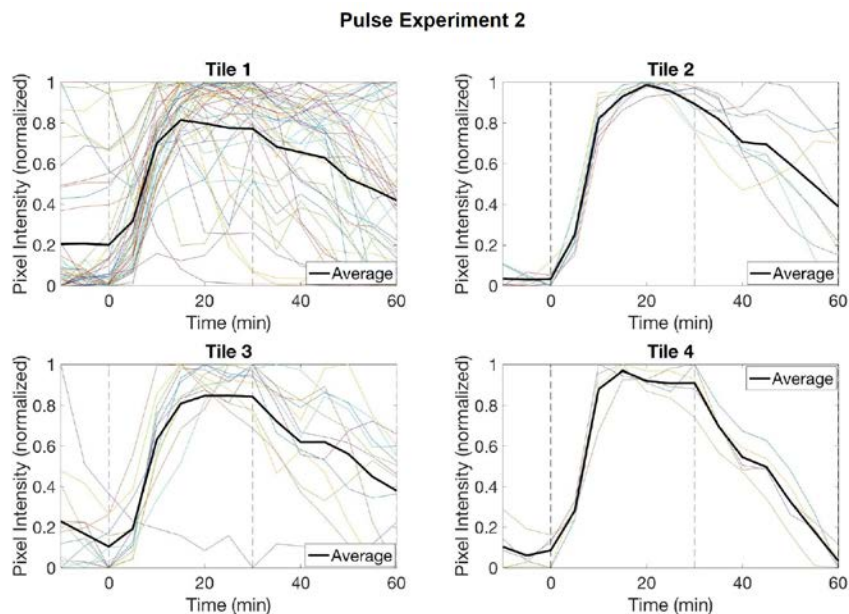


Figure 72: Results of the second pulse experiment. Each subplot contains the pixel intensity measurements for the ROIs of one tile. The different colored lines represent the data for each ROI. Data is normalized and the average is plotted.

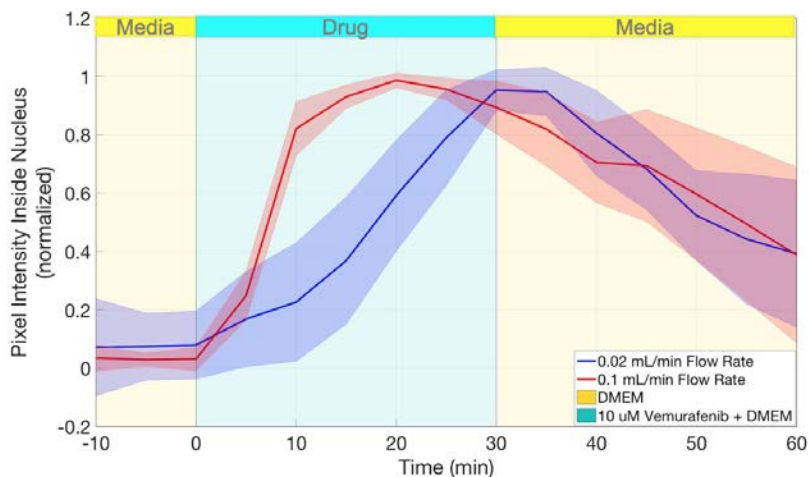


Figure 73: ERK translocation response times for the 0.02 mL/min and 0.1 mL/min flow rates.

The design team compared the results of the two biological experiments at flow rates 0.02 mL/min and 0.1 mL/min with the dye experiments described in Chapter 5 to characterize response times. The pump response time is defined as the time it takes between the moment a switch of media occurs and the moment a change in media is observed, as indicated by an increase in pixel intensity. Using dyes, the design team was able to quantify uniform media

distribution response time (time when a dye spreads uniformly and reaches maximum color intensity in the channel) for different flow rates: 4.765 min for 0.02 mL/min and 1.351 min for 0.1 mL/min (see Chapter 5). ERK translocation response time was significantly larger for vemurafenib pulse experiments: 30 min for 0.02 mL/min and 20 min for 0.1 mL/min (see Figure 73 above), indicating that there are additional delays of approx. 25 min and 18 min until pathway inhibition occurs, likely due to cell response time to the drug. Results demonstrate that, as expected, a faster flow rate increases the response time.

6.1.4 Pulse Experiment 3: Half hour stabilization period, one hour single drug pulse, 0.02 mL/min flow rate

Description:

This experiment still delivered only a single pulse of vemurafenib to the cells at the lowest flow rate of 0.02 mL/min, but the duration of the drug pulse was increased. In this experiment, the idea of a stabilization period was introduced. This stabilization period allowed the user to deliver regular media for a predetermined amount of time that differed from the regular alternation durations. For example, the cells in this experiment were subjected to the following drug profile: half an hour of media (stabilization period), one hour of drug, and one hour of media again (Fig. 74). The purpose of the experiment was to observe the effect that longer vemurafenib pulses had on the melanoma cells.

Experiment Duration: 2 ½ hours

Imaging Frequency: Every 2 minutes

Number of Tiles for Analysis: 4

Figure:

Drug Profile for Pulse Experiment 3

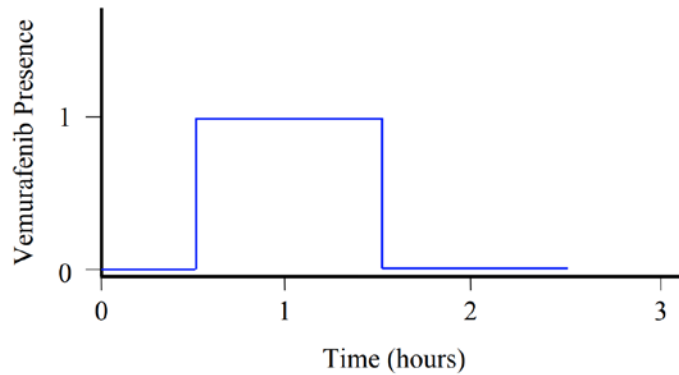


Figure 74: Drug Profile for Pulse Experiment 3

Results:

The same procedure for analysis in FIJI was performed, with the following results:

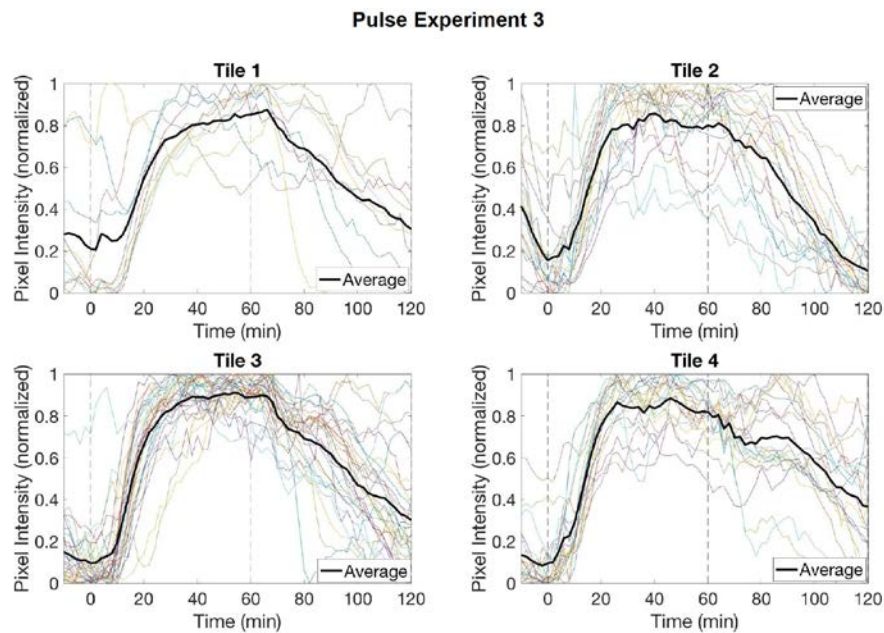


Figure 75: **Results of the third pulse experiment.** Each subplot contains the pixel intensity measurements for the ROIs of one tile. The different colored lines represent the data for each ROI. Data is normalized and the average is plotted.

A stabilization period was incorporated into this experiment, so that the cells could be exposed to flowing media and their behavior could stabilize before being exposed to drug. The pump. Despite the increase in the drug pulse duration and a slight difference in the shape of the curves, the overall pattern in ERK dynamics was similar to Pulse Experiment 1 and 2, where

pixel intensity increased when the switch from media to drug occurred (ERK pathway was inhibited) and decreased when the switch from drug to media occurred (ERK pathway was reactivated).

6.1.5 Pulse Experiment 4: Half hour stabilization period, one hour drug pulses (x2), one hour relaxation periods (x2), 0.02 mL/min flow rate

Description:

The next experiment was very similar to the previous experiment, but with one slight difference. This time, there were 2 pulses of drug rather than 1 pulse. The cells were subjected to the following drug profile: half an hour of media (stabilization period), one hour of drug, one hour of media, one hour of drug, and one hour of media (Fig. 76). The main purpose of this experiment was to observe the ERK dynamics when cells were exposed to multiple vemurafenib pulses.

Experiment Duration: 4 ½ hours

Imaging Frequency: Every 2 minutes

Number of Tiles for Analysis: 4

Figure:

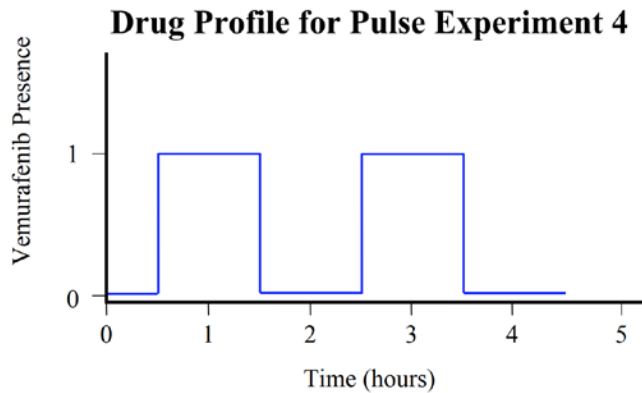


Figure 76: Drug Profile for Pulse Experiment 4

Results:

Pulse Experiment 4

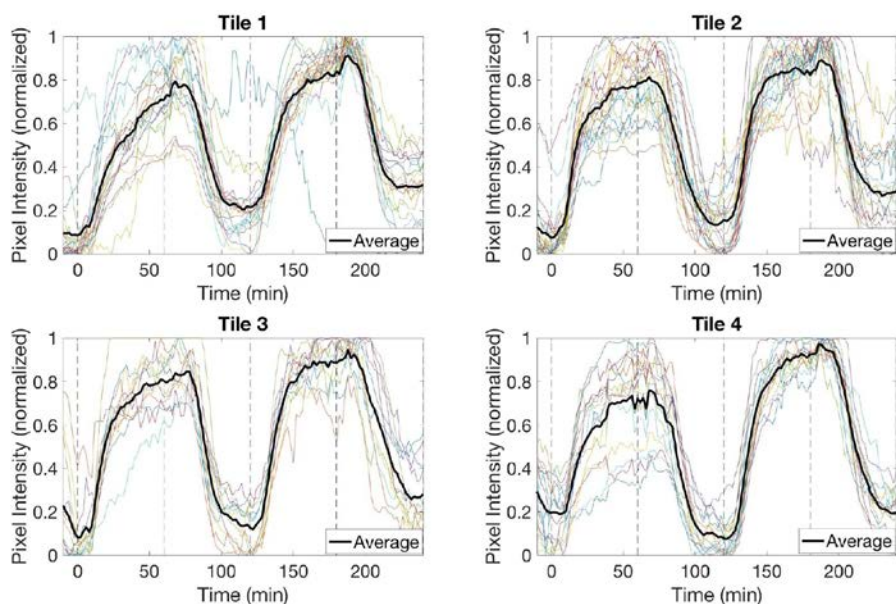


Figure 77: Results of the fourth pulse experiment. Each subplot contains the pixel intensity measurements for the ROIs of one tile. The different colored lines represent the data for each ROI. Data is normalized and the average is plotted.

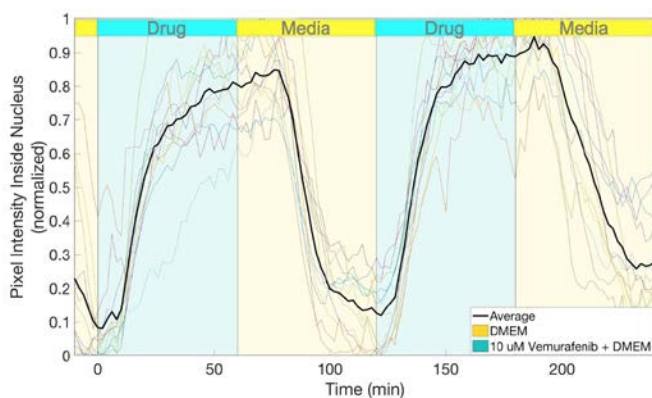


Figure 78: ERK translocation (0.02 mL/min) demonstrated reversibility for pathway activation and inhibition.

This experiment was fundamental in understanding the ERK dynamics that could be observed for more than one pulse of drug that is administered by the multi-pump system. The pump enabled the design team to perform an experiment that was longer in duration and that showed multiple alternations between pumps. Most importantly, these biological results demonstrated that there was a degree of reversibility achieved as a result of the dynamic doses that were administered by the pumps. This reversibility occurred as the ERK pathway was inhibited and reactivated two times in correspondence to the switch between media and drug.

This verified that the nuclear translocation in A375 cells in microfluidic chambers did indeed occur in response to multiple dynamic doses of vemurafenib.

6.1.6 Pulse Experiment 5: Half hour stabilization period, one hour drug pulses (x4), ½ hour relaxation periods, 0.02 mL/min flow rate

Description:

The next experiment was a continuation of the previous one. The length of time between drug pulses, in which regular media is administered to the cells, can be called the “drug holiday time,” since the cells receive a break from drug exposure. The client was interested in seeing the effects of different drug holiday times on the cellular response to vemurafenib. Of particular interest was if the cells would completely regain ERK pathway activity with the decreased drug holiday (i.e., decreased exposure to media between drug pulses). In this experiment, the overall pattern of drug profile was the same, except that the intervening periods of media between drug pulses was reduced to half an hour (as opposed to one hour).

Experiment Duration: 6 ½ hours

Imaging Frequency: Every 2 minutes

Number of Tiles for Analysis: 4

Figure:

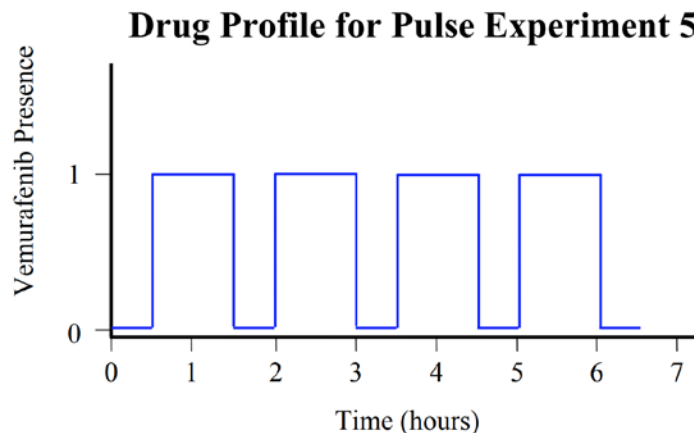


Figure 79: Drug Profile for Pulse Experiment 5

Results:

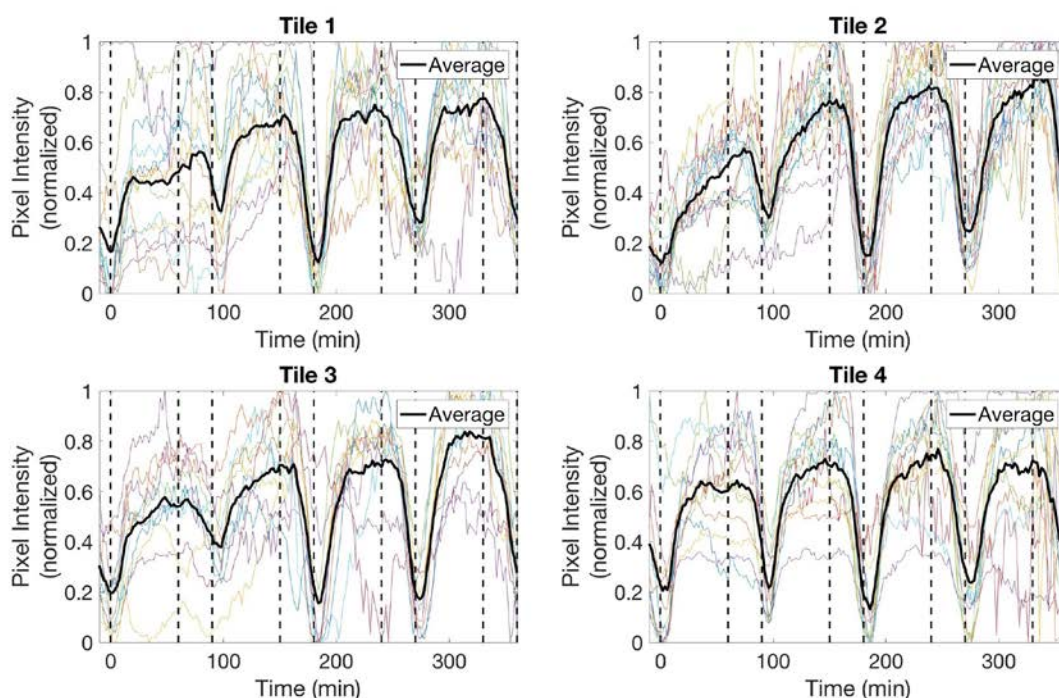


Figure 80: Results of the fifth pulse experiment. Each subplot contains the pixel intensity measurements for the ROIs of one tile. The different colored lines represent the data for each ROI. Data is normalized and the average is plotted.

This experiment demonstrated that the pump system was capable of even longer periods of testing. All of the tiles demonstrated similar results, which indicates that there was uniformity and consistency across the different regions of the chamber that were being imaged. Due to the decreased drug holiday period (whereas Pulse Experiment 4 had 1 hour intervals between drug pulses and could therefore be considered as a one hour drug holiday experiment), there was less reversibility observed. This makes sense intuitively because there was less time for the cells to recover their ERK activity between vemurafenib doses.

6.1.7 Pulse Experiment 6: Half hour stabilization period, one hour drug pulses (x4), $\frac{1}{4}$ hour relaxation periods, 0.02 mL/min flow rate

Description:

The next experiment also continued the previous one. To continue the study of varying drug holiday time, this experiment once again retained the overall pattern of drug profile, but reduced

the drug holiday to a quarter of an hour (as opposed to half an hour and one hour in the previous two experiments).

Experiment Duration: 5 ½ hours

Imaging Frequency: Every 2 minutes

Number of Tiles for Analysis: 5

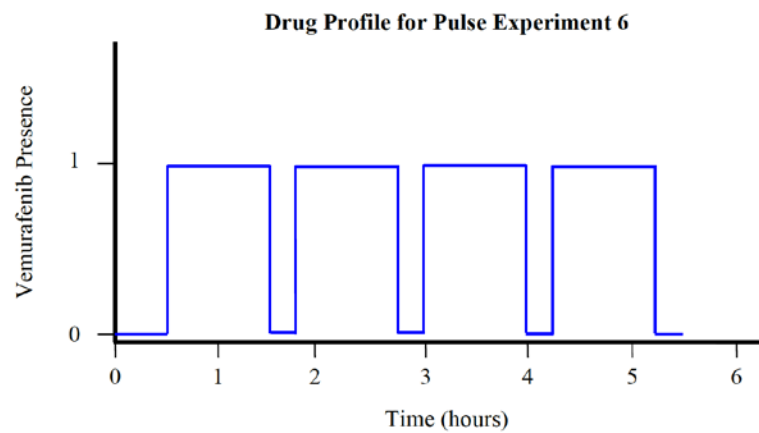


Figure:

Figure 81: Drug Profile for Pulse Experiment 6

Results:

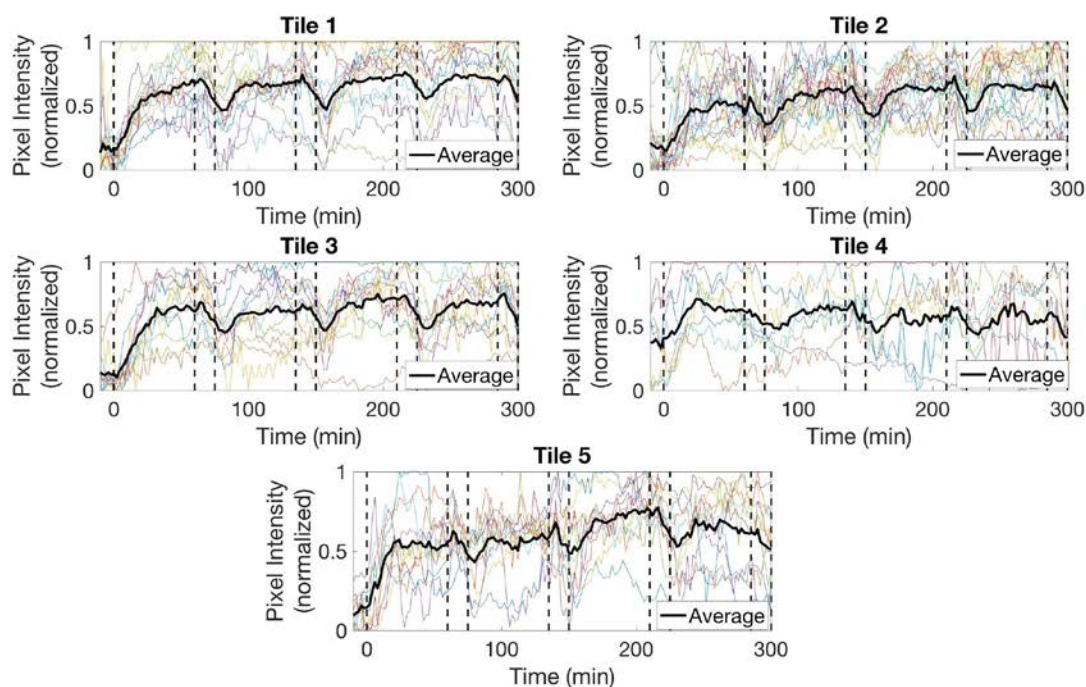


Figure 82: Results of the sixth pulse experiment. Each subplot contains the pixel intensity measurements for the ROIs of one tile. The different colored lines represent the data for each ROI. Data is normalized and the average is plotted.

From these experiments, it was noted that with the further reduction of the drug holiday time, there was an even lesser degree of reversibility. Shortening the holidays shows less reactivation in the ERK pathway, and this is expected because there is less time for the cells to recover their ERK activity between vemurafenib doses. Thus, this experiment demonstrated the least degree of reversibility.

6.1.8 Pulse Experiment 7: Three hours starvation media, 4 hours starvation media with vemurafenib (compared with the control)

Description:

The seventh pulse experiment began a new, promising study based on previous results on ERK dynamics obtained by Mitchell lab in their research. Researchers in Mitchell lab had treated cells with what they called “starvation media,” in which there were no growth factors (i.e., no FBS was added to DMEM) for 3 hours. They then manually delivered 10 μ M vemurafenib in starvation media to the cells for a resting period of 4 hours. In their analysis, they noticed that between 10-20% of cells had regained ERK activity despite having been

subjected to vemurafenib for 4 straight hours. However, because this study was performed statically, the growth factors that are naturally secreted by cells remained in the media for the duration of the experiment, which could affect ERK activity. Therefore, no conclusion can be made about vemurafenib resistance from this static study.

The multi-pump system can be a valuable component to this experiment. Because the pump can continuously deliver starvation media to the cells, the secreted growth factors can be washed away as the starvation media flows through the microfluidic chamber. The significance of this is that by repeating the experiment with continuously flowing media with the implementation of the pump, it can eliminate an extraneous variable that may be affecting the results of the experiment. If the same behavior of regained ERK activity is observed with this experiment, then a conclusion can be safely made about vemurafenib resistance.

This drug profile for this experiment was: 3 hours starvation media (DMEM without FBS), and 4 hours drug in starvation media (Fig 83).

Experiment Duration: 7 hours

Imaging Frequency: Every 4 minutes

Number of Tiles for Analysis: 4 (control) and 5 (starvation)

Figure:

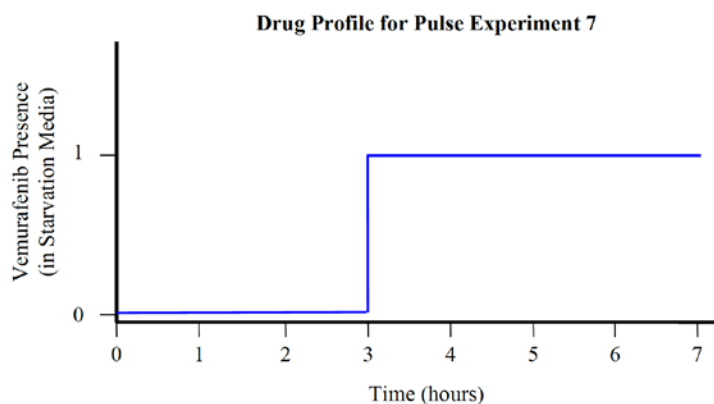


Figure 83: Drug Profile for Pulse Experiment 7

Results:

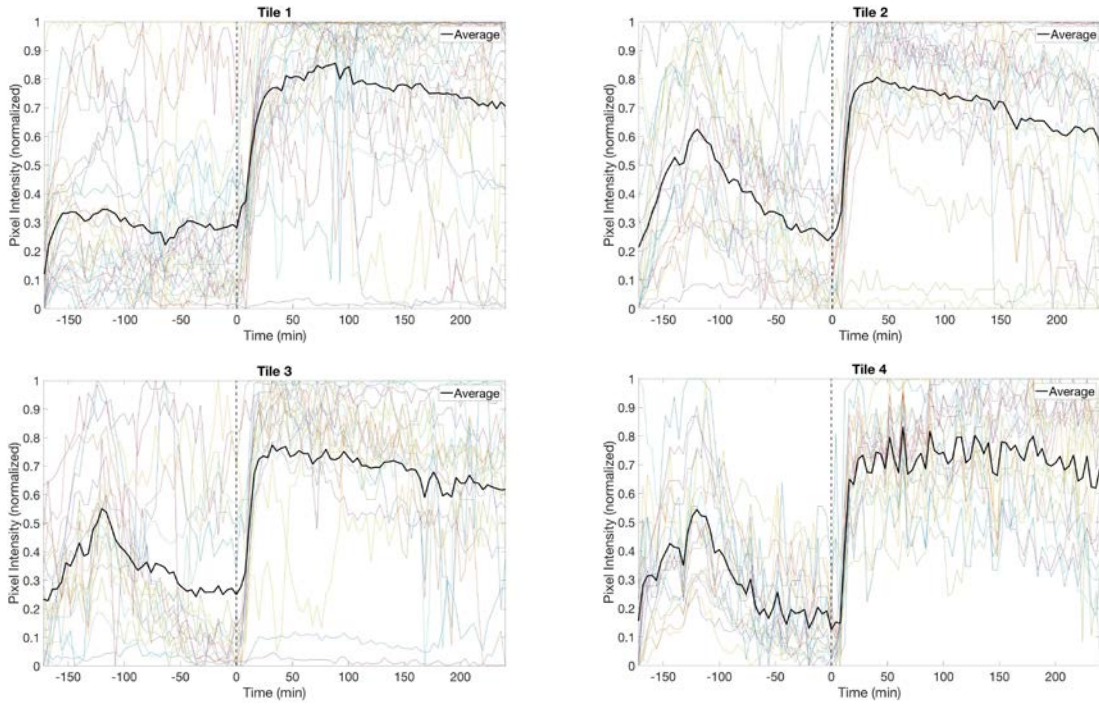
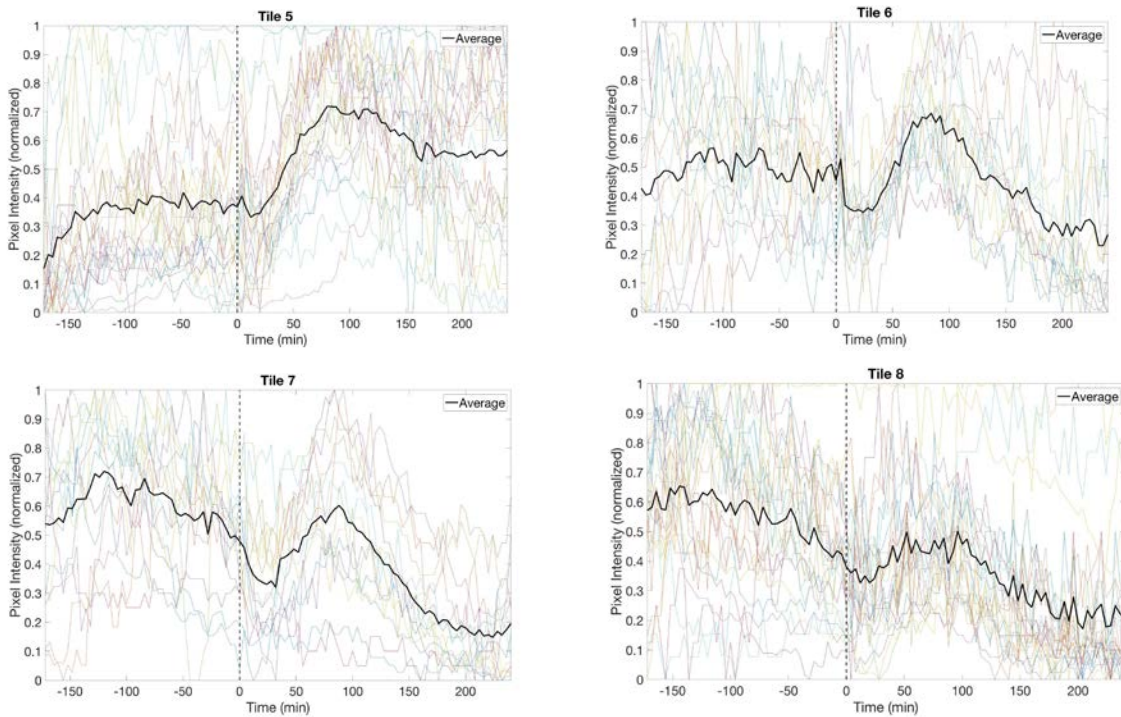
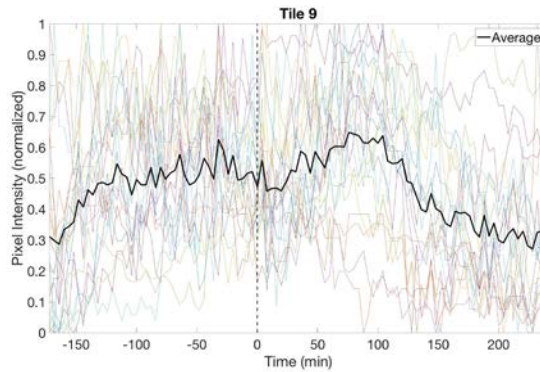


Figure 84: Results of the control for the starvation experiment. Each subplot contains the pixel intensity measurements for the ROIs of one tile. The different colored lines represent the data for each ROI. Data is normalized and the average is plotted.





*Figure 85: **Results of the starvation experiment.** Each subplot contains the pixel intensity measurements for the ROIs of one tile. The different colored lines represent the data for each ROI. Data is normalized and the average is plotted.*

Despite being a promising experiment and having been performed multiple times to ensure proper setup, the results did not give much insight biologically. While the graphs from the control channel clearly show ERK inhibition (since pixel intensity occurs after the switch from media to drug), the graphs from the starvation channel do not seem to exhibit any ERK inhibition activity. This is likely due to the fact that there may not have been any drug added to the starvation media that was pumped in the final 4 hours of the experiment. Therefore, these results are inconclusive.

6.1.9 Final Pulse Experiment: 6 multi-channel starvation experiment

Overall Description:

This final experiment served as a culmination of the work of the design team. It demonstrated that the multi-pump system designed by the team could successfully perform 6 parallel experiments, as requested by the client. This experiment was very important for verifying that multiple experiments in which different drug profiles were applied to cells could be performed simultaneously, for higher throughput and efficiency in gaining experimental results. Each channel within the microfluidic chip contained a different experiment, each of which are summarized below in Table 35.

Table 35: Experiment summary for the six multi-pump experiment

Channel Number	Experiment Duration (hours)	Drug Profile
1	12	30 min starvation media, 4 hours starvation media + drug, 7.5 hours starvation media
2	12	1 hour starvation media, 4 hours starvation media + drug, 7 hours starvation media
3	12	2 hours starvation media, 4 hours starvation media + drug, 6 hours starvation media
4	12	4 hours starvation media, 4 hours starvation media + drug, 4 hours starvation media
5	12	6 hours starvation media, 4 hours starvation media + drug, 2 hours starvation media
6	12	2 hours FBS media, 4 hours FBS media + drug, 6 hours FBS media

Imaging Frequency: every 10 minutes

Number of Tiles for Analysis: 3 per channel

6.1.9.1 Channel 1

Results:

The first channel did not have any results for two reasons. The first involved air bubbles that were introduced to the system during setup. Although the air bubble was not observed by the design team before the microfluidic was placed in the microscope, there was eventually air in the channel that disrupted the cells and resulted in data loss. The second reason was poor image quality due to the microscope settings.

6.1.9.2 Channel 2

Results:

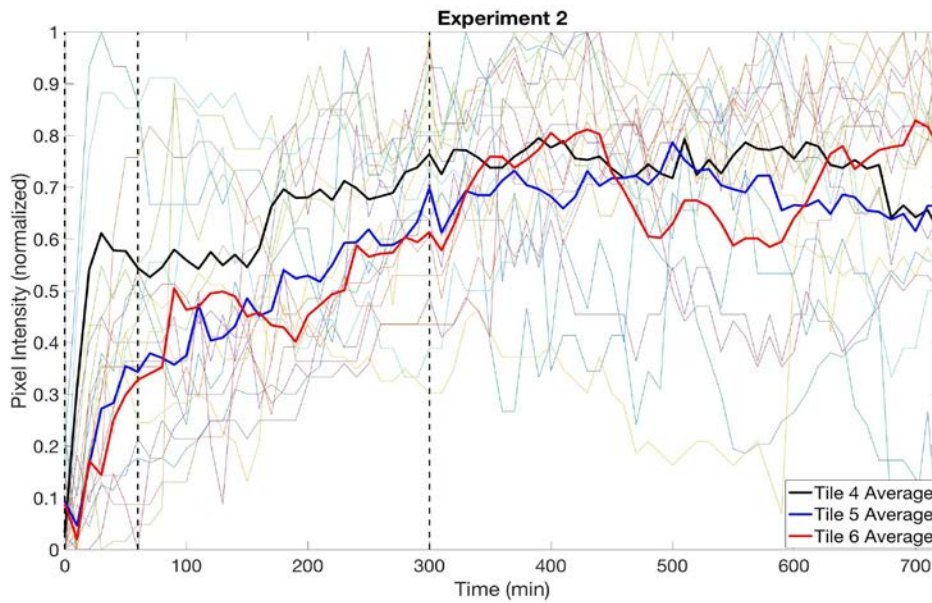


Figure 86: Results for channel 2 of the 6 pump starvation experiment

6.1.9.3 Channel 3

Results:

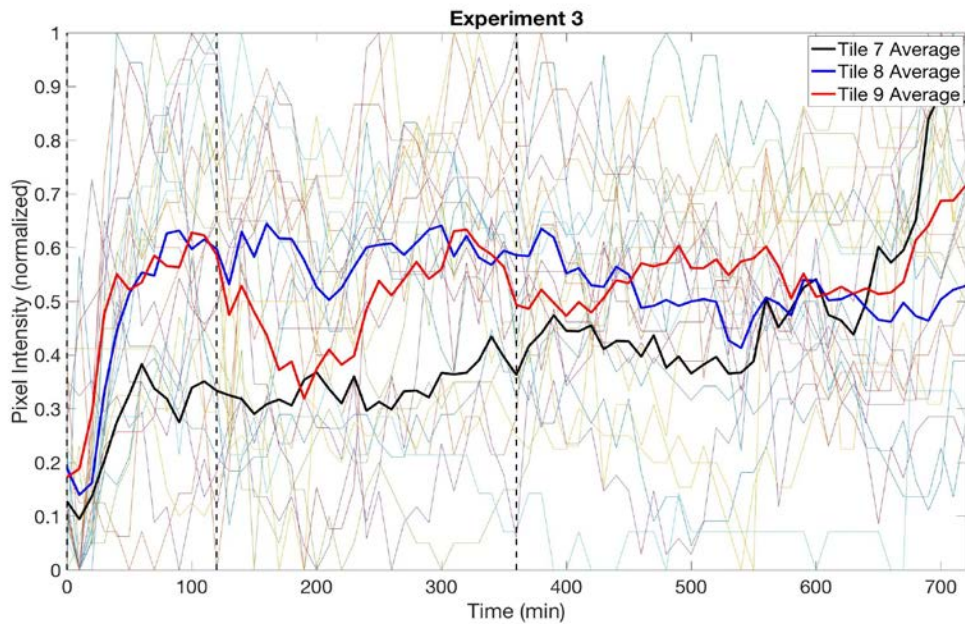


Figure 87: Results for channel 3 of the 6 pump starvation experiment

6.1.9.4 Channel 4

Results:

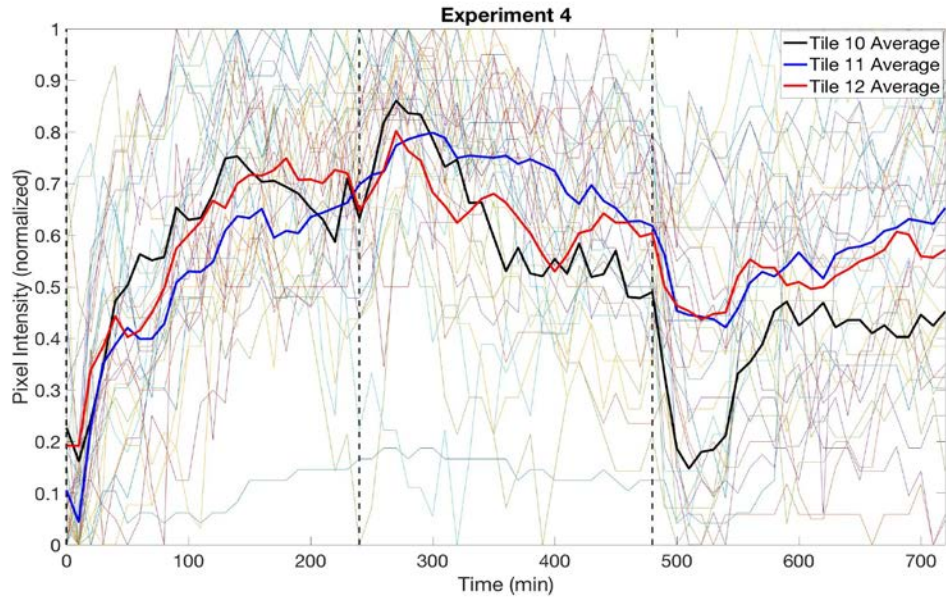


Figure 88: Results for channel 4 of the 6 pump starvation experiment

6.1.9.5 Channel 5

Results:

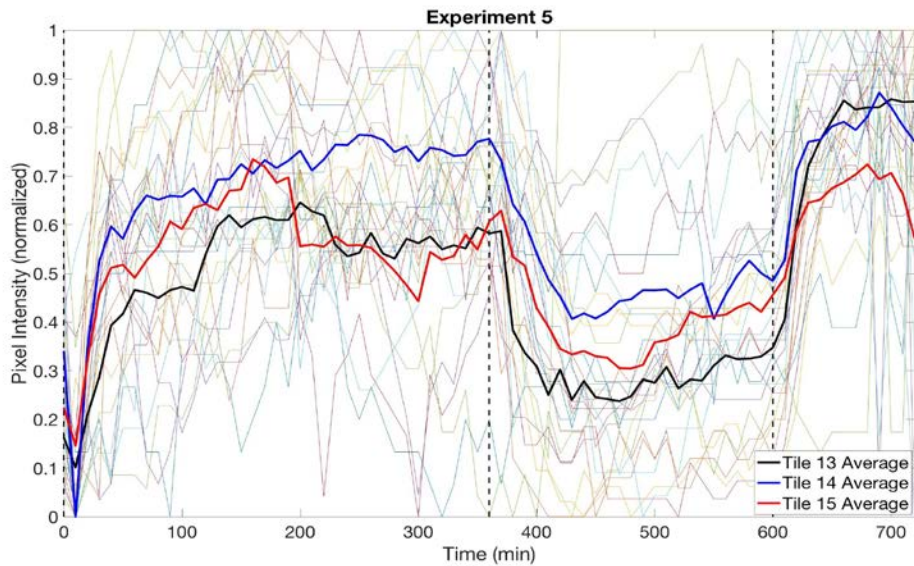


Figure 89: Results for channel 5 of the 6 pump starvation experiment

6.1.9.6 Channel 6

Results:

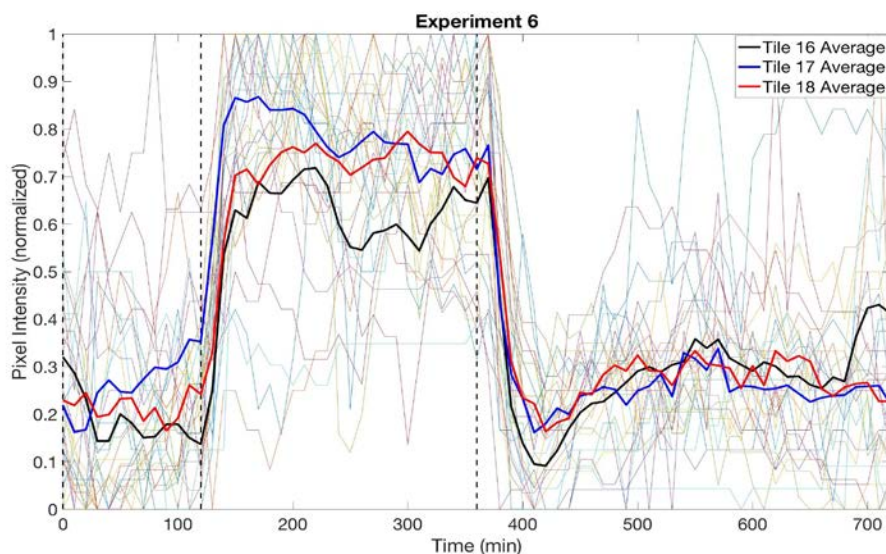


Figure 90: Results for channel 6 of the 6 pump starvation experiment

The data from this experiment were challenging to analyze, especially because all the data from an entire channel was missing due to air bubbles and poor image quality. In addition, resolution of all images were poor. Interesting things to note are that in Experiment 2, the ERK pathway seemed to be inhibited constantly after the switch was made from media to drug. In Experiment 3, the ERK dynamics remained relatively constant throughout, regardless of when the switch was made. In Experiment 4, there was a large dip in pixel intensity right after the switch from drug to media was made, but it then stabilized once more. In Experiment 5, pixel intensity started off high, decreased to a low value when the switch was made from media to drug, and then increased to a higher value when the switch was made from drug to media. These are the opposite results to the usual results, so there may have been some experimental error. One possible cause could be that, although the design team took extra care, the two syringes (one with media, one with drug) could have been placed on the wrong side of the pump, so drug was administered first before media, resulting in the different pattern. In Experiment 6, in which the media contained FBS, the results were very similar to previous experiments with FBS; the same pattern of ERK dynamics can be seen.

Additionally, when comparing the starvation media experiments to the FBS media, it seems that overall the drug has weaker effect in the starvation experiment, and the translocation reporter seems to move into the nucleus even before the switch occurs. This could be expected since not having growth factors in the media would affect the proliferation by decreasing, that otherwise would be high, suggesting that having starvation media leads to lower proliferation.

6.2 Reproducibility Experiment

Overall Description:

This experiment was performed by a member of Mitchell Lab, with the assistance of the design team. The goal of this experiment was twofold: to teach the procedure for setting up the multi-pump system to the researchers in Mitchell Lab so that they are able to perform them on their own, and to ensure that the results obtained from the experiment performed by the researcher are similar to the ones obtained previously.

This was a starvation experiment in which one channel had 1 hour starvation media, 4 hours starvation media with vemurafenib, and 2 hours starvation media. This was the starvation channel. The other channel had 1 hour FBS media, 4 hours FBS media with vemurafenib, and 2 hours FBS media. This was the control channel.

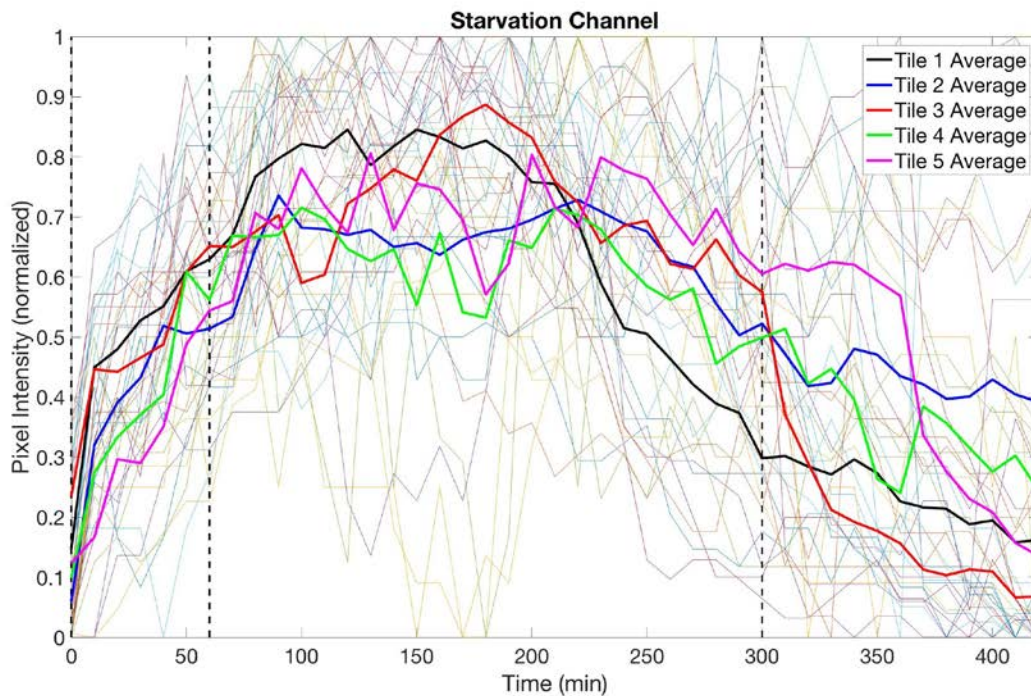


Figure 91: Starvation channel from the reproducibility experiment

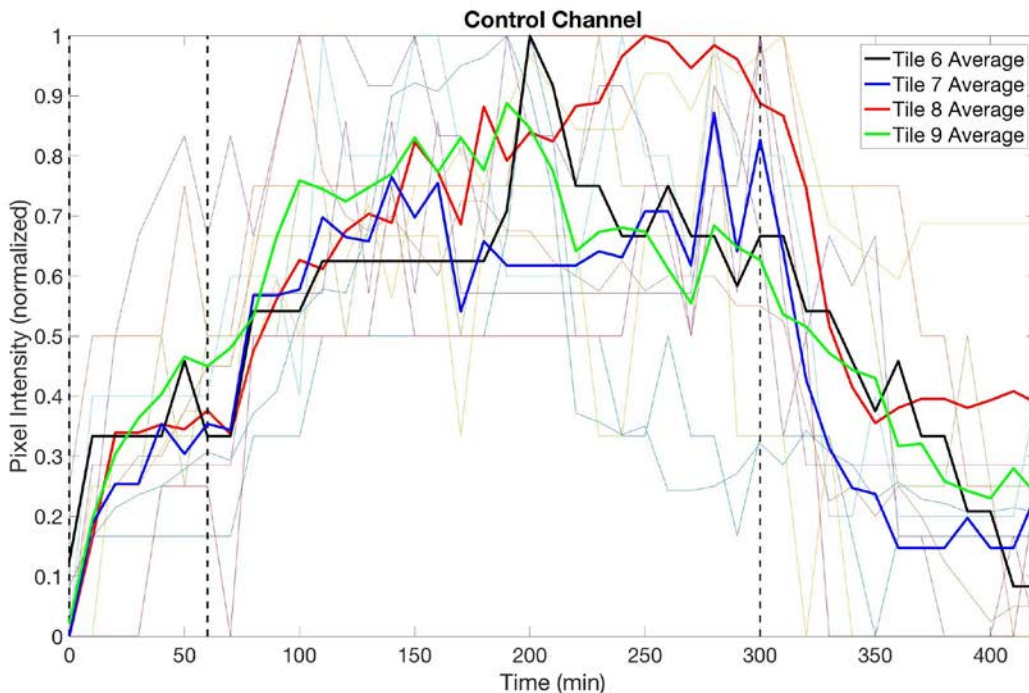


Figure 92: Control channel from the reproducibility experiment

Although analysis was plagued by poor image quality, the results overall demonstrated that the experiment was reproducible. The ERK dynamics of this experiment, which was performed by the researcher in Mitchell Lab, closely resembled the ERK dynamics from the experiments performed by the design team. As the switch from media to drug occurred, the pixel intensity increased as an indication of ERK inhibition. As the switch from drug to media occurred, the pixel intensity decreased as an indication of ERK reactivation.

6.3 Economics

The multi-pump system designed here provides laboratories with a cost-effective alternative to commercially available pump systems for biological research. Due to the DIY nature of the device, the 3D printed pieces of the pump can be constructed at minimal cost, as the material used is a relatively cheap acrylonitrile butadiene styrene (ABS) filament from www.imakr.com, at prices ranging from \$20 to \$40. The remainder of materials have a summed price that is much less expensive than syringe pumps on the market, which can be anywhere from \$300 to \$3000. Building this system is a much more economical alternative for Mitchell Lab, since purchasing 12 commercially available syringe pumps in order to run 6 parallel

experiments would be extremely costly. Overall, this multi-pump system is a very cost-effective choice for research laboratories.

6.4 Environmental Impact

The multi-pump system will not create a huge impact on the environment, as it does not produce any waste. The main area of concern is the 3D printed pieces, which are made of ABS plastic. ABS is recyclable, which will reduce its environmental effects. If the pumps are continuously being used in the laboratory, then these pieces will not need to be disposed of. However, should these pieces fracture or break from overuse, they can then be recycled, and new pieces can be 3D printed in the MakerSpace.

The users of the multi-pump system can also minimize waste in regards to materials used in standard experiments. Researchers will not have the need for standard tissue culture plates, meaning that they will discard fewer and have less waste. This is good for the environment because these plates are made of plastic. The microfluidic chambers are very expensive, at approximately \$50 a piece, but have 6 channels for experiments. Thus, with more channels, the user can still produce efficient experimental output while discarding less materials. Furthermore, the microfluidic chambers, tubes, and many other components of the system (such as the Luer stubs and small metal tubes) can be reused if properly cleaned, which also contributes to less waste when experiments are performed.

6.5 Societal Influence

The multi-pump system has both benefits for laboratory settings and for research. This system allows more efficient testing on cell cultures exposed to dynamically changing environments. This will enable laboratory settings to obtain multi-pump systems more economically accessible to develop complex models. These models can be applied for further disease research using a wide variety of cells types and evaluate their response to different types of drugs, treatments, or any dynamic alterations. Allowing six experiments to run at the same time will influence laboratories and research to be more cost and time effective.

In terms of research, this multi-pump system has the potential to advance scientific knowledge about cancer. As demonstrated in this project, the device facilitates cancer therapeutic research by delivering dynamic doses of vemurafenib to melanoma cells. This is simply one of the many cancer-related experiments that can be conducted with the pump.

Should these experiments prove fruitful, the resulting findings and possible cancer drug development can have a beneficial impact on patients. Other critical biological research questions that require constant fluid flow and syringe pumps can be made possible with the use of this pump.

6.6 Political Ramifications

Research tends to be expensive due to inefficient and time consuming testings. This system will provide the opportunity to run six experiments in parallel which would accelerate the process of testing and produce cost-effective research. Currently, cancer research is being done worldwide and allowing this system to be used in this field is a novel way of performing high-throughput experiments, which will enhance the finding of treatment or ideal drug dosing at determined pulses for specific types of cancer cells. In order to provide assurance of device effectiveness, the FDA could play a role in it, by assigning specific guidance and requirements of use for this type of devices.

6.7 Ethical Concerns

The device will be ethically beneficial to society because it would accelerate the research for any treatment to a specific disease, or in our case melanoma cancer. Additionally, it will provide input on how cells respond to the different forms of treatment, either to different drug concentration or to different pulses of drug, before sacrificing animal models for testing and before exposing human beings to clinical trials. The multi-pump system itself does not pose any ethical concerns, as it is simply a tool for researchers to perform their biological studies.

6.8 Health and Safety Issues

The device utilizes an Arduino system; however, this does not produce a high-level risk to human use even if a circuit shock is produced. Regarding the biological aspect, most of the research in which this device could be used involves cancerous cells which could expose the user to health and safety issues. Working with this type of cells or any other biological materials presents a health risk on Biosafety Level 2. Therefore, all users who wish to perform biological experiments that use the multi-pump system must be cleared for Biosafety Level 2 work and must receive the proper laboratory safety training.

6.9 Manufacturability

In order to manufacture the device, the costs were considered to be built at lower prices compared to the competitors commercially available. Syringe pumps for lab settings that can manage low flow rates as needed when working with microfluidic environments are found at high costs in the market, over \$1000. These devices are usually found on a one-by-one basis, and usually limited to very specific types of experiments at already determined flow rates. The device presented by the team can be easily manufactured at lower costs and adapted to the user needs. The syringe holder bases are 3D printed with a relatively inexpensive ABS material, which saves in cost production. The other components were bought in Amazon or Home Depot at very low prices. The syringe is powered and programmed by an Arduino and motor shield which are accessible and can be edited as needed. The user manual on how to build it can be found in Appendix C.

6.10 Sustainability

Our device is sustainable for laboratory settings. It is easily built and the parts that it is composed of are strong enough to withstand the stress the device might receive. However, in case of needing an extra piece, the syringe holders are easily 3D printed and any other parts are economic and can be easily purchased through Amazon or Home Depot. The syringes, tubing, plugs, and 6 channel microfluidic chamber is replaceable to run experiments multiple times as needed. Additionally, the device can be used for further purposes than the one described by the design team by implementing a different variety of treatment to distinct cell types. Because it is a durable device that can be used for long periods of time, and because it has potential for use in so many different types of biological experiments, this device is sustainable for the user.

6.11 Industry Standards

In order to complete the design and building of the device, some ISO standards were followed. As mentioned in Chapter 3, ISO 7 was followed for the amount of particles allowed in laboratory settings. The ISO 15190, was followed for guidance on proper working environment for *in vitro* diagnosis and guarantee safety for lab workers. The ISO 11737-2:2009 guide was also followed for sterility of medical or laboratory devices which have large effect on cell culture. Additionally, the ISO 10993-1 which covers the Biological evaluation and biocompatibility assessment as stated by the FDA.

Chapter 7: Discussion

7.1 Final Design Analysis

The team has designed a multi-pump system that satisfies all needs of the client. The system met all objectives, design requirements, and constraints, each of which will be described in detail below. The design team verified the functionality of the pump by performing biological experiments that demonstrate it worked with cell cultures in microfluidic chambers. These experiments also demonstrated that the device can enable cellular signaling studies that can provide meaningful biological data and subsequent analysis. For these reasons, the design and assembly of the multi-pump system was a success.

7.1.1 Accomplishing Objectives

The completed multi-pump system was able to meet each of the objectives for the project. The finished product was fully programmable through the use of an Arduino. The user of the system can interact directly with the Arduino code by inputting desired values of experiment parameters, such as flow rate, delay, and pulse frequency. Once the code is uploaded to the Arduino, the experiment can run with minimal human intervention and therefore provides an automated system.

The system is also very user-friendly. The User Manual in Appendix C provides a detailed, step-by-step guide to setting up the multi-pump system. The Arduino Code Documentation in Appendix B contains a full annotation of the code that is used to control the pumps, which can aid the user in setting up the desired experiment parameters. Furthermore, the protocol in Appendix D describes the procedure for performing biological cellular signaling experiments with the multi-pump system. These documents, as well as the relative simplicity of the pump, make the system easy to use.

Parallelization has also been achieved. The design team constructed 6 pump units, for a total of 12 syringe pumps, that make up the multi-pump system. Each pump unit will be attached with tubing to one channel of the ibidi® microfluidic chamber, which contains a total of six channels. This allows for side-by-side, simultaneous studies. It allows the user to perform 6 experiments in parallel for greater efficiency. The design team has demonstrated the

parallelization of the system by performing two different biological experiments that required the use of 6 pumps.

Cell viability is also maintained. The design team has shown that media delivered by the pumps at very low flow rates between 0.02 mL/min and 0.1 mL/min was able to maintain cell viability for the duration of experiments that last up to 24 hours.

7.1.2 Satisfying Constraints

Construction of the device remained within the the design constraints that were established at the beginning of the project. As proposed by the team, the device itself was constructed and validation testing was completed by the end of C term. Biological experiments related to cellular signaling studies were then performed for the entirety of D term, which was one of the main goals of the design team. Although expenses exceeded the team's budget provided by the BME department, the team was able to order all necessary materials with the help of Mitchell Lab, who covered any outstanding costs.

The system's components can undergo standard sterilization procedures, either by washing the system with ethanol or by autoclaving. The materials in direct contact with the cells are biocompatible. This is primarily the ibidi® microfluidic chamber, which also has a trade secret surface treatment to promote surface cell adhesion. The size of the system as a whole is quite large, but the microfluidic chamber itself is the only component which must be inside the microscope incubator, and it does fit. The weight has been minimized by attaching two pumps to a single base, which is important to reduce both the expenses of the system and the space that the device will occupy in the lab. The Arduino used in the system is compatible with the software and stepper motors for successful programmability.

Cell viability was one of the most critical constraints. Media delivery to the microfluidic chambers was set at a very low flow rate to not perturb the cells residing within them. These flow rates ranged from 0.02 mL/min at the low extreme, to 0.1 mL/min at the high extreme. Cell viability studies were able to verify that these flow rates did not have a deleterious effect on the cells. These flow rates also led to shear stresses that were ideal for this specific application. According to the ibidi® product guide, flow rates within the μ -Slide VI 0.4 microfluidic chamber used by Mitchell Lab can be used to calculate shear stresses that occur within the chamber (*Shear Stress and Shear Rates for ibidi μ -Slides*, 2016). The design team used only flow rates of 0.02 mL/min, 0.05 mL/min, and 0.1 mL/min. Based on the product guide, a flow rate of 0.08 mL/min

will result in a shear stress of 0.1 dyn/cm^2 within the channel, and a flow rate of 0.16 mL/min will result in a shear stress of 0.2 dyn/cm^2 . The flow rates used by this pump are within this range, and these associated shear stresses do not exceed the limit for cell viability, as discussed in previous chapters.

7.1.3 Meeting Design Requirements

The design team was able to successfully meet all design requirements, which were a combination of objectives, constraints, and functions of the system. Objectives and constraints were already discussed in the preceding two sections of this chapter. For functions, the multi-pump system can successfully deliver two different types of media in alternating fashion to enable pulse experiments involving different drug profiles. The flow rate, and by consequence shear stress, is controlled by the Arduino code. Furthermore, the design team has performed testing that involves tracking of induced bubbles in the flowing fluid to verify that the specified flow rate is accurate. The tubing used at the outlet of the microfluidic channels successfully removed media into a waste container after it had passed through the channel, and this did not damage cells in any way. The system was compatible with common sterilization techniques. It was also compatible with the microscope incubator, which was crucial to ensure that the system could provide and maintain the proper environment for cell cultures.

In addition, all needs were successfully met, many of which have already been discussed. The pump also accommodated live-cell imaging at single-cell resolution with time-lapse microscopy because it was compatible with the microscope incubator. The microscope incubator also provided the correct temperature and carbon dioxide control, and the addition of HEPES buffer provided stabilization of pH for the cell cultures.

7.2 Comparison with Existing Devices

The team evaluated three alternative designs from the ones available in literature. These were the gravity driven pump, and the DIY Syringe Pump. According to literature these were the most suitable design options for the team requirements. The hydrostatic pump consisted of simple mechanics and was easy and economical to build. However, the downside of this option consisted of the flow rate decreasing with time and challenging to achieve slow flow rates that would allow 30 ml of media to last 24 hours or more.

The other option alternative evaluated was syringe pumps, which are widely used in lab settings, but due to high prices, the team decided to develop DIY syringe pumps. These result very economical and can be built with simple materials mostly found in the lab setting. Two designs were tested and the Laser Cut syringe was discarded because the moving piece the pushed the syringe plunger to generate the flow immobilized at some time points of the experiment making the setting not be reliable enough for the team to trust doing experiments over 24 hours long.

Lastly the 3D printed syringe pump was built and tested to verify and validate the functioning of the device. This device was economically available and easy to build compared to those available commercially as already built syringe pumps or pressure driven systems as the ibidi pump system which are very expensive to obtain. This device has the advantage of being customizable to meet specifics of the end user and is flexible for different type of experiments for different types of cell study, which is an advantage compares to the automated syringe pump commercially available. The device was verified by performing, flow rate testing, stress testing, and uniform media distribution testing. Successfully, the pump was able to achieve slow flow rates and this was confirmed by ensuring the input flow rate in the arduino code matched the flow rate calculated from the outlet of the chamber. Regarding the uniform media distribution, this verification testing was done to provide information on how rapidly the switch between pumps occurred and how long did it last for the new media to cover the whole chamber. The results stated that even for the slowest flow rate (0.02 ml/min) that was tested the chamber was completely filled post pump switch after less than 5 minutes. This can be considered slow compared to the pressure driven pumps as the Ibidi pump system, which have the feature of rapid switching between reservoirs in seconds, however developing this kind of devices is very expensive that goes above the budget of the team and the lab.

The 3D printed pump was then validated by performing biological experiments in which the objectives of maintaining cell viability, performing high throughput experiments through parallelization, being automated and user friendly were met. The device demonstrated to be compatible with microfluidics by demonstrating that cell response studies can be achieved with this system.

7.3 Limitations

7.3.1 System must be stopped manually at the end of the experiment

The pump system was programmed to be automated and to function without any human interaction. However, the code has the limitation of not having a timer that can stop the pumps when the experiment is over. The biological experiments last for an intended duration, and the Zeiss microscope will perform time-lapse microscopy with the ZenPro software during the duration of the experiment. However, the pumps do not stop automatically when the images are done being taken. The implications for the end user are that the user must physically unplug the pumps or cut off the power source to the pumps when the experiment is over, which limits the flexibility for the user and requires manual intervention. Therefore, the user must coordinate their schedule around the timing of the experiment, which is very inconvenient. Additionally, if the system continues to run for longer than the designated experiment duration, the motors could overheat and the system could be damaged.

7.3.2 Air bubbles enter the system

When setting up experiments, especially when performing the six parallel pump experiment, bubbles tend to form inside the syringes and eventually could get into the system at any time point of the experiment. Bubbles enter the system during setup because of air that gets trapped in the system when inserting the plugs with the tubes, or because some of them were left in the syringes. Additionally, if insertion of the inlet plug, outlet plug, and tubes is not performed properly according to the protocol developed in Appendix D, then air could be trapped between the media and the plugs, giving the possibility for air bubbles to form and enter the microfluidic chamber. These bubble formations are a limitation because air bubbles that travel through the microfluidic channel will wash cells away, resulting in data loss. Any images taken in the regions that contain air bubbles cannot be analyzed, since there are very few cells remaining in the channel and the imaging quality of these regions is poor.

7.3.3 Cells suffer during experiment setup

In order to maintain cell viability, the appropriate pH and temperature must be provided at all times. Although the microfluidic chamber is placed inside the microscope incubator during the experiment and the media that flows through the chamber contains HEPES buffer to regulate the pH, the setup of the experiment is performed at ambient temperature and cells are originally

plated without HEPES in the media. For this reason, cells have a limited time in which they can survive while the experiment being set up. Some experiments present high complexity in the setup, especially when all six pump units are running, and if plugs and tubing are not placed and inserted rapidly, in some cases cells might suffer and die even before starting the experiment. Additionally, if the setup process takes too long, the cells become unhealthy, and this is evident in the very first images taken when the experiment is finally started.

7.4 Impact on Biological Research

7.4.1 Cell Viability under different flow rates

Since maintaining cell viability was considered one of the main objectives of the project, the team had to ensure the pump system was able to deliver a flow rate that was slow enough for cells to withstand and therefore allow the performance of biological experiments. The team successfully met this objective. However, the team found some interesting results. Unexpectedly, the lowest flow rate had the lower cell viability among all the tested flow rates. A possible reason could be cells that are initially exposed to a determined shear stress, even under low flow rates could have been washed out. For the 0.05 mL/min, the cell viability was measured as above 100%, possibly because cells near the inlet of the chamber could have moved around and by the end of its testing period some cells that initially weren't on the tile that was imaged, appeared and later attached to this same tile. For the 0.1 mL/min cell viability is also considered to be high, which is good indication that cells are able to survive to the shear stress generated by this flow rate. Overall, having a 88% of cell viability is considered high since cells survive when exposed to flow rates and shear stress generated by the pump system. Proving cell viability was high opened the path for other experiments of biological interest to be performed.

7.4.2 Promising studies in cancer research

The multi-pump system constructed by the design team provides a useful, unique, and valuable device to the Mitchell Lab for their research. This system will enable the experiments they wish to conduct related to their hypothesis. This hypothesis centers around the idea that dynamic doses of vemurafenib can effectively treat melanoma cells while at the same time minimizing drug exposure to the cells. While the lab was able to perform static experiments previously, they would like to observe the effects of dynamic experiments in which media and drug are continuously flowing in alternating fashion into the microfluidic channels that cells are

seeded in. This is particularly relevant for the starvation experiments, which are of great interest to the lab, as well as the drug holiday experiments, in which there are resting periods between each drug dose. Without the pump system, which provides the continuous flow that maintains cell viability and is fully programmable to alternate between media and drug doses in different profiles, these experiments would not be possible, and thus the system is crucial to their future research.

Chapter 8: Conclusions

8.1 Conclusions

The design team has demonstrated the functionality of the multi-pump system by performing biological experiments that monitor the temporal dynamics of signaling inhibition in an important model melanoma cell line. The team has designed a 3D-printed multi-pump system capable of delivering constant, controllable flow rates of media to cell cultures in microfluidic chambers that are subjected to dynamically changing environments.

Verifying the dynamics of a known cancer mutation in response to oscillatory therapeutic drug doses is informative and demonstrates the functionality and performance of the system. Initial biological experiments demonstrated that the system could deliver dynamic doses of vemurafenib to melanoma cell in microfluidic chambers. Starvation experiments revealed some insight on the effect that the lack of growth factors can have on the cells when being treated with drug (namely, that starvation media lowers proliferation due to the absence of these growth factors). Finally, reducing drug holidays (i.e., relaxation periods between drug doses) can yield a lesser degree of reversibility in the ERK dynamics and therefore less reactivation of the ERK pathway is observed in these periods.

The team achieved all of their objectives and met all design requirements set by the client. The pump system now enables the client's lab to perform meaningful research in melanoma treatment via dynamic doses of vemurafenib.

8.2 Recommendations

The following sections provide recommendations for future improvements of the multi-pump system.

8.2.1 Implement a method for stopping the pumps when an experiment has finished

Implementation of a timer in the Arduino Code will allow the pumps to stop running when the experiment has finished. This will prevent any potential damage to the system if the pumps keep running well after the experiments have finished. It will also give much more flexibility to the end user, because they will not have to accommodate their work schedule based on when the experiment finishes in order to manually unplug the pump.

Another possible option for stopping the pumps is a timer on the power source in the form of an electrical timer. This will be attached to the power source and will cut the power

when the designated time (based on the experiment duration) has passed, thereby stopping the pumps when the experiment has finished. In general, accomplishing some form of timer will give more flexibility to the end user.

8.2.2 Introduce a User Interface

Another recommendation would be to introduce a more user-friendly interface. For the purposes of this project, the client stated that changing experiment parameters directly in the Arduino code was sufficient. To increase user-friendliness of the system, a user interface can be implemented. This could take the form of the Adafruit LCD Shield, which consists of a screen display that can prompt the user to enter the experiment parameters and buttons for selecting the parameters the user wants for the experiment. This LCD Shield would be easy to implement because it can be connected directly to the Arduino, and it would be easy to use for the end user so that they are not required to interact directly with the Arduino code.

8.2.3 Establish a solution for preventing bubbles from entering the system

Bubbles entering the system is a limitation especially when these enter the channel affecting biological samples and cells ideal environment, as well as serving as obstacles for clear images being taken. For this reason the team proposed evaluating the option of a bubble trapper. One recommended option is the ElveFlow Microfluidic bubble trapper as seen in the image below [55]. This debubbler uses a Polytetrafluoroethylene (PTFE) microporous membrane in which the inlet fluid containing bubbles flows and traps the bubbles and expel them through a hydrophobic membrane even at low pressures.

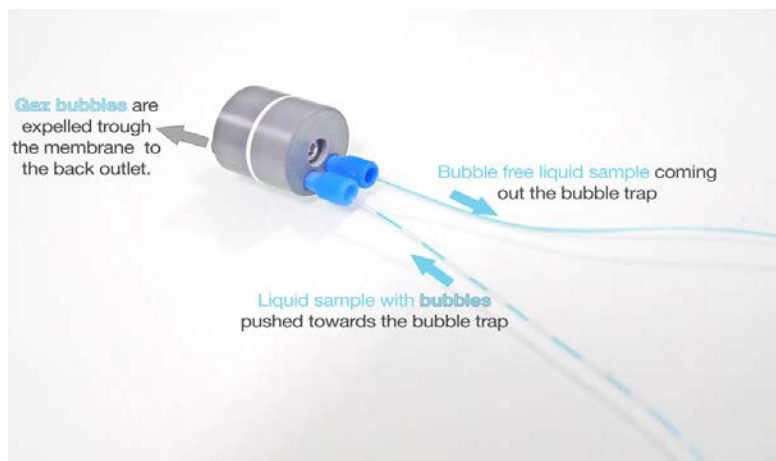


Figure 93: ElveFlow Microfluidic Bubble Trapper [59]

Another recommended option would be media degas already mounted in the syringes to eliminate all possible bubbles and prevent them from entering the tubing and chamber. The degassing of syringes can be done either by vacuum or by centrifuging.

8.2.4 Prevent cell suffering during experiment setup

In order for cell to survive long periods in cell cultures, these should be maintained in a proper environment. This means they should be exposed to appropriate temperature (37°C) and pH. The microscope incubator is not able to provide the pH through CO₂, and for this reason HEPES buffer is added to the media at the syringes that will be flowing through the chamber. However, the cells originally plated have suffered during experiments set up due to lack of HEPES, and the appropriate temperature. The setup of experiments can last for about an hour which is enough for cells to suffer or even die without having the appropriate environment. For this reason the team proposes to add HEPES to the media used to originally plate cells in the microfluidic for them to have the ideal pH. In order to have cells under adequate temperature during the setup, a solution would be to have a small portable and transportable incubator chamber that levels the temperature to 37°C and performing the setup of the experiments while the microfluidic is standing inside the chamber.

8.2.5 Other recommendations

Other recommendations include the possible use of an alternative material for the 3D printed parts of the syringe pump. The material that is currently used is acrylonitrile butadiene styrene, or ABS. Extensive use of the pump can cause the 3D printed pieces to fracture. Thus, an alternative material that is stronger than ABS could be used instead. Alternatively, the material can be kept the same but the 3D printing pattern can be altered to give the pieces more strength. This can be accomplished by increasing the fill density of the material during printing to give the pieces more strength.

Another recommendation would be to find an alternative coupler. This is the piece that connects the motor shaft to the threaded rod, which have two different diameters. The current coupler has the same diameter as the threaded rod, so it is a perfect fit on one side. However, the other side has an imperfect fit because the motor shaft is much smaller in diameter than both the threaded rod and the coupler hole. Additionally, there are 4 small screws on the coupler for

fastening, but they are all situated on the same side. When the coupler is tightened, this causes the motor shaft to be pushed against one side of the coupler's interior. This results in an elliptical movement of the rod as the motor turns, rather than a circular movement. Finding a different coupler that can accommodate the motor shaft and the threaded rod so that they are both centered can help achieve more smooth movement of the rod as it turns.

8.3 Future Work

The client initially proposed having three different types of experiments, as discussed in Chapter 4. These proposed experiments were the Pulse Experiment, Constitutive Level Experiment, and Slope Experiment. The first type, Pulse Experiment, was successfully achieved. Due to time constraints, the constitutive level and slope experiments were not implemented. These experiments would involve having one syringe with a 100% concentration of drug and another syringe with standard cell culture media that are being pumped simultaneously but at different rates in order to obtain either a constant level, increasing level, or decreasing level of drug concentration. The main difficulty here was achieving consistent, thorough mixing within the microfluidic chamber. As described in Chapter 2, mixing is difficult to obtain inside small channels of microfluidics because of the laminar flow that occurs. Furthermore, two streams inside a microfluidic channel will only occur by diffusion. Future work on this project can consist of searching for a reliable mechanism to achieve mixing in the channel in order to enable the constitutive level and slope experiments that will involve obtaining different gradients of drug doses by acquiring different drug concentrations. This could potentially be accomplished with the use of micromixers or modifying channel geometries to increase the amount of time that diffusion can occur between two fluids, both of which will facilitate mixing.

Important future work can be performed related to the biological experiments. As previously discussed, the completion of this pump system enables Mitchell Lab to continue researching their hypothesis regarding the treatment of melanoma cells to dynamic doses of vemurafenib. Many different experiments can be performed in the future to expand on the ones conducted by the design team. First, the multi-pump experiment can be repeated. This would consist of independent but parallel experiments, which each of the 6 pumps controlling the specific drug profile for a single channel in the microfluidic chamber. Each channel can run different frequencies of drug exposure, similar to the experiment that the design team conducted.

Since the multi-pump frequency experiment that was performed by the team had inconclusive results due to technical difficulties, this would be a very useful experiment to repeat. It would allow for greater experimental efficiency due to its parallel nature as well as the obtaining large amounts of data for analysis.

The starvation experiments can also be repeated. The team performed different variations of the starvation experiment, but more reliable data is needed by Mitchell Lab before definitive conclusions can be made. Since the outcome of starvation experiments is one of their main interests, the pump system can be used by members of the lab in the future to advance their research in this area.

Another option for future work is extending the experiment duration to 48 hours instead of 24 hours. This would have to involve the testing of other flow rates to ensure that cell viability can be maintained for longer experiment durations. This would be very valuable because melanoma cell behavior in response to dynamic vemurafenib doses in the long term is of great interest to the lab.

In conclusion, the multi-pump system built by the design team can be used by members of Mitchell Lab to continue research on their hypothesis. The pump system now enables the lab to perform interesting experiments in which they administer dynamic doses of vemurafenib to melanoma cells to see if this can more effectively treat melanoma cells while simultaneously reducing drug exposure.

References

- [1] M. Rastrelli, S. Tropea, C. Rossi and M. Alaibac, "Melanoma: Epidemiology, Risk Factors, Pathogenesis, Diagnosis, and Classification", *In vivo*, vol. 28, pp. 1005-1012, 2011.
- [2] R. Ossio, R. Roldán-Marín, H. Martínez-Said, D. Adams and C. Robles-Espinoza, "Melanoma: a global perspective", *Nature Reviews Cancer*, vol. 17, no. 7, pp. 393-394, 2017.
- [3] A. Mitchell, P. Wei and W. Lim, "Oscillatory stress stimulation uncovers an Achilles heel of the yeast MAPK signaling network", *Science*, vol. 350, pp. 1379-138, 2015.
- [4] C. Byun, K. Abi-Samra, Y. Cho and S. Takayama, "Pumps for microfluidic cell culture", *ELECTROPHORESIS*, vol. 35, no. 2-3, pp. 245-257, 2013.
- [5] E. Young and D. Beebe, "Fundamentals of microfluidic cell culture in controlled microenvironments", 2010. [Online]. Available: <http://dx.doi.org/10.1039/b909900j>. [Accessed: 10- Nov- 2017]
- [6] M. Mehling and S. Tay, "Microfluidic cell culture", *Current Opinion in Biotechnology*, 2014. [Online]. Available: <http://doi.org/10.1016/j.copbio.2013.10.005>. [Accessed: 23- Sep- 2017]
- [7] N. Sasaki, M. Shinjo, S. Hirakawa, M. Nishinaka, Y. Tanaka, K. Mawatari, T. Kitamori and K. Sato, "A palmtop-sized microfluidic cell culture system driven by a miniaturized infusion pump", *ELECTROPHORESIS*, vol. 33, no. 12, pp. 1729-1735, 2012.
- [8] "OEM solution pushes cell culture boundaries", 2018.
- [9] F. Zhao and T. Ma, "Perfusion bioreactor system for human mesenchymal stem cell tissue engineering: Dynamic cell seeding and construct development", *Biotechnology and Bioengineering*, vol. 91, no. 4, pp. 482-493, 2005.
- [10] J. Britton and T. Jamison, "The assembly and use of continuous flow systems for chemical synthesis", *Nature Protocols*, vol. 12, no. 11, pp. 2423-2446, 2017.
- [11] J. Tarbell and Z. Shi, "Effect of the glycocalyx layer on transmission of interstitial flow shear stress to embedded cells", *Biomechanics and Modeling in Mechanobiology*, vol. 12, no. 1, pp. 111-121, 2012.
- [12] S. Halldorsson, E. Lucumi, R. Gómez-Sjöberg and R. Fleming, "Advantages and challenges of microfluidic cell culture in polydimethylsiloxane devices", *Biosensors and Bioelectronics*, vol. 63, pp. 218-231, 2015.
- [13] T. Boone, Z. Fan, H. Hooper, A. Ricco, H. Tan and S. Williams, "Peer Reviewed: Plastic Advances Microfluidic Devices", *Analytical Chemistry*, vol. 74, no. 3, pp. 78 A-86 A, 2002.

- [14] D. Beebe, G. Mensing and G. Walker, "Physics and Applications of Microfluidics in Biology", *Annual Review of Biomedical Engineering*, vol. 4, no. 1, pp. 261-286, 2002.
- [15] Y. Çengel and J. Cimbala, *Fluid mechanics*. Boston: McGraw-Hill Higher Education, 2014.
- [16] L. Yi and J. Lin, "Development and Applications of Microfluidic Devices for Cell Culture in Cell Biology", *Molecular Biology*, vol. 1, 2016.
- [17] Z. Zhang and S. Nagrath, "Microfluidics and cancer: are we there yet?", *Biomedical Microdevices*, vol. 15, no. 4, pp. 595-609, 2013.
- [18] M. Wu, S. Huang and G. Lee, "Microfluidic cell culture systems for drug research", *Lab on a Chip*, vol. 10, no. 8, p. 939, 2010.
- [19] "Gravity driven Perfusion System - Elveflow", Elveflow, 2018. [Online]. Available: <https://www.elveflow.com/microfluidic-tutorials/cell-biology-imaging-reviews-and-tutorials/live-cell-perfusion/methods-and-techniques/perfusion-systems-for-live-cell-microscopy/automate-scientific-perfusion-system/>. [Accessed: 23- Mar- 2018]
- [20] Rsc.org. *Lab on a Chip*, 2018 [online] Available at: <http://www.rsc.org/journals-books-databases/about-journals/lab-on-a-chip/> [Accessed 20 Mar. 2018].
- [21] V. Shukla, T. Kuang, A. Senthilvelan, N. Higueta-Castro, S. Duarte-Sanmiguel, S. Ghadiali and D. Gallego-Perez, "Lab-on-a-Chip Platforms for Biophysical Studies of Cancer with Single-Cell Resolution", *Trends in Biotechnology*, vol. 36, no. 5, pp. 549-561, 2018.
- [22] "Research", Mitchell Lab, 2018. [Online]. Available: <https://mitchell-lab.umassmed.edu/research/>. [Accessed: 16- Mar- 2018]
- [23] "Brief", Mitchell Lab, 2018. [Online]. Available: <https://mitchell-lab.umassmed.edu/research/>. [Accessed: 16- Mar- 2018]
- [24] Cancer.org. What Is Melanoma Skin Cancer?. 2018 [online] Available at: <https://www.cancer.org/cancer/melanoma-skin-cancer/about/what-is-melanoma.html> [Accessed 18 Mar. 2018].
- [25] J. Barnes, J. Nauseef and M. Henry, "Resistance to Fluid Shear Stress Is a Conserved Biophysical Property of Malignant Cells", *PLoS ONE*, vol. 7, no. 12, p. e50973, 2012.
- [26] A. Kim and M. Cohen, "The discovery of vemurafenib for the treatment of BRAF-mutated metastatic melanoma", *Expert Opinion on Drug Discovery*, vol. 11, no. 9, pp. 907-916, 2016.
- [27] P. Ascierto, J. Kirkwood, J. Grob, E. Simeone, A. Grimaldi, M. Maio, G. Palmieri, A. Testori, F. Marincola and N. Mozzillo, "The role of BRAF V600 mutation in melanoma", *Journal of Translational Medicine*, vol. 10, no. 1, p. 85, 2012.

- [28] A. Plotnikov, K. Flores, G. Maik-Rachline, E. Zehorai, E. Kapri-Pardes, D. Berti, T. Hanoch, M. Besser and R. Seger, "The nuclear translocation of ERK1/2 as an anticancer target", *Nature Communications*, vol. 6, no. 1, 2015.
- [29] C. de la Cova, R. Townley, S. Regot and I. Greenwald, "A Real-Time Biosensor for ERK Activity Reveals Signaling Dynamics during *C. elegans* Cell Fate Specification", *Developmental Cell*, vol. 42, no. 5, pp. 542-553.e4, 2017.
- [30] Elveflow. "Syringe pumps and microfluidics- Elveflow". 2014 [online] Available at: <https://www.elveflow.com/microfluidic-tutorials/microfluidic-reviews-and-tutorials/syringe-pumps-and-microfluidics/> [Accessed 16 Mar. 2018].
- [31] Manufacturingchemist.com. (2012). *Peristaltic pumps - advantages and applications*. 2012 [online] Available at: https://www.manufacturingchemist.com/news/article_page/Peristaltic_pumps__advantages_and_applications/74693 [Accessed 17 Mar. 2018].
- [32]"A First Inherently Pulsation Free Peristaltic Pump", 58th Illmenau Scientific Colloquium, vol. 58, 2014.
- [33] M. Marimuthu and S. Kim, "Pumpless steady-flow microfluidic chip for cell culture", *Analytical Biochemistry*, vol. 437, no. 2, pp. 161-163, 2013.
- [34]M. Long, "What is a Syringe Pump? | Infusion Pump vs. Syringe Pump", Chemyx Inc, 2018. [Online]. Available: <https://www.chemyx.com/support/knowledge-base/getting-started/what-is-a-syringe-pump/>. [Accessed: 12- Sep- 2017]
- [35] Elveflow. "Perfusion for live cell imaging: Methods and techniques", 2018. [Online]. Available:<https://www.elveflow.com/microfluidic-tutorials/cell-biology-imaging-reviews-and-tutorials/live-cell-perfusion/methods-and-techniques/>. [Accessed: 10- Apr- 2018]
- [36] R. Gómez-Sjöberg, A. Leyrat, D. Pirone, C. Chen and S. Quake, "Versatile, Fully Automated, Microfluidic Cell Culture System", *Analytical Chemistry*, vol. 79, no. 22, pp. 8557-8563, 2007.
- [37]"ibidi Pump System | Perform Cell-Based Flow Assays", Ibidi.com, 2018. [Online]. Available: <https://ibidi.com/perfusion-system/112-ibidi-pump-system.html>. [Accessed: 20- Mar- 2018]
- [38] Microfluidic pump, "Microfluidic infusion only syringe pump", Darwin Microfluidics, 2018. [Online]. Available: <https://darwin-microfluidics.com/collections/syringe-pump/products/microfluidic-just-infusion-syringe-pump>. [Accessed: 20- Mar- 2018]

- [39] L. Shelledy, PharmD and D. Roman, PharmD, BCOP, "Vemurafenib: First-in-Class BRAF-Mutated Inhibitor for the Treatment of Unresectable or Metastatic Melanoma", *Journal of the Advanced Practitioner in Oncology*, vol. 6, no. 4, 2015.
- [40] G. Bancroft, V. Sikavitsas and A. Mikos, "Technical Note: Design of a Flow Perfusion Bioreactor System for Bone Tissue-Engineering Applications", *Tissue Engineering*, vol. 9, no. 3, pp. 549-554, 2003.
- [41] M. Mitchell and M. King, "Computational and Experimental Models of Cancer Cell Response to Fluid Shear Stress", *Frontiers in Oncology*, vol. 3, 2013.
- [42] "µ-Slide VI 0.4 | Channel Slide for Parallel Flow Assays | ibidi", *Ibidi.com*, 2018. [Online]. Available: <https://ibidi.com/channel-slides/57--slide-vi-04.html>. [Accessed: 28- Aug- 2017]
- [43] Iso.org. "35.240.10 - Computer-aided design (CAD)", 2018. [Online]. Available: <https://www.iso.org/ics/35.240.10/x/>. [Accessed: 24- Apr- 2018]
- [44] "Translational medicine and laboratory design", *Laboratory Design News*, 2018. [Online]. Available: <https://www.labdesignnews.com/article/2016/09/translational-medicine-and-laboratory-design>. [Accessed: 01- Oct- 2018]
- [45] Iso.org, 2018. [Online]. Available: <https://www.iso.org/obp/ui/#iso:std:iso:15190:ed-1:v1:en>. [Accessed: 01- Oct- 2017]
- [46] I. 11737-2:2009, "ISO 11737-2:2009 - Sterilization of medical devices -- Microbiological methods -- Part 2: Tests of sterility performed in the definition, validation and maintenance of a sterilization process", *Iso.org*, 2018. [Online]. Available: <https://www.iso.org/standard/44955.html>. [Accessed: 01- Oct- 2017]
- [47] *Fda.gov*, 2018. [Online]. Available: <https://www.fda.gov/downloads/medicaldevices/deviceregulationandguidance/guidancedocuments/ucm348890.pdf>. [Accessed: 26- Sep- 2017]
- [48] Z. Li, S. Mak, A. Sauret and H. Shum, "Syringe-pump-induced fluctuation in all-aqueous microfluidic system implications for flow rate accuracy", *Lab on a Chip*, vol. 14, no. 4, p. 744, 2014.
- [49] "Electric Motors and Drives - Fundamentals, Types, and Applications", *App.knovel.com*, 2006. [Online]. Available: https://app.knovel.com/web/toc.v/cid:kpEMDFTA3/viewerType:toc/root_slug:electric-motors-drives. [Accessed: 21- Sep- 2017]
- [50] "Arduino - Introduction", *Arduino.cc*, 2017. [Online]. Available: <https://www.arduino.cc/en/Guide/Introduction>. [Accessed: 30- Sep- 2017]
- [51] R. Wentk, *Teach yourself visually Raspberry Pi*. Visual, 2014.

- [52] L. Waite and J. Fine, "Applied Biofluid Mechanics", McGraw-Hill Companies, Inc, 2007.
- [53] D. Albrecht, "BME ISP DRA 3601: Microfluidics Laboratory Week 4: Microfluidic Physics I: Flow, Resistance, Diffusion (and Droplets?)", 2015.
- [54] D. Albrecht, "BME ISP DRA 3601: Microfluidics Laboratory Week 5: Microfluidic Physics II: Shear stress, Gradients, Flow networks", 2015.
- [55] "DIY Syringe Pump Using Stepper Motor", Instructables.com, 2018. [Online]. Available: <http://www.instructables.com/id/DIY-Syringe-Pump-Using-Stepper-Motor/>. [Accessed: 01-Nov- 2017]
- [56] "Open Syringe Pump", Hackaday.io, 2018. [Online]. Available: <https://hackaday.io/project/1838-open-syringe-pump>. [Accessed: 10- Nov- 2018] "Open Syringe Pump", 2018)
- [57] D. Zill and W. Wright, *Differential Equations with Boundary-Value Problems*, 8th ed. Boston: Brooks/Cole, Cengage Learning, 2013.
- [58] C. Edwards and D. Penney, *Differential Equations and Boundary Value Problems*, 5th ed. Upper Saddle River: Pearson Education, Inc., 2014.
- [59] "Avoid air bubbles during your microfluidic experiments - Elveflow", Elveflow, 2018. [Online]. Available: <https://www.elflow.com/microfluidic-tutorials/microfluidic-applications/avoid-air-bubbles-during-your-microfluidic-experiments/>. [Accessed: 22- Apr- 2018]
- [60] B. Kernighan and D. Ritchie, *The C programming language*. Englewood Cliffs, NJ: Prentice-Hall, 1988.
- [61] "short", *Arduino.cc*, 2018. [Online]. Available: <https://www.arduino.cc/reference/en/language/variables/data-types/short/>. [Accessed: 22- Apr- 2018].
- [62] "long", *Arduino.cc*, 2018. [Online]. Available: <https://www.arduino.cc/reference/en/language/variables/data-types/long/>. [Accessed: 22- Apr- 2018].
- [63] "unsigned long", *Arduino.cc*, 2018. [Online]. Available: <https://www.arduino.cc/reference/en/language/variables/data-types/unsignedlong/>. [Accessed: 22- Apr- 2018].
- [64] L. Fried, *Adafruit Motor Shield V2 for Arduino*. Adafruit Industries, 2018.

- [65] "setup()", *Arduino.cc*, 2018. [Online]. Available: <https://www.arduino.cc/reference/en/language/structure/sketch/setup/>. [Accessed: 22- Apr- 2018].
- [66] "loop()", *Arduino.cc*, 2018. [Online]. Available: <https://www.arduino.cc/reference/en/language/structure/sketch/loop/>. [Accessed: 22- Apr- 2018].
- [67] "begin()", *Arduino.cc*, 2018. [Online]. Available: <https://www.arduino.cc/en/serial/begin>. [Accessed: 22- Apr- 2018].
- [68] "pinMode()", *Arduino.cc*, 2018. [Online]. Available: <https://www.arduino.cc/reference/en/language/functions/digital-io/pinmode/>. [Accessed: 22- Apr- 2018].
- [69] "Serial.print()", *Arduino.cc*, 2018. [Online]. Available: <https://www.arduino.cc/reference/en/language/functions/communication/serial/print/>. [Accessed: 23- Apr- 2018].
- [70] "println()", *Arduino.cc*, 2018. [Online]. Available: <https://www.arduino.cc/en/Serial/Println>. [Accessed: 23- Apr- 2018].
- [71] "millis()", *Arduino.cc*, 2018. [Online]. Available: <https://www.arduino.cc/reference/en/language/functions/time/millis/>. [Accessed: 23- Apr- 2018].
- [72] "digitalWrite()", *Arduino.cc*, 2018. [Online]. Available: <https://www.arduino.cc/reference/en/language/functions/digital-io/digitalwrite/>. [Accessed: 23- Apr- 2018].
- [73] "Arduino Reference", *Arduino.cc*, 2018. [Online]. Available: <https://www.arduino.cc/reference/en/language/functions/time/delay/>. [Accessed: 23- Apr- 2018].

APPENDIXES

Appendix A: Arduino Code


```

/**
 * FORWARDING AND REWINDING CODE
 * @author Shaimae Elhajjajy
 *
 * Name: Forward and Backward Motion
 *
 * Purpose:
 * This program is intended for the forwarding and rewinding the pumps,
 * in which the moving piece of the pump can be moved either forwards
 * or backwards. It will achieve this functionality
 * by moving the pumps at a reasonable, pre-tested speed. This speed is
 * slow enough to forward or rewind the motors in a reasonable amount
 * of time, but not fast enough to damage the pump itself. The user
 * should only forward or rewind one motor at a time. To do this, comment
 * out the line of code below for the other motor that is not in use.
 * The user must also make sure that the direction of the motor's rotatin
 * specified by the second parameter of the step() function is correct.
 * If the pump is not moving in the desired direction, change this parameter
 * to the opposite (i.e., if FORWARD, change to BACKWARD, and vice versa).
 *
 * This code is especially useful for rewinding the motors to their
 * original position after an experiment has been finished, so that
 * a fully extended 30 mL syringe can be inserted into the pump
 * once again.
 *
 * Comments are provided throughout the code for explanation of specific commands.
 *
 * To view print statements contained within this code, click the magnifying
glass icon at the top right corner of the Arduino interface.
 *
 * Libraries and Functions provided by: Adafruit Motor Shield V2 Arduino Library
 * https://learn.adafruit.
com/adafruit-motor-shield-v2-for-arduino/install-software
 *
 */

// Include the proper libraries
#include <Wire.h>
#include <Adafruit_MotorShield.h>
#include "utility/Adafruit_MS_PWM_ServoDriver.h"

// Request the Stepper Motor with the Adafruit_MotorShield
Adafruit_MotorShield AFMS = Adafruit_MotorShield();

// Initialize the object for Motor 1

```

```

// Format --> AFMS.getStepper(Number of Steps Per Revolution, Port Number)
// For NEMA 17HS13-0404S1 Motor: Number of steps per revolution = 200 (1.8
degree turns)
// Terminals M3 and M4 = port 2
Adafruit_StepperMotor *myMotor1 = AFMS.getStepper(200, 2);

// Initialize the object for Motor 2
// Format --> AFMS.getStepper(Number of Steps Per Revolution, Port Number)
// For NEMA 17HS13-0404S1 Motor: Number of steps per revolution = 200 (1.8
degree turns)
// Terminals M1 and M2 = port 1
Adafruit_StepperMotor *myMotor2 = AFMS.getStepper(200, 1);

// Define Symbolic Constants
#define NUM_STEPS 10           // Define the number of steps that the motor
will move each time
#define DELAY 100             // Define the delay (in milliseconds) that will
occur between each specified number steps of the motor
                               // (Example: in this case, a 100 ms delay will
be inserted after every 10 steps)

/**
 * The Setup() Function
 *
 * The setup() function is called when the experiment first starts.
 * This function will only run once when the Arduino code is first
 * uploaded. The purpose of this function is to "set up" any
 * necessary components of the code, such as initializing
 * variables and pin modes.
 */
void setup() {

    Serial.begin(9600);           // Opens serial port, sets data rate
to 9600 bps
    Serial.println("Stepper test!"); // Print statements to see if the
code is working as expected (inserted for debugging purposes)

    AFMS.begin();                // Initializes the motor shield
object AFMS and sets the frequency
                               // To rewind, leave the parentheses
blank (for default frequency of 1600 Hz, which is faster)

    myMotor1->setSpeed(1);        // Set the speed of Motor 1 to 1 RPM

```

```

(the setSpeed function controls the speed of the stepper motor rotation)
  myMotor2->setSpeed(1);          // Set the speed of Motor 2 to 1 RPM
}

/**
 * The Loop() Function
 *
 * The loop() function allows active control of the Arduino by
 * continuously looping through the code within the function.
 * This function allows for continuous forward or rewinding motion.
 */
void loop(){

  // If motor 1 should be forwarded or rewinded,
  // leave this uncommented, and comment out the
  // line of code for motor 2.
  myMotor1 -> step(NUM_STEPS, BACKWARD, SINGLE);          // Move motor 1.
                                                         // The step()
function controls the motion of the stepper motor; Change the second parameter
based on the direction the motor turns (Forward or Backward)
  // If motor 2 should be forwarded or rewinded,
  // leave this uncommented, and comment out the
  // line of code for motor 1.
  myMotor2 -> step(NUM_STEPS, BACKWARD, MICROSTEP);      // Move motor 2.
                                                         // The step()
function controls the motion of the stepper motor; Change the second parameter
based on the direction the motor turns (Forward or Backward)

  // Insert a delay after each set of steps of the motor
  delay(DELAY);
}

```

```

/**
 * PULSE EXPERIMENT CODE
 * @author Shaimae Elhajjajy
 * @version 3.0 (3/23/2018)
 *
 * Name: Pulse Experiment
 *
 * Purpose:
 * This program is intended for the pulse experiment,
 * in which delivery of media and delivery of drug will be
 * alternated by the pump. It will achieve this functionality
 * by alternating the movement of the two stepper motors.
 * The user can specify various parameters such as
 * stabilization period, flow rate, the duration for which
 * motor 1 runs, and the duration for which motor 2 runs. Motors 1
 * and 2 will each run for their allotted time in alternating fashion
 * for the duration of the experiment.
 *
 * The following parameters are user-defined and indicate the parameters
 * of the experiment. They do NOT indicate parameters of particular
 * functions, despite the use of the @param tags. The parameters are
 * located below in the section labeled "PARAMETERS FOR PULSE EXPERIMENT".
 * There are no return values.
 *
 * @param stab_period      The desired stabilization period at the start of the
experiment
 * @param flow_rate        The desired flow rate at which the media or drug will
be pumped (typically, in the range 0.02083 mL/min and 0.1 mL/min)
 * @param motor1_interval  The desired period of time for which motor 1 will run
during each pulse (NOTE: motor 1 controls media)
 * @param motor2_interval  The desired period of time for which motor 2 will run
during each pulse (NOTE: motor 2 controls drug)
 *
 * Comments are provided throughout the code for explanation of specific commands.
 *
 * To view print statements contained within this code, click the magnifying
glass icon at the top right corner of the Arduino interface.
 *
 * Libraries and Functions provided by: Adafruit Motor Shield V2 Arduino Library
 * https://learn.adafruit.
com/adafruit-motor-shield-v2-for-arduino/install-software
 *
 */
// Include the proper libraries

```

```

#include <Wire.h>
#include <Adafruit_MotorShield.h>
#include "utility/Adafruit_MS_PWM_ServoDriver.h"

// Request the Stepper Motor with the Adafruit_MotorShield
Adafruit_MotorShield AFMS = Adafruit_MotorShield();

// Initialize the object for Motor 1
// Format --> AFMS.getStepper(Number of Steps Per Revolution, Port Number)
// For NEMA 17HS13-0404S1 Motor: Number of steps per revolution = 200 (1.8
degree turns)
// Terminals M3 and M4 = port 2
Adafruit_StepperMotor *myMotor1 = AFMS.getStepper(200, 2);

// Initialize the object for Motor 2
// Format --> AFMS.getStepper(Number of Steps Per Revolution, Port Number)
// For NEMA 17HS13-0404S1 Motor: Number of steps per revolution = 200 (1.8
degree turns)
// Terminals M1 and M2 = port 1
Adafruit_StepperMotor *myMotor2 = AFMS.getStepper(200, 1);

// Define Symbolic Constants
#define STEPS 1 // Define the number of steps that
the motor will move each time
#define MOTOR_1 0 // Constant for Motor 1 in the switch
statement
#define MOTOR_2 1 // Constant for Motor 2 in the switch
statement

// Declare variables
unsigned long start_time = 0; // Initialize the start time of the
experiment to zero
unsigned long end_time; // Declare the variable for end time
unsigned running_motor = MOTOR_2; // Initialize the default running
motor to Motor 2, which runs first at the start of the experiment
unsigned long motor_intervals_sum; // Declare the variable for the sum
of the motor intervals
unsigned long motor1_delay; // Declare the variable for the delay
of Motor 1
unsigned long motor2_delay; // Declare the variable for the delay
of Motor 2
int ledPinGreen = 11; // Initialize the pins for the Green
LED (Pin 11)
int ledPinRed = 10; // Initialize the pins for the Red
LED (Pin 10)

```

```

// ----- PARAMETERS FOR PULSE EXPERIMENT -----

unsigned long stab_period = 1800000;          // Enter in the stabilization period
at the start of the experiment (in milliseconds)
double flow_rate = 0.02;                    // Enter in the desired flow rate for
the experiment (in mL/min)
unsigned long motor1_interval = 3600000;     // Enter in the desired duration to
run motor 1 for each cycle (in milliseconds)
unsigned long motor2_interval = 3600000;     // Enter in the desired duration to
run motor 2 for each cycle (in milliseconds)

// ----- END OF PARAMETERS FOR PULSE EXPERIMENT -----

/**
 * The Setup() Function
 *
 * The setup() function is called when the experiment first starts.
 * This function will only run once when the Arduino code is first
 * uploaded. The purpose of this function is to "set up" any
 * necessary components of the code, such as initializing
 * variables and pin modes.
 *
 * This function contains the code that controls the stabilization
 * period at the beginning of the experiment.
 */
void setup() {

    Serial.begin(9600);                      // Opens serial
    port, sets data rate to 9600 bps

    AFMS.begin(50);                          // Initializes the
    motor shield object AFMS and sets the frequency to 50

    myMotor1->setSpeed(10);                   // Set the speed of
    Motor 1 to 10 RPM (the setSpeed function controls the speed of the stepper motor
    rotation)
    myMotor2->setSpeed(10);                   // Set the speed of
    Motor 2 to 10 RPM

    pinMode(ledPinGreen, OUTPUT);            // Initialize the
    pin for the Green LED (Pin 11 on the Arduino)
    pinMode(ledPinRed, OUTPUT);              // Initialize the
    pin for the Red LED (Pin 10 on the Arduino)

```

```

// For MICROSTEP
motor1_delay = (0.139689/flow_rate)*1000;           // This equation
calculates the appropriate delay between motor steps based on the desired flow
rate

// Print statements to see the value of motor delays (inserted for debugging
purposes)
Serial.print("Motor 1 Delay: ");
Serial.println(motor1_delay);
Serial.print("Motor 2 Delay: ");
Serial.println(motor2_delay);

motor2_delay = motor1_delay;           // Make sure the
flow rates of both motors are the same by making the delays equal.

end_time = millis();                   // Use the
millis() function to grab the time since the code started

motor_intervals_sum = motor1_interval + motor2_interval; // Find the sum
of the motor intervals

// Stabilization period
while ((end_time - start_time) <= stab_period) // Execute if
difference between start and end times is less than interval of first motor;
during this time, motor 1 will run
{
    digitalWrite(ledPinGreen, HIGH); // Turn the Green
LED on for duration that motor 1 runs
    digitalWrite(ledPinRed, LOW); // Turn the Red
LED off for the duration that motor 1 runs
    Serial.print("Motor 1 On\n"); // Print statment
for debugging
    myMotor1 -> step(STEPS, BACKWARD, MICROSTEP); // The step()
function controls the motion of the stepper motor; Change the second parameter
based on the direction the motor turns (Forward or Backward)
    delay(motor1_delay); // Insert a delay
after each step of the motor; the length of this delay period will be calculated
based on the user-defined flow rate
    end_time = millis(); // Use the
millis() function to grab the time since the code started
} // end while

start_time = end_time; // Reset the
start time

```

```

}

/**
 * The Loop() Function
 *
 * The loop() function allows active control of the Arduino by
 * continuously looping through the code within the function.
 * This function allows multiple cycles of the drug pulses
 * to occur consecutively by repeating the pulse pattern in a loop.
 */
void loop(){

    end_time = millis(); // Use the
    millis() function to grab the time since the code started

    switch (running_motor)
    {
        case MOTOR_2: // Start by
            running Motor 2 (Stabilization period has run for Motor 1)

                if ((end_time - start_time) <= motor2_interval) // Execute if
                    difference between start and end times is less than interval of first motor
                {
                    digitalWrite(ledPinGreen, LOW); // Turn Green
                    LED off for duration that motor 2 runs
                    digitalWrite(ledPinRed, HIGH); // Turn Red LED
                    on for duration that motor 2 runs
                    Serial.print("Motor 2 On\n"); // Print
                    statement for debugging
                    myMotor2 -> step(STEPS, FORWARD, MICROSTEP); // The step()
                    function controls the motion of the stepper motor; Change the second parameter
                    based on the direction the motor turns (Forward or Backward)
                    delay(motor2_delay); // Insert a
                    delay after each step of the motor; the length of this delay period will be
                    calculated based on the user-defined flow rate
                } // end if

            // As soon as condition is no longer satisfied, begin running motor 1
            else
            {
                running_motor = MOTOR_1; // Switch turns
                to motor 1 (for when the code loops around)
            }
        }
    }
}

```



```

    // Since it is the turn for motor 1, we start it here and continue at the
switch case statement for later turns after the first delay
    digitalWrite(ledPinGreen, HIGH); // Turn the
Green LED on for duration that motor 1 runs
    digitalWrite(ledPinRed, LOW); // Turn the Red
LED off for duration that motor 1 runs
    Serial.print("Motor 1 On\n"); // Print
statement for debugging
    myMotor1 -> step(STEPS, BACKWARD, MICROSTEP); // The step()
function controls the motion of the stepper motor; Change the second parameter
based on the direction the motor turns (Forward or Backward)
    delay(motor1_delay); // Insert a
delay after each step of the motor; the length of this delay period will be
calculated based on the user-defined flow rate
} // end else

break;

case MOTOR_1: // Continue by
running Motor 1 (after Motor 2's interval has completed)

    if ((end_time - start_time) <= motor_intervals_sum) // Execute if
difference between start and end times is greater than interval of first motor
but less than the sum of the two intervals
    {
        digitalWrite(ledPinGreen, HIGH); // Turn the
Green LED on for the duration that motor 1 runs
        digitalWrite(ledPinRed, LOW); // Turn the Red
LED off for the duration that motor 1 runs
        Serial.print("Motor 1 On\n"); // Print
statement for debugging
        myMotor1 -> step(STEPS, BACKWARD, MICROSTEP); // The step()
function controls the motion of the stepper motor; Change the second parameter
based on the direction the motor turns (Forward or Backward)
        delay(motor1_delay); // Insert a
delay after each step of the motor; the length of this delay period will be
calculated based on the user-defined flow rate
    } // end if

    // As soon as condition is no longer satisfied, begin running motor 2
else
{
    start_time = end_time; // Reset the
start time
    running_motor = MOTOR_2; // Switch turns

```

to motor 2 (for when the code loops around)

```
    digitalWrite(ledPinGreen, LOW);           // Turn the
Green LED off for the duration that motor 2 runs
    digitalWrite(ledPinRed, HIGH);           // Turn the Red
LED on for the duration that motor 2 runs
    Serial.print("Motor 2 On\n");           // Print
statement for debugging
    myMotor2 -> step(STEPS, FORWARD, MICROSTEP); // The step()
function controls the motion of the stepper motor; Change the second parameter
based on the direction the motor turns (Forward or Backward)
    delay(motor2_delay);                     // Insert a
delay after each step of the motor; the length of this delay period will be
calculated based on the user-defined flow rate
} // end else

break;

default:           // Do nothing. It should never be executed.

break;

} // end switch

} // end loop function
```

```

/**
 * CONSTITUTIVE LEVEL EXPERIMENT
 * @author Shaimae Elhajjajy
 *
 * Name: Constitutive Level Experiment
 *
 * Purpose:
 * This program is intended for the constitutive level experiment,
 * in which a constant concentration is maintained for the duration
 * of the experiment. The desired concentration is achieved by
 * having one syringe filled with standard media and the other syringe
 * filled with 10 uM vemurafenib in standard media. The goal is to have the
 * two motors moving simultaneously at different rates such that the two
 * fluids can mix to achieve the desired concentration. This code was
 * not used in biological experiments due to problems with achieving
 * sufficient mixing in microfluidic chambers.
 *
 * Comments are provided throughout the code for explanation of specific commands.
 *
 * To view print statements contained within this code, click the magnifying
glass icon at the top right corner of the Arduino interface.
 *
 * Libraries and Functions provided by: Adafruit Motor Shield V2 Arduino Library
 * https://learn.adafruit.
com/adafruit-motor-shield-v2-for-arduino/install-software
 *
 */

// Include the proper libraries
#include <Stepper.h>
#include <Wire.h>
#include <Adafruit_MotorShield.h>
#include "utility/Adafruit_MS_PWM_ServoDriver.h"
#include <AccelStepper.h>

// Request the Stepper Motor with the Adafruit_MotorShield
Adafruit_MotorShield AFMS = Adafruit_MotorShield();

// Initialize the object for Motor 1
// Format --> AFMS.getStepper(Number of Steps Per Revolution, Port Number)
// For NEMA 17HS13-0404S1 Motor: Number of steps per revolution = 200 (1.8
degree turns)
// Terminals M3 and M4 = port 2
Adafruit_StepperMotor *myMotor1 = AFMS.getStepper(200, 2);

```

```

// Initialize the object for Motor 2
// Format --> AFMS.getStepper(Number of Steps Per Revolution, Port Number)
// For NEMA 17HS13-0404S1 Motor: Number of steps per revolution = 200 (1.8
degree turns)
// Terminals M1 and M2 = port 1
Adafruit_StepperMotor *myMotor2 = AFMS.getStepper(200, 1);

// Define Symbolic Constants
#define NUM_STEPS          1
#define DELAY              0
#define BASE_FLOW_RATE    0.0997

// ----- PARAMETERS FOR EXPERIMENT 2 ----- //
unsigned conc = 50;
float total_flow_rate = 0.02083;
// ----- END OF PARAMETERS FOR EXPERIMENT 2 ----- //

// ----- INITIAL CALCULATIONS ----- //

// Calculate respective flow rates for Motor 1 and Motor 2
float flow_rate_Motor1 = ((float)conc/100)*total_flow_rate;
float flow_rate_Motor2 = ((float)(100-conc)/100)*total_flow_rate;

// Calculate the respective delays for Motor 1 and Motor 2
float delay_Motor1 = (BASE_FLOW_RATE/(float)flow_rate_Motor1);
float delay_Motor2 = (BASE_FLOW_RATE/(float)flow_rate_Motor2);

// Calculate the steps per minute, based on the delay, for Motor 1 and Motor 2
float stepsPerMin_1 = 60/(float)delay_Motor1;
float stepsPerMin_2 = 60/(float)delay_Motor2;

// Calculate the steps per second for Motor 1 and Motor 2
float temp1 = (float)stepsPerMin_1/60;
float temp2 = (float)stepsPerMin_2/60;

float stepsPerSec_1 = (float)temp1*10;
float stepsPerSec_2 = (float)temp2*10;

// ----- END OF INITIAL CALCULATIONS ----- //

// ----- WRAPPERS FOR THE MOTORS ----- //

void forwardstep1() {
    myMotor1->onestep(BACKWARD, MICROSTEP);

```

```

}
void backwardstep1() {
  myMotor1->onestep(FORWARD, MICROSTEP);
}
// wrappers for the second motor!
void forwardstep2() {
  myMotor2->onestep(BACKWARD, MICROSTEP);
}
void backwardstep2() {
  myMotor2->onestep(FORWARD, MICROSTEP);
}

// Now we'll wrap the 2 steppers in an AccelStepper object
AccelStepper stepper1(forwardstep1, backwardstep1);
AccelStepper stepper2(backwardstep2, forwardstep2);

// ----- END OF WRAPPERS FOR THE MOTORS ----- //

void setup() {

  Serial.begin(9600); // Opens serial port, sets data
rate to 9600 bps
  Serial.println("Stepper test!"); // Print statements to see if the
code is working as expected (inserted for debugging purposes)

  AFMS.begin(); // Initializes the motor shield
object AFMS and sets the frequency // To rewind, leave the
parentheses blank (for default frequency of 1600 Hz, which is faster)

  // Print statements (for debugging purposes)
  Serial.print("Motor 1 Flow Rate: ");
  Serial.println(flow_rate_Motor1, 4);
  Serial.print("Motor 2 Flow Rate: ");
  Serial.println(flow_rate_Motor2, 4);

  Serial.print("Motor 1 Delay: ");
  Serial.println(delay_Motor1, 4);
  Serial.print("Motor 2 Delay: ");
  Serial.println(delay_Motor2, 4);

  Serial.print("Motor 1 Steps Per Sec: ");
  Serial.println(stepsPerSec_1, 4);
  Serial.print("Motor 2 Steps Per Sec: ");
  Serial.println(stepsPerSec_2, 4);

```

```
stepper1.setSpeed(stepsPerSec_1);           // Set the speed of motor 1
stepper2.setSpeed(stepsPerSec_2);           // Set the speed of motor 2
}

void loop(){

    stepper1.runSpeed();                      // Make motor 1 move
    stepper2.runSpeed();                      // Make motor 2 move
}
```

Appendix B: Arduino Code Documentation

B1. Introduction

B1.1 Purpose

The purpose of this document is to provide the user of the multi-pump system with a guide to the accompanying Arduino code. The multi-pump system was built for this MQP by the design team in order to enable biological experiments conducted by Mitchell Lab at UMMS's Program in Systems Biology to explore melanoma cell response to dynamic dosing regimens of vemurafenib.

B1.2 Scope

This document is intended to serve as a reference for users of the multi-pump system by describing the Arduino code that controls the system

B1.3 Definitions, Acronyms, and Abbreviations

All information cited from [60] unless otherwise noted.

#include - a prefix used to at the top of the program to include all information from a library, which contains a collection of classes, functions, and other useful data that will be used in the program.

Symbolic Constants - a name or symbol, conventionally written in all uppercase letters, that is assigned a value that is not changed throughout the program. Symbolic constants are preceded by “#define” and are followed by their numerical value, with no assignment operator. Every occurrence of the symbol in the remainder of the program will be replaced by its assigned value at compile time.

Variable - a name that stores a value, which can be used in computation. The value held by a variable can be changed. The value is assigned to the variable name by the assignment operator, =. Variables are generally written in lowercase letters.

Global Variables - variables that are visible and can be used in any part of the program, regardless of which function the user is in.

Data Types - different classifications of data. Some data types include:

- char - character

- int - integer
- float - floating point (numbers that contain decimals)
- double - double-precision floating point
- short - short integer that can hold numbers in the range “-32,768 to 32,767 (minimum value of -2^{15} and a maximum value of $(2^{15}) - 1$)”. [61]
- long - long integer that can “store 32 bits (4 bytes), from -2,147,483,648 to 2,147,483,647”. [62]
- unsigned long - a long integer of extended size due to the fact that it does not carry negative numbers. This data type ranges “from 0 to 4,294,967,295 ($2^{32} - 1$)”. [63]
- void - used in functions to indicate that no value will be returned.

Function - a series of statements or instructions that specify what operation or task should be performed by the program.

While loop - a type of control flow statement that will continue evaluating a certain region of code as long as the specified conditional statement remains true. As soon as the conditional statement becomes false, the control exits the loop.

Switch Statement - a type of control flow statement that implements a multiway decision branch. The portion of code executed by the switch statement depends on the value of a particular expression. The switch statement contains multiple different “cases” that are each labeled by a constant value. When the expression matches one of the values, it will execute the portion of code for that case.

If/Else Statement - a type of conditional statement in which a specified action will be performed based on the outcome of a particular condition. For example, if a particular condition is satisfied (If), then one action will be performed. If that condition is not satisfied (Else), a different action will be performed. If/Else statements are an important component of control flow.

B2. Overview

B2.1 Description of Problem

The goal of the code is to provide control over the stepper motors which power the pumps. The Arduino needed to be programmed in order to perform specific types of experiments.

B2.2 Technologies Used

The open source Arduino software was used for this project. Because this software accompanies the Arduino microcontroller, it is easy to use and fully documented at Arduino’s web page and

forum. To download the software, visit <https://www.arduino.cc/> then select “Downloads” from the “Software” menu. Scroll down to the section labeled “Download the Arduino IDE” and select the option for the operating system of choice.

B2.3 Installation

Once the Arduino software has been downloaded, the Adafruit motor shield library must also be downloaded. This is necessary in order to control the stepper motors, which are connected to the motor shield. Follow the instructions in [64] in the sections called “Install Software” and “Install Adafruit Motor Shield V2 library” to download and install this library for use.

B3. Built-in Function Descriptions

B3.1 setup()

The setup() function is called when the Arduino is turned on or when the Arduino is reset. It runs only once at the start of the program, when the code is first uploaded to the Arduino. The setup() function is called when the experiment first starts. The purpose of this function is to "set up" any necessary components of the code, such as initializing variables and pin modes. In the code for multi-pump system, the setup() function contains the code that controls the stabilization period at the beginning of the experiment. [65]

B3.2 loop()

The loop() function allows active control of the Arduino by continuously looping through the code within the function. For the multi-pump system, this function allows multiple cycles of the drug pulses to occur consecutively by repeating the pulse pattern in a loop. This alternates the running of each motor, which enables the dynamic dosing regimens by alternating between media and drug for the specified time intervals. [66]

B3.3 Arduino Built-In Functions

Serial.begin()

The Serial.begin() function takes a speed as its argument, which “sets the data rate in bits per second (baud) for serial data transmission.” For this project, the rate is set at 9600 bits per second. [67]

Example:

```
Serial.begin(9600);
```

pinMode()

The `pinMode()` function specifies which pin on the Arduino is being controlled (first argument), and whether that pin will behave as either input or output (second argument). For this project, `pinMode()` was used to control the pins to which the green and red LED lights were attached to, and they behave as output. [68]

Example:

```
int ledPinGreen = 11;
int ledPinRed = 10;
pinMode(ledPinGreen, OUTPUT);
pinMode(ledPinRed, OUTPUT);
```

Serial.print()

The `Serial.print()` function prints text to the serial monitor so that it is visible to the user. Messages are printed as human-readable ASCII text. For this project, the function was used primarily for debugging purposes (for which print statements are a common practice). [69]

Example:

```
Serial.print("Motor 1 On\n");
Serial.print("Motor 2 On\n");
```

Serial.println()

The `Serial.println()` function is similar to the `Serial.print()` function, except that it prints data to the serial monitor rather than text. This function is often used to print the value of a particular variable for the user to see, which are human-readable ASCII format and followed by a carriage return (newline). For this project, the function was also used primarily for debugging purposes. [70]

Example (used in conjunction with `Serial.print()`):

```
Serial.print("Motor 1 Delay: ");
Serial.println(motor1_delay);
Serial.print("Motor 2 Delay: ");
Serial.println(motor2_delay);
```

millis()

The `millis()` function returns the number of milliseconds that have passed since the current program has started running. It will overflow after 50 days, in which case the number will start at 0 again. For this project, the function is used to keep track of elapsed time since the beginning of the experiment, in order to make the switches between motors occur at the correct time. [68]

Example:

```
end_time = millis();
```

digitalWrite()

The digitalWrite() function is used to set a digital pin (first argument) to either a LOW or a HIGH value (second argument). For this project, the function is used to turn an LED on (digital pin set to LOW) or to turn an LED off (digital pin set to HIGH). [71]

Example:

```
digitalWrite(ledPinGreen, HIGH);  
digitalWrite(ledPinRed, LOW);
```

delay()

The delay() function pauses the program for a specified amount of time, which is passed in as an argument in units of milliseconds. For this project, the function was used to insert a delay between each single step of a motor; the length of the delay determines the flow rate. [70]

Example:

```
delay(motor1_delay);
```

B3.4 Adafruit Motor Shield Built-In Functions [72]

getStepper()

This function is part of the Adafruit_MotorShield class and is used to create a stepper motor object. It takes two arguments: the number of steps per revolution for the particular stepper motor being used, and the port number on the motor shield that the motor is connected to. If the motor has been attached to terminals M1 and M2 on the motor shield, the port number will be 1. If the motor has been attached to terminals M3 and M4, the port number will be 2.

Example:

```
Adafruit_StepperMotor *myMotor1 = AFMS.getStepper(200, 1);  
Adafruit_StepperMotor *myMotor2 = AFMS.getStepper(200, 2);
```

begin()

This function is part of the Adafruit_MotorShield class and is required to initialize the motor shield. It must be called in setup(). It can take no arguments, or it can take a frequency parameter. For this project, the frequency was set to 50.

Example:

```
AFMS.begin(50);
```

setSpeed()

The function `setSpeed()` “controls the speed of the stepper motor rotation...specified in RPM.” For this project, the speed was set to 10 RPM.

Example:

```
myMotor1->setSpeed(10);  
myMotor2->setSpeed(10);
```

step()

The `step()` function controls the movement of the stepper motor. It takes three parameters. The first is an integer which dictates how many steps the motor will move. The second takes a symbolic constant which dictates the direction (either `FORWARD` or `BACKWARD`) that the stepper motor will move in. This directionality dictates only the direction of the motor’s rotation, but not necessarily the direction that the pump moves in. The third takes another symbolic constant which dictates the style in which the stepper motor moves (either `SINGLE`, `DOUBLE`, `MICROSTEP`, or `INTERLEAVE`). More information on the style of movement of the motor can be found on in [64]. For this project, the number of steps is always 1 and the style of movement is always `MICROSTEP`. The direction of movement depends on each motor, and must be changed to either `FORWARD` or `BACKWARD` depending on which direction the pump moves. [64]

Example:

```
myMotor1 -> step(STEPS, BACKWARD, MICROSTEP);  
myMotor2 -> step(STEPS, FORWARD, MICROSTEP);
```

B4. Arduino Code Description

Although all programs went through multiple iterations, the ones included here are the final versions. There are three main programs.

B4.1 Simple Forward and Backward Motion

This code can be used to rewind the pumps. This is particularly useful after an experiment has finished, and the moving piece has been pushed all the way forward. Upload this code to each of the Arduinos in order to rewind the pumps and return each of the moving pieces to their original positions, so that a fully extended 30 mL syringe can be inserted once again. Conversely, the

The title of this program is called “Foward_Backward_Motion”. The number of steps (10) and the delay (100 ms) have already been set as symbolic constants.

```
#define NUM_STEPS 10  
#define DELAY 100
```

These values have been chosen based on a reasonable speed for forwarding and rewinding the pumps (i.e., a speed that does not take too long for the moving piece to move but that is not too fast to damage the pumps). In loop(), there are two lines of main importance for the user.

```
myMotor1 -> step(NUM_STEPS, BACKWARD, SINGLE);  
myMotor2 -> step(NUM_STEPS, BACKWARD, MICROSTEP);
```

Each of these lines will control one of the motors. It is best to rewind only one motor at a time; therefore, when the user wishes to rewind motor 1, comment out the line for motor 2 by inserting two forward slashes (//) before “myMotor2”. When the user wishes to rewind motor 2, uncomment the line for motor 2 (i.e., remove the two forward slashes) and comment out the line for motor 1.

As mentioned previously, the actual direction of the motor movement is specific to each motor. The directionality likely has to do with the order in which the different colored wires are connected to the terminals in the motor shield. If the motor is not moving in the desired direction, change the second parameter to the opposite direction. For example, if the second parameter in the step() function above is BACKWARD but the motor is moving in the forward direction, then change the second parameter to FORWARD. If the second parameter in the step() function is BACKWARD and the motor is being rewound, then it is correct and nothing needs to be changed.

B4.2 Pulse Experiments (Alternating Motors)

This code is intended for the pulse experiments, in which dynamic doses of drug are delivered to cells. This is the main code used by the design team for each of the biological experiments. The title of this program is called “Pulse_Experiment.”

The user must specify the experiment parameters in the section labeled “Parameters for Pulse Experiment,” as seen below.

```
// ----- PARAMETERS FOR PULSE EXPERIMENT -----  
  
unsigned long stab_period = 1800000;      // Enter in the stabilization period at the start of the experiment (in milliseconds)  
double flow_rate = 0.02;                 // Enter in the desired flow rate for the experiment (in mL/min)  
unsigned long motor1_interval = 3600000; // Enter in the desired duration to run motor 1 for each cycle (in milliseconds)  
unsigned long motor2_interval = 3600000; // Enter in the desired duration to run motor 2 for each cycle (in milliseconds)  
  
// ----- END OF PARAMETERS FOR PULSE EXPERIMENT -----
```

The variable stab_period contains the length of time (in milliseconds) for which motor 1 (media) will be run at the very beginning of the experiment, for the stabilization period. The variable flow_rate will contain the desired flow rate of the fluid, which can be either 0.02 mL/min, 0.05 mL/min, or 0.1 mL/min (based on previous cell viability testing). The variable motor1_interval contains the length of time (in milliseconds) for which motor 1 (media) will run for its

alternation. Similarly, the variable `motor2_interval` contains the length of time (in milliseconds) for which motor 2 (drug) will run for its alternation. In the example above, the flow rate is 0.02 mL/min. The media will run for a 30 minute stabilization period with media, followed by a 1 hour period of drug, 1 hour period of media, 1 hour period of drug, 1 hour period of media, and so on.

The control flow of this program is accomplished through the implementation of while loops, if statements, and switch statements. Many of the variables are global variables so that they can be easily accessed in all areas of the code. In `setup()`, many variables are initialized. The amount of delay required between each step of the motor is also calculated in order to achieve the desired flow rate.

```
// For MICROSTEP
motor1_delay = (0.139689/flow_rate)*1000;
```

The stabilization period also occurs in `setup()`, because it will only run once. This is useful because it's duration can be different than its repeated alternating duration, like in the example mentioned before. The code which controls the stabilization period is the following:

```
// Stabilization period
while ((end_time - start_time) <= stab_period)
{
    digitalWrite(ledPinGreen, HIGH);
    digitalWrite(ledPinRed, LOW);
    Serial.print("Motor 1 On\n");
    myMotor1 -> step(STEPS, BACKWARD, MICROSTEP);
    delay(motor1_delay);
    end_time = millis();
} // end while
```

Motor 1 runs for the stabilization period, since it controls media. The green LED light will be on (indicating that Motor 1 is running), while the red LED light will be off.

In `loop()`, a switch statement is used to pass control to each of the motors when it is their turn to run. Since motor 1 controls media, which already ran during the stabilization period, the switch statement begins with motor 2, which controls drug. Motor 2 will run for its interval, according to the following code:

```
case MOTOR_2:

    if ((end_time - start_time) <= motor2_interval)
    {
        digitalWrite(ledPinGreen, LOW);
        digitalWrite(ledPinRed, HIGH);
        Serial.print("Motor 2 On\n");

        myMotor2 -> step(STEPS, FORWARD, MICROSTEP);

        delay(motor2_delay);
    } // end if
```

The red LED light will be on (indicating that Motor 2 is running), while the green LED light will be off.

The next case of the switch statement passes control back to motor 1, in a similar manner:

```
case MOTOR_1:

    if ((end_time - start_time) <= motor_intervals_sum)
    {
        digitalWrite(ledPinGreen, HIGH);
        digitalWrite(ledPinRed, LOW);
        Serial.print("Motor 1 On\n");
        myMotor1 -> step(STEPS, BACKWARD, MICROSTEP);
        delay(motor1_delay);
    } // end if
```

The two motors will then keep alternating until the end of the experiment.

This code can also be adapted for the starvation experiments, as was done by the design team.

B4.3 Six Pump Experiments

When performing multi-pump experiments, it may be easier to set up the code before hand. Make a note of how each of the parameters should be entered in the code for each experiment. Upload the code to each Arduino with the correct parameters, one at a time. When the user has uploaded the code to all the Arduinos, plug in their power sources and they will run independently according to the program the user uploaded.

B5. User Interface

B5.1 Current

Currently, the user will interact directly with the Arduino code, as suggested by the client. The parameters are marked in a clear section near the top of the code, as seen below:

```
// ----- PARAMETERS FOR PULSE EXPERIMENT -----

unsigned long stab_period = 1800000; // Enter in the stabilization period at the start of the experiment (in milliseconds)
double flow_rate = 0.02; // Enter in the desired flow rate for the experiment (in mL/min)
unsigned long motor1_interval = 3600000; // Enter in the desired duration to run motor 1 for each cycle (in milliseconds)
unsigned long motor2_interval = 3600000; // Enter in the desired duration to run motor 2 for each cycle (in milliseconds)

// ----- END OF PARAMETERS FOR PULSE EXPERIMENT -----
```

These parameters are the only values that the user will need to change for their experiment, and have been described previously. Having this section clearly demarcated from the rest of the code help the user to know where the experiment parameters can be changed.

B5.2 Future

To improve user-friendliness, a user interface can be implemented. This can be in the form of an LCD shield, available from Adafruit (<https://www.adafruit.com/product/714>). This device can be attached directly to Arduino. It has a screen to display prompts or options to the user, and it has a keyboard with buttons for the user to select different options from. This shield could provide an alternative to the user, so that they can select their experiment parameters rather than input them directly in the Arduino code.

B6. Troubleshooting

The following section deals with troubleshooting. Each subsection includes commentary on potential challenges encountered when working with the code, and their associated possible solutions. The challenges mentioned here are the ones which the design team encountered most often.

B6.1 The Arduino code won't compile

The user should click the “Verify” icon (seen as a checkmark) at the top left-hand side of the screen before uploading the code to the Arduino. This will compile the program, and the status can be seen in the black bar situated along the bottom of the screen. If it compiles correctly, the message will read “Compiling sketch...” followed by “Done Compiling.” If it does not compile, then something is wrong in the code itself. This could have happened accidentally when the user changed experiment parameters. The section at the bottom will be orange in the case of an error, and a compile warning will be displayed. Use this compile warning to help debug the problem. In addition, make sure to double check your code to see what has been changed and what may have gone wrong. Ensuring that all syntax is correct (including semicolons at the end of every line!) can help to resolve the issue.

B6.2 The Arduino code won't upload

The user must click the “Upload” icon (seen as a right arrow) at the top left-hand side of the screen in order to upload the code to the Arduino. Once this has been completed, the Arduino will be activated a couple of seconds later to perform the actions specified in the code. If the code will not upload, the message “Problem uploading to board. See <https://www.arduino.cc/en/Guide/Troubleshooting#upload> for suggestions”. This could be due to a number of problems. One possible reason is that the code has not been compiled; refer to the previous section if this is the case. Another reason may have to do with the USB port that connects the Arduino to the laptop. Change the ports by going to the menu Tools → Port →, and then select the port that is listed there (not the one labeled Bluetooth).

If there are still issues uploading the code, but everything seems to look okay with your code and your port connections, try pushing the “RESET” button on the Arduino, and then try again.

B6.3 The Arduino code will not open

There are multiple reasons why an Arduino sketch may not open, but the most common is that the file has not been saved properly. Make sure that the file is saved inside a folder that has the same name as the file itself. If you happen to rename an Arduino sketch, you must also rename the folder that it is in. This is one of the constraints that the Arduino software enforces. Once this has been done, the file should open.

B6.4 The Arduino code timing is incorrect






This issue is related to the experiments itself. If the user has noticed that the timing of the motors is not happening as expected, this could be due to the way parameters have been entered into the code. Make sure that the times entered for the parameters `stab_period`, `motor1_interval`, and `motor2_interval` have been entered in units of milliseconds, and that the flow rate entered for the parameter `flow_rate` has been entered in units of mL/min. Also make sure that the times have been entered for the correct variables.






Appendix C: User Manual






HOW TO BUILD A SYRINGE PUMP




This document provides step-by-step instructions for building one unit of the syringe pump, where one unit involves two syringe pumps attached to the same base. Images are provided for reference.

Materials needed to build one syringe pump unit:




Material	Vendor	Quantity needed	Price (\$)	Image of Material
Base: 80/20 Inc., 1020, 10 Series, 1" x 2" T-Slotted Extrusion x 18"	Amazon: https://www.amazon.com/gp/product/B00BMU3XBA/ref=oh_aui_detailpage_o01_s00?ie=UTF8&psc=1	1	8.97	
3D-printed Syringe Holders: (4 per syringe pump, 8 per unit)	MakerSpace: Files at https://hackaday.io/project/1838-open-syringe-pump	2 of each piece		Part 1 (Motor Base)  Part 2 (Moving Piece)  Part 3  Part 4 

<p>Smooth rod: Linear Motion 8 mm Shaft, 330 mm Length, Chrome Plated, Case Hardened, Metric</p>	<p>Amazon: https://www.amazon.com/gp/product/B0045DUX5A/ref=oh_aui_detailpage_o00_s00?ie=UTF8&psc=1</p>	<p>2 (one for each pump of the unit)</p>	<p>7.76</p>	
<p>Threaded Rod (5/16 inch Diameter, 1 ft in Length)</p>	<p>Home Depot</p>	<p>2 (one for each pump of the unit)</p>	<p>1.75 (for 2, 1 for each syringe pump)</p>	
<p>5/16 inch Hex Nut (0.4 cm thickness)</p>	<p>Home Depot</p>	<p>2 (one for each pump of the unit)</p>	<p>0.80 (2 nuts)</p>	
<p>Bolts and T-nuts: 80/20 Inc., 3393, 10 Series, Bolt Assembly: 1/4- 20 x .5" Button Head Socket Cap Screw (BHSCS) and Slide-In Economy T- Nut (25 Pack)</p>	<p>Amazon: https://www.amazon.com/gp/product/B00FDSEOWY/ref=oh_aui_detailpage_o02_s00?ie=UTF8&psc=1</p>	<p>1 bag (contains enough pieces to build 2 complete units; 12 screws and 12 caps are needed for 1 unit)</p>	<p>6.27 (6, 3 for each pump)</p>	
<p>Shaft couplers: Aideepen 10PCS 6.35 x 8mm CNC Motor Jaw Shaft Coupler 6.35mm To 8mm Flexible Coupling</p>	<p>Amazon: https://www.amazon.com/Aideepen-Coupler-Flexible-Coupling-Gadgets/dp/B01K9QPCXY</p>	<p>1 bag (contains enough pieces to build 5 complete units; 2 couplers are needed for 1 unit)</p>	<p>2.78 (2 pieces)</p>	

Gadgets				
<p>Linear Bearings: Easy RepRap - 12 LM8UU Linear Bearings for 3D Printer. Prusa Mendel, reRap</p>	<p>Amazon: https://www.amazon.com/gp/product/B00ED150S4/ref=oh_aui_detailpage_o09_s00?ie=UTF8&psc=1</p>	<p>1 bag (contains enough pieces to build 6 complete units; 2 bearings are needed for 1 unit)</p>	<p>5.56 (2 pieces)</p>	
<p>Stepper Motor: STEPPERON LINE 17HS13-0404S1 Stepper Motor for 3D Printer DIY CNC Robot, -10 - 50 Degree C, 0.4 Amp, Black</p>	<p>Amazon: https://www.amazon.com/gp/product/B00PNEQ9T4/ref=oh_aui_detailpage_o05_s00?ie=UTF8&psc=1</p>	<p>2 (one for each pump of the unit)</p>	<p>23.98 (2 motors)</p>	
<p>Arduino UNO Rev3</p>	<p>Arduino: https://store.arduino.cc/usa/arduino-uno-rev3</p>	<p>1 (A single Arduino can control 2 syringe pumps at the same time)</p>	<p>22.00</p>	
<p>Motor shield:</p>	<p>Adafruit: https://www.adafruit.com/product/1438</p>	<p>1</p>	<p>19.95</p>	
<p>M2.5 Standoffs and Screws: (Male to Female 12+6mm)</p>	<p>Adafruit: https://www.adafruit.com/product/3299 Alternative option - Amazon:</p>	<p>4</p>	<p>3.50 (4 pieces)</p>	

10pcs)	https://www.amazon.com/HOBBYIMATE-Standoffs-Assorted-Quadcopter-Raspberry-Pi/dp/B06XW978ZP/ref=sr_1_5?ie=UTF8&qid=1521641714&sr=8-5&keywords=m2.5+standoff			
M3 Screws M3 x 6mm 304 Stainless Steel Phillips Pan Head Screws Bolt 60pcs	Amazon: https://www.amazon.com/Stainless-Steel-Phillips-Screws-60pcs/dp/B012TE12CY/ref=sr_1_10?s=industrial&ie=UTF8&qid=1522296167&sr=1-10&keywords=m3+screws	8 (4 for each motor)	0.81 (8 pieces, 4 for each motor)	
Acrylic Arduino Box: Laser Cut (1/8 inches thick)	MakerSpace	1		**include picture when ready**
Stacking Headers: Shield stacking headers for Arduino (R3 Compatible)	Adafruit: https://www.adafruit.com/product/85	1	1.94	
1K Ohm Resistor (Brown, Black, Red, Gold)	SparkFun: https://www.sparkfun.com/products/14492	2	1.90 (0.95 each)	

<p>LEDs</p>	<p>SparkFun: Red https://www.sparkfun.com/products/9590 Green https://www.sparkfun.com/products/9592</p>	<p>1 Green 1 Red</p>	<p>0.70 (0.35 each)</p>	
<p>Jumper Wires: Premium Male/Male Jumper Wires - 20 x 3" (75mm)</p>	<p>Adafruit: https://www.adafruit.com/product/1956</p>	<p>4</p>	<p>1.94</p>	
<p>USB Connector: USB Cable - Standard A-B - 3 ft/1m</p>	<p>Adafruit: https://www.adafruit.com/product/62</p>	<p>1</p>	<p>3.95</p>	
<p>Power Supply: AC/DC Power Supply, Switch Mode, 1 Output, 12 W, 12 V, 1 A</p>	<p>Newark: http://www.newark.com/triad-magnetics/wsu120-1000-r/ac-dc-converter-external-plug/dp/83T4339?st=ac%20adaptor%2012v</p>	<p>1</p>	<p>8.35</p>	
<p>Power Outlet Strip: GE 6 ft. 10-Outlet and 2-USB Port, 2.1 Amp, 3000 Joules Surge Protector</p>	<p>Home Depot: https://www.homedepot.com/p/GE-6-ft-10-Outlet-and-2-USB-Port-2-1-Amp-3000-Joules-Surge-Protector-13476/205727495</p>	<p>1</p>	<p>29.50</p>	

<p>Wire Spool: Hook up Wire Kit (Stranded Wire Kit) 22 Gauge (6 different colored 25 Foot spools included) - EX ELECTRONIX EXPRESS</p>	<p>Amazon: https://www.amazon.com/Stranded-different-colored-spools-included/dp/B00B4ZQ3L0/ref=sr_1_10?ie=UTF8&qid=1522297930&sr=8 = 10&keywords=arduino+wire</p>	<p>1</p>	<p>\$2 (whole package \$18)</p>	
<p>Phillips Screwdriver</p>	<p>Lab materials</p>			
<p>Allen Wrench (CR-V 5/32)</p>	<p>Lab materials</p>			

Procedure:

1. Organize all of the materials needed to ensure you are able to build a complete device.



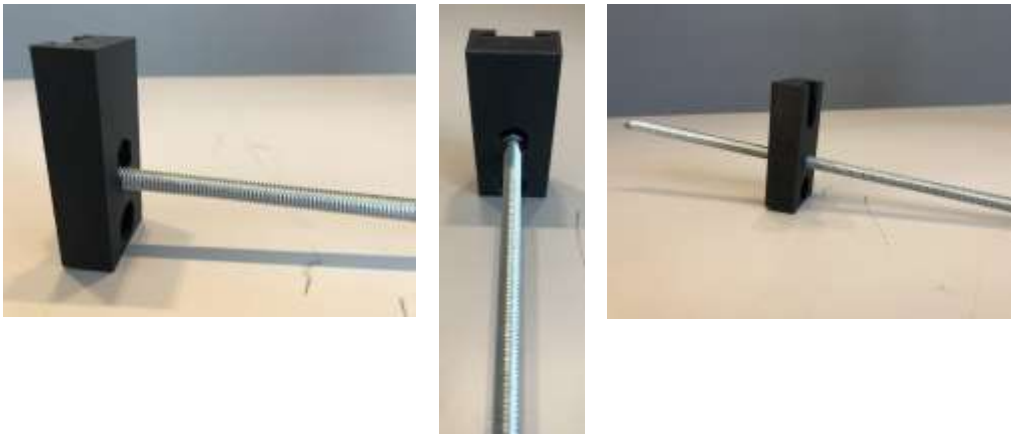
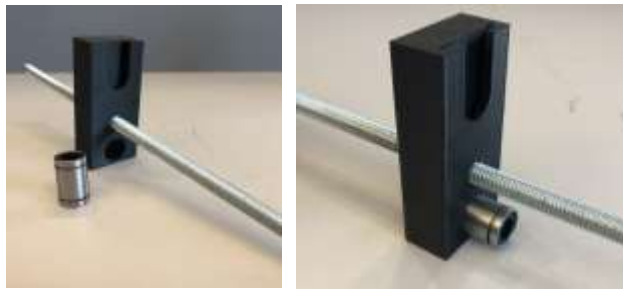
Building the First Syringe Pump

2. Place the 5/16 inch Hex Nut into the slot of the 3D Printed Moving Piece (Part 2) as shown in the images. Make sure the Hex Nut slides all the way down into place.

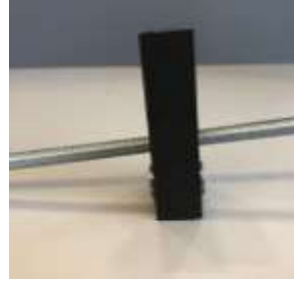


3. Insert the Threaded Rod into the Hex nut. Keep turning the rod until the Hex Nut is about halfway down the length of the rod.

3. Insert the metal Linear Bearing into the hole at the bottom of the 3D Printed Moving Piece



(Part 2).



4. Insert the Threaded Rod into the stable 3D printed Part 3 by sliding it through the top hole.



5. Insert the Threaded Rod in the stable 3D Printed Part 4 by sliding it through the top hole.

6. Place the Stepper Motor on the Motor Base (Part 1) and attach it by inserting the small M3 screws in each of the 4 corners. Tighten the screws in the little holes by using a Phillips screwdriver.



7. Insert the metal Bolts into each of the stable 3D printed parts (Parts 1, 3, and 4) using a CR-V 5/32 Allen Wrench (This is required if the 3D printed piece holes and the bolt are very tight, if not by push it, it will be inserted) Loosely insert the T-nuts on the end part of the Bolt. Do the same for each of the holes in the stable parts.



8. Slide the Motor Base (Part 1) onto the T-Slotted Extrusion Base, as depicted below.



9. Use the CR-V 5/32 Allen Wrench to tighten the Bolts into the T-nuts of the Motor Base (Part 1), until the piece cannot move. Make sure that the part is aligned straight with the T-Slotted Extrusion Base.



10. Slide the other three pieces (Parts 2, 3, and 4) with the Threaded Rod onto the T-Slotted Extrusion Base.

11. Before tightening the rest of the Bolts, make sure that the distance between the stable 3D Printed Parts (Parts 3 and 4) is large enough that it can fit the 30 mL syringe into the system, as shown in the image below.



12. Tighten all the Bolts into the T-nuts of 3D Printed Parts 3 and 4 while the syringe is still in place, to make sure the measurement is correct. Once again, make sure that the parts are aligned straight with the T-slotted Extrusion Base.

13. Slide the Threaded Rod so that it moves away from the motor. This will allow some room to insert the Joint Coupler between the Stepper Motor shaft and the Threaded Rod.

14. Insert the Threaded Rod into the hole of the Coupler that has the larger diameter. Now slide the Threaded Rod towards the motor, so that the Stepper Motor shaft fits into the Coupler's smaller diameter. Make sure that the Stepper Motor shaft and the Threaded Rod meet at the middle in the interior of the Joint Coupler.



15. Confirm that all parts are tightened securely to the base. Adjust if necessary.

16. Insert the Smooth Rod through all the holes at the bottom of the of the stable parts (Parts 1, 3, and 4), and through the Linear Bearing of the 3D Printed Moving Piece (Part 2) until it touches the wall of the Motor Base (Part 1). The first syringe pump of the unit is now complete.



Building the Second Syringe Pump

17. Repeat steps 2 through 16, using the other side of the same T-slotted Extrusion Base to insert/attach the parts and build another whole unit. In particular, make sure to do the following:

- a. Place the first syringe pump and T-slotted Extrusion Base on its side, so as to be able to insert the other pump on the opposite side.
- b. Insert the second Stepper Motor through the back part of the T-Slotted Extrusion Base.

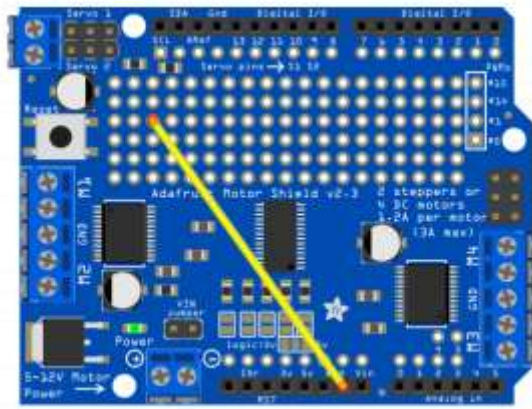


- c. Introduce the other 3 parts together with the threaded rod into the base by sliding the nuts loosely attached to the bolts in the holes of the 3D printed parts. Tighten everything securely in place. The complete syringe pump unit is now complete.

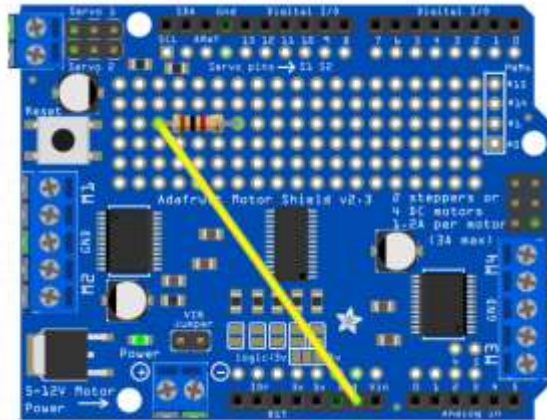


Connecting the LED indicators

21. Place one end of a jumper wire into one of the small holes in the Adafruit Motor Shield. Connect the other end to a Ground pin (GND).

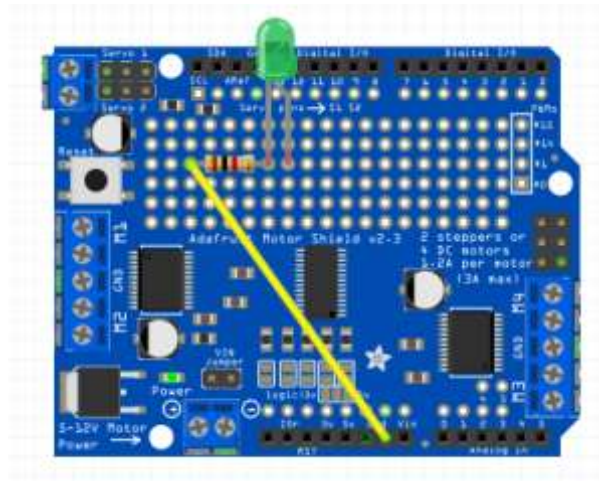


22. Insert one end of a 1K Ohm resistor into the same hole as the first jumper wire. Insert the

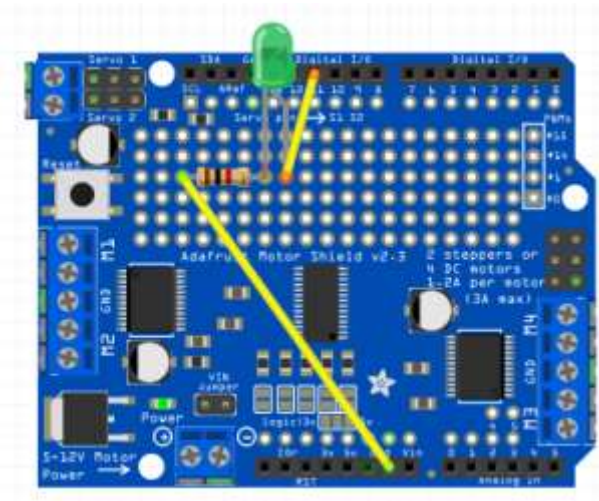


other end of the resistor into another hole to the right.

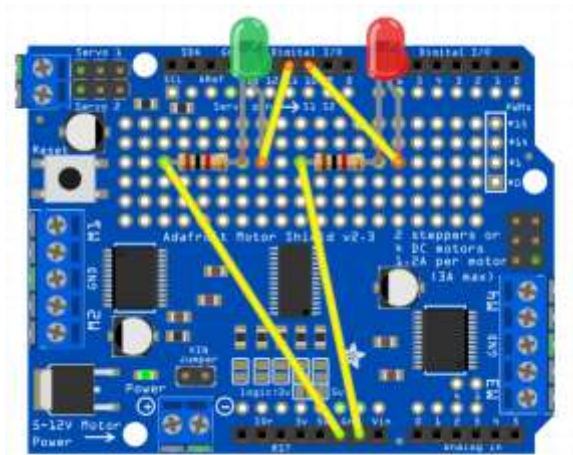
23. Insert the longer end of the Green LED into the same hole as the right end of the resistor. Insert the shorter end of the LED into the adjacent hole.



24. Insert one end of a second jumper wire into the same hole as the shorter end of the LED. Insert the other end to a numbered Pin 11.



25. Repeat steps 21 - 24 for the Red LED.



26. Solder all pieces in place. An image of the finished product can be seen below.



Arduino Set-Up and Connection to Pump

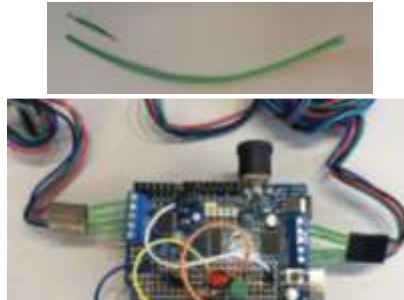
27. Solder the headers into the Motor Shield. To do this, follow the procedure stated in [61], in the section called “Installing Headers and Terminals”.

28. Laser cut the acrylic box. The CorelDraw files for the box are located on the Desktop of the computer that is connected to the laser cutter, in a folder called “Arduino Box for Multi-Pump System.”

29. Place the Motor Shield on top of the Arduino by inserting the headers in the appropriate places. Place the combined electronics in the Acrylic Box.

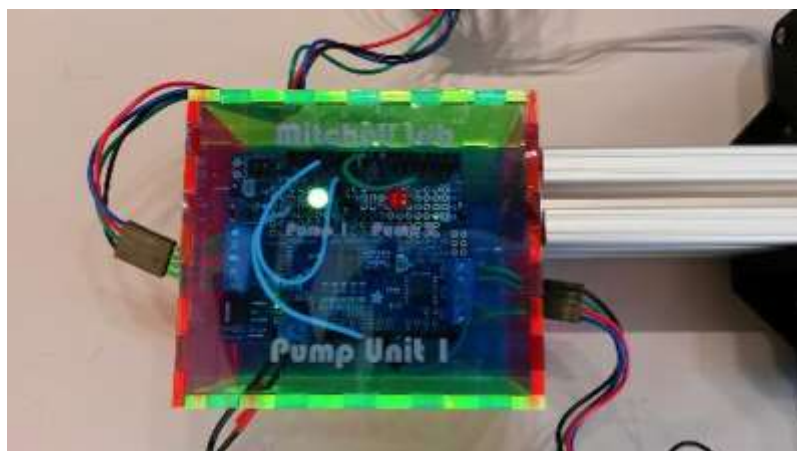


30. Cut a portion of wire from the Wire Spool into small pieces and peel off the ends to connect the Stepper Motor to the Motor Shield that is sitting on top of the Arduino. See image for reference.



There are five connections in each terminal (seen above as 5 small screws in each rectangular blue piece). Two wires from the motor will be connected to the two leftmost connections, and the other two wires will be connected to the two rightmost connections. When selecting the two wires for each side, make sure that the green and black wires are connected on the same side, and that the red and blue wires are connected on the same side. In other words, green and black wires should always be paired, as should red and blue wires.

31. Insert the Power Supply into the Panel Mount DC Barrel Jack. If the Motor Shield has no DC Barrel Jack attached, insert the ends of the wires of the power supply into the small blue piece on the side of the Motor Shield that has two connections. This piece is in front of the VIN jumper and is labeled “Power”. Make sure that the side of the plug that is marked with a piece of red tape is inserted into the right side (negative) of this small blue piece, while the other side of the plug is inserted into the left side (positive). The final setup of the box should look like this:



When making all of these connections, they must be done while the Arduino is already inside the box. Leave the cover of the box unattached until all connections are made. Insert the wires for

the motor and power source through the holes that are cut in the acrylic box in the appropriate places. When finished, place the cover on the box and secure with clear tape.

32. Plug the Power Supply into the Power Outlet Strip. The green light on the Motor Shield should turn on.

33. Use the USB Cord to connect the Arduino to a laptop or computer. Upload the Arduino code to the Arduino. The pump is now ready to begin experiments!

Appendix D: Biological Experiment Protocol

Treatment of A375 Melanoma Cells with Dynamic Doses of Vemurafenib

This document is a protocol for the biological experiments performed with the automated, programmable syringe pump constructed for this MQP. Included are procedures for preparing cell cultures, microfluidic plating of cells, implementation of the syringe pump, and setting up the experiment.

The overall purpose of the study is to understand cellular response to different dynamic dosages of drugs. For this, an automated, programmable syringe pump system was built to allow dynamic flow of media for up to 24 hours without any human interaction. Two pumps are used for each of the microfluidic chambers, of which there are 6 in total per microfluidic device. One pump controls the flow of regular media, while the other controls the flow of media infused with the therapeutic drug vemurafenib, a BRAF-inhibitor for the treatment of melanoma (Kim, 2016).

Each microfluidic chamber is exposed to different profiles of drug to study how cells react to the different dosing regimens. Melanoma cells are able to withstand high flow rates to the limit of 250 $\mu\text{L/s}$ (14.9 ml/min) (Barnes et al., 2012). Flow rates for this testing will be in the range of 0.02 mL/min to 0.1 mL/min, with 0.02083 mL/min being the ideal flow rate to ensure that the total syringe capacity of 30 mL can last for experiments up to 24 hours.

The main goals of the study are:

- To determine the cell viability after subjecting cells to fluid flow exposure at a minimum and maximum flow rate generated by the syringe pump. This will ensure cells survive the exposure and that the syringe pumps can be used for further experiments to analyze how cells react to different doses of drugs.
- Determine cellular response to the drug vemurafenib at when delivered at different frequencies of pulses, which is achieved by alternating the two different types of media.

Materials:

For the cell cultures:

- A375 Melanoma Cells (A375-KTR-ERK-Clover-Neo-H2B-mCherry-Hygro)
- Dulbecco's Modified Eagle's Medium (DMEM) with L-glutamine, 4.5g/L glucose, and Sodium Pyruvate (*Corning, Cat. No. 10-013-CV*)
- Fetal Bovine Serum (*Fisher Scientific, Cat. No. 26140079*)
- 1X Phosphate-Buffered Saline, w/o calcium and magnesium (*Corning, Cat. No. 21-040-CV*)
- 1M HEPES Buffer Solution (*gibco, ThermoFisher Scientific, Cat. No. 15630080*) (for maintaining proper pH levels in case of fluctuating CO₂ levels in microscope incubator)

- Penicillin Streptomycin (Pen Strep) (for prevention of contamination)
- Trypsin (TrypLe)
- 0.4% Trypan Blue Solution
- 70% Ethanol (EtOH) in a spray bottle
- Tissue Culture (TC) Plates (sterilized)
- Glass Pasteur Pipettes (sterilized)
- Motorized Pipette Controller
- Serological Pipettes (sterilized)
- Micropipettes (all sizes)
- Micropipette Tips (sterilized) (all sizes)
- Invitrogen™ Countess™ Cell Counting Chamber Slides (*Fisher Scientific, Cat. No. C10228*)
- Conical Microcentrifuge Tubes (all sizes)
- Nitrile examination gloves
- Biological Safety Cabinet (BSC)
- Vacuum Aspirator
- Bead Bath
- Standard Incubator (5% CO₂, 37°C)

Adapters	Female Luer
Volume per reservoir	60 µl
Number of channels	6
Volume of each channel	30 µl
Height of channels	0.4 mm
Length of channels	17 mm
Width of channels	3.8 mm
Growth area per channel	0.6 cm ²
Coating area per channel	1.20 cm ²
Bottom: ibidi Polymer Coverslip	

- ibidi® µ-Slide VI 0.4 with ibiTreat surface modification (*ibidi, Cat. No. 80606*)
Figure 1: Specifications of the microfluidic chamber (*µ-Slide VI 0.4, 2018*)

For the PDMS fabrication:

- Sylgard 184 Silicone Elastomer Kit
- Digital Measuring Scale
- Plastic Weigh Boats
- Wooden stick for mixing

- Tissue Culture (TC) Plates
- Oven

For the experiment:

- One complete syringe pump unit
- 1 Laptop with a USB port
- USB cable
- Vemurafenib (PLX4032, RG7204) (*Selleckchem, Cat. No. S1267*)
- Tygon tubing, 0.020 in ID, 0.060 in OD (*Cole-Parmer, Cat. No. AAQ02103-CP S-54-HL*)
- 22 gauge x ½” Luer Stubs (*Instech, Cat. No. LS22*)
- 23 TW x 0.500” small metal tubes (*New England Small Tube Corporation, Cat. No. NE-1300-01*)
- 0.75 mm surgical punch (*Electron Microscopy Sciences, 69039-07*)
- 4.5 mm surgical punch (AcuPunch) (*Acuderm, Cat. No. P4525*)
- Poly(dimethylsiloxane) (PDMS), 1:3 ratio, 0.5 cm height
- Triad Magnetics AC/DC Power Supply, 12V, 1A (*Newark, Cat. No. 83T4339*)
- Power outlet strip
- Self Sticking Labeling Tape (*Fisher Scientific, 159015R*)
- 30 mL syringes (*BD, Cat. No. 302832*)
- Glass beaker
- Zeiss Microscope Incubator XL DARK S1
- Zeiss software (with ZenPro)
- Desktop Computer

Passaging of A375 melanoma cells

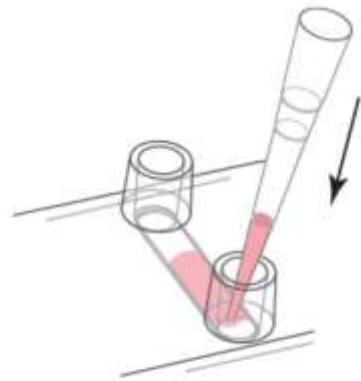
1. Place the DMEM, PBS, and trypsin bottles in the bead bath for 15-20 minutes to warm up.
2. Spray with each of the three bottles with 70% ethanol before placing inside the BSC.
3. Retrieve the TC plate of A375 melanoma cells from the incubator.
4. Attach one Pasteur pipette to the vacuum. Aspirate the current media from the TC plate.
5. Attach a serological pipette to the motorized pipette controller. Add 10 mL of DPBS to the TC plate to wash the cells. Move the plate in a circular motion to ensure full coverage of the dish.
6. Aspirate PBS completely, leaving none remaining in plate.
7. Add 1 mL of TrypLE to the plate.
8. Incubate the cells for 5 min, to allow complete detachment of the cells from the surface of the TC plate.

9. Remove the plate from the incubator and check the state of cell detachment under a microscope. Once cell detachment is satisfactory, return the plate to the BSC.
10. Add 2 mL of DMEM to the plate to neutralize the TrypLE.
11. With a 1mL pipette, perform thorough repeated pipetting (i.e. pipette up and down multiple times) to mix the cell suspension and break down larger cell clumps.
12. Remove 1 mL of cell suspension from the TC plate and pipette into a 2 mL microcentrifuge tube. Label the tube as appropriate.
13. In another microcentrifuge tube, add 10 μ L Trypan Blue to the tip at the bottom. Label the tube as appropriate.
14. Next, transfer 10 μ L cell suspension from the TC plate to the microcentrifuge tube containing Trypan Blue. Mix well with a 10 μ L pipette via repeated pipetting.
15. Insert 10 μ L of the Trypan Blue - cell suspension mixture into each of the two chambers on the cell Counting slides.
16. Using an automated cell counter, obtain a cell count for both chambers. Average the two resultant numbers to obtain the final cell count.
17. Using the average cell count and the dilution equation $C_1V_1 = C_2V_2$, perform the appropriate calculation required to make 1 mL of a cell sample with concentration 1×10^6 cells/mL. Prepare this sample in a 2 mL microcentrifuge tube, and label the tube as appropriate.
18. Repeat the calculation, this time to make 1 mL of a cell sample with concentration 4×10^5 cells/mL from the 1 mL sample prepared in the previous step. This can be prepared by adding 400 μ L cell suspension and 600 μ L DMEM to a 2 mL microcentrifuge tube. Label the tube as appropriate.
19. Add 8 mL media to the petri dish with the melanoma cells source and return to incubator.

Seeding Cells in the Microfluidic

Cell seeding procedure for ibidi® microfluidic adapted from (Horn, 2012).

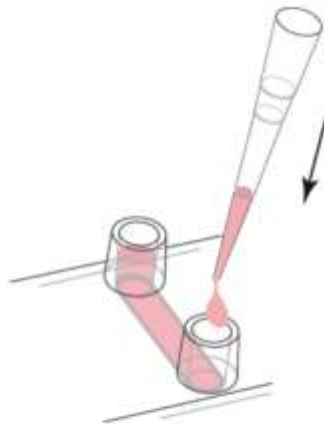
1. Using the cell sample with concentration 4×10^5 cells/mL, plate 30 μ L of this final cell concentration into each chamber of the ibidi® microfluidic device. When plating, place the micropipette tip securely inside the inlet well so that it is in contact with the chamber inlet (as shown below). Release the cell suspension quickly but carefully to fill the entire chamber.



Filling in a cell suspension into one cell culture channel of the μ -Slide VI 0.4.

Figure 2: Seeding the cells in the microfluidic (Horn, 2012)

2. Place the microfluidic device in the incubator for 1 hour, to allow the cells to adhere to the surface of the chambers.
3. Remove the microfluidic from the incubator and return to the BSC.
4. Add 60 μ L of DMEM to both the inlet and outlet well for each of the chambers (as shown below).



Filling the Luer reservoirs of the μ -Slide VI 0.4.

Figure 3: Filling the inlet and outlet wells with 60 μ L DMEM (Horn, 2012)

5. Place the microfluidic back in the incubator. It is ideal to wait 6 hours before beginning any experiments, to ensure full cell adhesion to the microfluidic chamber surface.

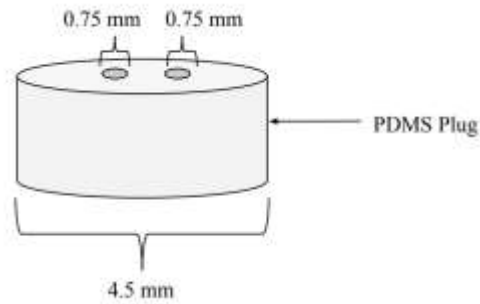
PDMS fabrication

1. Use Sylgard 184 Silicone Elastomer Kit.
2. Measure 50 grams of elastomer in a scale by placing in a plastic plate.
3. In order to do 1:3 ratio add 16.6 ml of curing agent with the electrical pipette
4. Mix with a small wooden stick until uniform.
5. Transfer to 5 different petri dish as a mold to create about 0.5 cm height.
6. Vacuum for half an hour to extract any bubbles
7. Bake PDMS on oven for 4 hours at 100°C.

Setting Up the Experiment

1. Turn on the Zeiss microscope incubator at least one hour before the experiment to allow the temperature within the microscope to reach 37°C. In particular, make sure each of the 5 hardware units is turned on in the correct order as indicated by the corresponding labels.
2. Once all hardware units are on, open the Zeiss software on the desktop computer. Select ZenPro.
3. Prepare the regular DMEM media solution, with 5% FBS, 1% Pen Strep, and 25 mM HEPES buffer.
4. Prepare a 10 μ M vemurafenib concentration, and add to a sample of regular media solution.
5. Perform the appropriate calculations to determine the amount of regular media and the amount of drug media will be needed for the duration of the planned experiment. These volumes can be found by multiplying the desired flow rate by the duration of the experiment.
6. Use a 30 mL syringe to draw out the correct volume of regular media. Repeat for the drug media.
7. Place both syringes in the incubator to allow them to warm up.
8. Create the PDMS plug for the inlet and outlet wells of the microfluidic chamber by doing the following:
 - a. Inlet plug
 - i. First, create two small holes using the 0.75 mm surgical punch. Make sure the remnants of PDMS from these holes are extracted completely. Also make sure that the two holes are close to each other, and that they are vertically straight.

- ii. Place the 4.5 mm surgical punch on the PDMS so that the two small holes are centered inside the punch. Apply force to create a plug over the two



small holes. The end product should look as follows:
Figure 4: The inlet plug

b. Outlet plug

- i. First, create one small hole using the 0.75 mm surgical punch. Make sure the remnants of PDMS from this hole is extracted completely. Also make sure that the hole is vertically straight.
- ii. Place the 4.5 mm surgical punch on the PDMS so that the small hole is in the center of the punch. Apply force to create a plug over the small hole. The end product should look as follows:

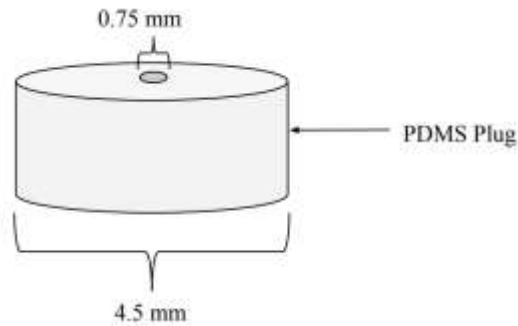


Figure 5: The outlet plug

9. Cut two tubes with length 50 cm; these will be used for the connection of syringe and the inlet plug
10. Cut one tube of length 20 cm; this will be used for the outlet plug and passage of media waste products.
11. Insert the metal portion of a Luer Stub halfway into one end of the 50 cm length of tubing. Repeat for the second 50 cm tube.

12. Insert one small metal tube halfway into the other end of the 50 cm length of tubing. Repeat for the second 50 cm tube. These metal tubes will be inserted later on into the inlet plug.
13. Insert one small metal tube halfway into one end of the 20 cm length of tubing. This metal tube will be inserted later on into the outlet plug.
14. Attach the Luer Stub to the end of the 30 mL syringes.
15. Place the syringes in the pump as instructed. Prime the syringes by gently turning the threaded rods of the pump manually. Wait until drops of media start forming at the end of the tube, then wait a little more for the droplets to stop forming; this ensures the tubes have been completely primed. Make sure that no bubbles have formed in the tubes.
16. Retrieve the microfluidic chamber from the incubator. Make sure that the media level in both the inlet and outlet wells is a little higher than the halfway height. If not, add some media to both wells.
17. Insert the inlet plug into the inlet well of the microfluidic chamber. Wait a few seconds for the media level to equilibrate on both sides. There should be no space of air between the media and the PDMS plug (i.e., the media level should rise to meet the plug). This is an important step to avoid the introduction of air bubbles in the chamber.
18. Insert the outlet plug into the outlet well of the microfluidic chamber.
19. Insert the small metal tubes at the end of the 50 cm plastic tubing into the inlet plug, one in each small hole. Make sure they are inserted completely until the bottom of the inlet well.
20. Insert the small metal tubes at the end of the 20 cm plastic tubing into the small hole of the outlet plug. Make sure it is inserted completely until the bottom of the outlet well.
21. Place a beaker inside the microscope incubator on the right-hand side. This will be the general waste container for disposal of media that falls from the outlet tube.
22. Carefully insert the microfluidic chamber into the microscope. Tape down the inlet tubes to the left of the chamber, to avoid movement during the experiment and prevent collision with the moving imaging camera. Tape down the outlet tube to the beaker so that the waste media falls securely inside the beaker; this is an important step to prevent leakage within the microscope.
23. Focus the microscope so that the image of the cells is clear.
24. Select 3 to 4 regions of the microfluidic chamber that have a large number of cells. Save these regions as tiles in ZenPro.
25. Properly set up the focus for the Bright, mCherry, and EGFP channels in ZenPro.
26. Define the experiment by setting the desired experiment duration and frequency of imaging. Make sure the images will be saved to the desired location.
27. On the laptop, start the Arduino software and open the correct file for the desired experiment. Fill in the necessary parameters for the experiment. See the Arduino code documentation for details.

28. Start the experiment. When the first set of images has been taken, upload the code to the Arduino board.
29. Watch and observe the experiment until the first drop is seen in the waste beaker and no leakage occurs.
30. Let the experiment run for the determined duration. Check periodically to make sure everything is running smoothly (i.e., no air bubbles, camera remains in focus, etc.).
31. When experiment has completed, clean the area and obtain the saved .czi file of time lapse images.

Parameters to consider for Flow Rate and Delay Time

Time chamber completely filled with new media and time cells respond to drug

Flow Rate (mL/min)	Time it takes for whole chamber to be covered with new media (min)	Time cells respond to dose of drug (min)
0.1	1.351	20
0.05	1.991	
0.02	4.765	30

Cleaning Up the Experiment

1. Unplug each of the pump systems from the power source, or turn off the power source.
2. Make sure your data has been saved to the destination folder on the computer.
3. Carefully remove the microfluidic chamber from the microscope.
 - a. Make sure outlet tubes are covered when extracting them so that no drops of media fall into the microscope. It is essential that no liquids spill inside the microscope.
4. Remove the waste beaker from the microscope. Dump the waste media in the sink, directly in the drain. Fill the beaker with 10% bleach and leave it in the sink. After a while, pour out the bleach and put the beaker away to be cleaned.
5. Take the syringes from the pump and unplug the tubes from the tip of the syringe.
6. If there is still media remaining in the syringes, place them back in the refrigerator. If not, discard the syringes in Biohazard box
7. Grab the tubes and move to the lab bench for cleaning and sterilization, so that the tubes can be reused.
8. Use three different syringes to wash the tubes using the following method:
 - a. First clean with water by connecting the tube to the end of the syringe and applying pressure to the plunger. Make sure it runs for at least 10 seconds.
 - b. Second, clean the tubes with 70% ethanol to sterilize them.
 - c. Third, clean the tubes with PBS to make sure all ethanol has been removed.
9. Leave space organized and label tubes if cleaned or not for the purpose of the next experiment. Wipe down counters with 70% ethanol if any liquids have been spilled.

10. Turn off the microscope. Make sure each of the 5 hardware units is turned off in the correct order as indicated by the corresponding labels.

Troubleshooting

Challenging situations to be aware of during experiments

1. Bubbles entering the system

a. How do bubbles enter the system?

In some cases the end user might face challenges involving bubbles entering the system. The reason for this could be that air got trapped in the inlet or outlet of the chamber when placing the plugs, or that a bubble left in the syringe when setting up the experiment that enters the tubing and gets to the chamber.

b. Why is it important to remove the bubbles?

Having bubbles in the system is equivalent of data loss. Whenever a bubble enters the chamber, this is harmful for the biological samples (in this case, A375 cells) as well as affect the images taken. Those images that have a bubble at a specific time point cannot be analyzed since no cells can be seen, nor the biological response they have during the experiments.

c. How to avoid bubbles

- i. Be extremely careful while inserting the inlet and outlet plug, by following the exact procedure stated above.
- ii. Add extra media to the inlet and outlet, so that when inserting plugs these are touching the media and there is no air in between them.
- iii. Make sure tubes are completely primed before inserting them in the inlet holes of the plug.
- iv. CAUTION: If when placing the plugs and tubes you observe a bubble or any air present in one of the tubes or in the inlet or outlet, you must start the setup again (remove the tubes, the outlet plug, and inlet plug and start the indicated procedure above again)

2. Cells surviving the setup process

a. What is the main challenge?

Temperature and pH during setup

- Set up can take a long time to do, and during this process cells lack the appropriate environment. The media cells are originally plated in does not contain HEPES buffer, which means cells lack the appropriate pH during the setup process. The setup is performed outside the microscope incubator at room temperature, which is lower than the ideal temperature for cell survival.

b. How to make cells survive through the setup process

- i. Temperature: provide a transportable mini incubator chamber that contains the property of achieving a temperature of 37°C. This will be used to cover the cells while inserting the plugs and tubes into the chamber. However, this chamber must allow the manual insertion of the plugs and tubes without being an obstacle in doing so.

- ii. pH: A proposed solution is adding HEPES to the media cells are initially plated with, which will give them a longer period of survival and be able to withstand the setup process.
- iii. Both of these options will relieve stress over the end user, and therefore lead to better outcomes.

3. Microscope live imaging

a. Focus

- i. Make sure the focus has been set up correctly for better image quality. If this is not done, images obtained for analysis can be very pixelated and it will be hard to distinguish biological response.

b. Selection of tiles to image

- i. Select tiles for imaging, at least 3 in each chamber.
- ii. Select completely distinct areas that can provide a large number of cells.

c. mCherry and eGFP channels

- i. Make sure these have an appropriate signal resolution for better outcome in analysis (especially mCherry channel).